Understanding the mechanistic uptake and exploring the applications of novel amino acid based ion pair complexes

Annsar Ahmad Warraich

Doctor of Philosophy

Aston University

September 2019

Aston University

Understanding the mechanistic uptake and exploring the applications of novel amino acid based ion pair complexes

Annsar Ahmad Warraich

Doctor of Philosophy

2019

Thesis summary

High throughput screening has resulted in a significant increase in the rate at which new chemical entities are discovered. However, major hurdles such as poor solubility, permeability and efflux limit their application. Not only is it difficult to get a drug into the body from the most convenient routes, once inside, challenges such as increasing resistance to drugs in cancer cells, fungi, bacteria and viruses present significant drug delivery challenges. To address these challenges, we have investigated the role and application of amino acids for solubility enhancement and in increasing drug uptake. Tetracycline (TC), ciprofloxacin (Cip) and digoxin were chosen as model drugs along with acidic and basic amino acids as counterions.

Saturated solubility was studied in different concentrations of the acidic (L-aspartic acid and L-glutamic acid) and basic (L-arginine, L-lysine and L-histidine) amino acids. We have shown that solubility of both TC and digoxin can be enhanced using amino acids, with the extent depending on the ionisation ability of the solution. Whilst both acidic and basic amino acids led to increased TC solubility, acidic amino acids were considered suitable counterions due better stability of TC in solution. Likewise, basic amino acids were determined to be suitable for digoxin compared to acidic since the latter led to drug degradation. Permeability of digoxin was studied using caco-2 cell line. Basic amino acids L-arginine and L-lysine led to a decrease in efflux ratio of digoxin. In parallel, the same counterions enhanced the permeability of digoxin through caco-2 monolayers via mechanisms which are likely to involve tight junction modulation triggered para-cellular transport, transcellular transport through ion-pair formation or reduced efflux thorough P-glycoprotein inhibition.

Use of amino acids as antimicrobial agents on their own as well as counterions to antibiotics, in a bid to investigate the potential optimisation of antibiotic activity, was investigated in planktonic cells as well as biofilms. For this, accumulation assays using ethidium bromide as an efflux competitor were done, showing that acidic L-amino acids were able to enhance both TC and Cip accumulation within *Staphylococcus aureus* (*S. aureus*) and *Pseudomonas aeruginosa* (*P. aeruginosa*). This translated into specific combinations of the amino acids and the antibiotics exhibiting synergistic hindrance in the growth of both bacteria. Pyocyanin and pyoverdine pigment production was also inhibited in *P. aeruginosa*; both with amino acids alone and synergistically when the amino acids were combined with the antibiotics. Antimicrobial activity of acidic D-amino acids was also investigated on *S. aureus* biofilms, specifically on their effect on biofilm density (both D- and L-amino acids), colony forming units (CFU), rate of cell attachment to surface and biofilm architecture. A concentration dependent ability to inhibit *S. aureus* biofilm formation and disperse already formed ones was observed with these amino acids; effecting both biofilm density and CFU. Synergy with Cip in the anti-biofilm activity of acidic amino acids was witnessed at specific combinations. Most interestingly, confocal imaging with the nucleic acid dyes SYTO 9 and propidium iodide, revealed that the amino acids disrupt the honeycomb-like extracellular DNA (eDNA) meshwork whilst also preventing its formation; a finding which was not observed with the use of Cip on its own. It is likely that the acidic amino acids act through mechanisms which modulate the acid base interactions involved in anchoring eDNA to cells. Being very non-specific, mechanisms such as modulation of acid-base interactions or ionic interactions may hold a key in evading evolutionary challenges, since overcoming these would require, if at all possible, drastic changes within bacteria. Our work has concluded that the amino acids present a wide functionality, ranging from solubility and permeability enhancement to overcoming antimicrobial resistance.

Key Words: **Solubility, permeability, efflux, antimicrobial resistance, biofilms.**

Acknowledgements

In the name of Allah (God), the Gracious, the Merciful.

(The Holy Quran, Al-Fatihah, 1:1)

All praise belongs to God who has given me strength to undertake this PhD. I have not the capacity to be grateful to Him enough for He never forgot me, even when I was week in His remembrance. He has been my hope at times of ease and at times of hardship. He is the one who is the source of all peace for me and the one Who continually brings me out of all forms of darkness into light. And I seek His protection from any difficulties I may encounter and His support throughout any challenges I may face. Peace and blessings of God be upon His Messenger, Muhammad (s.a.w), whose life has been a guiding principal for me in all aspects of my life including balancing work and other commitments. I am also sincerely grateful to my beloved Khalifatul Masih, Hazrat Mirza Masroor Ahmad (atba), whose guidance and prayers enabled me to embark on and journey through this PhD. His wise words of reminders for the community have helped me overcome many challenges along the way, aiding my personal development.

Now I would also like to convey my gratitude to Professor Afzal R Mohammed, who gave me the priceless opportunity to do this PhD and carry out this research. His enthusiasm has helped me through the four years and he has been there to supervise, guide and support me throughout my time at Aston. I would also like to thank Dr Ayesha Rahman for her continuous support and time with the microbiology part of the work. Thanks also goes to my associate supervisors Professor Yvonne Perrie and Dr Majad Hussain.

I am extremely grateful to my family; my father, brothers and especially my lovely Umi Jaan (mother) who continually and tirelessly supports and encouraged me throughout this undertaking, as well as the rest of my life. No matter how much I try, I can never repay my parents for their favours and just hope and pray that:

'My Lord, have mercy on them even as they nourished me in my childhood.'

(The Holy Quran, Bani Isra'il, 17:25)

I have been fortunate to have wonderful colleagues during my time at Aston, both within my research group and outside, and am extremely tankful for their friendship and support. I would also like to thank all the technical staff from Aston University, particularly Christine Jakeman, Jiteen Ahmed and Rachel Heath as well as the technical staff from University of Wolverhampton who have thought me a lot and supported me throughout this research. I must acknowledge the time and support of Matthew Walden for the mass spectrometry work undertaken within this research. Here I would also like to thank Dr Hazel Gibson from University of Wolverhampton for reviewing the biofilm paper.

I am also grateful to Dr Tony Worthington and Professor Anthony C Hilton for access to the lab facility (Aston University) where part of the work was undertaken. I also thank Charlie Clarke-Bland from the Aston Research Centre for Healthy Ageing for fluorescence and confocal microscope training and access.

I would also like to thank BBSRC and Dr Majad Hussain from Quest Healthcare Ltd for providing the studentship to fund this research.

Contents

List of Figures

List of Tables

List of Abbreviations

AA	Amino acid
A-B	Apical to basolateral
ABC	ATP-binding cassette superfamily
AMR	Antimicrobial resistance
Arg	Arginine
Asp	Aspartic acid
ATC	Anhydrotetracycline
ATP	Adenosine triphosphate
B-A	Basolateral to apical
BCS	Biopharmaceutical classification system
BP	British Pharmacopeia
CAA	Calcein accumulation assay
CFU	Colony forming units
Cip	Ciprofloxacin
CPEs	Chemical permeation enhancers
CV	Crystal violet
DMSO	Dimethyl sulfoxide
EATC	4-epianhydrotetracycline
eDNA	Extracellular DNA
EDTA	Ethylenediaminetetraacetic acid
EMEM	Minimum essential medium eagle
EtBr	Ethidium Bromide
ETC	Epitetracycline
FBS	Fetal bovine serum
FDA	Food and Drug Administration
GAPDH	Glyceraldehyde-3-phosphate dehydrogenase
GI	Gastrointestinal
Glu	Glutamic acid
glu	Glucose
HBSS	Hank's balanced salt solution
His	Histidine
HPLC	High-performance liquid chromatography
HTS	High Throughput Screening
Log *P*	Log Partition coefficient

LPS	Lipopolysaccharide
Lys	Lysine
MDR	Multidrug resistance
MFS	Major facilitator superfamily
MIC	Minimum inhibitory concentration
MLC	Minimum lethal concentration
MS	Mass spectrometry
NCEs	New chemical entities
O.D.	Optical density
OP	Overall potential
P. aeruginosa	*Pseudomonas aeruginosa*
Papp	Permeability coefficient
PBPs	Penicillin binding proteins
PBS	Phosphate buffered saline
P-gp	P-glycoprotein
p*I*	Isoelectric point
PI	Propidium Iodide
PIA	Polysaccharide intercellular adhesin
PMF	Proton motive force
PPZ	Phenyl piperazine
PVP	Ppolyvinylpyrrolidone
RND	Resistance-nodulation-division superfamily
S. aureus	*Staphylococcus aureus*
SDDS	Supersaturated drug delivery system
SEDDS	Self-emulsifying drug delivery system
SESD	Solvent evaporated solid dispersions
SMR	Small multidrug resistance family
SMSD	Surface modified solid dispersions
SNEDDS	Self-nanoemulsifying drug delivery system
TC	Tetracycline
TEER	Transepithelial Electrical Resistance
TSA	Tryptone soya agar
TSB	Tryptone soya broth
USP	United States Pharmacopeia
WHO	World Health Organisation

List of Publications

Peer reviewed articles

Annsar A Warraich, Afzal R Mohammed, Yvonne Perrie, Majad Hussain, Hazel Gibson and Ayesha Rahman (2019). Anti-eDNA: insights into a new mechanism of Staphylococcus aureus biofilm inhibition and dispersal using acidic amino acids. Scientific Reports (Submitted – under review).

Conference proceedings:

Annsar A Warraich, Ayesha Rahman, Yvonne Perrie, Majad Hussain and Afzal R Mohammed. Evaluation of acidic amino acids as counterions on the solubility of model zwitterionic drug tetracycline. UKICRS. April 2016.

Annsar A Warraich, Ayesha Rahman, Yvonne Perrie, Majad Hussain and Afzal R Mohammed. Evaluation of acidic amino acids as counterions on the solubility of model zwitterionic drug tetracycline. PharmSci. September 2016

Annsar A Warraich, Ayesha Rahman, Yvonne Perrie, Majad Hussain and Afzal R Mohammed. New insights into the mechanism of Staphylococcus aureus biofilm inhibition and dispersal using amino acids. Aston Postgraduate Day. June 2018. (Poster prize winner)

Annsar A Warraich, Yvonne Perrie, Majad Hussain, Afzal R Mohammed and Ayesha Rahman. New insights into the mechanism of Staphylococcus aureus biofilm inhibition and dispersal using D-amino acids BSAC Spring Conference. March 2019

Chapter 1: Introduction

Introduction

High throughput screening (HTS) has resulted in a significant increase in the rate at which new chemical entities (NCEs) are discovered (1). However, in delivering these drugs to where they are required, major hurdles stand and continue to emerge. Not only is it difficult to get a drug into the body from the most convenient routes, once inside challenges such as increasing resistance to drugs in cancer cells, fungi, bacteria and viruses are ever emerging (2-5). This has compounded the challenge for targeted drug delivery.

1.1 Drug delivery in humans via

1.1.1 Oral drug absorption

Once a drug enters via the oral route of administration, it is absorbed, distributed, metabolised and finally excreted. Since the therapeutic effect of the drug is highly influenced by its bioavailability, it is important that a sufficient level of the drug is reached and maintained at the target site. Bioavailability itself is effected by the amount and rate of drug absorption. So it is of vital importance that drug absorption is well understood to develop formulations with good efficacy and safety (6).

Absorption can be described as the migration of the drug from the site of administration to the extracellular compartment of the body. Since oral route is the most commonly used route of drug administration, the gastrointestinal (GI) tract plays a key role in drug absorption. Drug absorption is influenced by three main factors; physiological, physiochemical and biopharmaceutical factors (6). Physiological factors relate to the GI tract and include GI pH, GI perfusion, surface area of absorption, gastric emptying, small intestinal transit time and absorption mechanisms (6, 7). Physiochemical factors on the other hand relate to factors about the drug including pKa, solubility, lipophilicity, particle size and polar-nonpolar surface area. Biopharmaceutical factors refers to the formulation characteristics of the dosage form, which influence drug absorption (6, 8, 9).

1.1.2 Factors affecting absorption of solid oral dosage forms

1.1.2.1 Disintegration

An oral drug in the solid dosage form must first disintegrate into smaller particles. As the particles get smaller, it increases the surface area of the drug within the solid dosage from that is in contact with the gastrointestinal fluids (10). This ultimately leads to a higher rate of dissolution of the drug (10). Thus the rate of drug absorption is expected to be greater for a formulation with a faster disintegration time when compared to formulation with a lower disintegration time (6, 11). However, disintegration of a solid dosage form such as a tablet only increases the rate of dissolution of the drug rather than the solubility. In other words, with disintegration of the tablet, the maximum amount of drug which would dissolve in the medium would remain the same, only the rate at which it dissolves would increase.

1.1.2.2 Dissolution and solubility

As hinted above, though dissolution and solubility sound very similar, the words do not refer to the same phenomenon. When referring to the solubility of a substance, two main aspects can be described. First being the maximum amount of the substance which can dissolve in a given solvent, referred to as the solubility of the substance. Second being the time it takes for this to occur and this is referred to as the dissolution rate. Thus solubility is a capacity whilst dissolution is a kinetic process.

Dissolution is the next step after disintegration of a solid dosage form, and refers to the process in which the drug becomes dissolved in a solvent. It is a vital requirement before a drug in the solid dosage form can be absorbed; if a drug is unable to dissolve in aqueous fluids of the GI tract, it will be unable to gain access to and interact with the epithelial cell surface where it needs to be for absorption. The extent of dissolution is dependent upon the solubility of the drug. The rate of drug absorption is thus influenced by the rate at which the drug dissolves; this is even more important for poorly soluble drugs (6, 11, 12).

Amount of drug that gets absorbed is also affected by its solubility. Solubility is expressed as the mass of the solute (drug) that dissolves in a given volume of solvent at a given temperature (6, 12). As presented in Table 1.1, a substance can be categorised from very soluble to practically insoluble, depending on how many parts of solvent are required to dissolve per part of it (13). Whilst drugs with good solubility are more likely to be absorbed within the gut, those

expressing poor solubility get eliminated from the body without being absorbed by the small intestine. Thus poorly soluble drugs with low rates of dissolution are candidates that are least likely to be absorbed (6, 11, 14).

Table 1.1: USP and BP criteria for in describing the solubility a substance.

Descriptive term	Part of the solvent required per part of solute
Very soluble	Less than 1
Freely soluble	From 1 to 10
Soluble	From 10 to 30
Sparingly soluble	From 30 to 100
Slightly soluble	From 100 to 1000
Very slightly soluble	From 1000 to 10,000
Practically insoluble	10,000 and over

1.1.2.2.1 Factors affecting the solubility of solids substances in liquids

There are many factors which influence the solubility of a substance and some of these will be briefly discussed here. These include temperature, nature of solvent and the solute, molecular structure of the solute and pH (10, 15).

1.1.2.2.1.1 Temperature

Generally being an endothermic process, an increase in temperature aids the dissolution process. Thus in such endothermic systems, if the temperature is raised, the amount of substance which can dissolve increases. However if a substance undergoes the rarer exothermic dissolution process, an increase in temperature of the solution would instead decrease its solubility (10, 15).

1.1.2.2.1.2 Nature of solvent and the solute

The nature of the solvent and the solute is another factor which impacts the ability of the solute to dissolve. This interaction is usually explained with the saying that like dissolves like (16). Whereby, if the solvent is made up of polar molecules, such as water, solutes which are also polar are much easily dissolved than those which are non-polar (15). This is because of the

attraction between the polar solute molecules and the polar solvent molecules. Despite this, minute amounts of non-polar solutes can dissolve in polar solvents, probably due to the much weaker dipole-induced dipoles attractions induced by polar solvent molecules on non-polar solute molecules (10, 15, 16).

1.1.2.2.1.3 pH

Another factor which influences the solubility of a solute is the pH of the solution. This is specially the case with weakly acidic, basic and zwitterionic drugs. Since majority of the drugs are either weakly acidic or weakly basic, pH of the solution plays a crucial role in their solubility (10). Once in solution, these drugs exist as either the unionised or the ionised form in an equilibrium where proportion of either is dependent upon the pH of the solution. For weakly acidic drugs (HA) and weakly basic drugs (B), this equilibrium is usually expressed using the following equations (10, 15).

For a weak acid:

$$HA \rightleftharpoons H^+ + A^-$$

For a weak base:

$$B + H^+ \rightleftharpoons HB^+$$

The equilibrium between the ionised and the unionised form is dependent upon the pH in relation to the pKa of the ionisable sites of the drug (10). pKa is the pH at which 50% of a drug, whether weakly acidic or weakly basic, exists in the ionised form whilst the other 50% exist in the unionised form. Another simple rule to keep in mind is that an acidic group becomes ionised in a more basic pH whilst a basic group becomes ionised in a more acidic pH. This means that for weakly acidic drugs, an increase in pH above the pKa of the acidic ionisable site, increases the proportion of its ionised form, whilst decreasing the pH has the opposite effect. On the other hand, for a drug which is a weak base, an increase in pH above the basic group's pKa will increase the amount in the unionised form whilst decreasing the pH would increase the proportion in the ionised form. This means that a formulation scientist can control the solubility of weakly acidic or basic drugs by experimenting with the solution pH (10, 15).

Zwitterionic drugs have both an acidic group and a basic group. Therefore, like weakly acidic and weakly basic drugs, the solubility of a zwitterionic drug can also be altered by ionising either the acidic or the basic group. To add to this, the problem of pH dependent drug

degradation is more easily resolved with zwitterionic drugs due to the choice of using acidic or basic pH in solubility control.

Although the behaviour of the ionisable sites can be predicted through the study of its pKa values and determination of solvent pH, exact degree of the ionisation of a weakly acidic and a weakly basic drug can be calculated using the Henderson-Hasselbalch equations below (10, 15):

For a weak acid:

$$pH = pK_a + log10\frac{[A^-]}{[HA]}$$

For a weak base:

$$pH = pK_a + log10\frac{[B]}{[BH^+]}$$

Ultimately, the rise of solubility attributed to a rise in ionisable form of a drug is due to the ability of the ionised or polar species to interact with polar water molecules. As mentioned above, solutes which are polar are more easily able to dissolve in polar solvents (10).

1.1.2.3 Permeability

After becoming dissolved, a drug can now be absorbed into the systemic circulation. At this stage, the absorption of the drug can be affected by both physiological factors as well as factors relating to the drug. Physiological factors include but are not limited to the availability of transport mechanisms through the selective phospholipid membrane and efflux of the drug back out from the cells. To add to this, factors relating to the drug also affect its absorption. These include lipid solubility, size and number of hydrogen bonds (10).

Like with solubility, poorly permeable drugs will not be absorbed as much as highly permeable ones. However, unlike solubility greatly hydrophilic drugs are poorly permeable and thus are poorly absorbed through the phospholipid bilayer membrane (17). Since dissociation of weakly acidic and basic drugs into its ions makes them less lipophilic and more hydrophilic, the pH around the membrane at the site of absorption plays a crucial role in absorption. This has been covered in the pH-partition hypothesis by Overton in 1899 and takes into account passive

diffusion, the most common route of drug permeation (10). Briefly, only drugs present in the unionised form, which exist in an equilibrium whose proportion is effected by the pH around the absorption site, will passively diffuse through the membrane. However this hypothesis does not explain why drugs that are predicted to exist in the ionised form at physiological pH are absorbed through the gastrointestinal tract. One theory put forward for these drugs is the formation of ion-pairs, resulting in neutral species which are then able to be absorbed (10).

A drugs ability to be absorbed through the membrane can predicted by determining its partitioning behaviour between water and a lipid-like solvent such as octanol (10). Partition coefficient (*P*) of a particular drug under set condition can therefore be calculated using the following equation:

$$Partition\ coefficient = \frac{concentration\ of\ drug\ in\ organic\ phase}{concentration\ of\ drug\ in\ water\ phase}$$

The value of *P* obtained is then converted to log*P*. Drugs with log*P* values between 3 and 6 are optimal for passive diffusion through the lipid membrane (11, 12).

Cell culture techniques using the well-established caco-2 cell line are quite common and well accepted model of intestinal absorption (10, 18). Along with permeability data, this cell model can provide useful insights into the mechanism of transport. Transport experiments on caco-2 cells can be done in both apical to basolateral (A-B) direction as well as the basolateral to apical (B-A) direction. Passive transport can be assumed if the transport of a drug is equal in both directions. On the other hands, efflux by efflux pumps such as P-glycoprotein, is hinted by greater transport in the B-A direction (10, 18).

Various other ways for determining the permeability of drugs are available. These include tissue studies and perfusion studies both in animals and humans (10). Permeability tests directly measure the rate of mass transfer across human intestinal membrane and therefore indirectly measure the extent at which the drug would be absorbed in a human (6).

1.1.2.4 The solubility permeability paradox

One of the factors required for a drug to dissolve is also the one which hinder its permeation and vice versa. In another words, both very hydrophilic drugs and hydrophobic drugs will have poor absorption in the GI tract since they will have very poor permeability and solubility respectively. Thus for a drug to be readily absorbed, it must be able to permeate the lipid

bilayer whilst also being able to dissolve in water. Optimal requirements therefore are that the drug be mainly hydrophobic whilst also being able to dissolve in water. This is one of the reasons why majority of the drugs tend to be either weak acids or weak bases (19).

1.1.2.5 Biopharmaceutical classification system

Depending on a drugs solubility and intestinal permeability the Food and Drug Administration (FDA) approved Biopharmaceutical Classification System (BCS) classifies it into one of four broad categories (20). These classes are presented in the Table 1.2.

Table 1.2: Biopharmaceutical classification system

	High Solubility	*Low Solubility*
High Permeability	Class 1	Class 2
Low Permeability	Class 3	Class 4

As presented in the table above, class 1 drugs are those which demonstrate both a high solubility and a high permeability. In normal circumstance, this allows for rapid uptake into the bloodstream and an excellent bioavailability (10).

Having poor solubility, the absorption of class 2 drugs is limited by its low dissolution rate. Since solubility and dissolution rate is easier to modulate for a formulation scientist, drugs with a low solubility and high permeability are preferred over those with a low permeability and high solubility (10).

Class 3 drugs are those which have high solubility but low permeability. Although high solubility helps, a formulation scientist can maximise permeation by ensuring very rapid dissolution (10, 20). This would allow exposure to the site of absorption for maximum time, increasing the total percentage able to permeate (10).

Lastly, out of the four classes, class 4 drugs are the most challenging for a formulation scientist. As expected, they exhibit poor bioavailability. For oral delivery, prodrug formation or other novel strategies are need to adopted for drugs in this class to attain sufficient bioavailability (10).

FDA guidelines state that the BCS approach can be used to justify biowaivers for class 1 and class 3 immediate release drugs that demonstrate at least rapid in vitro dissolution rates (20, 21). Biowaivers renders the need for in vivo bioavailability and/or bioequivalence studies unnecessary for the drug to be approved. The criteria required for meeting the high solubility, high permeability and rapid dissolution requirements of the biowaivers are outlined next.

1.1.2.5.1 High solubility

To meet the high solubility requirement, the highest dose of a drug which a biowaiver is requested for must be able to dissolve in 250 ml or less of water throughout the pH range of 1-6.8 at 37 °C. The 250 ml represents the estimate amount of fluid available after oral dosage form ingestion along with a glass of water by a fasting individual. The requirement therefore ensures that all the drug within the highest dosage form is able to dissolve easily when taken by most patients.

1.1.2.5.2 High permeability

For a drug to be classified as highly permeable, it must demonstrate systemic bioavailability or absorption in humans of greater than 85% (20). FDA guidelines stipulate many methods to demonstrate high permeability including rate of mass transfer across human intestinal membrane and absolute bioavailability along with methods which predict absorption in humans including in situ intestinal perfusion using animal models and in vitro permeability studies using the caco-2 cell line (10, 20, 21).

1.1.2.5.3 Rapid dissolution

The third requirement for the eligibility of a biowaiver is the demonstration of rapid or very rapid dissolution. For this, the drug must be proven to exhibit 85% or more dissolution within 15 minutes (very rapid dissolution) or 30 minutes (rapid dissolution) using USP apparatus 1 or 2. Apparatus 1 must be set at 100 rpm whilst apparatus 2 must be set at 50 rpm and dissolution must be demonstrated in 500 ml of three different media; 0.1 N HCl, a buffer of pH 4.5 and a buffer of pH 6.8 (20).

1.1.2.6 Lipinski's rule of five

Lipinski et al highlighted that HTS provides higher efficiency in lead generation and more therapeutic opportunities, however it is unable to predict for oral activity (22). This results in more leads, but they have less favourable physical properties resulting in worse oral activity profiles. Because of this, in 1995 Lipinski et al proposed 'the rule of 5' as a tool to predict for poor absorption or permeation. According to the rule, a formulation scientist should be aware of potentially poor lead absorption or permeation when two of the following are met (22):

- "There are more than 5 H-bond donors (expressed as the sum of OHs and NHs)"
- "The MWT is over 500" in daltons
- "The Log P is over 5"
- "There are more than 10 H-bond acceptors (expressed as the sum of Ns and Os)" (22)

These rules are suggestive of solubility or permeability issues for the drug in question (23). It is worth highlighting that this rule only applies to such drugs which are not substrates of transport proteins (22).

1.1.3 Mechanisms of oral drug absorption

After successful dissolution, a drug must cross the lipid bilayer of the epithelial cells before it can reach its site of action. Whilst a comparably small amount of drug is absorbed in the stomach, majority of the drugs taken by mouth are absorbed in the small intestine due to the greater surface area available for absorption (17). Cell membranes are selective barriers due to their hydrophobic core and substrate specific proteins (6, 17). Three main mechanisms are well known which enable the transport of drugs across the membranes. These include ATP independent transport, active transport and endocytosis (6, 17).

After being transported into the cell, some drugs can undergo efflux back out into the lumen of the small intestine. A common efflux transporter responsible for this is P-glycoprotein. This will be covered in more detail under the section 'efflux pumps'.

1.1.3.1 ATP independent transport

Passive diffusion can occur through the lipid membrane (lipid diffusion) or aqueous channels. It is the mechanism through which most of the drugs are absorbed from the GI tract. Since

this mechanism is passive, no energy is expended and the driving force for this mechanism is the concentration gradient. Drugs diffuse from an area of high concentration to an area of low concentration until equilibrium is reached. Other than concentration gradient, the main drug characteristics governing the diffusion rate are molecular size and shape, degree of ionisation, lipid solubility. Passive diffusion generally only enables small molecules to diffuse through. A specific type of passive diffusion, known as facilitated diffusion is the mechanism through which larger molecules are able to diffuse into the cell (7, 12, 17).

Lipid soluble drugs show the highest rate of passive diffusion. However this relationship is not linear. This is because for a drug to passively diffuse across a lipid membrane, it must not only be able to partition into the membrane but back out of it from the other side (Figure 1.1). In other words, hydrophilic (Log*P* <3) drugs would find it difficult to partition into the membrane bilayer. On the flip side although drugs that are very hydrophobic (Log*P* >6) would rapidly partition into the membrane, they would find it difficult to partition out from the other side into the cell (11, 12). Membranes also contain aqueous channels through which drugs with higher hydrophilicity can penetrate (17).

Figure 1.1: Polar drugs would find it difficult partitioning into the membrane bilayer, whereas very nonpolar drugs would find it as had to partition out the membrane, once in it (12).

Since most drugs are weak acids or bases, in aqueous GI fluids they exist as both ionised and the unionised form, with the equilibrium dependent upon the pH of the surroundings. The ionised form is hydrophilic and thus is unable to be absorbed through passive diffusion whereas the unionised form is largely lipid soluble and is therefore able to be transported (Figure 1.2) across the membrane (12, 17).

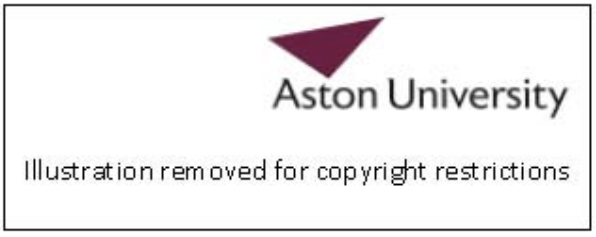

Figure 1.2: Ionised form of the weak acid (A) and weak base (B) is passively able to diffuse through the membrane whereas the unionised version of the weak acid (B) and weak base (B) is not (17).

Although facilitated diffusion utilises specialised transmembrane carrier proteins, like simple passive diffusion it also does not require any energy. The proteins enable the passage of larger molecules into the cell, again down the concentration gradient. During the process of transportation the carriers are able to undergo conformational changes to facilitate the passage of large molecules such as glucose (12, 17).

1.1.3.2 Active transport

Active transport utilises specific carrier proteins. Since these transmembrane proteins require energy, unlike in passive diffusion, active transport enables the passage of molecules against their concentration gradient. The energy for the process is derived from hydrolysis of

adenosine triphosphate. Drugs that are similar to natural endogenous metabolites are able to utilise this passage (17).

1.1.3.3 Endocytosis

Endocytosis enables the transport of very large drugs into the cell. In this process, the drug is engulfed by part of the cell membrane which then gets pinched off inside the cell and forms a vesicle containing the drug. Like active transport, this mechanism also requires energy (17).

1.1.4 Challenges and strategies for oral drug absorption

Oral drug delivery is the most widely used route of drug administration due to its cost effectiveness as well as the comparably high patient compliance it offers as a consequence of its convenience in use. One of the most challenging hurdles is attaining a sufficient solubility which about 40-70% of all new chemical entities (NEC's) fail to reach (8, 9).

1.1.4.1 Oral drug delivery

A drug can be administered to a patient through various routes, the choice of which is influenced by many factors. These routes include the oral route, parenteral route, topical route, respiratory route as well as the rectal and vaginal route. However oral drug administration is often the route utilised and preferred by both the patient and the physician. From the patient's perspective, taking the drug orally is often more convenient, simple, safe as well as less time consuming. Whereas from a physician's perspective the preference of the oral route is influenced by cost effectiveness as well as patient compliance which results from the ease of use this route presents to the patient (6, 12, 17). Thus this route offers convenience to the patients and a higher adherence rate is expected, which is mutually beneficial to both the patient and the health care system.

However formulating a drug for oral administration is not always simple. The drug must be able to withstand enzymatic degradation within the gut while being stable in both acidic and alkaline pH. It must also show good level of stability with the food it will inevitably come in contact with. It must be resistant to efflux from the small intestine as well as survive first pass metabolism. Importantly, before the drug becomes available it must solubilise in water for it to be absorbed, and then be able to permeate through the gut lining into the blood stream (7, 17).

1.1.4.2 The challenges

Low solubility and low permeability are the most common causes of low oral bioavailability. Around 40-70% of NEC's that are discovered, do not reach the market due to their poor water solubility profile. Thus herein lies one of the biggest challenges for a formulation scientist of today (8, 9).

Even though challenging, enhancing the apparent solubility of drugs is therefore a crucial research area. Many methods have been developed in a bid to tackle this problem. When enhancing the solubility of a drug, the method chosen is dependent upon the drug characteristics and dosage requirements. These methods can be divided into three main categories; physical modifications, chemical modifications and other methods. Physical modifications include particle size reduction and solid dispersions. Chemical modifications include salt formation. Other methods such as supercritical fluid process and use of adjuvant like surfactant are also available (8, 9).

1.1.4.2.1 Ways of overcoming challenges with solubility

1.1.4.2.1.1 Self-emulsifying drug delivery systems

Mohsin et al optimised self-nanoemulsifying drug delivery system (SNEDDS) to improve the solubility and bioavailability of the anticholesterol drug fenofibrate (24). Highest solubility was obtained with formulations containing mixed glycerides. They showed in vivo studies that the oral bioavailability of fenofibrate improved 1.7 times using SNEDDS as compared to the pure drug itself (24).

Balata et al used self-emulsifying drug delivery system (SEDDS) to improve the solubility of resveratrol. The optimal formulation was then used to determine the effect of the formulation on the efficacy of the drug through in vivo studies (25). Various oils, surfactants and cosurfactants were screened for their individual effect on the solubility of resveratrol. Olive oil, Tween 80 and propylene glycol were found to be the best oil, surfactant and cosurfactant respectively in solubilising the drug. Therefore these components were combined with the drug to form the most optimal system.

They found that the solubility of the drug was dependent on the concentration balance of the oil, surfactant and cosurfactant used. The proportion of each component effected the size of

the droplets; the smaller droplets with more surface area to volume ratio was generally found to solubilise more drug. The composition of oil to surfactant to cosurfactant weight ratio of 200:266.7:533.3 was determined to be the best formulation and was used for further studies. In vivo studies showed significant results; the new formulation was nearly as effective as the unprocessed drug in decreasing the total cholesterol (25). The hypoglycemic effect of the drug followed a similar pattern and is likely due to higher bioavailability of the drug through the use of optimised SEDDS (25).

Alqahtani et al prepared mixed micelles using cremophor EL, labrasol, captex and ethanol as a surfactant, co-surfactant, oil and co-solvent respectively. This SEDDS was prepared to increase the solubility and bioavailability of the poorly soluble and permeable drug ɣ-Tocotrienol (26). To assess solubility, lipolysis was used to release the entrapped drug in the system. The drug was then quantified using HPLC. The group found that SEDDS formulation, had a better release profile (60% at 120 min) compared to the commercially available product Tocovid (20% at 120 min) (26).

1.1.4.2.1.2 Liposomes

Wang et al used the thin film hydration method to prepare liposomes which they loaded with naringenin to increase the solubility and bioavailability of poorly soluble drug. The liposomes consisted of phospholipid, cholesterol, sodium cholate, and isopropyl myristate. Liposomal characterisation studies revealed that stable liposomes were formed (27).

Dynamic light scattering measurements using particle size/zeta potential analyser revealed an average particle of liposome to be 70.53nm whilst transmission electron microscopy showed that these naringenin loaded particles were spherical in shape. Furthermore since the average particle size of free naringenin particles was 21.35µm, 0.22µm filters were used to remove the naringenin which was not encapsulated into the liposome. This enabled the quantification of remaining encapsulated drug within the samples, using HPLC, and allowed the encapsulation efficiency of the liposomes to be determined. The results indicate majority (72.2%) of the drug was entrapped in the liposome (27).

In vitro release profile revealed the dissolution rate of liposome loaded drug to be much higher (>90% in 72 hours) than free drug (<32%). It is likely that the dissolution rate was enhanced due to higher solubility of the drug in the liposome formulation compared to the free drug (27).

For tissue distribution study, fasted Kunming mice were orally administered with free and liposome loaded drug. Next the tissues of interest were dissected and the amount of drug in the respective tissue quantified. The study found that the liposome loaded drug, had a significantly higher distribution throughout all tissues compared to the free drug (27).

1.1.4.2.1.3 Solid Dispersion

Fong et al used freeze drying to formulate solid phospholipid dispersions for the poorly soluble drug celecoxib in order to increase its solubility and its effect on permeability. In the formulations, different concentrations of phospholipids were used to form the matrix around the drug (28).

They found that the enhancement of solubility of the drug depended upon the concentration of the phospholipid in the formulation. Greater than 200 fold increase in solubility was observed for the formulations. The reason for the apparent enhancement in this solubility is twofold. Firstly the solubilising effect of liposomes contributes to this enhanced solubility. Secondly, freeze drying changed the state of the drug from the crystalline state to an amorphous state. Since the forces between the molecules of a substance in the amorphous state are weaker than those in the crystalline form, it is more easily dissolved. Due to this reason, they also found that freeze drying on its own caused a seven fold increase in the apparent solubility of celecoxib (28).

Choonara et al used various concentrations of the hydrophilic substance menthol to make solid dispersions of sulfamethoxazole. This drug has low solubility and high permeability and therefore falls under class II of the BCS (29).

The group used the co-melt technique in which heat and mixing was utilised to mix menthol and the drug to form the solid dispersions. They used various concentrations of menthol ranging from 1g to 10g, whilst the concentration of the drug was kept constant at 50mg per solid dispersion. They melted the menthol at 37°C, after which they added the drug to the melted menthol and raised the temperature to 160°C to melt the drug. Throughout this process magnetic stirring was utilised to ensure homogenous mixture of the two components in the melt state as well as when the solid dispersion is formed. Next 5% sucrose was added as a cryoprotectant; to prevent freezing and desiccation of menthol during the freeze-drying process. The resultant mix was freeze-dried and later mixed with hydroxypropyl

methylcellulose, sodium carboxymethyl cellulose and magnesium stearate before being compressed into tablets (29).

To determine change in solubility of the drug through the formation of the drug loaded solid dispersion, as compared to the drug own its own, both the control and the solid dispersion were mixed for 48h in simulated human intestinal fluid and quantified thereafter. They found that the solubility of the drug was higher in the drug-loaded solid dispersions compared to control. Furthermore, the higher the content of menthol in the dispersion, the higher the resulting solubility was (29). The increase in menthol concentration and solubility was also in line with a decrease in crystallinity and therefore and increase in amorphous form of the product as well as decrease particle size and therefore an increase in surface area to volume ratio (29).

1.1.4.2.1.4 Complex formation

Sanka et al used skimmed milk as the host to form inclusion complexes with the poorly soluble drug piroxicam. They made this complex using the rotary evaporator technique. They found that skimmed milk was a good carrier in not only increasing solubility (2.5 times) but it also significantly decreased the gastric side effects, such as ulceration, associated with such non-steroidal anti-inflammatory drugs (30). Milk contains amino acids so it may be possible that interaction of the drug with these amino acids may be one of the potential underlying causes for the enhancement of solubility.

1.1.4.2.1.5 Supersaturated Drug Delivery System

Ganesh et al developed a supersaturated drug delivery system (SDDS) where chitosan was used to form cocrystals of aceclofenac which were embedded within alginate beads. The aim was to enhance the solubility of the drug through co crystal formation to enable controlled released through the formation of an alginate matrix around the cocrystals (31). Various mechanisms are underplay in the enhancement of dissolution rate through the use of chitosan. These include particle size reduction, enhanced wettability of the system as well as alteration in the surface morphology of the drug (31).

1.1.4.2.1.6 Other solid dispersions

Rashid et al conducted a study to compare the effectiveness of various solubility enhancing techniques in enhancing the physicochemical characteristics of the drug ezetimibe. In this study the group compared SNEDDS, surface modified solid dispersions (SMSD) as well as solvent evaporated solid dispersion (SESD). All systems were loaded with the drug and aqueous solubility, dissolution and oral bioavailability was investigated (32).

Spray drying techniques were used to prepare all formulations. The group found that SNEDDS were the best in improving the physicochemical characteristics of the drug followed by SESD and lastly but not least, since it also improved the characteristics, SMSD. This pattern correlates with the particle size achieved with each formulation; SNEDDS gave the smallest particle size (6 µm) whilst SMSD gave rise to the larges particle size (24µm). Also of interest is that the drug was present as an amorphous form in SNEDDS and SESD but as a crystalline form in SMSD formulations (32).

1.1.4.2.2 Technology for overcoming challenges with solubility

1.1.4.2.2.1 Electrospray

Yousaf et al developed nanoparticles (referred to as nanospherule) using the electrospraying technique. These nanoparticles were loaded with a BCS class II drug fenofibrate to increase the solubility of the drug (33). The matrix composed of the polymer polyvinylpyrrolidone (PVP) and the surfactant Labrafil M 2125.

Increasing the concentration of Labrafil in the formulation was seen to enhance the apparent solubility and hence also the dissolution rate of the drug. Thus the highest drug to Labrafil weight ratio of 1:0.5 was chosen to determine the effect of changing PVP concentration on the formulation. Like with Labrafil, increasing the PVP concentration also raised the solubility, but only up to a drug to PVP weight ratio of 1:4. Further increasing the PVP concentration did not give rise to any significant advancement in solubility. Finally the optimal formulation was chosen to be drug/PVP/Labrafil 1:4:0.5 and was used to do characterisation studies as well as in vivo oral bioavailability in rats. The oral bioavailability was found to be 2.5 times greater in the optimised formulation compared to the free fenofibrate (33).

1.1.4.2.2.2 Hot melt extrusion

Ashour et al utilised the hot melt extrusion technique to increase the solubility, permeability and oral bioavailability of piperine using various polymers. Soluplus was found to be the most optimal polymer, enhancing the apparent solubility of piperine by 160 fold with the formulation containing 10% w/w piperine/Soluplus (34).

1.1.4.2.2.3 Antisolvent Precipitation

Sadeghi et al used the antisolvent precipitation or crystallisation technique to increase the solubility of curcumin which is an anticancer drug with poor solubility. They did this in the presence of polyvinylpyrrolidone K30 (PVP). Untreated curcumin was used as the control, whereas physical mixture of curcumin and PVP were used to distinguish the difference of effect of just PVP and the effect of antisolvent crystallisation on curcumin (35).

For crystallisation, curcumin which was dissolved in acetone was added dropwise to aqueous solutions containing different amounts of PVP to give final weight ratios of curcumin to PVP of 1:0, 1:1, 1:2 and 2:1. The resulting suspension was frozen and 24 hours later freeze dried. Physical mixtures of curcumin and PVP were prepared using a tumbling mixture using appropriate ratios of both substances (35).

Solubility studies showed that curcumin in precipitated samples of curcumin and PVP had up to a twenty fold higher solubility compared to curcumin on its own or to the physical mixtures of curcumin with PVP. Curcumin which has been precipitated with PVP displays an amorphous state as compared to the curcumin precipitated without PVP or the untreated curcumin, both of which displayed crystalline structures (35).

1.1.4.2.3 Ways of overcoming challenges with permeability

1.1.4.2.3.1 Inhibition of efflux pumps

Having been solubilised and absorbed into or through the membrane, the drug may be susceptible to efflux. Hence low bioavailability due to efflux of drugs is another challenge faced in oral drug delivery. Apart from low bioavailability, increased luminal concentration of the drug resulting from its efflux into the intestine can lead to intestinal toxicity. This highlights the need to overcome drug efflux to improve bioavailability.

A novel application of phospholipids were investigated by Simon S et al (36). They showed that two phosphatidylcholine (PC) derivatives 1,2-dicotanoyl-*sn*-glycero-3-phosphocholine (8:0 PC) and 1,2-didecanoy-*sn*-glycero-3-phosphocholine (10:0 PC) had significant in vitro P-glycoprotein (P-gp) inhibitory activity (36). In this study the group only used phospholipids which demonstrated good formulation and no cytotoxicity to assess their interferences with P-gp activity. They also suggest that the lipid molecules themselves were accountable for the inhibition of P-gp, whilst the shape and size of the aggregates and whether they formed liposomes or not did not seem to influence P-gp activity. They also concluded that intact phospholipids were required for their inhibitory effect on P-gp; free fatty acids, on the other hand, either did not have a significant inhibitory effect or led to decreased monolayer integrity evident from a significant drop in transepithelial electrical resistance (TEER) values. Further evidence to confirming P-gp inhibition by these phospholipids was found when P_{app} ratio decreased in P-gp transfected MDCKII mdr1 cell line to a much higher degree compared to those that were not transfected with P-gp (wild type) (36).

Two main methods were used to determine a phospholipids inhibitory effects. The first involved the study of the transport of Digoxin, whilst the second was the calcein accumulation assay (CAA). In these studies the inhibitory effect of verapamil was taken to be 100%. The results for the test compounds were thus expressed as the relative inhibition compared to verapamil. In CAA, 8:0 PC displayed a relative inhibition of 50% and 80% in caco-2 and MDCKII mdr1 cell lines respectively. For 10:0 PC, the relative inhibition of P-gp was 80% in caco-2 cell lines, whilst the inhibitory effect of this phospholipid was 20% better then verapamil in MDCKII mdr1 cell lines at 120% relative inhibition (36).

They showed using wildtype MDCKII cell lines that the P-gp inhibition was the mechanism involved. After incubation with the test phospholipids and as compared to control the fluorescence of calcein increased dramatically (up to 9 fold) in cells with P-gp expressed (MDCKII mdr1) as compared to wildtype cells which do not express P-gp (36).

The P-gp ATPase activity studies showed that the mechanism of p-gp inhibition of cis-22:6 PC was indirect, since this phospholipid did not affect P-gp ATPase activity. 8:0 PC and 10:0 PC on the other hand both reduced the P-gp ATPase activity which was induced by verapamil. Furthermore, 10:0 PC was also shown to reduce basal activity of P-gp ATPase. The group concludes that both 8:0 PC and 10:0 PC act through a direct mechanism to induce P-gp inhibition (36).

Further in vivo work by the same group showed that these phospholipids can also be used to increase bioavailability (37). They investigated the effect of incorporating phospholipids on the bioavailability of orally administered ritonavir. To do this they used the animal model Wistar rats and administered 20mg/kg suspension of ritonavir along with 1mM of test compound into their stomach.

Although 8:0 PC and 10:0 PC did not match the P-gp inhibiting effects of verapamil or Tween®, nevertheless they exhibited a significant increase in bioavailability of ritonavir represented by an 18 and 14 fold increase in the area under the curve respectively (37).

Derivatives of PC are present in a normal diet and thus it is hoped that as long as the total administrated lipid is not more than that which classifies it as a xenobiotic, it is unlikely to have any adverse effects. It is also suggested that a systemic side effect of using phospholipids is unlikely due to their degradation by digestive enzymes. The author highlights that use of surfactants such as Tween® may have adverse effects. Thus it is suggested that the phospholipids, although less effective then Tween®, may be a safer option since although synthetic, they are made up of moieties natural to the body (37).

1.1.4.2.3.2 Balancing toxicity verses permeability approach

Intestinal permeation enhancers offer a good way to improve bioavailability. However their use has been limited due to a somewhat toxicity concerns. Whitehead et al studied 51 permeation enhancers generating a database highlighting their potency and toxicity (38).

Whitehead et al studied 51 different permeation enhancers at three different concentrations (0.01%, 0.1% and 1% w/v); thus a total of 153 formulations were studied. Whitehead et al found that both permeation enhancement and toxicity of the 51 chemical permeation enhancers (CPEs) were dependent upon their concentration. However they also found that the extent of permeation enhancement and toxicity significantly varied across all chemical categories (38).

Their study confirmed the commonly held perception that if CPEs are strong enhancers of permeability, they are also very toxic or that if CPEs are not very toxic, they are weak enhancers of permeability. However the production of this database allows the recognition of a few formulations that are potentially best of both; significantly low toxicity whilst having a significantly high permeation enhancement effect (38). Thus considering both the

enhancement potential and toxicity, the authors created a new parameter called overall potential (OP). The largest OP was observed for the chemical category of anionic surfactants and was followed by zwitterion surfactants. Furthermore, using OP values the authors were able to rank the formulations and found that six out of the top ten best and safest enhancers were of the low concentration (0.01% w/v). According to the author this highlights the need to study a chemical enhancer at different concentrations before ruling it out (38).

The highest OP value was obtained for Phenyl piperazine (PPZ) which identified it as the most optimal permeability enhancer. 0.1% PPZ was found to enhance the permeability of mannitol and dextran by 14 and 11 fold respectively. Furthermore TEER values returned to original with 24 hours of removal of PPZ from the media. This shows the potential applicability of not only PPZ but also the database to pinpoint the most safe and effective CPEs (38).

1.1.4.2.3.3 Ion-pair formation

Isabel et al used the concept of ion-pairing to improve the permeability of atenolol at the colon. The counterions used were acidic, brilliant blue and bromophenol blue (39). Histological assessment was carried out using microscopy to determine membrane integrity (39). No significant damage to the colon was observed through microscopy and therefore it is likely that the enhancement in permeability was due to ion pairing and not due to loss of membrane integrity (39).

Since majority (>87%) of atenolol was present in the aqueous phase for each assay, whether or not ion pairing occurred was unclear form the partitioning studies (39).

Nevertheless, In situ permeability studies were carried out on the male Wistar rats. 500µM concentrations of both atenolol and the counterions were used in the study; that is a 1:1 molar ratio. The use of these counterion did attain the desired outcome of enhancing the permeability of atenolol. Of particular note is that permeability was found to be better in brilliant blue (Papp 0.508 X^{10-4} cm/s) compared to bromophenol blue (0.405 $X10^{-4}$ cm/s). Bromophenol blue has previously been found to be a suitable counterion, however it is toxic. This study therefore shows that brilliant blue, a food additive, may be a suitable counterion. However, the author states that majority of brilliant blue is excreted without being absorbed (39). Therefore, if the lack of toxicity associated with brilliant blue is due to lack of its absorbance, this formulation may lead to brilliant blue associated toxicity since ion pairing will increase its absorption from the colon.

Interestingly, ion-pair formation is not only linked to permeability enhancement, but has shown evidence to overcome both solubility and permeability. To add to this, the same substance which enhances solubility has also been linked to the enhancement of permeability. ElShaer et al, has used the concept of ion pairing to assess its impact on the apparent solubility and permeability of model drugs. The concept utilises amino acids as counterions to drugs with the aim that the drug would form an ion pair with an oppositely charged amino acid in solution, thereby modifying the drugs physicochemical characteristics. ElShaer et al, has shown that the apparent solubility and permeability of drugs can be improved through the use of amino acids as counterions (40).

1.2 Drug delivery in bacteria

Challenges with delivering drugs are not restricted to just absorption of orally administered drugs through the GI tract. Bacteria present a more sophisticated level of barrier to antimicrobial agents, a barrier which is also ever evolving. The effectiveness of the bacterial envelop to function as a barrier differs depending on which two of the broad class of bacteria it belongs to; gram-positive or gram negative. This is because of the difference in bacterial envelop between these two classes, some of which, along with mutual features are presented in Table 1.3 (41).

Table 1.3: Features of gram-positive and gram-negative bacterial envelop.

	Gram-positive	**Gram-negative**
Peptidoglycan	Thick	Thin
Outer membrane	Absent	Present
Periplasm	Absent	Present
Inner membrane	Present	Present

Although gram-positive bacteria have a thicker cell wall comprising of peptidoglycan, it does not present much resistance to diffusion of antimicrobial agents. The outer membrane of gram-negative bacteria on the other hand confers substantial resistance acting as an effective barrier. The diffusion of otherwise permeable hydrophobic molecules is greatly hindered by the outer membrane due its outer leaflet being composed of lipopolysaccharide (LPS) (42). There is a presence of asymmetry in the outer membrane, caused by LPS being exclusively present in the outer leaflet, whilst the inner leaflet is composed of the typical phospholipid (43). Along with this asymmetry, the saturated fatty acid chains of LPS drastically reduce the fluidity of the interior of the outer membrane, which in phospholipid bilayers is fluid (41). Ultimately, this reduction in fluidity is understood to be the cause of reduced permeation (44, 45).

1.2.1 Antimicrobial resistance

Along with the barrier, bacteria themselves are ever evolving. This evolution has given rise to antimicrobial resistance (AMR) to such extents that it has become a threat to global public health with the World Health Organisation (WHO) referring to it as a crisis (46). Fearing a post-antimicrobial era, where even common infections may prove fatal, the World Health Assembly held on May 2015 implemented a global action plan outlining the following five objectives (46):

- “to improve awareness and understanding of AMR through effective communication, education and training;
- to strengthen the knowledge and evidence base through surveillance and research;
- to reduce the incidence of infection through effective sanitation, hygiene and infection prevention measures;
- to optimize the use of antimicrobial medicines in human and animal health;
- to develop the economic case for sustainable investment that takes account of the needs of all countries and to increase investment in new medicines, diagnostic tools, vaccines and other interventions (46).”

To add to this WHO has published a list of priority pathogens to focus research and development. After declaring Mycobacterium tuberculosis caused infection tuberculosis to be the number one killer, WHO provides a list of 12 pathogens grouped into critical, high and medium priority (47). This list is presented in the Table 1.4.

Table 1.4: List of priority pathogen proposed for research and development published by WHO (47).

Critical Priority	High Priority	Medium Priority
Acinetobacter baumannii	*Enterococcus faecium*	*Streptococcus pneumoniae*
Pseudomonas aeruginosa	*Helicobacter pylori*	*Haemophilus influenzae*
Enterobacteriaceae	*Salmonella species*	*Shigella species*
	Staphylococcus aureus	
	Campylobacter species	
	Neisseria gonorrhoeae	

1.2.2 Origin of antimicrobial resistance

The role of human use of antibiotics as a cause of AMR is well established and links between antibiotic consumption and AMR shows strong correlation (3). However, it seems that all AMR does not have to be anthropogenic in origin. Bacteria strains resistant to as many as 14 distinct antibiotics have been discovered in caves isolated from apparent human influence for 4 million years (48). Thus, AMR is an ancient, naturally occurring by-product of bacteria fighting to survive in various environments and communities. To add to this, resistance is not always acquired. Bacteria also exhibit intrinsic resistance, which is resistance conferred by genes which are already present in the genome of a species or genus (49). Acquired resistance on the other hand occurs in the presence of selection pressure, most likely due to exposure to antibiotics. These antibiotics also include naturally secreted substances by neighbouring

species. Nevertheless, the selection pressure can confer resistance by two different mechanisms; mutation of genes to a more resistance genotype and acquisition of resistance DNA through horizontal gene transfer (50).

1.2.2.1 How does mutation lead to resistance?

During natural cell division, mutations in genes are likely to occur. Since bacteria generally have a much higher rate of cell division compared to eukaryotic cells, this confers them high rates of mutation also. Ultimately mutations in genes can lead to a phenotype which can affect the activity of a particular drug (50). In the presence of such a drug all susceptible bacterial cells would be wiped out, leaving only those with the mutation to survive. Finding no competition and no drug to kill them, these resistant cells continue to divide and ultimately become the dominant phenotype, giving rise to resistance. This shows that use of antimicrobial agents selects for the resistant phenotypes, since without it the natural phenotype would predominate and the mutated cells would eventually die out. Misuse of course would only speed up this process; bringing to light why WHO in their global action plan hope to optimise antibiotic use (46). The exact mechanism of resistance will be covered under the section ‘conventional resistance mechanism’.

1.2.3 Extent of the crisis of antimicrobial resistance

Table 1.5 presents some of the common antimicrobial agents along with their mechanism of action, classification, aqueous solubility, type of bacteria it is effective against, known mechanisms of resistance, whether it is effluxed or not and also the route of administration. It also serves as a reminder that resistance has been established for all common antibiotics.

To add to this, AMR is not restricted to particular locations. Instead it is a global threat. The WHO first published a report on the global surveillance of AMR in 2014, stating that AMR resistance has reached “alarming levels” in many parts of the world (51). Realising global AMR surveillance to be the key in deploying global strategies, in 2015 the WHO initiated the Global Antimicrobial Resistance Surveillance System (GLASS) (51).

Despite this, most of the pharmaceutical companies have stopped research into new antimicrobial agents (46). This in combination with increasing rise in clinical resistance to antibiotics highlights why the 5th objective of the global action plan was necessary and reiterates the need for research into novel strategies in combating AMR globally.

Table 1.5: List of common antimicrobial agents including their mechanism of action, classification, aqueous solubility (E: experimental, P: predicted), type of bacteria it is effective against, mechanisms of resistance, whether it is effluxed or not and also the route of administration (3, 52-54).

MoA	*Classification*	*Antibiotic*	*Solubility in water*	*Type of bacteria it is effective against*	*Mechanism of Resistance*	*Effluxed?*	*Administration*
Interference with cell wall Synthesis	Beta Lactams	Penicillins	Penicillin G	E = 210 mg/l P = 0.285 mg/ml	Gram +ve and some Gram –ve cocci	Hydrolysis, Efflux, Altered Target	Possible	Parenteral
			Ampicillin	P = 0.605 mg/ml	Above and more Gram -ve	Hydrolysis, Efflux, Altered Target	Possible	Oral
			Methicillin	P = 0.31 mg/ml	Above and penicillinase producing Staph. Aureus.	Hydrolysis, Efflux, Altered Target	Possible	Parenteral - inactivated by gastric acid
			Ticarcillin	P = 0.0716 mg/ml	Above + Pseudomonas aeruginosa	Hydrolysis, Efflux, Altered Target	Possible	IV
		Cephalosporins	Cephalexin	E = 1789 mg/L P = 0.297 mg/ml	Gram +ve and Gram -ve	Hydrolysis, Efflux, Altered Target	Yes	Oral
		Other	Glycopeptides	Vancomycin	P = 0.225 mg/ml	MRSA	Target modification / removal of susceptible target	No	Parenteral
Protein Synthesis Inhibition	Anti-30S ribosomal subunit	Aminoglycosides	Gentamicin	P = 12.6 mg/ml	Aerobic Gram –ves Enterobacteriaceae Pseudomonas	Phosphorylation, Efflux, Altered target	Yes	Oral, Parenteral
		Tetracyclines	Tetracycline	E = 231 mg/L P = 1.33 mg/ml	Rickettsia, Mycoplasma, Spirochetes (Lyme's Disease)	Monooxygenation, Efflux, Altered target	Yes	Oral
	Anti-50S ribosomal subunit	Macrolides	Erythromycin	E = 2000 mg/L P = 0.459 mg/ml	Streptococcus, H. Influenzae, Mycoplasma pneumonia	Hydrolysis, Glycosylation, phosphorylation, Efflux, Altered target	Yes	Oral
		Phenicols	Chloramphenicol	E =2500 mg/L P = 0.461 mg/ml Lipid-soluble	H. Influenzae, Bacterial meningitis, Brain abscess	Acetylation, Efflux and Altered target	Yes	Oral, Parenteral
DNA synthesis Inhibitors	Inhibit DNA Gyrase	Fluoroquinolones	Ciprofloxacin	P = 1.35 mg/ml	Strep., Mycoplasma, Aerobic Gram +ves, Pseudomonas	Acetylation, Efflux and Altered Target	Yes	Oral

1.2.4 Conventional resistance mechanisms

Resistance in bacteria whether intrinsic or acquired through mutation, vertical gene transfer or horizontal gene transfer can be looked at mechanistically. Some of the more conventional mechanisms of antimicrobial resistance will be covered in this section, whilst the following section will explore resistance of bacteria within biofilms.

1.2.4.1 Enzymatic inhibition, deactivation or destruction of the antibiotic

Being one of the most common and successful forms of antimicrobial resistance mechanisms, enzymatic action on the antimicrobial agent refers to the process where the antibiotic is inactivated by modification or destruction through the aid of enzymes. These processes include hydrolysis, transference of functional groups as well as other chemical modifications. The end result is that the drug is unable to function as intended.

Aminoglycoside modifying enzymes (AMEs) are a prime example of enzymes which chemically modify the aminoglycoside antibiotics. Covalent modification of the hydroxyl or amino groups of the aminoglycoside antibiotics leads to such an alteration which renders the antibiotic inactive (50). Likewise, enzymes which destroy the antibiotic also exist. β-lactamases such as penicillinases are well known examples for this category and they pose major problems specially in gram-negative bacteria (50, 55). Breakdown of the amide bond by these enzymes leads to destruction of the β-lactam ring in antibiotics possessing these rings (50).

1.2.4.2 Decreased drug influx or increased efflux

Since majority of antimicrobials have targets within the cell or on the inner membrane, to illicit the desired effect, the drug must be able to penetrate through at least one or in some cases through both of the membranes (50). This presents bacteria for another opportunistic route to develop resistance. A decrease in intracellular levels of the active compound can be either due to a decrease in its uptake or an increase the rate at which it is pumped back out. Efflux will be covered later in its own section. Since one of the mechanism of drug penetration into the cell is via porins, a reduction in their expression can lead to reduced uptake as is the case with β-lactams and fluoroquinolones (54). Being hydrophilic, these antibiotic generally prefer to use the water-filled porins to migrate into cells (50).

1.2.4.3 Interference with the target site

Another common mechanism of resistance bacteria utilise is preventing the interaction between the drug and its target. They do this in two primary ways; target protection and target modification. Examples of target protection are the TetO and TetM proteins which dislodge tetracycline from its binding site on the ribosome (50).

Target modification can be due to mutation of the target site, target site alteration via enzymes or complete replacement or bypass of the target. Some bacteria are also able to become resistant by overproducing the target of the antibiotic, requiring no modification of the target site (50). Mutation of the genes coding for a specific target site greatly reduces the affinity of the antibiotic. Rifampin is an antibiotic effected by this mechanism of resistance. Mutation in the genes coding for RNA polymerase reduce the affinity of Rifampin for the enzyme, the binding of which would otherwise interrupt transcription (50). Thus mutation leading to binding site alteration allows transcription and hence protein production and normal cell physiology to continue, leading to resistance.

Enzymatic modification of the target site leads to resistance in a similar manner. A good example which represents this mechanism is the enzyme coded by the erm (erythromycin ribosomal methylation) genes (50). Macrolides are a class of antibiotics which prevent protein synthesis by binding to the 50s subunit of the ribosome (56). The enzyme causes mono- or demethylation of a residue of the 50s ribosomal subunit. This modifies the target site preventing binding of macrolide antibiotics to its target, and resistance ensues (50).

The final mechanism which can be grouped under target modification is complete replacement of the target. It refers to the ability of bacteria to no longer require a component which is a target of an antibiotic. This is achieved by the production of new components which serve the same function as the original component (50). Meaning that antibiotic inactivation of the original component is unable to hinder normal functioning of the bacteria. To demonstrate this, the example of penicillin binding proteins (PBPs) will be used. PBPs play a crucial role in the synthesis of peptidoglycan through transpeptidation and transglycosylation of peptidoglycan units. Peptidoglycan is a major component of bacterial cell wall and since β-lactam antibiotics function by binding to PBPs, this leads to incomplete and thus unstable cell wall, unable to sustain the life of the bacteria. Returning back to the mechanism of resistance, horizontal gene transfer resulted in *Staphylococcus aureus* (*S. aureus*) to acquire the gene *mecA*, a gene which codes for the production of PBP2a. Not only do β-lactams have low affinity for PBP2a,

the protein can also replace the function of PBPs (50). Thus although the antibiotic can still bind to PBPs, it is unable to stop peptidoglycan synthesis.

1.2.5 Biofilms

Biofilms utilise a unified behaviour of its microbes to facilitate their survival in an otherwise adverse environment. Biofilms are increasingly gaining attention because of their role in antimicrobial resistance (57). They are communities of sessile microorganisms (bacteria or fungi) living in a self-produced matrix (matrix of extracellular polymeric substances) which aids the survival of these microorganisms (58). Biofilms are not restricted to comprising of one species, instead they can contain communities of multiple species. Yet these communities within biofilms are highly organised and function cooperatively (59). Lawrence et al, showed through scanning confocal laser microscopy, the structure of biofilms to be micro-colonies separated by a network of open water channels (59, 60). This simple example demonstrates the level of interspecies and intercolonial signalling required to direct colonial growth in a structured way that it does not obstruct the water channels (59). Even though researchers have only begun to look into the interspecies communication that result in such highly functional and thriving multispecies communities; yet it is clear that a level of interspecies cooperation and tolerance is undoubtedly in play (59).

The formation of biofilm can be divided into stages. Firstly planktonic bacteria attach to a surface reversibly (58). At this stage the bacteria are still susceptible to antibiotics; hence prophylaxis in alloplastic surgery proves very useful as at this stage the bacteria are able to act on the planktonic forms which become reversibly attached (57). In the next stage, the bacteria become irreversibly attached through self-adhesion structures such as pili, multiplying and forming colonies. Furthermore, extracellular polymeric substances, which form the matrix, then become secreted and become deposited around the colonies (57). The matrix is very resourceful for the communities and consists of water, polysaccharides, proteins, lipids and DNA (57). Hydrogen bonding between water molecules and hydrophilic polysaccharides holds water within the biofilms whilst polymers such as glycopeptides, lipids and lipopolysaccharides aid in scaffolding and holding the biofilm together (57). As the biofilm grows thicker, it becomes mature; a process which is coordinated through quorum sensing and other signalling (57). Finally, the sessile bacteria in the biofilm are able to become free and spread to other surfaces to form new biofilms (57, 58).

These functional and structural adaptations which lead to the interrelationships present in biofilms are due to expression of genes which make the phenotypes of the bacteria within biofilms profoundly different from the planktonic forms of the same species (59). Biofilms are highly evolved systems, so much so that on estimate >99.9% of microbes are present as the biofilm form whilst planktonic phenotypes only account for <0.1% of the total microbial biomass (59). This demonstrates the survival advantage that bacteria in biofilms have compared to planktonic forms and hints at their clinical significance. Bacteria within biofilms can exhibit resistance to antibiotics, disinfectant chemicals and many components of the immune system (57). Furthermore biofilms can grow in many environments and on both biotic and abiotic surfaces (57). The survival advantage due to the adaptations ultimately enables biofilms to exhibit harmful clinical manifestations.

Resistance to antibiotics can be up to 1000 times higher for bacteria in biofilms and the underlying mechanisms of resistance are likely to be a combination of conventional resistance mechanisms found in planktonic phenotypes as well as those specific to biofilm phenotypes (58). Such specific mechanisms include retardation of antibiotic diffusion by the biofilm matrix as well as slowed growth of bacteria due to decreased metabolic rate in biofilms (57). The latter leads to resistance because most antibiotics have their effect on rapidly dividing cells (58).

Another theory which may bring light to the resistance observed within biofilms is that of persisters (61). These are a small population of bacterial cells which are able to survive despite aggressive antibiotic exposure (61). Whereas small populations of planktonic forms, which may remain after antibiotic therapy, would be eliminated by the immune system, in biofilms these would survive and lead to the restoration of the biofilm post-antibiotic therapy (62). It is proposed that these persisters are able to survive within biofilms due to damaged apoptotic mechanisms (63). Although other mechanisms mentioned above specific for biofilm resistance are likely to also be involved.

Biofilms forming bacteria are commonly associated with chronic infections, which are infections that persist despite antibiotic therapy and the body's immune response (57). The sessile communities in biofilms can give rise to planktonic forms, which in turn give rise to the disease state (58). Since the bacteria in biofilms are highly evolved in survival, biofilms act as a base which poses constant threat to the body through continuous release of virulence factors and planktonic forms (57). Hence a chronic state of infection is maintained due to the inability of the immune system or drugs to eradicate the biofilm.

Their ability to grown on abiotic surfaces can result in complications with implants as well as catheters. A good example which highlights the danger associated with biofilms is a biliary stent in which the growth of *Escherichia coli* (*E.coli*) biofilm led to repeated incidents of sepsis. Antibiotic therapy was of no avail and the second episode of sepsis proved fatal. DNA typing revealed that the same *E.coli* clonal type was present in the biofilm as the one responsible for sepsis (57).

There is an urgent need therefore for strategies which can successfully and safely prevent as well as those which can treat a biofilm infection. The strategies studied can be divided into four major categories; prevention of biofilm formation, weakening of the biofilm, disruption or dispersal of the biofilm and killing of bacteria specially the subpopulation which persists (58).

One strategy utilises D-amino acids to inhibit and disperse biofilms. Their role was seen after factors D-leucine, D-methionine, D-tryptophan and D-tyrosine, isolated prior to disassembly of Bacillus subtilis were found to prevent biofilm formation as well as cause its dispersal. It was found that D-amino acids caused cells in the biofilm to release amyloid fibres which were involved in linking cells in the biofilm together. YqxM was found to be the protein required in the formation and anchoring of the Tas A amyloid fibres to the cells (64). Strains with mutations in this protein were able to form biofilms in the presence of D-amino acids (65).

Since this understanding, D-amino acids have also proved to be effective as strategies for the prevention and dispersal of biofilms in other bacteria (66). It has been observed that using L-amino acids has no effect (65). They have also been studied and proved effective in combination with antimicrobials in a bid to overcome the antimicrobial resistance of biofilms.

1.2.6 Combinatorial therapy

One of the strategies used by clinicians with the aim of overcoming AMR is the use of antibiotic combinations (67). Though this was effective, and also holds the benefit of decreasing the chance of AMR occurrence, resistance can still occur (67). An issue related to using multiple antibiotics in combination is that bacteria can emerge with resistance to multiple drugs instead of just one. Dependent on extent, this can give rise to what is known as multidrug resistance, extensive drug resistance and pan drug resistance (68).

Another way to enhance the efficacy of antibiotics prone to resistance is the use of adjuvants. Antibiotic adjuvants are substances that can enhance the activity of a drug, most likely by

interfering with the resistance mechanisms. Generally, they show no antibiotic activity on their own (67). One example of antibiotic adjuvants which are in use and in clinical development are β-lactamase inhibitors (69, 70). Bacteria can develop resistance to the class of β-lactam antibiotics by producing enzymes (β-lactamases) which are able to hydrolyse the antibiotic rendering it ineffective (70). Knowing this however, opens the opportunity to develop compounds which can inhibit the enzymes. Thus, β-lactamase inhibitors structurally mimic the β-lactam and work by irreversibly or reversibly binding on or near the active site of the enzyme, thus rendering the enzyme ineffective, and overcoming resistance to β-lactam antibiotics (70). However, given the nature of resistance, it is probably not long before enzymes that are resistant to these inhibitors are produced by bacteria, leaving room for research into adjuvants which are resistant to inducing resistance. Such has been the case with Sulbactam (71).

1.3 Ion Pairs

Ion pairs are neutral species formed in a solution through the columbic (electrostatic) attraction between oppositely charged ions. They are often sufficiently lipophilic, enabling them to dissolve in non-aqueous solvents (72). Since ion-pair formation can be used to enhance solubility and permeability of drugs, they are looked at in some depth here.

1.3.1 Ion pair formation

In a solution, the charge of a free ion polarises the surrounding solvent molecules. This leads to a solvent-ion interaction between the newly polarised solvent molecules and the ion. Once this interaction is strong enough, the ion is said to exhibit a tight solvation shell (72, 73).

Once a counterion approaches an ion possessing a solvation shell, one of the two outcomes are possible. First possibility is that the solvation shell is maintained and the association is that of a loose ion pair. These can be of two types depending on whether the primary solvation shells of both ions are maintained (solvent separated ion pair) (Figure 1.3A) or both ions share one solvation shell (solvent shared) (Figure 1.3B) (74). In the second case, the solvent molecules (of the solvation shell) separating the two ions are pushed aside, leading to a stronger interaction and the formation of a tight (contact) (Figure 1.3C) ion pair (73, 74).

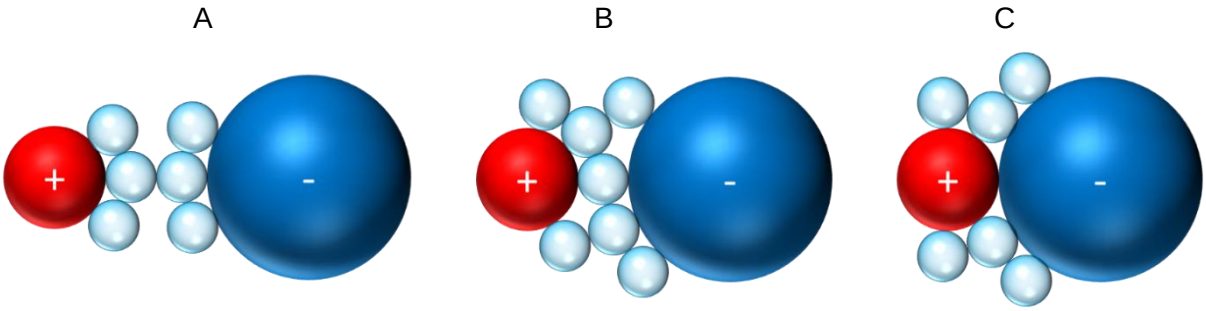

Figure 1.3: Types of ion pairs. A) Solvent separated ion pair. B) Solvent shared ion pair. C) Contact ion pair.

Therefore one of the requirements for the formation of a loose ion pair is the availability of solvent molecules with which the free ions can form a solvation shell. If such medium is not present, only tight ion pairs will form (72-74).

The two ions must breach a critical separation distance (D) in order to form and be classified as an ion pair. This distance is dependent upon the cationic charge (Z+), anionic charge (Z-),

electron charge (e), dielectric constant (ε) and absolute temperature (T) (72, 73). The relationship of these values to the critical separation distance can be seen through the Bjerrum's equation (where k is the Boltzmann's constant):

$$D = z^{+}z^{-}\frac{e^{2}}{2\varepsilon kT}$$

The dielectric constant is therefore an important parameter in ion pair formation. According to the above equation, ion pairs would form more readily in solvents with a lower dielectric constant, corresponding greater critical separation distance in such medium (72, 73).

1.3.2 Ion pair solubility

The solubility of an ion pair is dependent upon the charge accessibility on the ion pair by the solvent molecules. Utilising this concept, Higuchi proposed the solvation of ion pairs through three (Figure 1.4) distinct cases (74). Case one (Figure 1.4A) represents an ion pair with a large cation (mainly lipophilic except the positively charged centre) and a small anion. Due to their size, the anion carries a relatively high charge per unit area compared to the cation. Therefore, this ion pair would be solvated by lipophilic molecules carrying exposed positively charged surfaces (alcohols and dipolar molecules with acidic protons e.g. phenol). Being next to the anion, these positive charges would be 'buried', portraying this system as relatively nonpolar (74).

Complete opposite was proposed for the second case (Figure 1.4B) of ion pairs; the ion pair would be solvated by lipophilic molecules with exposed negatively charged surfaces, surrounding the cation (74). Third case (Figure 1.4C) represents an ion pair with no exposed polar surfaces due to deeply buried charges, and hence cannot undergo solvation in polar media. This ion pair can be extracted by non-polar solvents (74).

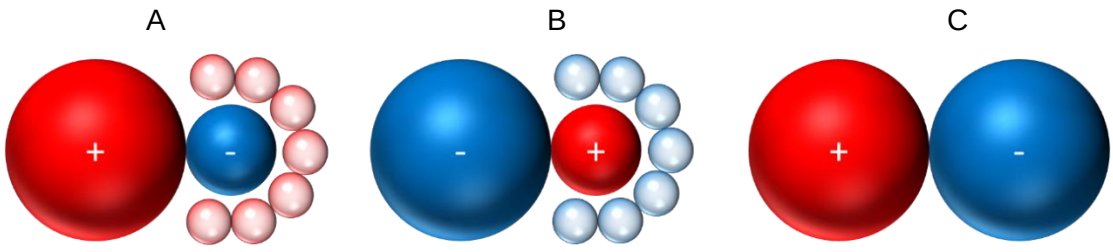

Figure 1.4: Three cases of ion pair solvation. A) Large cation and a small anion. B) Large anon and a small cation. C) Both cation and anion are large.

1.3.3 Ion pair aqueous solubility

Despite water having a high dielectric constant (ε = 78.5) Diamond used the term "Water structure enforced" to explain the formation of ion pairs in such medium (75). Ion pairs in water can form if both the cation and the anion are large and hydrophobic. In such a case the ions are forced together due to the hydrophobic interactions between ions and the hydrogen-bonded water structure. Ion pair formation in water is therefore due to solvent mediated effect as well as electrostatic attraction, with relative contribution of either depending upon the properties of the ions and solvents in question. Given that this electrostatic interaction is likely to be comparatively weaker, and that ion pairing is limited to low concentrations (due to low solubility), the usefulness of ion pairing in aqueous solutions is questionable (73, 75). Yet as evident of ion-pairing in aqueous solutions and its role in transport across membranes, ion pairing in water does occur. As will become apparent later, ion pairs forming in water are probably solvent-separated. This would be ideal as after permeation, the formulation scientist generally hopes for ion pair dissociation, enabling the active substance to carry out its intended function.

1.3.4 Formation of tight or loose ion pairs

Grunwald has described that as two ions approach each other, the potential energy slowly decreases (76). This occurs until the solvation shells come in contact, or one of the ions comes into contact with the others solvation shell (76). Considerable energy would be required to overcome this barrier, if a tight ion pair was to form. Considering Coulomb's law, the electrical force between the two ions would increase as their separation decreases. Therefore, if at this point the attraction is strong enough, the interionic distance would slowly decrease and potential energy rapidly increase, until in line with Coulomb's law the attraction becomes strong enough, to overcome the energy required in penetrating the solvation shell (76).

Increase in the solvents dielectric constant and ion-solvating power favours solvent-shared and solvent-separated ion pair (72, 73, 76, 77). It is therefore deducible that a solvent with a lower dielectric constant and a lower solvating power would favour the formation of contact ion pairs.

Furthermore, Naseer Ahmad and Day found that the higher the donicity (effectiveness as electron pair donors) of a solvent, the greater their ability to transform contact ion pairs into

solvent-separated ion pairs. This transformation was not observed in solvents with a lower donicity such as diethyl ether (78).

1.3.5 Amino acids as ion pairs

ElShaer et al, has been investigating both anionic (glutamate, aspartate) and cationic (arginine, lysine and histidine) amino acids as counterions for various model drugs. It has been found that both solubility and permeability of model drugs can be increased utilising this concept (40, 79).

1.3.6 Molar conductivity

Decrease in molar conductivity is a useful method for the detection of ion pair formation since ion pairs do not contribute to both ionic strength and electrical conductivity (80).

Ohm's law:

$$E = iR$$

Where *E* represents the applied potential, i is the measured current and the resistance between the two electrodes is denoted *R* (81).

While resistance quantifies the difficulty by which an electric current passes through a conductor, conductance (Symbol: *S*, Units: siemens – *S*) is the opposite and measures the ease by which the current passes and can be expressed as the reciprocal of R (81):

$$S = \frac{1}{R}$$

Conductivity is a quantity expressed by the symbol κ (S cm^{-1}). The ratio (*d/A*) of the distance between the two electrodes (*d*) and the surface area (*A*) of each electrode is a constant for a particular measurement cell and is called the cell constant (θ) (81). Conductivity can be given as:

$$\kappa = S\theta$$

For comparison between two samples, conductivity can be converted into molar conductivity. Molar conductivity Λ (S cm^2 mol^{-1}) is given by the following equation where *C* (mol/cm^3) the total ionic concentration (81):

$$\Lambda = \frac{\kappa}{C}$$

The following equation can also be used for simplicity (less unit conversion is needed and the molar *C* can be used) (81):

$$\Lambda = \frac{\kappa \times 1000}{C}$$

1.3.7 Enhancing permeation through ion pair formation

The concept of enhancing the permeation of ionised drugs, through the use of counterions, rests in the 'burial' of charges that occurs with the formation of an ion pair. In other words the formation of ion pairs transforms the hydrophilic drugs into more lipophilic complexes, thus enhancing their transport through hydrophobic membranes. This was first tested by Irwin et al, and found support in many later studies (73, 82).

However, some studies indicated that ion pair formation may not always be the cause of enhanced drug absorption and instead other mechanisms relating to the counterion may be involved. Thus to exclude the direct effect of counterions, neutral molecules (which cannot form ion pairs) such as caffeine can be used in permeation enhancement studies (73).

1.4 Efflux Pumps

1.4.1 Background

Transporters are not only restricted to transporting substances into a cell. Often they are involved in transporting substances, including drugs, out of cells. These transporters are generally termed efflux pumps. This evolutionary trait which functions to keep the body safe from harmful substances, has also become one of the major challenges in the field of health today. Efflux pumps in humans and efflux pumps in microorganisms are big contributors to the resistance to chemotherapy and antimicrobials respectively (83). This section will cover one well studied and clinically relevant efflux pump in humans and one in bacteria.

Three main criteria can be used for the classification of transporters; the energy source, phylogenic relationship, substrate specificity (84). There are two main classes of active transporters. Primary active transporters account for majority of drug efflux pumps in eukaryotic cells and utilise various forms of energy for their function. The energy source classically utilised is ATP. Secondary active transporters on the other hand are predominant in bacteria and function by acting as symports and antiports (84). Within these two classes three subclasses have been formed; superfamilies, families and clusters. These subclasses are divided in accordance with their substrate specificity (84). Even then, amazingly, most drug efflux pumps exhibit a multi-drug resistance phenotype.

1.4.2 Substrate specificity

Interestingly minimal common structural properties are necessary to obtain detectable efflux (Table 1.6). It is a commonly agreed hypothesis that most transporters recognize molecules with a polar, often slightly charged head associated with a hydrophobic domain (84).

Table 1.6 Superfamilies and their substrate specificities. Efflux pumps demonstrate a broad substrate specificity (84).

SMR (small multidrug resistance family)	RND (resistance-nodulation-division superfamily)	MFS (major facilitator superfamily)	ABC (ATP-binding cassette superfamily)	
			MDR1 (P-glycoprotein)	MRP1
Lipophilic, multicationic substrates	Amphiphilic, charged substrates	Amphipilic, mono- or dicationic substrates	Amphiphilic, neutral or cationic substrates.	Organic, anionic substrates (sometimes, hydrophobic, neutral or mildly cationic substrates)

Since majority of drug efflux pumps have a broad substrate specificity, this enables them to deal with many drugs of potentially unrelated pharmacological classes (84). Furthermore, efflux pumps are not restricted to bacteria; they have been recognised in almost all cell types (84). One of the way efflux pump activity can be bypassed, and which may be relevant is by increasing intracellular antibiotic concentration by enhancing permeability. A novel way of bypassing efflux pumps is being explored in this study through the utilisation of amino acid counterions.

1.4.2.1 Basis of substrate specificity

Proton motive force (PMF) dependent efflux proteins of the SMR, MFS and RND superfamilies tend to possess broad substrate specificity. However the molecular basis underlying their specificity is not yet clear. Currently studies indicate that instead of substrate structure, physical properties such as charge, hydrophobicity or amphipathicity may be the key determinants for the recognition of substrates by these proteins (84).

For the MFS transporters VMAT1 and VMAT2 the common substrate characteristics were the presence of a cationic moiety and an aromatic ring. Interestingly, the introduction of a negative charge to some VMAT substrates impressively decreased their affinities for the transporter binding site (84).

1.4.3 Efflux pumps in bacteria

Evolution is a fascinating phenomenon, one which has enabled the humans to flourish into the most advanced species witnessed today. Yet, evolution in the smallest of scales continues to

present us with some of the greatest challenges in combating infectious diseases. Microbes such as bacteria, utilise evolution to survive in otherwise lethal environments, resulting in devastating consequences in an infected individual. One of the key mechanisms is the active removal of antibiotics through the overexpression of efflux pumps. This results in sub-lethal concentrations of the antibiotic within the organism, which in turn can lead to emergence of antibiotic resistance. Although efflux pumps are nothing new, increasing insight into their structure and function make them attractive targets for restoring antibiotic susceptibility to resistant strains (84). However given the nature of evolution, it may be fair to say that resistance will find a way to persist.

Drug efflux pumps present in bacteria are categorised into five superfamilies: ABC (ATP-binding cassette superfamily), MFS (major facilitator superfamily), MATE (multidrug and toxic compound extrusion family), SMR (small multidrug resistance family) and RND (resistance-nodulation-division superfamily) (84). Efflux pumps in Gram-positive bacteria belong to the MFS, SMR, ABC and MATE families whilst the RND family exporters play a key role in clinically relevant Gram-negative antibiotic resistance (84). For now this section will look at some detail into RND transporters.

1.4.4 RND Transporters

RND efflux pumps are found throughout Prokaryotes and Eukaryotes. These are widespread in Gram-negative bacteria, but are not the only family of efflux pumps found in these bacteria (85). They function as proton/drug antiporters, catalysing the efflux of a wide variety of substrates including antibiotics and chemotherapeutic agents. Extensive studies have been done with most typical RND pump complexes: AcrAB-TolC of *E-coli* and MexAB-OprM of *Pseudomonas aeruginosa* (*P. aeruginosa*) (86).

1.4.4.1 Structure and Function

In Gram-negative bacteria the RND efflux pump complex (Figure 1.5) spans the inner and outer membrane. The RND efflux pump AcrB is situated within the inner membrane and functions in complex with two other proteins: AcrA and TolC (87). AcrA is a periplasmic adaptor protein and TolC is an outer membrane channel. These together form a tri-partite efflux pump (87). AcrB functions as a PMF dependent transporter, catalysing drug/H+ antiport (87). AcrB is also responsible for drug selectivity. AcrA on the other hand connect the other two proteins together (86, 87).

AcrB is associated with the drug efflux pathway from the periplasm/outer leaflet (inner-membrane) through the periplasmic domain of AcrB. MexB on the other-hand may have the ability to remove antibiotics from the cytoplasm/inner leaflet (inner-membrane) (86, 87).

Figure 1.5: Structure and function of the RND efflux pump (86).

Key residues (Asp407, Asp 408, Lys940 and Thr978) in the transmembrane domains of AcrB have been identified which likely function as the proton relay network (86).

Mutations around the residues Phe178 and Phe615 in the periplasmic domain of AcrB can lead to no change, or an increase or a decrease in resistance to various substances (86). This hints to the involvement of the periplasmic domain in substrate recognition (86, 87). Studies on the AcrD exporter showed that substrates could be captured from the cytoplasm as well as the periplasm, suggesting the presence of binding sites on both regions of the protein (86).

The AcrB is a homotrimer consisting of three organized protomers. The pump action is now understood to utilise a three-step functionally rotating mechanism (86). The protomers are however asymmetrical, with their conformation depending upon what state of the transport cycle they are in (86). These functional states are access (loose), binding (tight) and extrusion (open). It is suggested that the extrusion of a substrate bound at the periplasm is triggered by the protonation of one of the residues of the proton relay network (86, 87).

1.4.5 Efflux pumps in humans

Development of multi drug resistance is not only an issue in infectious diseases but also in oral bioavailability in general as well as in cancers (83). The physicochemical properties which allow for active transport of substances also render those substances more susceptible to recognition by efflux pumps (88). If a drug is being effluxed back out of GI tract endothelial cells, it will lead to poor bioavailability, whereas if the drug is effluxed out of a cancer cell it would lead to refractory disease.

One of the most implicated and well-studied efflux pump superfamily is the ABC superfamily (83). They are present in cellular and intracellular membranes and show a wide tissue distribution. They transport substances against the concentration gradient and therefore are energy dependent; energy is obtained from the hydrolysis of ATP. The genes coding for ABC superfamily are further subdivided into seven families from ABCAA to ABCG (89). Three of these families, ABCB, ABCC and ABCG, are the most important because they code for the proteins P-glycoprotein, multidrug resistance proteins (MRP) and ABCG2 (also known as breast cancer resistance protein) respectively. The following section will look at some detail at the efflux pump P-glycoprotein (83, 88, 89).

1.4.5.1 P-glycoprotein

P-glycoprotein has a wide tissue distribution and as well as being present in cancer cells is also found in normal tissues such as the blood-brain barrier, intestine, kidneys, liver along with others (89). P-glycoprotein (P-gp) is coded by the ABCB1 gene and is sometimes also referred to as PGY1 or multidrug resistance protein-1 (MDR1) (89). This is because the transporter has broad substrate specificity, recognising amphiphilic, neutral or positively charged drugs; that is it recognises and is involved in the efflux of multiple drugs of unrelated chemical structure and function. P-gp shares this broad substrate specificity with cytochrome P450 3A4 (88). Considering the wide tissue distribution, the broad substrate specificity and the function of P-gp and cytochrome P450, it is hypothesised that both work in a united fashion to protect the host from harmful and xenobiotic substances. Drugs that associate with P-gp can act as substrates or inhibitors, or as is the case with cyclosporine, both as a substrate and as an inhibitor (88, 89).

P-glycoprotein has been implicated in both limiting oral drug absorption and resistance to chemotherapy (88). Studies with human Caco-2 cells show that drug absorption is increased

upon inhibition of the pumps function via verapamil (88). It has also been observed that the expression of P-gp increases in cancer cells after chemotherapy and its expression has been linked to a worse response to treatment (88, 89).

1.5 Amino Acids

Proteins are composed of up to twenty amino acids, varying in size, shape, charge and chemical reactivity (90). There are two naturally occurring acidic (aspartic acid and glutamic acid) amino acids and three naturally occurring basic (arginine, lysine and histidine) amino acids (90, 91). The general chemical structure of these amino acids is the same; they only differ in their side chain (R group). The consistent part of the amino acid structure which is the same in all of these amino acids, is known as the backbone and is composed of an alpha carbon, an amino group (NH_2), a carboxyl group (COOH). All three of the groups, the amino group, the carboxyl group and the R-group are attached to the central alpha carbon (92).

All amino acids apart from glycine can occur in two isomeric forms; the L-isomer or the D-isomer. This is due to the presence of a carbon atom with four different groups attached (chiral centre), allowing the formation of two different non-superimposable structures differing only in the spatial orientation of their groups in three-dimensional space (90, 91).

Since amino acids possess both a basic (amino group) and an acidic (carboxyl group) group, they can exist as zwitterions. A zwitterion can be defined as a species carrying both a negative and a positive charge. Presence of both acidic and basic centres allows amino acids to remain ionised at any given pH, as a cation, anion or a zwitterion. This makes amino acids ideal candidates as counterions for the model drugs which will be studied. Even though zwitterions carry zero net charge, a truly neutral species does not exist (90, 91, 93).

Table 1.7: Acidic and Basic amino acids with their pK_a and isoelectric points (*pI*) (91).

Amino Acid	α-carboxylic acid pK_a	α-amino pK_a	Side chain pK_a	p*I*
Aspartic Acid	1.88	9.60	3.65	2.77
Glutamic Acid	2.19	9.67	4.25	3.22
Arginine	2.17	9.04	12.48	10.76
Lysine	2.18	8.95	10.53	9.74
Histidine	1.80	9.33	6.04	7.69

1.6 Aims and Objectives

It is clear that once discovered, getting the drug to its sight of action is a challenge. Challenges range from generally the solubility and permeability of the drug to, more specifically, resistance of the drug where possible. The overarching aim of this project was to study the physiochemical and physiological, both in mammalian cells and in bacteria, effects of using naturally occurring acidic and basic amino acids as counterions for various model drugs. The underlying hypothesis being that amino acids can enhance drug solubility, and therefore indirectly lead to enhanced drug permeability and decreased drug resistance. Formulation of the hypothesis also considered that amino acids can directly enhance permeability and decrease drug resistance through potential mechanisms including, but not restricted to ion pairing and utilisation of amino acid transport channels.

Thus the overall objective of the project was to determine the use of amino acids as solubility and permeability enhancers and as anti-resistance agents. Considering that permeation into the body was not enough, since the inevitable resistance would render this effort useless, both a permeability (Caco-2 cell line) and resistance model (bacteria) was used. Tetracycline (TC), ciprofloxacin and digoxin were chosen as model drugs along with acidic and basic amino acids as counterions.

The following were the objectives of this project:

- To investigate the solubility and octanol-water partitioning of tetracycline in the presence of amino acids
- To investigate the effect of using amino acids as counterions to tetracycline, on the accumulation of the drug in planktonic *S. aureus* and *P. aeruginosa* cells and determine whether this translates to an effect in growth of the bacteria, whilst elucidating any synergy between the drug and the amino acids
- To investigate the effect of using amino acids as counterions to ciprofloxacin, on the accumulation of the drug in planktonic *S. aureus* and *P. aeruginosa* cells and determine whether this translates to an effect in the growth of bacteria, whilst elucidating any synergy between the drug and the amino acids
- To investigate the effect of using D-isomers of acidic amino acids on biofilm inhibition and dispersal whilst delving to their effect on biofilm architecture and determining synergy between the amino acids and ciprofloxacin
- To investigate the solubility, caco-2 monolayer permeability and efflux ratio of digoxin in the presence of amino acids

Chapter 2: Tetracycline: Evaluation of the impact of acidic and basic amino acids on solubility, octanol-water partitioning and bacterial efflux

The work presented in this chapter comprises of two subchapters. The first subchapter investigates the role of charged amino acids on solubility and octanol water partitioning of tetracycline. The second subchapter evaluates the impact of optimised counterions on bacterial efflux of tetracycline.

2.1 Investigating the effect of acidic and basic amino acids as counterions on the solubility and octanol-water portioning of the zwitterionic drug, tetracycline

2.1.1 Introduction

Tetracyclines are a class of bacteriostatic antibiotics which inhibit protein synthesis by binding to the 30s ribosomal subunit (94). Tetracycline (TC) is one of the oldest antibiotic of this class, and was first introduced into clinical practice in the 1950s (95). In 1966 tetracycline was the second most dispensed antibiotic after penicillin with prescriptions reaching an estimated 12.6 million (96).

Tetracycline is prescribed as a tetracycline hydrochloride salt, with percentage absorption ranging from 77-88%. It is usually administered as an oral formulation although intravenous formulations are also available (95). Being administered in doses of 250 or 500mg, TC serum peak concentrations vary between 2 and 5mg/L with the dose. Time to peak concentration (*t*max) of 2-4h indicates that serum concentrations of TC rise slowly (95).

Being amphoteric TC is able to act as an acid and a base. Three pKa values (3.3, 7.7 and 9.7) are revealed upon titration (Figure 2.1), while a fourth pKa value of 12 is also possible (97, 98). TC has an isoelectric point of around pH 5 (97). In accordance with the USP and BP solubility criteria TC is only ‘very slightly soluble’ in water, with 1 part TC requiring 2500 part water to dissolve (99). At 25°C TC has a solubility of 231 mg/L in water whereas in methanol it has a solubility of 20 mg/ml at 28°C (100). This is why it is generally prescribed as the salt tetracycline hydrochloride, which is freely soluble in water (101).

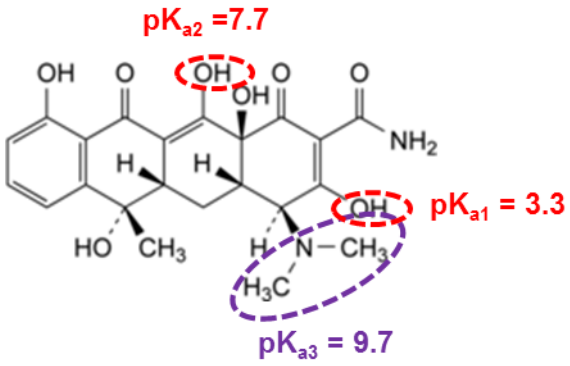

Figure 2.1: Chemical structure of TC with its functional groups highlighted which give rise to pKa values of 3.3, 7.7 and 9.7. Image adapted from British Pharmacopeia (102).

The stability of tetracycline (TC) has been studied in detail in aqueous solutions while its stability in methanol has also been examined. The best understood scheme of TC instability is epimerisation followed by dehydration (103, 104). Both have been described as degradation by many papers and their products as degradation products. Although many degradation products of TC have been suggested, three are well recognised (103). These are 4-epitetracycline (ETC), anhydrotetracycline (ATC) and 4-epianhydrotetracycline (EATC) (105).

Most likely drugs to undergo epimerisation are of the TC family (106). Epimerisation occurs most rapidly in solution between pH 2 and 6 (although also possible above pH 7.5) and results in the formation of its epimer ETC (107). The equilibrium is pH dependent and favours TC at higher pH values (104). Although ETC has a much lower antibiotic activity (5% of natural epimer), it is not known to be toxic (105, 107). Furthermore, this epimerisation is a reversible process meaning that ETC can turn back into the more potent epimer (107).

At lower pH values, a toxic degradation product is formed via two pathways (Figure 2.2). TC can undergo dehydration and form ATC which can in turn undergo epimerisation to become EATC. Along with this, ETC can also dehydrate to form EATC (97, 105). EATC is toxic to kidneys and is associated with Fanconi-like syndrome which may be fatal in extreme circumstances (97). Therefore a limit has been placed on the permitted quantity of these degradation products in the pharmaceutical dosage forms (tablets and capsules) containing tetracycline hydrochloride (the prescribed form) by British Pharmacopoeia (BP) (102).

Figure 2.2: Epimerisation of TC and its instability in acidic pH. Image taken from Foye's principles of medicinal chemistry (97).

The table below (Table 2.1) highlights the limit established by British Pharmacopoeia for these degradation products (102). The limit established for EATC by United States Pharmacopeia is 2.0% (108).

Table 2.1: Limit of impurities in TC by British Pharmacopeia (102).

Impurity	*Limit in TC hydrochloride (%)*	*Limit in TC (%)*
ETC	2.0	5.0
ATC	0.5	1.0
EATC	0.5	0.5

Stereoisomers are molecules that have the same molecular formula and bonding connectivity but differ only in the relative spatial orientations of their atoms and groups. Epimers are stereoisomers which are not mirror images of each other and convert from one epimer to another by the process of epimerisation. Epimerisation is the configurational inversion of one of the chiral centres in a molecule exhibiting more than one chiral centre. This process yields an epimer of the original molecule (109).

The C-4 dimethylamino functional group is the most studied moiety in TC since its stereo orientation is essential for antibacterial bioactivity (107). Epimerisation of TC is made possible due to the presence of the tricarbonyl system of ring A. This system allows enolization (enol formation) which involves the loss of C-4 hydrogen. Once reprotonation occurs either TC is reformed or ETC is formed (Figure 2.3), depending upon whether reprotonation occurred from the top (TC) of the enol or bottom (ETC) (97).

Figure 2.3: Diagram depicting that reprotonation of tetracycline can lead to epimerisation depending on whether the reprotonation was from the top or bottom of the enol. Image taken from Foye's principles of medicinal chemistry (97).

Adverse storage conditions such as light exposure, high temperature and humidity can increase TC degradation (110).

Various studies have shown ETC to be eluted first followed by TC and according to the British Pharmacopoeia the 1st, 2nd and 3rd peaks represent ETC, TC and EATC (in a sample containing these molecules) respectively (102, 103, 105).

The rational for choosing tetracycline base form was that it is a zwitterion and therefore able to potentially form ion pairs or at least become ionised by both acidic and basic amino acids. Furthermore working with tetracycline enables us to use bacteria as a model for investigating the impact of amino acids as counterions in studying drug efflux (Chapter 2.2).

Thus the aim of this study was to investigate the effect of acidic and basic amino acids on the solubility of TC and its partition behaviour from aqueous to an organic phase. For this, first a HPLC method able to precisely quantify TC was validated. Then TC saturated solubility was investigated at different concentrations of amino acids in aqueous medium. Finally, octanol-water partitioning studies were conducted to determine the effect of optimised amino acids on the partitioning of TC from water to octanol.

2.1.2 Materials and methods

2.1.2.1 Materials

Tetracycline ≥98.0% (NT), Oxalic Acid Dihydrate ≥99.0% (GC), L-Aspartic Acid 98%(T) and L-Glutamic Acid (N) were purchased from Sigma Aldrich, UK. HPLC grade Methanol and Aacetonitrile were both purchased from Fisher Scientific UK.

2.1.2.2 HPLC analysis

Calibration curve and sample quantification was carried out using a HPLC system; Dionex 1100 system consisting of an autosampler (AS50), gradient pump (GP50), UV detector (UVD 170U). Gemini 5µm C18 110Å 150 x 4.6 mm column was purchased from Phenomenex. The method was adapted from Castellari et al., (111). Mobile phase consisted of aqueous Oxalic acid dihydrate 0.01 M: Methanol: Acetonitrile (75:12.5:12.5 *v/v/v*). Analysis was carried out at ambient temperature with the flow rate of 1 ml/min and an injection volume of 60 µL. λmax for TC was determined using Genesys 10s UV-Vis Spectrophotometer to be 364 nm and the UV detector for HPLC analysis was set at 364 nm.

To obtain the calibration curve, single stock solutions were prepared by dissolving Tetracycline in methanol with a concentration of 1 mg/ml. This stock solution was used to make chromatographic standard solutions by diluting with appropriate volume of the mobile phase, as and when required.

2.1.2.3 Tetracycline solubility study

Saturated solubility of TC in different concentrations of amino acids were determined. Stock solution of amino acids (glutamic acid and aspartic acid) with a concentration of 1 mg/ml was prepared. Serial dilutions were prepared from this stock solution ranging from 1000 µg/ml down to 62.5 µg/ml in screw-capped tubes. Excess amounts of TC was added to each amino acid solution and pH recorded (Xisherbrand Hydrus 500 pH meter). The mixture was stirred at ambient temperature for up to 24 hours until excess TC had deposited. The pH was obtained again after which the tubes were left to rest for 2 hours. The supernatant was filtered through 0.45 µm syringe filter. The filtrate was diluted adequately with the mobile phase and the concentration determined through HPLC.

2.1.2.4 Preparation of Mutually saturated 1-octanol and distilled water

Shake flask method outlined in the Organisation of Economic Cooperation and Development (OECD) guidelines was used for the octanol-water partitioning experiment (112). Since water and octanol are not fully immiscible, mutually saturated solutions of octanol saturated with water and water saturated with octanol were prepared (113). Stock solution of octanol saturated with water was prepared by adding sufficient amount of water and stirring overnight with a magnetic stirrer. The solution was then left long enough for the octanol and water to separate. The water saturated octanol was then separated from water using a separating funnel. Stock solution of octanol saturated water was prepared in the same manner.

2.1.2.5 Octanol-water partitioning experiment

TC concentration of 100 µg/ml used based on the average of the controls for L-aspartic acid and L-glutamic acid solubility profiles. 100 ml stock solution of 200 µg/ml TC was made in octanol saturated distilled water. Stock solutions for L-aspartic acid and L-glutamic acid were made with the concentrations representing the molar ratio of TC to amino acid of 1:32, where the concentration of TC is 100 µg/ml. 2.5 ml of amino acid solution was mixed with 2.5 ml of 200 µg/ml TC solution to achieve a 5 ml solution with molar ratios of TC to amino acid of 1:16. At each stage of serial dilution from the stock solution of the amino acid, 2.5 ml of TC stock solution was mixed with 2.5 ml of amino acid solution to obtain the molar ratios of TC to amino acid of 1:16, 1:8. 1:4, 1:2 and 1:1. 5 ml of this TC with amino acid solution was mixed with 5 ml of water saturated octanol. The two phases were then stirred overnight with a magnetic stirrer, after which the two phases were left to rest for separation. A sample of the aqueous phase was obtained using a needle and syringe and used to determine the TC concentration using HPLC.

2.1.2.6 Calculation of percentage ionisation

The percentage ionisation of TC and the amino acids were calculated using equations derived from the Henderson-Hasselbalch equation below (97).

$$pK_a = pH + \log\frac{[acid\ form]}{[base\ form]}$$

Equation for percentage ionisation is given below, where x is -1 for an acidic site and 1 for a basic site (97, 114).

$$Percentage\ ionisation = \frac{100}{1 + 10^{x(pH-pKa)}}$$

Since both the drug and the amino acids are zwitterions, percentage ionisation at any given pH was calculated for individual ionisable groups. After this, the percentage ionisation of both acidic groups and both basic groups were added together before subtracting with the opposite. This enabled the calculation of the overall percentage ionisation.

2.1.2.7 Mass spectrometry analysis of degradation products of TC

In order to investigate what each peak in the chromatogram represents, samples were run through the column using the HPLC system mentioned above. Fractions representing each peak on the chronograms were collected as they were separated through the column. These fractions were then used for mass spectrometric (MS) analysis, and *m/z* spectra for each fraction was obtained. Positive ion mode was used to ionise the samples using the electrospray ionisation (ESI) method.

2.1.2.8 Statistics

Statistical analysis was conducted using GraphPad Prism. One way ANOVA was used to see whether there was overall statistical significance in the results. This was followed by Dunnett's multiple comparisons test to see which treatment was significantly different to the control. Dunnett's procedure was used over other multiple comparison tests because it is specialises in comparing each treatment against the control. P values below 0.05 for the results were taken as statistically significant.

2.1.3 Results

2.1.3.1 Validation of tetracycline HPLC method

2.1.3.1.1 Specificity and selectivity

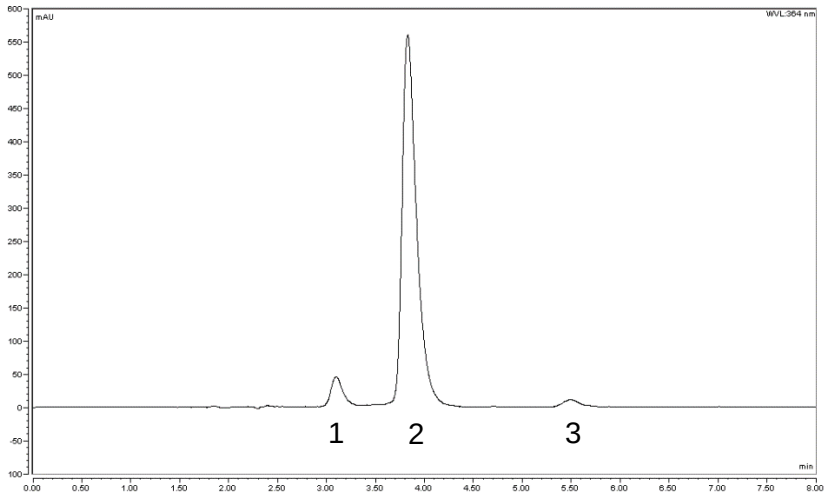

Figure 2.4: Three peaks of TC analysis through HPLC. Peak one (left), two (middle) and three (right) represent 4-epitetracycline, TC and 4-epianhydrotetracycline respectively.

In the analysis of TC three peaks (Figure 2.4) were observed on the chromatograms. According to the British Pharmacopoeia the 1st, 2nd and 3rd peaks represent ETC, TC and EATC (in a sample containing these molecules) respectively (102). Studies have shown the elution order of TC and its major degradation products to be ETC, TC, EATC and ATC from first to last (103, 105). ETC has a much lower antibiotic activity compared to TC. However, since ETC is not associated with toxicity and under some conditions can convert back into TC, the sum of the two peaks representing ETC and TC was used in quantifying the total amount of TC in a sample (105, 107). This total was used in plotting the calibration curve as well as in the analysis of unknown samples.

2.1.3.1.2 Linearity and range

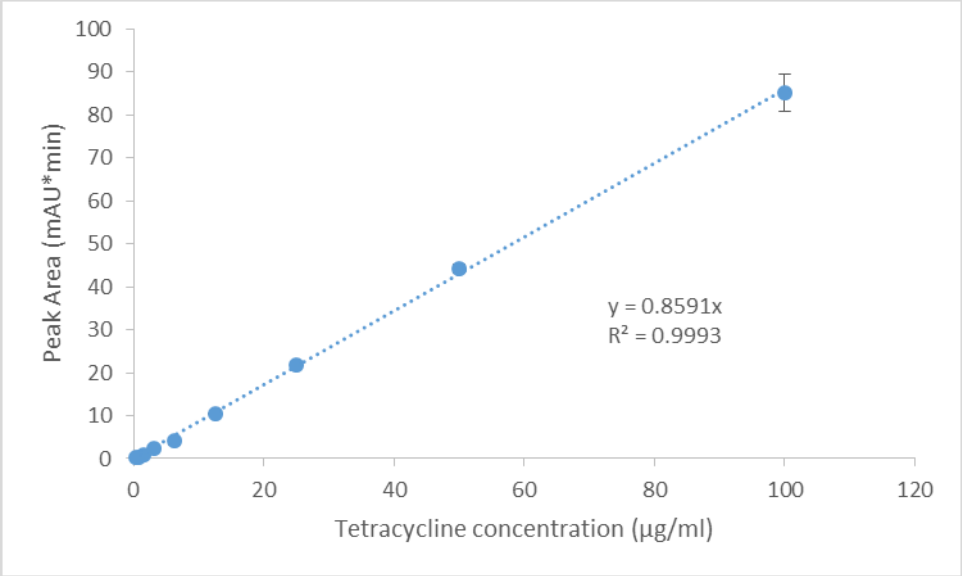

Figure 2.5: Calibration curve for TC with concentrations of TC ranging from 1.56 to 100 µg/ml; n=3.

Standard solutions of tetracycline at concentrations of 0.098, 0.20, 0.39, 0.78, 1.56, 3.13, 6.25, 12.5, 25, 50 and 100 µg/ml were prepared as described in the method. Calibration curve (Figure 2.5) was obtained with tetracycline standard solutions of concentration above the limit of visual detection; concentration ranging from 1.56 to 100 µg/ml. The equation of straight line and coefficient of determination (R^2) were obtained:

$$y = 0.8591\ x$$
$$R^2 = 0.9993\ (n = 27)$$

The Centre of Drug Evaluation and Research (CDER) recommends that criteria for establishing good linearity should be equal to or above a coefficient of determination of 0.999 (115). Therefore the obtained value for R^2 indicates good linearity since it is above 0.999.

2.1.3.1.3 Limit of detection (LOD) and limit of quantification (LOQ)

Visual evaluation was used to identify the concentration at which the limit of detection is achieved. The data for the mentioned range of concentrations obtained was then used to plot the calibration curve and establish the slope of the calibration curve (S) and the standard deviation of the response (σ). The standard deviation of the regression line was used as the

σ. The values obtained for S and σ were then used to determine LOD and LOQ using the following equations:

$$LOD = \frac{3.3\,\sigma}{S}$$

$$LOQ = \frac{10\,\sigma}{S}$$

LOD and LOQ was calculated to be 3.80 and 11.53 µg/ml respectively.

2.1.3.1.4 Precision

Precision was determined by testing two batches of six replicates at 100% of the test concentration; 100 µg/ml. One batch was tested twice in one day to determine the intra-day (intra-batch) precision (Table 2.3) whilst a second batch was tested on a different day allowing the determination of inter-day (inter-batch) precision (Table 2.2). The inter-day % relative standard deviation (RSD) was 5.86 and 6.47 for the first and second day respectively. The intra-day %RSD was 3.26 and 6.47. It is recommended that %RSD should not exceed 15%, therefore these results suggest good precision of the method (116).

Table 2.2 Inter-day (inter-batch) precision of the HPLC method in the analysis of TC.

Tetracycline concentration (µg/ml)	Day	Mean measured concentration (µg/ml)	SD	RSD (%)
100	1	106.36	6.23	5.86
100	2	99.37	6.43	6.47

Table 2.3 Intra-day (intra-batch) precision of the HPLC method in analysis of TC.

Tetracycline concentration (µg/ml)	Day	Mean measured concentration (µg/ml)	SD	RSD (%)
100	1	98.41	3.21	3.26
100	1	99.37	6.43	6.47

2.1.3.1.5 Accuracy

Accuracy was assessed by evaluating the concentration values obtained from the analysis of samples of three different known concentrations. TC solutions of 80, 60 and 40 µg/ml were prepared and analysed. Accuracy (Table 2.4) was then determined and expressed as the mean percentage recovery of the known concentrations. A mean recovery of 96.09% ± 0.48% for the three concentrations was found. These results suggest good accuracy of the method (116).

Table 2.4: Accuracy of the HPLC method in analysis of TC.

Standard solution (µg/ml)	Recovery (%)	RSD (%)
80	96.53	1.97
60	96.16	5.39
40	95.57	4.63

2.1.3.2 Solubility

Solubility of TC was investigated in different concentrations of both acidic and basic amino acids as counterions. This provided data identifying suitable counterions for TC while quantifying the extent of solubility enhancement with such amino acids.

2.1.3.2.1 Acidic amino acids

Initially solubility of TC was investigated in aqueous solutions of acidic amino acids (L-aspartic acid and L-glutamic acid) of increasing concentrations up to 1000 µg/ml. The concentrations used were 62.5, 125, 250, 500 and 1000 µg/ml. This identified both L-aspartic acid, L-glutamic acid as suitable counterions. Solubility of TC in higher concentrations (1500, 2500, 3500 and 4500µg/ml) of these amino acids was investigated subsequently.

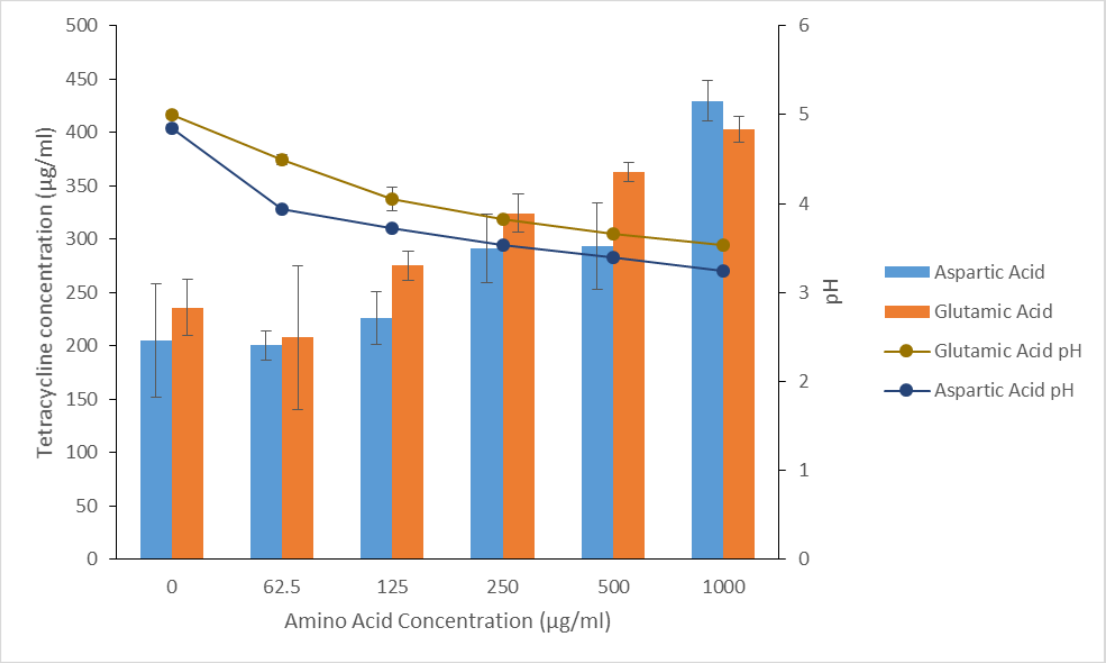

Figure 2.6: Apparent TC solubility increased with increasing concentrations of both L-aspartic acid and L-glutamic acid. Significant rise in solubility was observed with 1000µg/ml (p 0.0004, n = 3) aspartic acid and at 250µg/ml (p 0.0138, n = 3), 500µg/ml (p 0.0004, n = 3) and 1000µg/ml (p 0.0001, n = 3) glutamic acid.

Table 2.5: Fold change in solubility of TC with increasing concentration of L-aspartic acid and L-glutamic acid (62.5, 125, 250, 500 and 1000µg/ml) compared to control. Solubility increased with increasing aminoacid molarity.

L-Aspartic Acid (µg/ml)	Fold change	L-Glutamic Acid (µg/ml)	Fold change
62.5	0.98	62.5	0.88
125	1.10	125	1.17
250	1.42	250	1.37
500	1.43	500	1.54
1000	2.10	1000	1.71

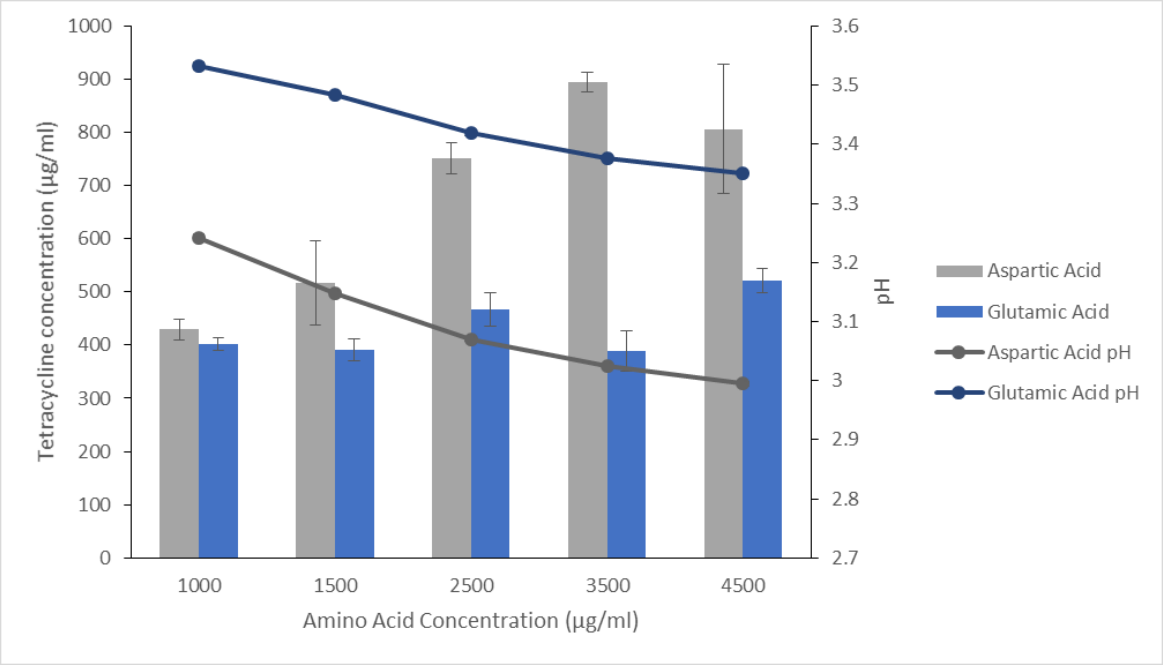

Figure 2.7: Change in TC solubility with increasing concentration of L-aspartic acid and L-glutamic acid. At these higher concentrations (>1000µg/ml), L-aspartic was the better acidic amino acid in enhancing apparent solubility of TC. Compared to contro, a significant (p 0.0001, n = 3) enhancement in apparent solubility was observed at all concentrations above 1000µg/ml with both acidic amino acids.

Table 2.6: Fold change in solubility of TC with different concentrations of L-aspartic acid and L-glutamic acid (1500, 2500, 3500 and 4500µg/ml) compared to control. Solubility of TC increased with increasing aminoacid molarity.

Aspartic Acid (µg/ml)	Fold increase	Glutamic Acid (µg/ml)	Fold increase
1500	2.53	1500	1.66
2500	3.67	2500	1.98
3500	4.37	3500	1.65
4500	3.94	4500	2.21

Solubility of TC increased with increasing concentration of both acidic amino acids; L-aspartic acid and L-glutamic acid (Figure 2.6). At L-aspartic acid and L-glutamic acid concentration of 1000 µg/ml, the solubility of TC increased by 2.10 and 1.71 fold (Table 2.5) respectively, when compared to control. The highest solubility in the L-aspartic acid solution was observed at a concentration of 3500 µg/ml of the amino acid (Figure 2.7). At this concentration, the solubility of TC peaked to 895.15 µg/ml (p 0.0001, n = 3), representing a 4.37 fold increase compared to control (Table 2.6). On the other hand, the enhancement of solubility observed in L-glutamic acid peaked to only 2.21 fold greater than control at 4500 µg/ml.

The pH data gathered was used to obtain theoretical percentage ionisation of TC and the corresponding amino acid. This was done using the Henderson-Hasselbalch equation, and the results were plotted on graphs (Figure 2.8 and Figure 2.9). The purpose of this was to see how the ionisation of the drug and amino acid changed with a change in amino acid concentration, and how this linked with the changes in solubility observed. Diagrams enabling easy visualisation of the effect of change in pH on ionisable sights were also constructed for both the amino acids and TC, separately and are presented in the discussion later.

With increasing concentration of both amino acids, percentage of TC in the ionised state also increased. It is worth highlighting that with L-aspartic acid, the percentage of TC in the ionised form reached up to 66.88 % at 4500 µg/ml. This was substantially higher than the 47.04 %of TC in the ionised form with 4500 µg/ml of L-glutamic acid.

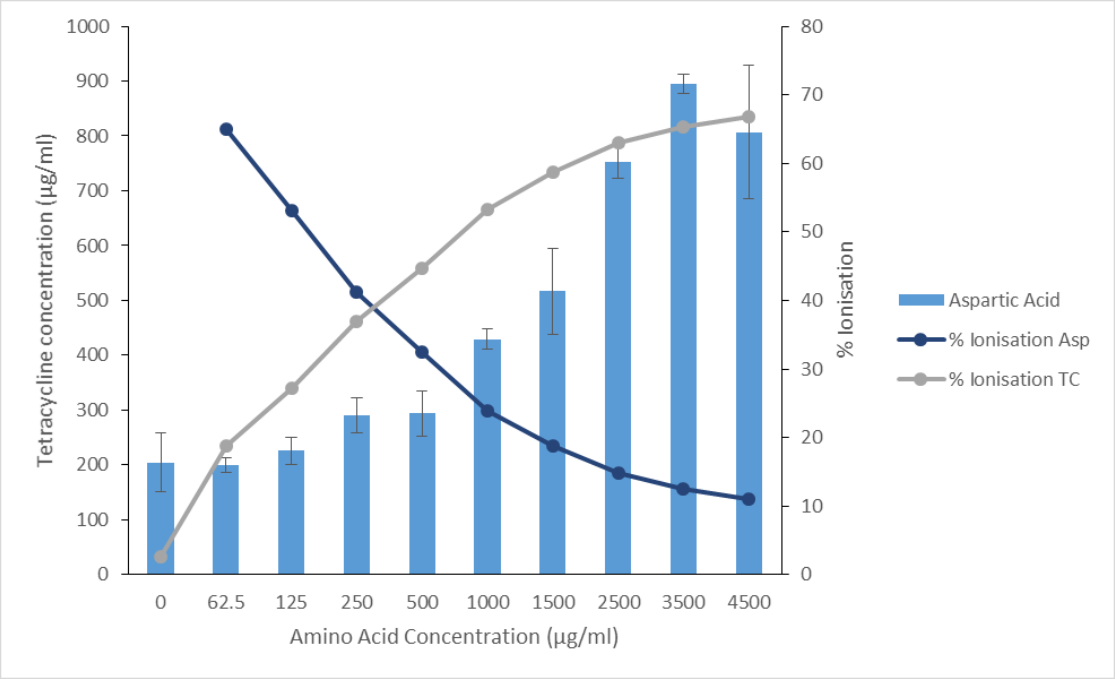

Figure 2.8: % Ionisation of TC and L-Aspartic acid. With increasing L-aspartic acid concentration and decreasing pH, the % ionisation of L-aspartic acid decreased whereas the % ionisation of TC increased; n=3.

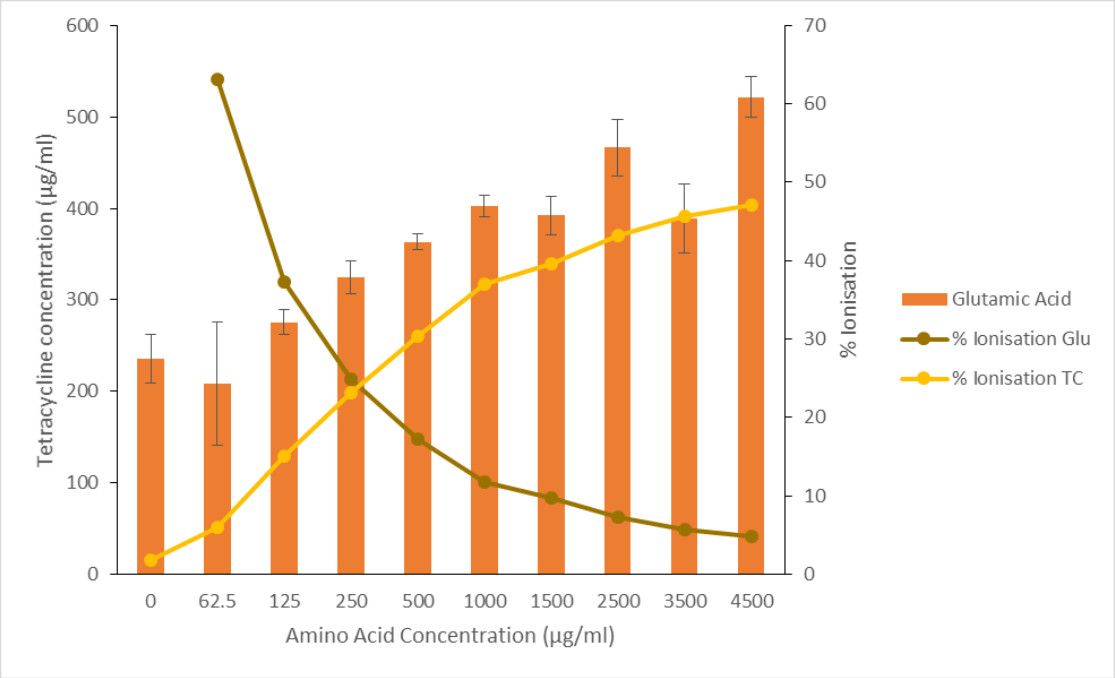

Figure 2.9: % Ionisation of TC and L-glutamic acid. With increasing L-glutamic acid concentration and decreasing pH, the % ionisation of L-glutamic acid decreased whereas the % ionisation of TC increased; n=3.

2.1.3.2.2 Basic amino acids

2.1.3.2.2.1 Solubility of tetracycline with basic amino acids over 24 hour

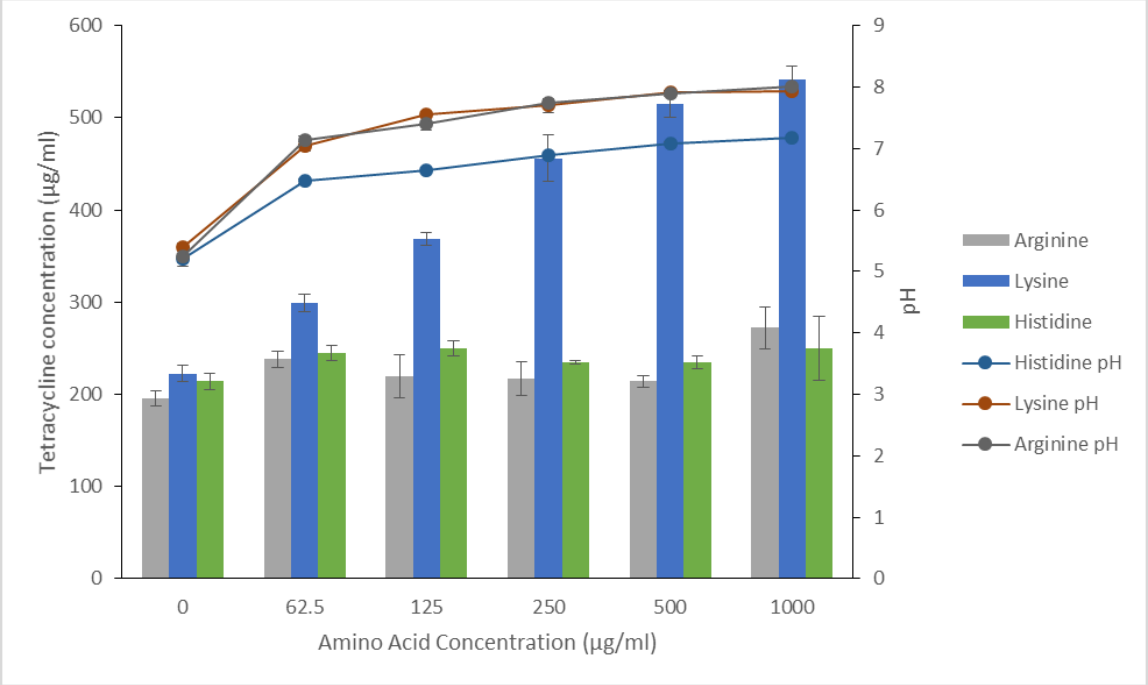

Figure 2.10: In the initial study TC solubility only increased appreciably with increasing concentration of L-lysine. Significant rise in solubility was observed with 62.5µg/ml (p 0.0274, n = 3) and 1000µg/ml (p 0.0004, n = 3) of arginine and at 62.5µg/ml (p 0.0004, n = 3), 125µg/ml (p 0.0001, n = 3), 250µg/ml (p 0.0001, n = 3), 500µg/ml (p 0.0001, n = 3) and 1000µg/ml (p 0.0001, n = 3) of lysine. No significant (p 0.1225, n = 3) rise in the apparent solubility of TC was observed with histidine.

Table 2.7: Amino acid molarity (representing concentrations of 62.5, 125, 250, 500 and 1000 µg/ml) and the associated fold change in solubility of TC from control.

Arginine (µg/ml)	Fold change	Lysine (µg/ml)	Fold change	Histidine (µg/ml)	Fold change
62.5	1.22	62.5	1.35	62.5	1.14
125	1.12	125	1.66	125	1.17
250	1.11	250	2.05	250	1.10
500	1.10	500	2.32	500	1.10
1000	1.39	1000	2.44	1000	1.17

Solubility of TC was also investigated in aqueous solutions of basic amino acids (L-arginine, L-lysine and L-histidine) of increasing concentrations maxed at 1000 µg/ml (Figure 2.10). The concentrations used were 62.5, 125, 250, 500 and 1000 µg/ml. This identified L-lysine as a

suitable counterion. Solubility of TC in higher concentrations (1500, 2500, 3500 and 4500µg/ml) of this amino acid was investigated subsequently.

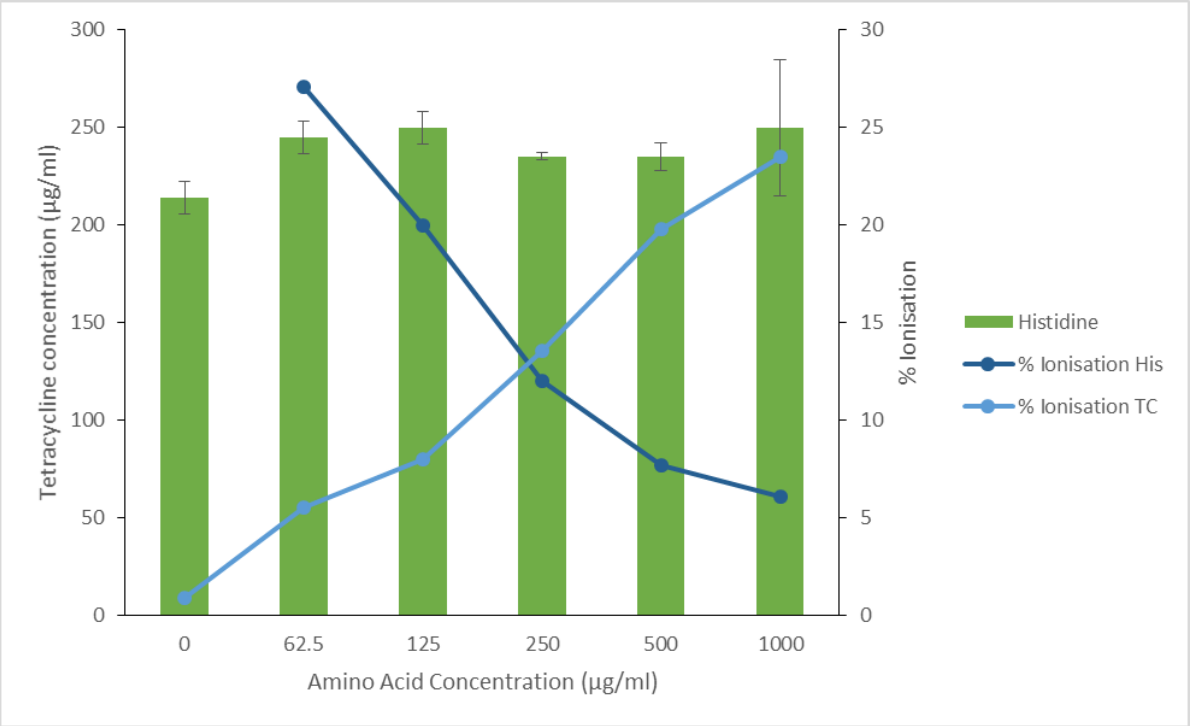

Figure 2.11: % Ionisation of TC and L-histidine. With increasing L-histidine concentration and therefore increasing pH, the % ionisation of L-histidine decreased whereas the % ionisation of TC increased; n=3.

At amino acid concentration 1000 µg/ml and with a 2.44 fold enhancement of solubility (Table 2.7) more than control, L-lysine seemed the best candidate as a counterion for TC out of all acidic and basic amino acids. Consequently, solubility with higher concentrations (up to 4500 µg/ml) of L-lysine were investigated (Figure 2.12). Interestingly, although the solubility of TC continued to rise with increasing concentration of L-lysine, the solubility maxed a 2.98 fold increase (Table 2.8) compared to the 3.94 fold increase (Table 2.6) with L-aspartic acid solution.

Even more surprisingly the pH of the L-lysine-TC solution was found to decrease instead of the expected rise in pH with increasing concentration of the basic amino acid above 1000 µg/ml. This along with other observations made whilst working with L-lysine and L-arginine prompted further investigations.

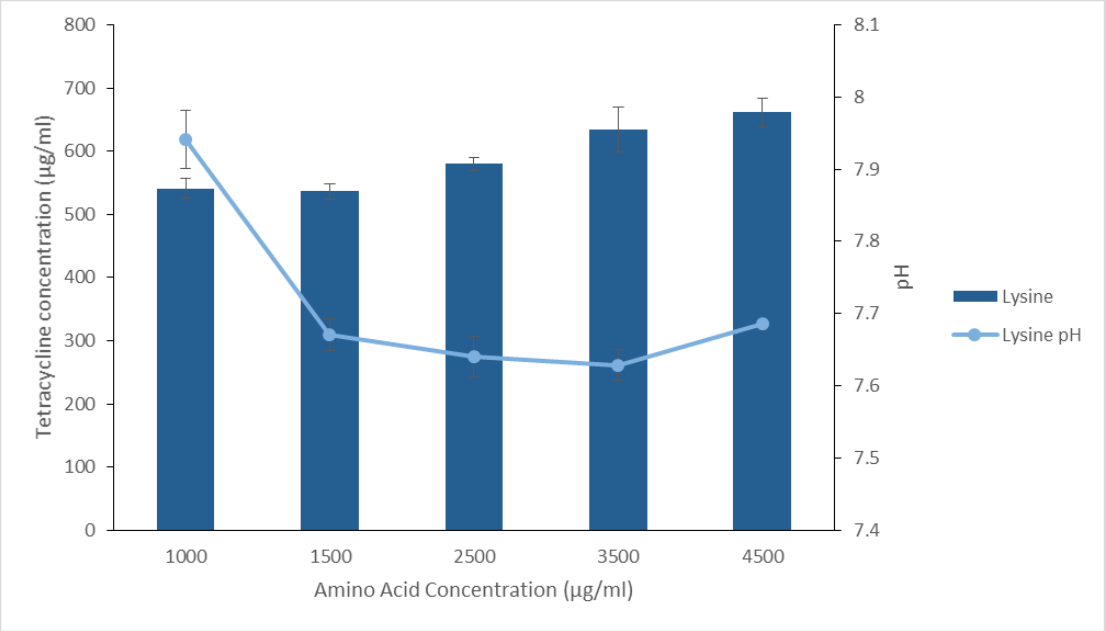

Figure 2.12: A shalow rise in TC solubility between 1000 and 4500µg/ml of L-lysine. The apparent rise in solubility was significant (p 0.0001, n = 3) at all these concentrations compared to control. The pH decreased despite increasing concentration of basic amino acid.

Table 2.8: Amino acid molarity (representing concentrations of 1500, 2500, 3500 and 4500 µg/ml) and the associated fold change in solubility of TC from control.

Lysine (µg/ml)	Fold change
1500	2.41
2500	2.61
3500	2.85
4500	2.98

2.1.3.2.2.2 Additional observations with tetracycline using basic amino acids

It was visually observed that much more TC seemed to dissolve in L-lysine and L-arginine solution than in any of the acidic amino acid solutions (Figure 2.13). Secondly, over the 24 hour stirring time, the colour of the L-lysine-TC solution and L-arginine-TC solution changed from the original yellow to a dark brown (Figure 2.14). And finally, the chromatogram revealed additional peaks (Figure 2.15) of TC degradation products in L-arginine and L-lysine solutions at higher concentrations of the amino acids.

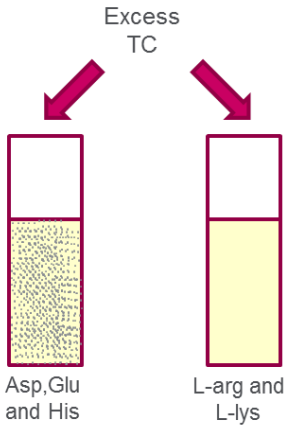

Figure 2.13: Upon visual evaluation, much more TC dissolved in L-arginine and L-lysine solutions compared to L-histidine or any of the acidic amino acids.

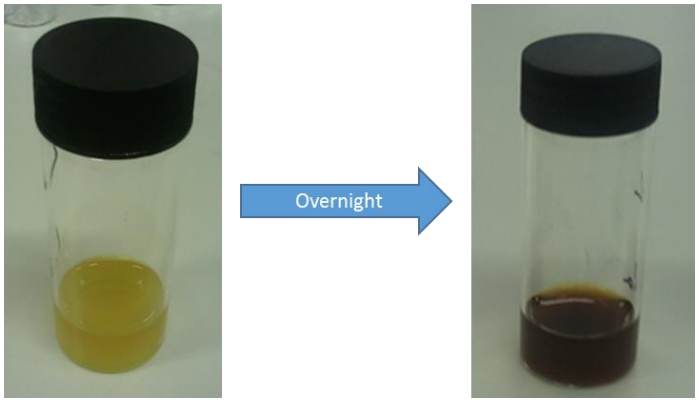

Figure 2.14: Overnight, L-arginine-TC and L-lysine-TC solution underwent colour change from yellow to brown.

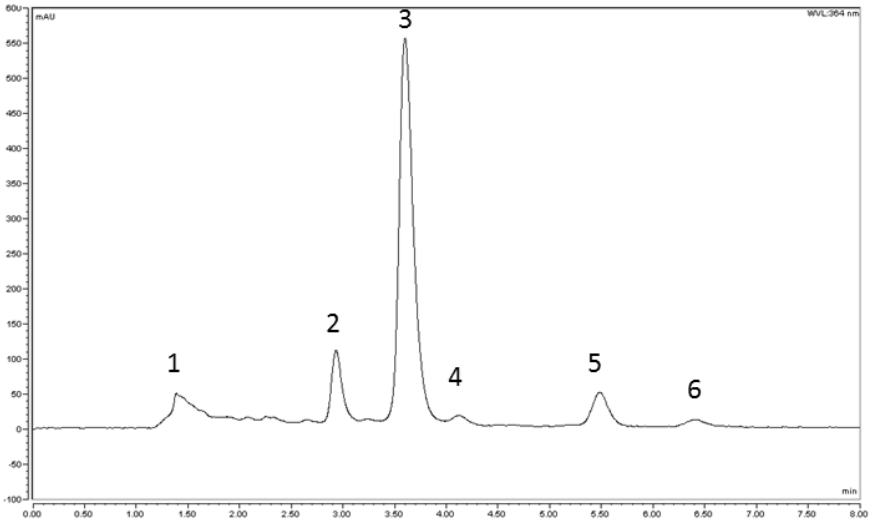

Figure 2.15: Additional peaks of degradation products observed with L-arginine and L-lysine.

2.1.3.2.2.3 Tetracycline degradation kinetics with basic amino acids and identification of degradation products

The degradation of TC over time in the presence of basic amino acids L-arginine (Figure 2.16) and L-lysine (Figure 2.17) was studied and order of degradation reaction was determined. TC was left in basic amino acid solutions without stirring or shaking. By 192 hours more than 90% of TC had degraded with both of the basic amino acids. To determine the order of degradation reaction, concentration over time (Figure 2.16a and Figure 2.17a), log10 concentration over time (Figure 2.16b and Figure 2.17b) and 1/concentration over time scatter charts were plotted (Figure 2.16c and Figure 2.17c). Whilst plotting concentration over time tests for zero order reaction, log10 concentration over time tests for first order reaction and 1/concentration over time tests for second order reaction. Since log10 concentration over time plot gave the straightest line, indicated by higher r^2 values compared to other two plots, the order of degradation reaction of TC was determined to be first order in both L-arginine and L-lysine solutions. Since the rate constant (k) is negative k ($-k$) in the equations of zero order and first order reactions, the gradient was multiplied by -1 to determine the rate constant. This gave k of 0.0062 h^{-1} and 0.0064 h^{-1} for L-lysine and L-arginine respectively. Half-life ($t_{1/2}$) of TC in these basic solutions was determined using the following equation.

$$t\frac{1}{2} = 0.693/k$$

This gave a half-life of 111.77 h for TC in L-arginine solution of 4500 µg/ml and 108.28 h for TC in L-lysine solution of 4500 µg/ml.

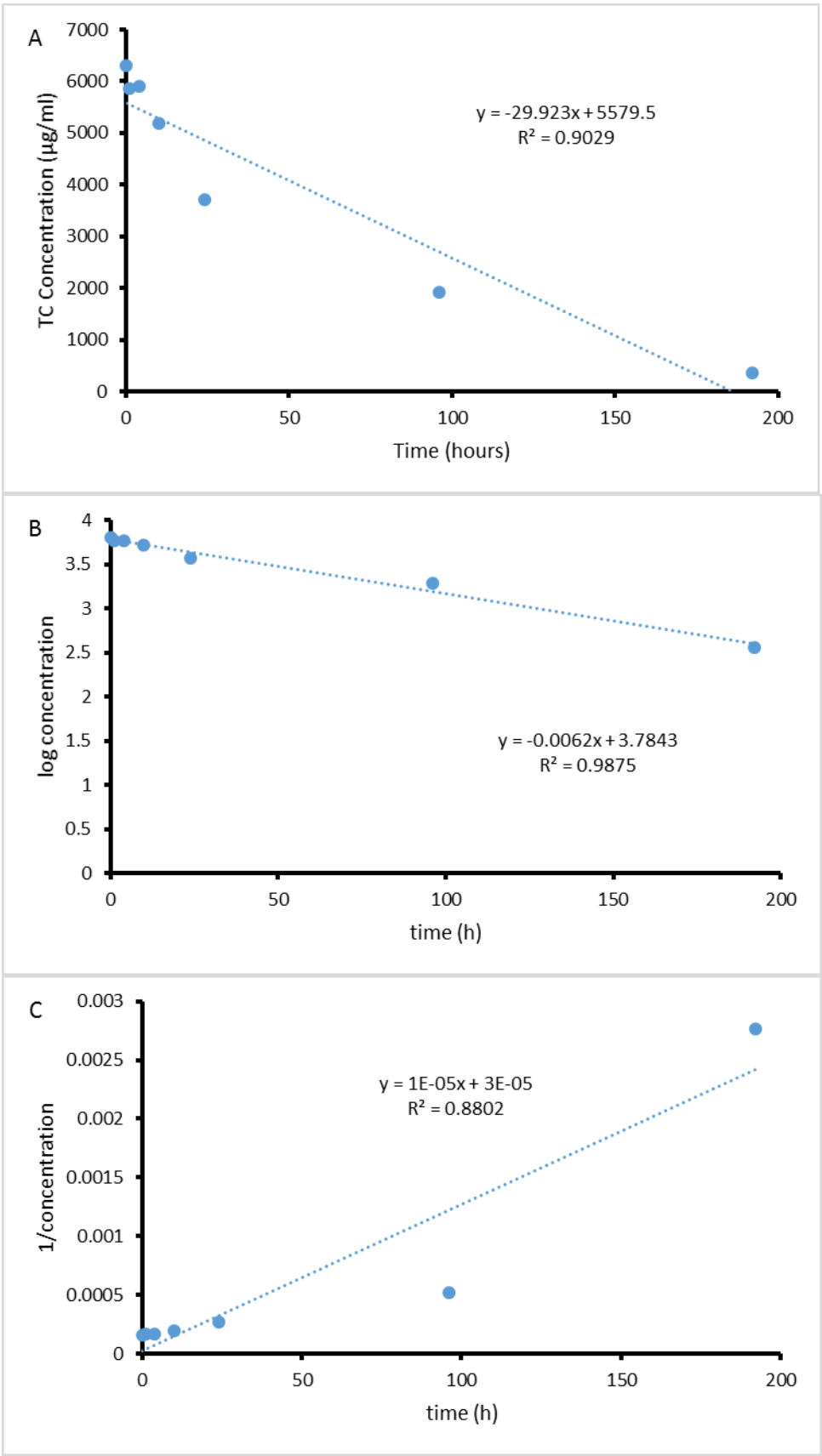

Figure 2.16: Degradation of TC over 192 hours in L-arginine solution of 4500 µg/ml. A) Concentration over time B) log concentration over time C) 1/concentration over time.

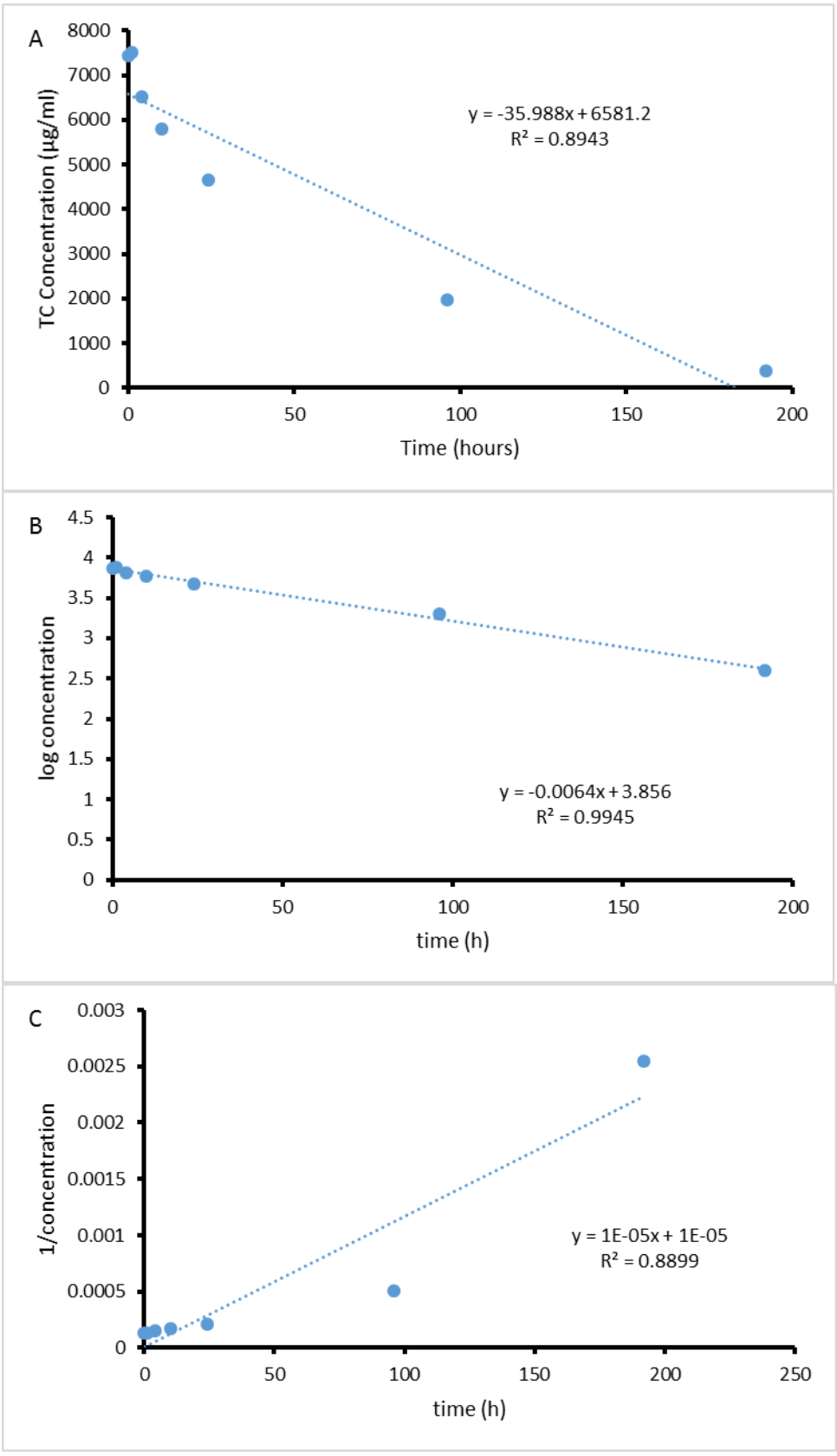

Figure 2.17: Degradation of TC over 192 hours in L-lysine solution of 4500 µg/ml. A) Concentration over time B) log concentration over time C) 1/concentration over time.

To confirm the formation of degradation products, MS of TC solution stirred in 4500 µg/ml of L-lysine overnight was conducted. Fractions were obtained as described in the methods section corresponding to each peak visible in the chromatogram. Fraction A corresponded to Peak 1 or the solvent front, fraction B for peak 2, fraction C for peak 3, fraction D for peak 4, fraction E for peak 5 and fraction F for peak 6 (Figure 2.15). Figure 2.18 to Figure 2.24 present MS spectra for blank (mobile phase) and fraction A to F.

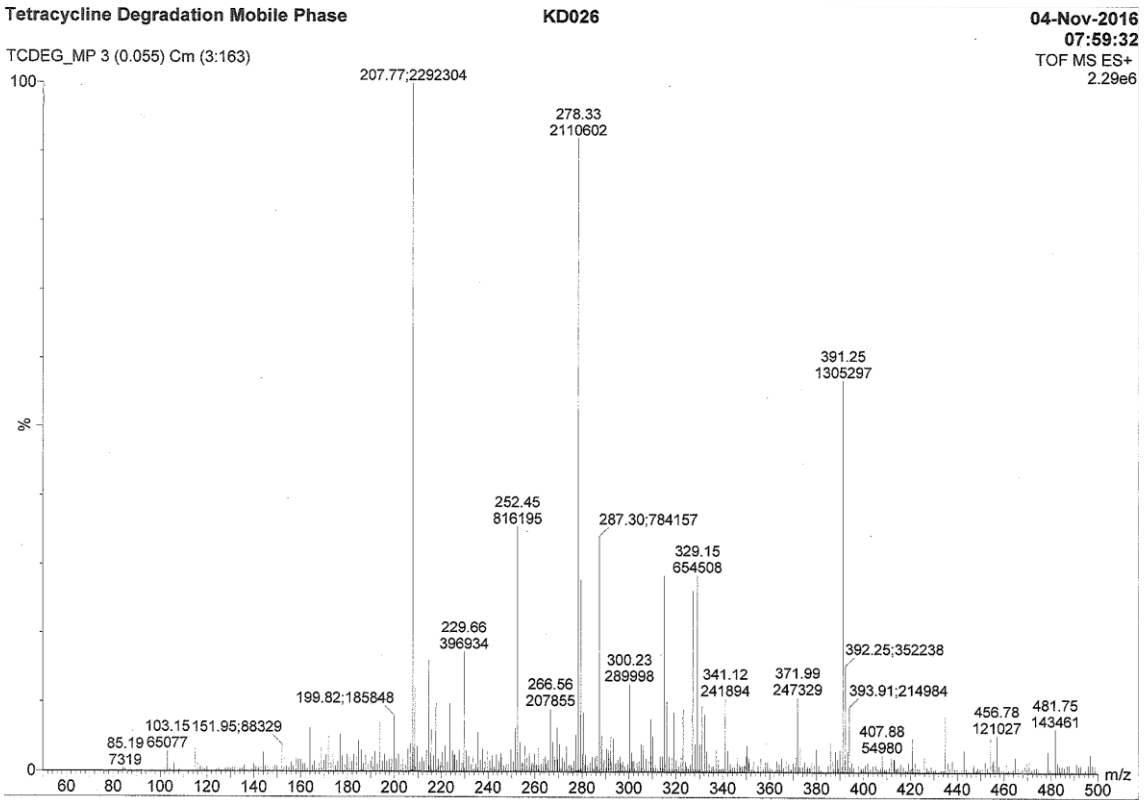

Figure 2.18: MS spectra for mobile phase.

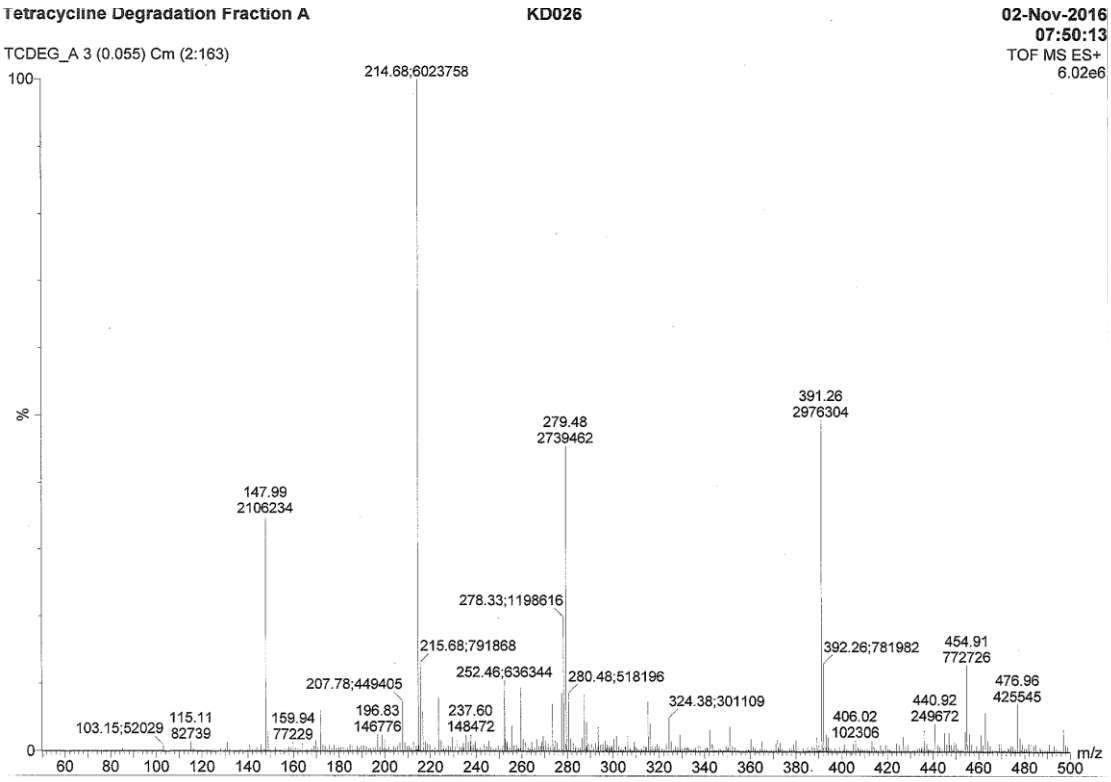

Figure 2.19: MS spectra for fraction A.

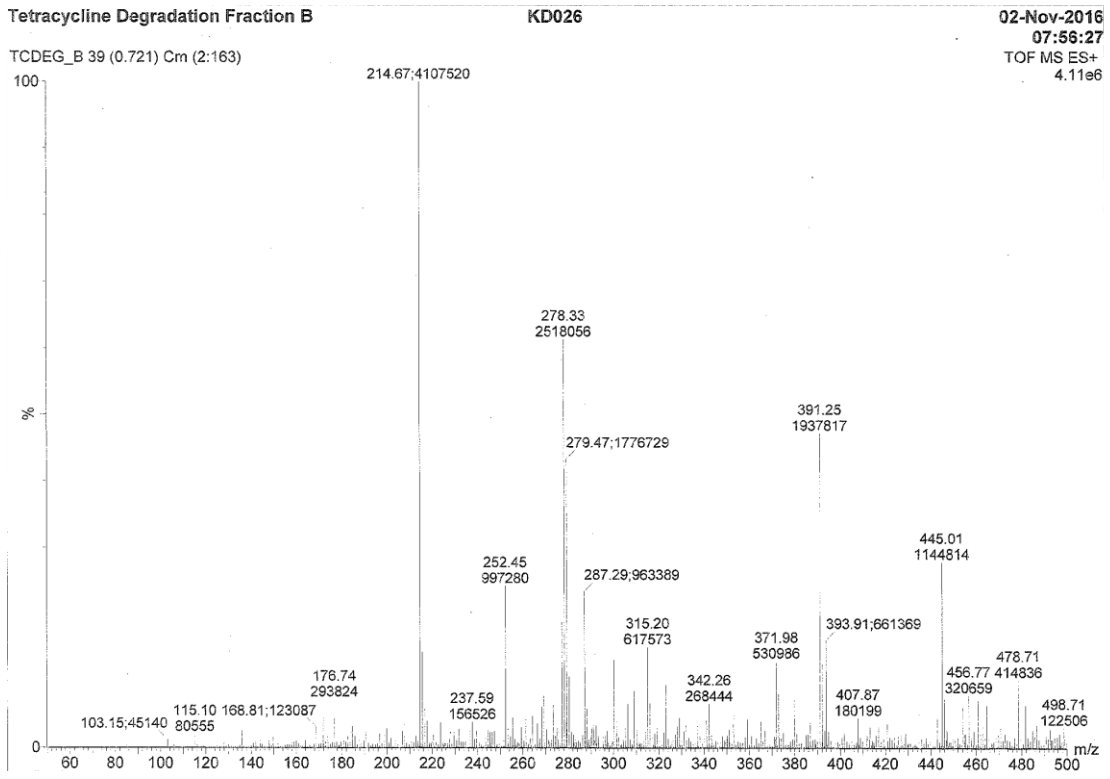

Figure 2.20: MS spectra for fraction B.

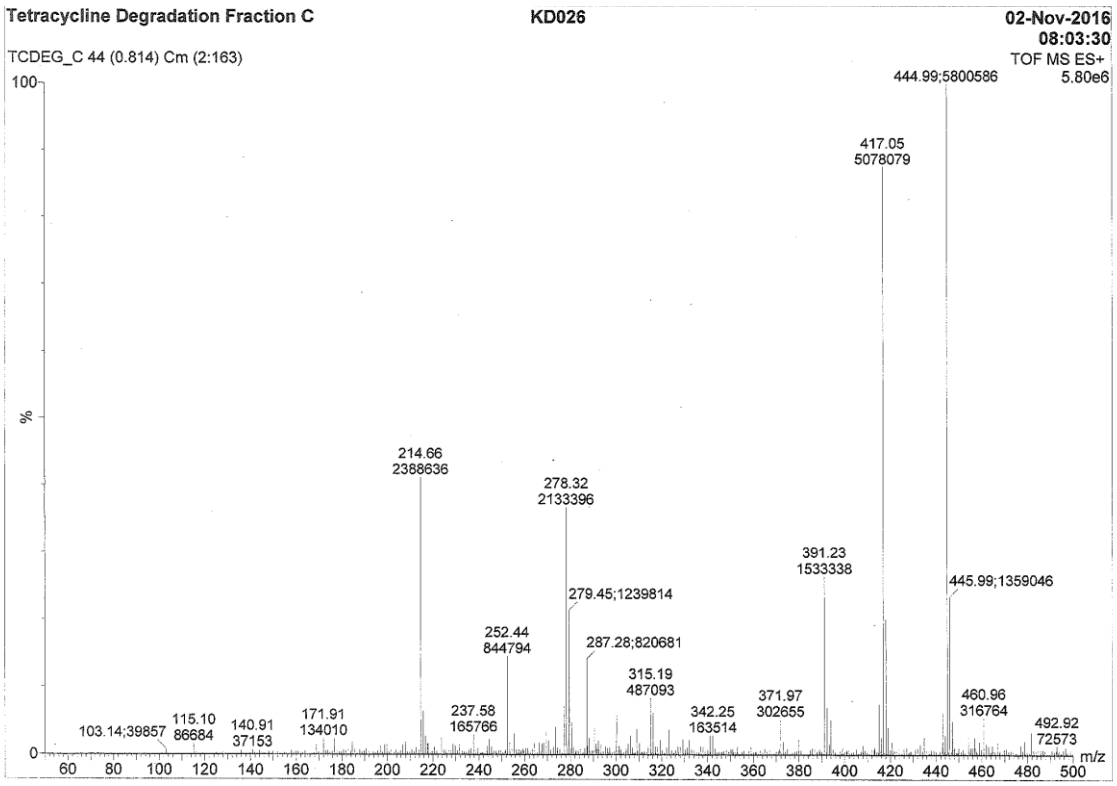

Figure 2.21: MS spectra for fraction C.

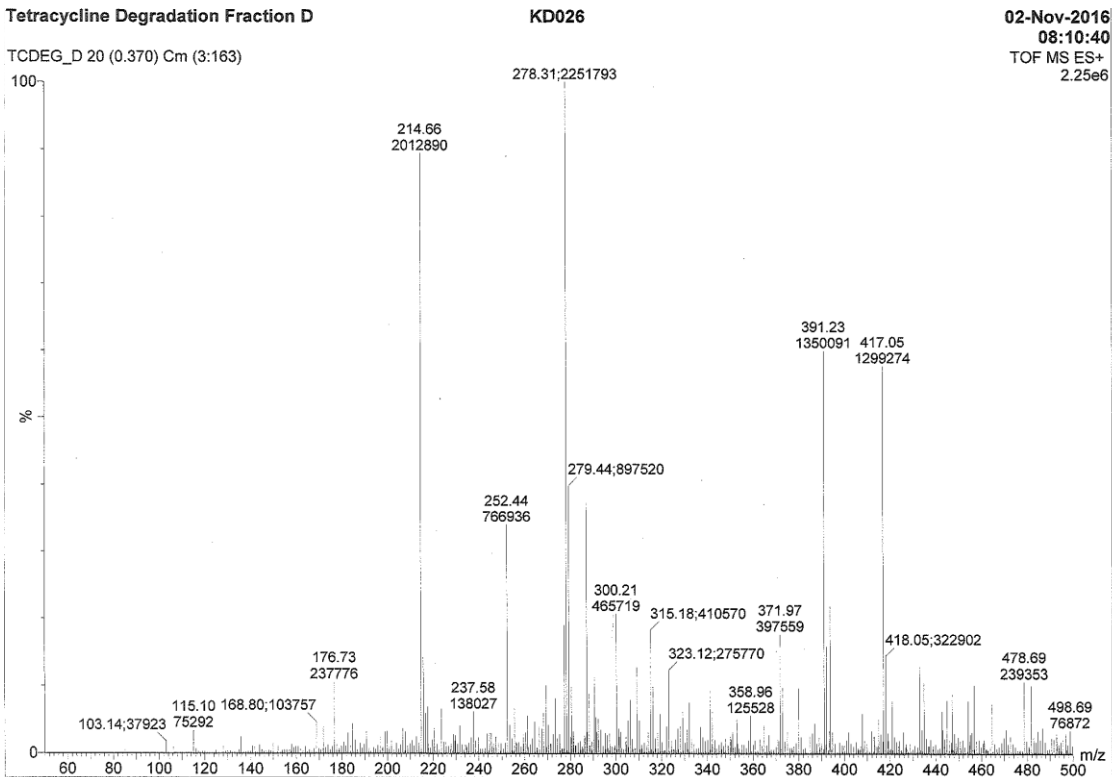

Figure 2.22: MS spectra for fraction D.

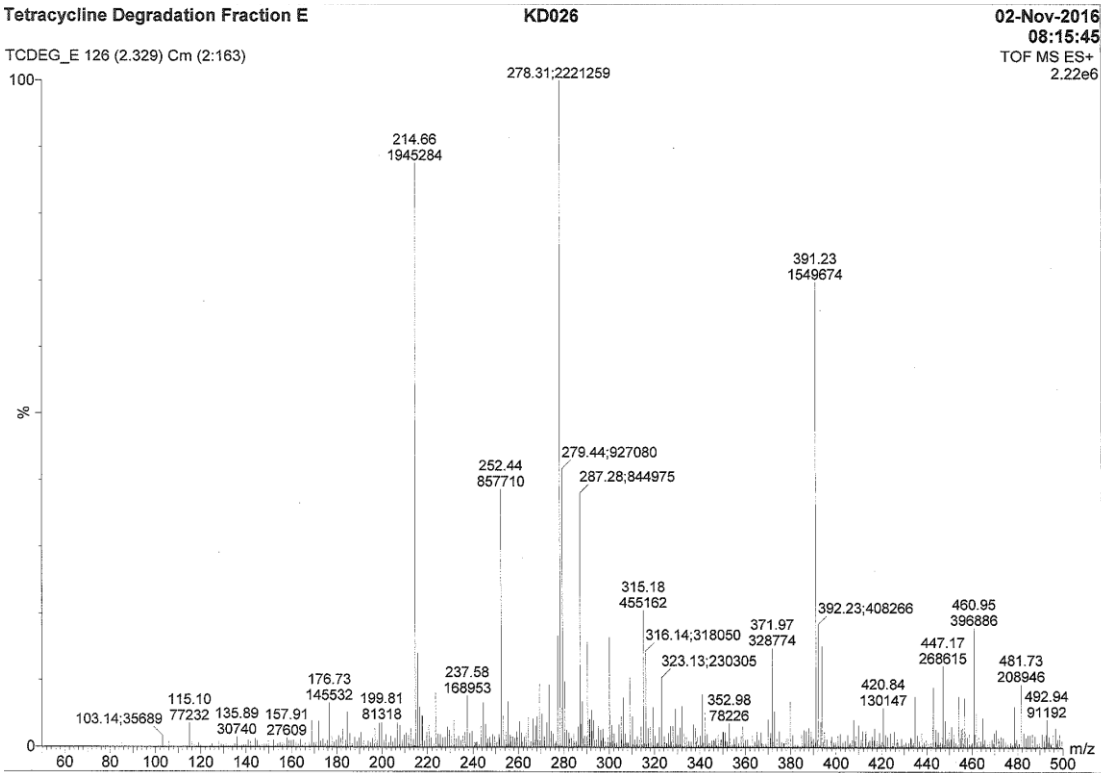

Figure 2.23: MS spectra for fraction E.

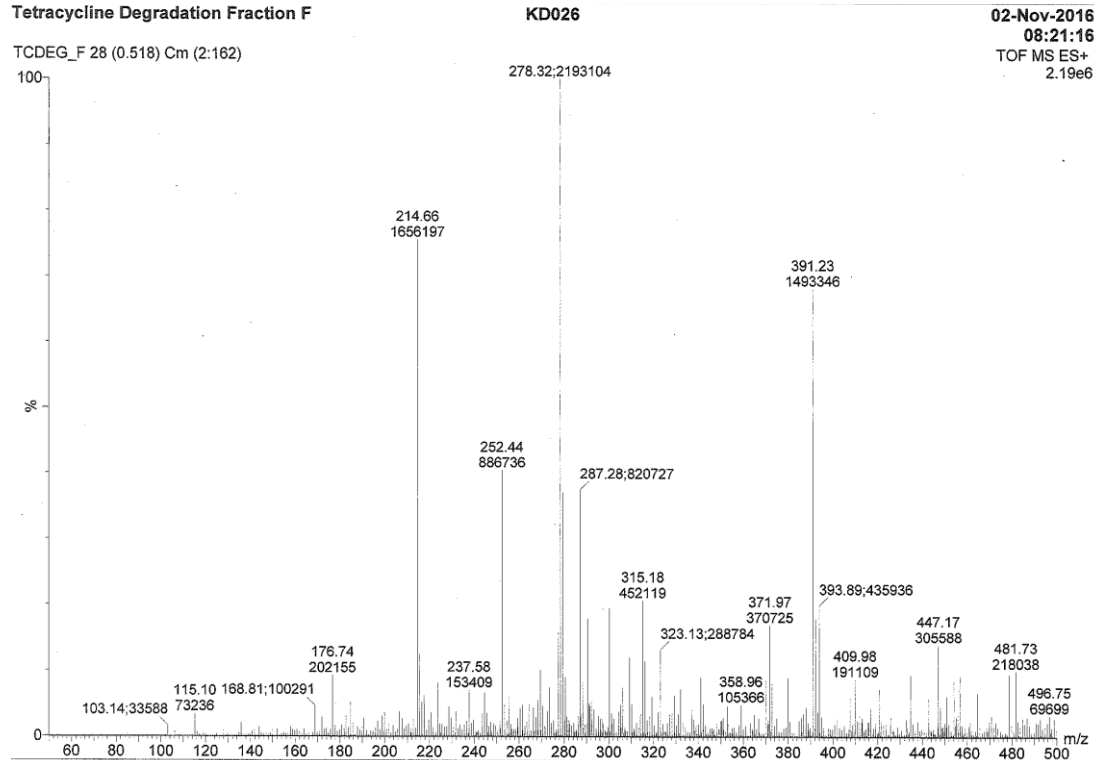

Figure 2.24: MS spectra for fraction F.

For simplicity, when considering peaks which were also present in the mobile phase sample, *m/z* peaks around or above 20% of relative intensity were taken into account. Peaks that were present in the mobile phase were used to blank the spectra from all the fractions in a bid to obtain the peaks of interest which were not present in the blank. All the major peaks are summarised in Table 2.9, whilst the peaks not present in the blank were taken to represent L-lysine (*m/z* 148), TC (*m/z* 445) or the degradation products of TC (*m/z* 410, 417, 441, 447, 460 and 477).

Table 2.9: Summary of MS of chromatograph fractions.

Fraction no.	Major *m/z* peaks present in blank	*m/z* not present in blank
A	215, 278, 391	148, 441, 477
B	215, 278, 287, 391	445
C	215, 252, 278, 287, 391	417, 445
D	215, 252, 278, 300, 315, 371, 391	417
E	215, 252, 278, 287, 315, 391	447, 460
F	215, 252, 278, 287, 315, 391	410, 447

2.1.3.2.2.4 Instant solubility of tetracycline with basic amino acids

In light of the above observations, it was decided to investigate the instant solubility of TC in the presence of the basic amino acids L-arginine and L-lysine. Instant solubility refers to solubility studies where TC was exposed to the basic amino acids solution for a minimal time before quantifying the amount of TC which had dissolved and excludes the overnight stirring of TC within the solution.

In line with visual observation, the results revealed that the instant solubility of TC in L-arginine and L-lysine solution much greater than its solubility in acidic amino acid solutions. The increase in TC solubility was dependent on the concentration of the amino acid, with higher concentration of either L-arginine or L-lysine generally resulting a higher amount of TC dissolved (Figure 2.25 and Figure 2.26). Highest solubility of TC was reached at 4500 µg/ml of L-arginine and L-lysine and was found to be 5891.05 and 6534.96 µg/ml (Figure 2.25 and Figure 2.26), representing a 16.30 and 25.70 (Table 2.10) fold increase in solubility from control, respectively. The increase in amino acid concentration is calculated to result in increasing amounts of TC being in the ionised (Figure 2.27 and Figure 2.28) form despite lowering the percentage ionisation of the amino acid. This presents another correlation that TC solubility increases in basic amino acid solutions with increasing amounts of TC present in the ionised form. The percentage of TC in the ionised form reached a maximum of 119.08 % and 121.71 % for L-arginine (Figure 2.27) and L-lysine (Figure 2.28) respectively. Note that a value above 100% represents two charges on TC. This is around double of the TC percentage ionisation achieved with same concentrations of L-aspartic acid and L-glutamic acid (Figure 2.8 and Figure 2.9). It is worth highlighting though that although the percentage of TC in the ionised form was barely 2 fold greater in basic amino acids as compared to acidic amino acids, the solubility of TC was around 7-8 fold greater in basic amino acids than L-aspartic acid and 11-13 fold greater than L-glutamic acid.

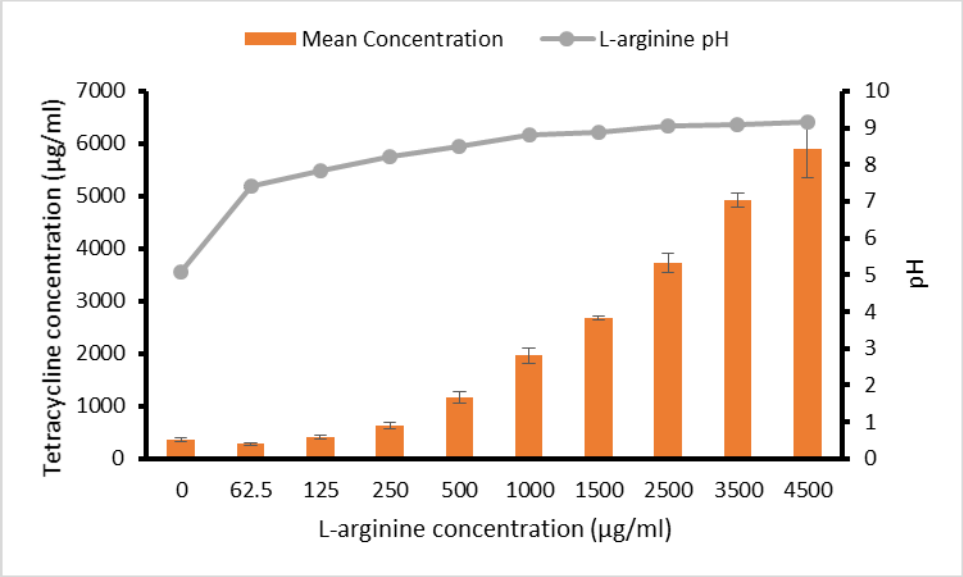

Figure 2.25: Apparent TC solubility increased with increasing concentrations of L-arginine. Solubility of TC in L-arginine solution was much greater when analysed instantly after mixing with the amino acid solution as compared to when analysed after overnight stirring. Significant rise in solubility was observed at L-arginine concentrations of 500 µg/ml (p=0.00056), 1000 µg/ml (p<0.0001) 1500 µg/ml (p<0.0001), 2500 µg/ml (p<0.0001), 3500 µg/ml (p<0.0001) and 4500 µg/ml (p<0.0001); n=3.

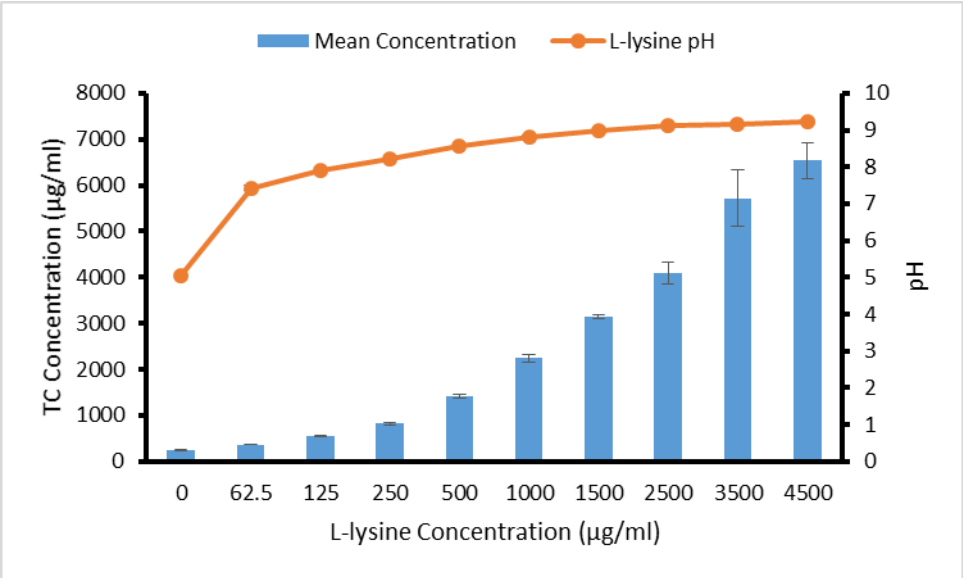

Figure 2.26: Apparent TC solubility increased with increasing concentrations of L-lysine. Solubility of TC in L-arginine solution was much greater when analysed instantly after mixing with the amino acid solution as compared to when analysed after overnight stirring. Significant rise in solubility was observed at L-arginine concentrations of 500 µg/ml, 1000 µg/ml, 1500 µg/ml, 2500 µg/ml, 3500 µg/ml and 4500 µg/ml; p<0.0001, n=3.

Table 2.10: Fold change in solubility of TC with increasing concentration of L-arginine and L-lysine (62.5, 125, 250, 500, 1000, 1500, 2500, 3500 and 4500 µg/ml) compared to control. Solubility increased with increasing aminoacid molarity.

L-Arginine (µg/ml)	Fold increase	L-lysine (µg/ml)	Fold increase
62.5	0.77	62.5	1.45
125	1.32	125	2.14
250	1.72	250	3.22
500	3.22	500	5.59
1000	5.44	1000	8.81
1500	7.38	1500	12.38
2500	10.29	2500	16.11
3500	13.60	3500	22.47
4500	16.30	4500	25.70

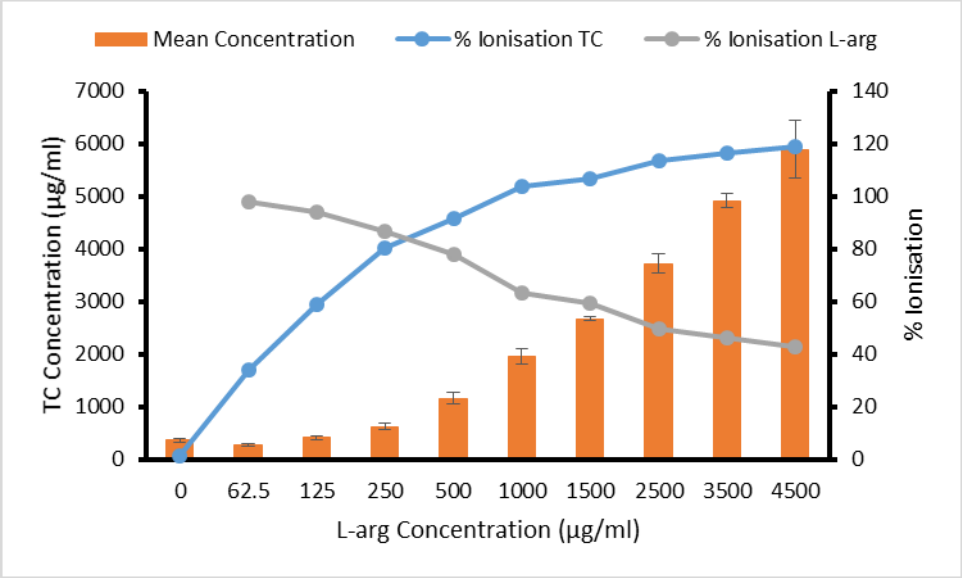

Figure 2.27: % Ionisation of TC and L-arginine. With increasing L-arginine concentration and decreasing pH, the % ionisation of L-arginine decreased whereas the % ionisation of TC increased; n=3.

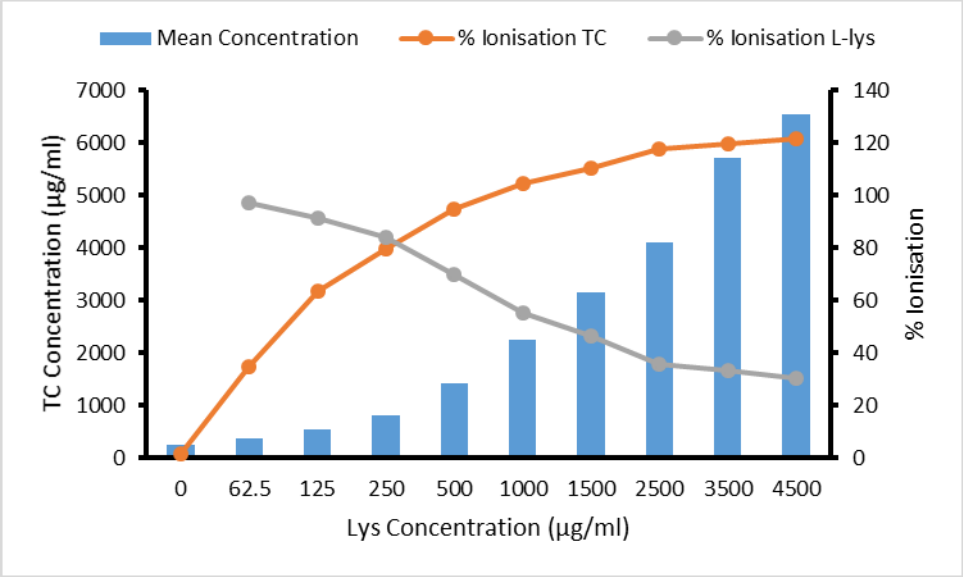

Figure 2.28: % Ionisation of TC and L-lysine. With increasing L-lysine concentration and decreasing pH, the % ionisation of L-lysine decreased whereas the % ionisation of TC increased; n=3.

2.1.3.2.3 Formation of tetracycline epimer

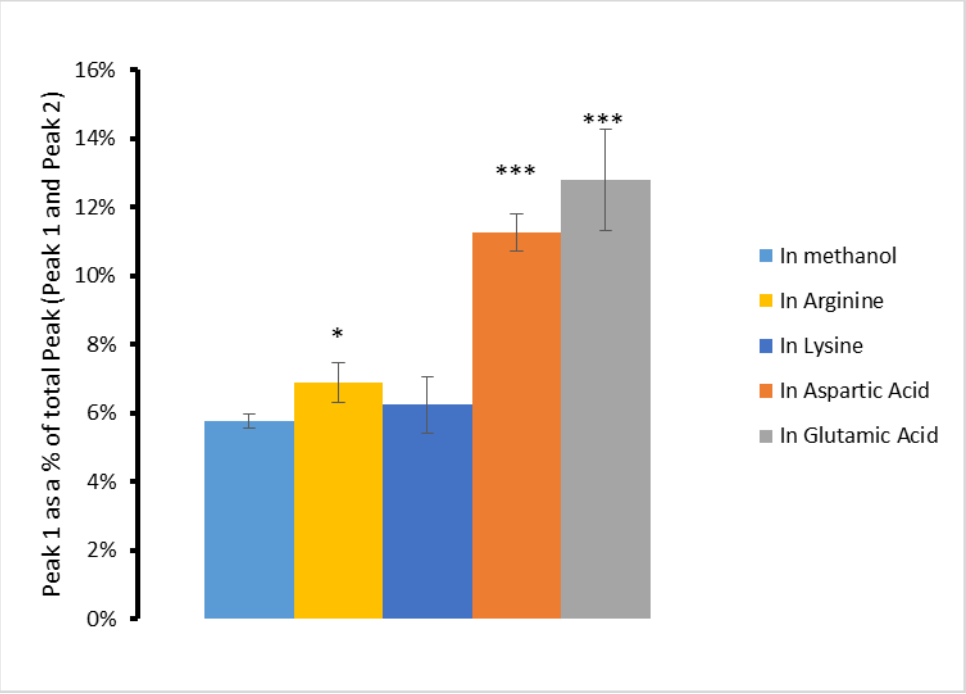

Figure 2.29: Proportion of peak 1 (ETC) as compared to the sum of peak 1 and peak 2 (TC) in different solutions; n=3.

Although an increase in solubility has been observed with both sets of amino acids, the ratio of the two peaks in the chromatogram changed significantly (Figure 2.29), in solubility

experiments conducted with acidic amino acids. With basic amino acids, such a substantial change was not observed in the ratios. When TC was analysed for obtaining calibration curves the peak area of peak 1 (ETC) was on average 5.77% (Figure 2.29; in methanol) of the total peak area; sum of peak 1 and peak 2 (TC). However this significantly increased to an average of 11.25% (p=0.000000024) and 12.78% (p=0.0000055) when analysed in L-aspartic acid and L-glutamic acid solutions respectively. The proportion of peak 1 was even greater at higher concentrations of the amino acids (results not presented).

2.1.3.3 Octanol-water partitioning

Before moving onto experimentation in bacteria, it was important to see how the partitioning of TC from water to octanol was effected by amino acids. For this purpose L-aspartic acid was used since it gave the highest enhancement in TC solubility without leading to its degradation. The concentrations used were molar ratios of 1, 2, 4, 8 and 16 of L-aspartic acid for every TC. As seen in Figure 2.30, increasing the concentration of L-aspartic acid resulted in less TC partitioning into the octanol phase and more into the water phase. This translates to a reduction in Log*P* of TC with increasing concentration of L-aspartic acid.

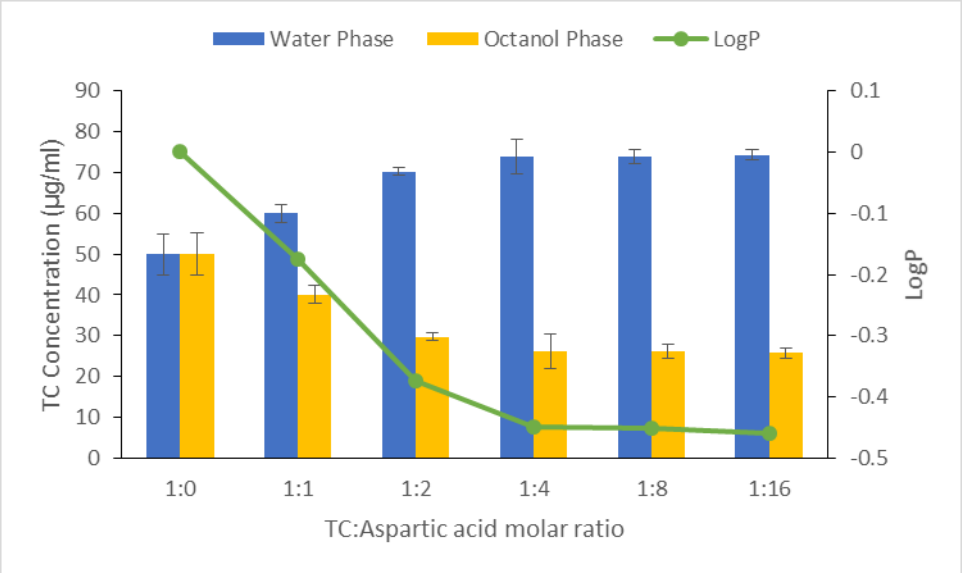

Figure 2.30: TC concentration and its log*P* values in different concentrations of L-aspartic acid. With increasing concentration of L-aspartic acid, Log*P* decreased in line with more TC partitioned into the water phase; n=3.

2.1.4 Discussion

2.1.4.1 Acidic amino acids

Although both L-aspartic acid and L-glutamic acid were able to enhance the solubility of TC, there was a considerable difference in their respective abilities to do so. Nevertheless, these results suggest that TC acted mainly as a base in the solution of both of the acidic amino acids. The results also suggest that the drug may have formed ion pairs with both L-aspartic acid and L-glutamic acid.

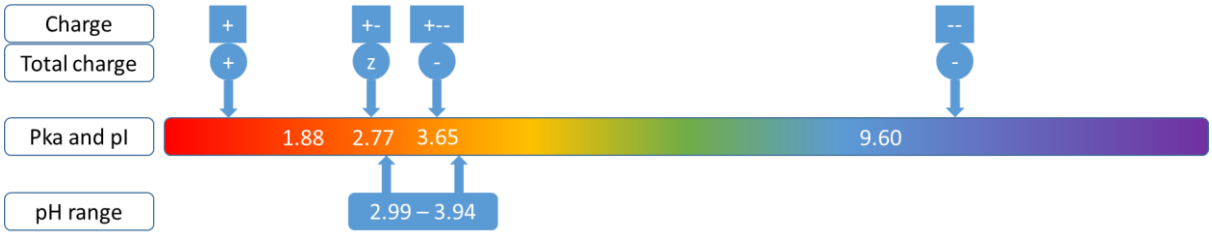

Figure 2.31: Diagram depicting the predominant charges at a given pH as well as the three ionisable sites (pK_a 1.88, 3.65 and 9.60) and the isoelectric point (2.77) of L-aspartic acid. At the pH range of 2.99-3.94, majority of L-aspartic acid was either in the zwitterionic form or the anionic form.

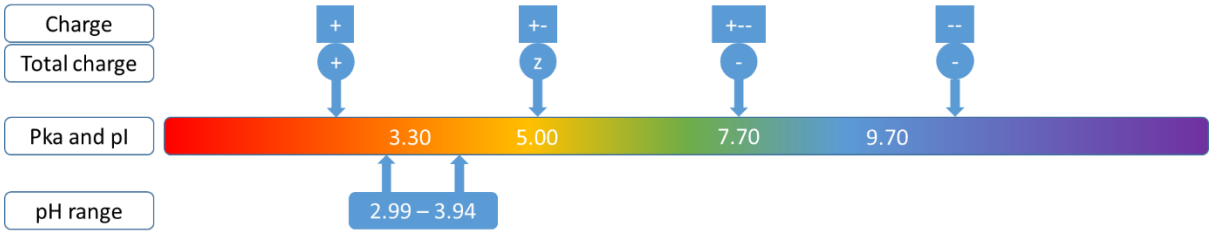

Figure 2.32: Diagram depicting the predominant charges at a given pH as well as the three ionisable sites (pK_a 3.30, 7.70 and 9.70) and the isoelectric point (5.00) of TC. At the pH range of 2.99-3.94, in L-aspartic acid-TC solution, majority of TC was in the cationic or the zwitterionic form.

Increasing L-aspartic acid concentration from 62.5µg/ml resulted in a decrease in pH from 3.94 to 2.99. In this pH range TC exists as a cation and a zwitterion in an equilibrium where the ratio of the two species depends on the pH of the solution. The reason for this is clear upon analysis of the pK_a values of TC and considering that generally an acidic group will ionise in a basic solution and a basic group will ionise in an acidic solution. With this general rule, in this pH range the basic group of TC with the pK_a of 9.70 will be greater than 99.99% ionised, since the difference between this pK_a value and the closest pH value of the solution is greater than 4 (7). With the basic group ionised, TC attains positive charge. Although the solution is

too acidic for the second acidic group of pK_a 7.7 to be ionised, the first acidic group of pK_a 3.30 is ionised in this pH range, and this gives TC a second but negative charge. However as the pH of the solution decreases with increasing concentration of L-aspartic acid, the conditions become too acidic and less favourable for even the first acidic group to be ionised. At a pH 2.99, only around 33.11% of the acidic group is ionised, and it also means that 33.11% of TC is present as the zwitterionic form. Therefore, around 66.88% of TC is present as a cation at pH 2.99. And since the amount of TC present as a cationic species increased with a decreasing pH, an increase in the apparent solubility of TC in water is observed.

The solubility of TC increases with an increasing concentration of its cationic form because there are more polar molecules which are able to interact with polar water molecules and become solubilised. Likewise, since zwitterions have zero net charge, they are unable to interact with polar water molecules. Thus it is also observed that the solubility is higher when the zwitterionic concentration is lowest, and vice versa.

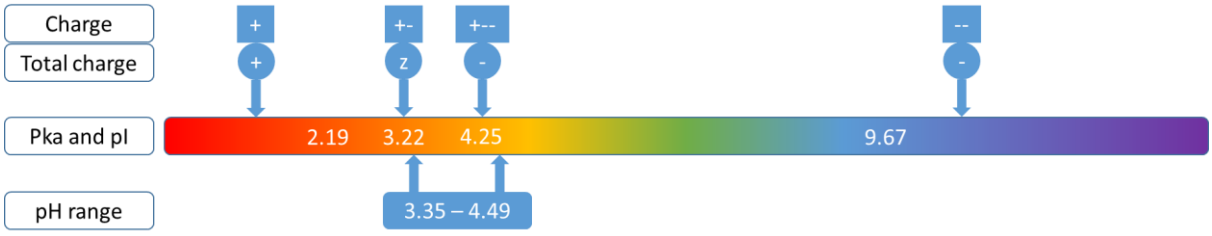

Figure 2.33: Diagram depicting the predominant charges at a given pH as well as the three ionisable sites (pK_a 2.19, 4.25 and 9.67) and the isoelectric point (3.22) of L-glutamic acid. At the pH range of 3.35-4.49, majority of L-glutamic acid was either in the zwitterionic form or the anionic form.

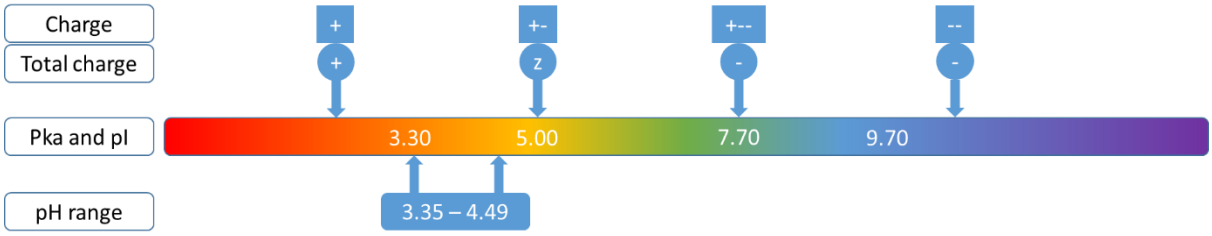

Figure 2.34: Diagram depicting the predominant charges at a given pH as well as the three ionisable sites (pK_a 3.30, 7.70 and 9.70) and the isoelectric point (5.00) of TC. At the pH range of 3.35-4.49, in L-glutamic acid-TC solution, majority of TC was in the cationic or the zwitterionic form.

As the concentration of L-glutamic acid increased from 62.5 to 4500µg/ml, the pH of L-glutamic acid-TC solution decreased from 4.49 to 3.35 respectively. Both the cationic and the zwitterionic form of TC exists in this pH range. The amount of each species is dependent upon

the pH of the solution. Analysis of the pKa values of TC, aid in the understanding of this relationship between pH and the ionic state of TC. As mentioned earlier, an acidic group will mainly ionise in a more basic solution, and vice versa. In L-glutamic acid-TC solution, the basic group of TC (pKa of 9.70) is more than 99.99% ionised, leaving TC with a positive charge. This is because the difference between the pKa of this group and highest pH value (4.49) of the solution is greater than 4 (7). Furthermore, the second acidic group of pKa 7.7 will only be 0.2% ionised at the highest pH of the pH range of this solution. The first acidic group (pKa 3.30) on the other hand will be 93.97 to 52.95% ionised, representing the increasing L-glutamic acid concentration and therefore the decreasing pH from 4.49 to 3.35 respectively. As the ionisation of the acidic group gives TC a negative charge, TC in L-glutamic acid-TC solution exists as both a zwitterion and a cation. The proportion of zwitterion is highest at the higher pH values since TC has both a positive charge and a negative charge from the ionisation of the basic and the acidic groups respectively. However, as the pH decreases, and the acidic group is less able to ionise at lower pH values, the proportion of TC in the cationic form increases and the zwitterionic form decreases. Thus increase in the cationic form of TC correlates with the enhancement of apparent solubility observed with L-glutamic acid as the counterion.

This apparent enhancement in solubility observed with increasing concentration of ionic form of TC can be attributed to the higher hydrophilicity that polar molecules have as compared to non-polar molecules. On the other hand, with higher concentrations of zwitterions, the solubility is lower. This can be attributed to the net zero charge which is exposed to the surroundings of a zwitterion; due to the positive and negative charge of the zwitterion cancelling each other out.

Although both L-aspartic acid and L-glutamic acid are acidic amino acids, there is a difference to the extent of which each one enhances the solubility of TC whilst serving as the counterion. Since polar molecules dissolve in water, the higher quantity of polar molecules that exist, the more of that molecule will dissolve. At amino acid concentration of 4500µg/ml, 66.88% of TC is ionised in the L-aspartic acid-TC solution, whilst in L-glutamic acid-TC solution 47.04% of TC is ionised. Thus herein lies the reason for the difference in solubility enhancement observed between the two amino acids; L-aspartic acid causes a higher percentage of TC to become ionised as compared to L-glutamic acid and therefore more TC dissolves in L-aspartic acid-TC solution compared to L-glutamic acid-TC solution.

Unlike TC the percentage ionisation of both acidic amino acids decreased with the increase of their concentration. Nevertheless, the total amount of ionic amino acids did increase

although their percentage ionisation decreased; due to substantial increase in the concentration of the amino acids relative to the decrease in percentage ionisation. Furthermore, although they acted as counterions for TC in terms of causing ionisation of TC, whether they acted as counterions in terms of ion pair formation with TC is not clear from these results. It is likely that ion pairs did not form. However it is also likely that ion pairing was involved in the apparent enhancement of TC solubility which was observed. For the latter case, one hypothesis may be that ion pair formation between the zwitterionic drug and ionic amino acid, or vice versa, enabled one of the zwitterionic charges to be buried whereas the second remained exposed. Thus the newly formed polar species between a zwitterion and an ion would dissolve, just like the TC which is already in ionic form. For a second hypothesis, the cationic TC forms ion pairs with anionic amino acid. Here solvation may occur like the first case (Figure 1.4A) described by Higuchi (74). TC is larger and cationic. The amino acid is anionic and since it is also smaller, it may have a greater charge per unit area compared to TC. In other words, not all of the negative charge becomes buried. Thus solvation may occur through interactions between water and this relatively negative half of the ion pair. Nevertheless, these are theories which need to be investigated through ion pair characterisation studies.

As seen in Figure 2.29, proportion of the epimer ETC significantly increased ($p<0.00001$) in both L-aspartic acid and L-glutamic acid solutions up to a concentration of 1000 µg/ml. Since the pH of these amino acid solutions ranged from 3.09 to 4.13, these findings find support in the literature which highlights that epimerisation occurs most rapidly between the pH of 2 and 6 (105). Although inactive, ETC is a non-toxic isomer of TC and the process of epimerisation is reversible, making the increase in solubility a sensible trade-off (105).

2.1.4.2 Basic amino acids

2.1.4.2.1 Solubility of tetracycline with basic amino acids over 24 hour

L-lysine was the only basic amino acid found to raise TC solubility by an appreciable amount. Surprisingly, L-arginine was not able to raise the apparent solubility of TC by a comparable amount to L-lysine, despite similar pK_a values.

The pH of L-histidine-TC solution ranged from 6.47 to 7.18, representing an amino acid concentration of 62.5 to 1000 µg/ml. Majority of TC was present in the zwitterionic form in this pH range. The largest percent (23.47%) of anionic TC was present at the pH of 7.18. In another

words since L-histidine did not greatly ionise TC, a significant rise in its solubility was not observed (p 0.1225, n = 3).

2.1.4.2.2 Evidence for tetracycline degradation with basic amino acids

Unlike the other amino acids, the change in pH with increasing concentration of L-lysine was bidirectional. Therefore the pH range of 7.04 (at 62.5 µg/ml) to 7.94 (at 1000 µg/ml) does not accurately represent an increasing amino acid concentration since at higher L-lysine concentrations the pH was below 7.94. Nevertheless throughout this concentration range, majority of L-lysine existed in the cationic form whilst some was also present in the zwitterionic form. Zwitterions exist due to both the carboxyl (pK_a 2.18) and amino (pK_a 10.53) group being ionised, giving L-lysine a negative and a positive charge respectively. However, since the pH range is greater than one less than the pKa of the second basic centre (amino group; pK_a 8.95), >90% of this group will also be charged, giving L-lysine an additional positive charge. This leaves L-lysine with an overall positive charge whilst TC was present mainly in the anionic form in this pH range. Since in this pH range, the percentage of TC which is in the ionised form (>90%) is greater than the percentage of TC in the ionised form with L-aspartic acid (66.88%) at 4500 µg/ml, it was surprising that TC did not reach as high a solubility enhancement with L-lysine (2.98 fold increase) as compared to L-aspartic acid (3.94 fold increase).

This lack of TC solubility enhancement in L-arginine solution despite similar pK_a values to L-lysine, as well as the relatively shallow rise in solubility above concentrations of 1000 µg/ml can be explained by additional observations made during the study. Previous studies suggest that colour change indicates the formation of degradation products such as ATC and EATC (103). This together with additional peaks observed in chromatograms after overnight stirring indicates that TC gradually degrades, resulting in colour change of the solution, with the degradation products showing as additional peaks. This gives reason to the deceptively low solubility of TC observed in the initial study of L-arginine and L-lysine solutions as well as the bidirectional change in pH with increase in the concentration of the amino acid.

Degradation of TC and oxytetracycline leading to red, red-brown or brown colouration in basic pH has been reported in the past (117, 118). Although photolysis and high temperature (50 °C) were suggested to be contributing to this degradation, this study found degradation to occur in the absence of light and at room temperature. In addition, both studies suggested oxidation to play a role in colour change. Observations made during this study support this

mechanism; browning of TC in basic amino acid solutions was concentrated in the air water interface, from which the degraded TC would diffuse down, allowing non-degraded TC to take its place for the cycle to begin again (Figure 2.35).

Figure 2.35: Browning of TC in L-arginine and L-lysine solutions was concentrated in the air/water interphase.

Half-life of TC has been determined in the past by Sah H to be 329.2 h (119). Although the reported half-life by Sah H is specifically for tetracycline hydrochloride, it is almost three times greater than the $t_{1/2}$ of TC in basic amino acid solutions determined in this study. Considering that the $t_{1/2}$ would be even less (data not presented), possibly under 12 h, if the rate of degradation experiment was done whilst stirring the solution, it was decided to continue the microbiology work with acidic amino acids instead. However, out of interest and to add scientific knowledge it was decided to do instant solubility experiments of TC in basic amino acid solutions. It may be that further research may lead to techniques whereby solubility enhancement ability of basic amino acids can be maintained whilst also preventing TC degradation (117).

To confirm degredation of TC, MS was carried out to analyse TC exposed to L-lysine solution at 4500 µg/ml. Majority of the peaks present in the blank sample can be either attributed to plasticisers or other background ions from the mobile phase. From those the peaks not present in the blank, peak with *m/z* of 148 can be attributed to L-lysine which has a molecular weight of 146.19. Peaks at *m/z* in fraction B and C correspond to ETC and TC. Due to their size, peaks at *m/z* 410, 417, 441, 447, 460 and 477 not present in the blank are likely to be degradation products of TC. Considering its relative abundance greater than other peaks, the major degradation peak seems to be of *m/z* 417.

For the major fragment at *m/z* 417, the change in mass from 445 is 28. This can be explained by the loss of two methyl groups from nitrogen on carbon 4 of TC. This would result in a *m/z* of 415. However, the 2 valance electrons on nitrogen may quickly allow bonding to hydrogen resulting in the observed *m/z* of 417.

Liang Y et al have shown using standards that the *m/z* of 4-epi-anhydrotetracycline hydrochloride and anhydrotetracycline hydrochloride to be 427 (103). Subtracting 36 from this, which is the predominant *m/z* for HCl, gives a *m/z* of 391. Narukawa M et al have shown that oxalic acid can be detected in the positive-ion spectrum predominantly as ions with *m/z* of 40, 24 and 12 (120). Cluster formation between C_2^+ (*m/z* of 24) and the fragment with *m/z* of 391 may be contributing to the peak at 417.

These are of course proposals. TC degradation can follow complex pathways, many of which have been proposed by Liang Y et al (103). To confirm what structures these peaks represent, NMR and IR would be needed. Nevertheless, MS results spectra do confirm the presence of degradation products whilst also validating that peak 1 and peak 2 do correspond to ETC and TC.

2.1.4.2.3 Instant solubility of tetracycline with basic amino acids

Both L-arginine and L-lysine were able to enhance the instant solubility of TC considerably. These results suggest that TC acted mainly as an acid in the solution of both of the basic amino acids and suggests that ion pair formation may have occurred between TC and both L-arginine and L-lysine.

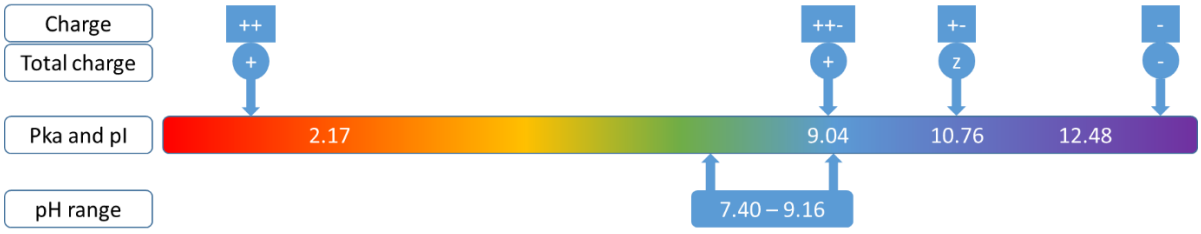

Figure 2.36: Diagram depicting the predominant charges at a given pH as well as the three ionisable sites (pK_a 2.17, 9,04 and 12.48) and the isoelectric point (10.76) of L-arginine. At the pH range of 7.40-9.16, majority of L-arginine was either in the zwitterionic form or the cationic form; proportion of zwitterion increases at higher values of this pH range.

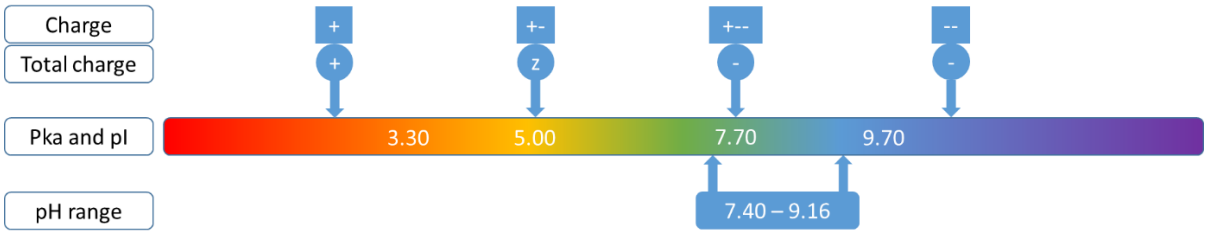

Figure 2.37: Diagram depicting the predominant charges at a given pH as well as the three ionisable sites (pK_a 3.30, 7.70 and 9.70) and the isoelectric point (5.00) of TC. At the pH range of 7.40-9.16, in L-arginine solution, majority of TC was in the cationic or the zwitterionic form; proportion of the anionic form increases as the pH in this range increases.

Increasing L-arginine concentration from 62.5µg/ml resulted in an increase in pH from 7.40 to 9.16. In this pH range TC exists as an anion and a zwitterion in an equilibrium where the ratio of the two species depends on the pH of the solution. The reason for this is clear upon analysis of the pK_a values of TC. Generally an acidic group will ionise in a basic solution and a basic group will ionise in an acidic solution. With this general rule in mind, in this pH range the acidic group of TC with the pK_a of 3.3 will be greater than 99.99% ionised, since the difference between this pK_a value and the closest pH value of the solution is greater than 4 (7). With this acidic group ionised, TC attains a negative charge. The second negative charge on TC in this pH range is dependent on the pH and is due to the second acidic group of pKa 7.7. As the pH rises from 7.40 to 9.16, ionisation of this group rises from 33.31% to 96.65%. In other words, some TC molecules have one acidic group ionised whilst some have both ionised giving them two negative charges. Ionisation of the basic group of TC (pKa 9.7) is also dependent on the pH in this pH range; with increasing pH from 7.40 to 9.16 inoisation of TC basic group decreases from 99.50% to 77.58%. This means in the pH range of L-arginine solution, some TC molecules have single negative charge and some have two negative charges whilst some also have a positive charge which acts to neutralise one of the negative charges. This computes to an overall rise in TC ionisation from 33.81% to 119.08% representing a rise in pH from 7.40 to 9.16. Note that since this percentage is a sum of percentage ionisation of both acidic groups subtracted by percentage ionisation of the basic group, the value for example of 33.81% representing TC ionisation at a pH of 7.40 does not mean that 33.81% of all TC is ionised. In actuality, the value can be higher, since the basic group can be ionised in either the TC molecule with a single charge or the TC molecule with two charges; in the latter, TC will still have an overall negative charge. The calculation therefore predicts the lowest amount of TC likely to be in the ionised form. On the other hand, TC ionisation above 100% of course does not mean that more than 100% of TC in ionised. It means that some TC molecules have two charges, and we can quite confidently assume that near to 100% if not 100% TC would be ionised in these cases. Ultimately, since the amount of TC present as an ionic (anionic)

species increased with an increase in pH, an increase in the apparent solubility of TC in water is observed.

The solubility of TC increases with an increasing concentration of its anionic form because there are more polar molecules which are able to interact with polar water molecules and become solubilised. Likewise, since zwitterions have zero net charge, they are unable to interact with polar water molecules. Thus it is also observed that the solubility is higher when the zwitterionic concentration is lowest, and vice versa.

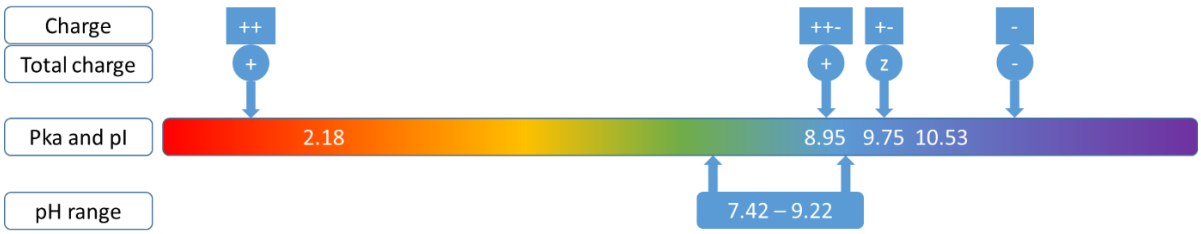

Figure 2.38: Diagram depicting the predominant charges at a given pH as well as the three ionisable sites (pK_a 2.18, 8.95 and 10.53) and the isoelectric point (9.75) of L-lysine. At the pH range of 7.42-9.22, majority of L-lysine was either in the zwitterionic form or the cationic form; proportion of zwitterion increases at higher values of this pH range.

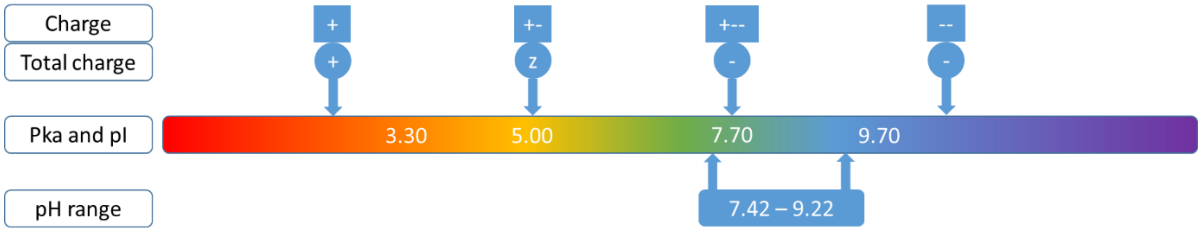

Figure 2.39: Diagram depicting the predominant charges at a given pH as well as the three ionisable sites (pK_a 3.30, 7.70 and 9.70) and the isoelectric point (5.00) of TC. At the pH range of 7.42-9.22, in L-lysine solution, majority of TC was in the cationic or the zwitterionic form; proportion of the anionic form increases as the pH in this range increases.

As the concentration of L-lysine increased from 62.5 to 4500µg/ml, the pH of L-lysine-TC solution increased from 7.42 to 9.22 respectively. Both the anionic and the zwitterionic form of TC exists in this pH range. The amount of each species is dependent upon the pH of the solution. Analysis of the pKa values of TC, aid in the understanding of this relationship between pH and the ionic state of TC. As mentioned earlier, an acidic group will mainly ionise in a more basic solution, and vice versa. In L-lysine-TC solution, the first acidic group of TC (pKa of 3.30) is more than 99.99% ionised, leaving TC with a negative charge. This is because the difference between the pKa of this group and lowest pH value (7.42) of the solution is greater than 4 (7). Furthermore, the ionisation of the second acidic group of pKa 7.7 will

change from 34.18% to 97.04% ionised as the pH of the solution increases from 7.42 to 9.22. This will leave some TC molecules with 2 negative charges. Some of these charges will be buried at this pH range by the ionisation of the basic group (pKa 9.70). The percentage ionisation of this basic group decreases from 99.48% to 75.32% as the concentration of L-lysine, and hence the pH increases from 7.42 to 9.22. As the ionisation of the basic group gives TC a positive charge, TC in L-lysine solution exists as both a zwitterion and an anion. The proportion of anionic form is highest at the higher pH values since at higher pH values, the acidic groups remain or become more ionised whereas the percentage ionisation of the basic group decreases. For the opposite reason, prevalence of the zwitterionic form is higher at lower pH values. Thus increase in the anionic form of TC correlates with the observed enhancement of apparent solubility of TC with L-lysine as the counterion.

With L-arginine and L-lysine, the apparent enhancement in TC solubility observed with increasing concentration of its ionic form can be attributed to the higher hydrophilicity that polar molecules have as compared to non-polar molecules. Polar TC molecules are able to interact with polar water molecules and become solubilised. On the other hand, with higher concentrations of zwitterions, the solubility is lower. This can be attributed to the net zero charge which is exposed to the surroundings of a zwitterion; due to the positive and negative charge of the zwitterion cancelling each other out. Hence, they are unable to interact with polar water molecules and become solubilised. Thus it is also observed that the solubility is higher when the zwitterionic concentration is lowest, and vice versa.

Unlike TC the percentage ionisation of both basic amino acids decreased with the increase of their concentration. Furthermore, although they acted as counterions for TC in terms of causing ionisation of TC, whether they acted as counterions in terms of ion pair formation with TC cannot be confirmed without experimentation. It is likely that ion pairs did not form. However it is also likely that ion pairing was involved in the apparent enhancement of TC solubility which was observed. For the latter case, one hypothesis may be that ion pair formation between the zwitterionic drug and ionic amino acid, or vice versa, enabled one of the zwitterionic charges to be buried whereas the second remained exposed. Thus the newly formed polar species between a zwitterion and an ion would dissolve as well as the TC which is already in ionic form. For a second hypothesis, the anionic TC forms ion pairs with the cationic amino acid. Here solvation may occur like the first case (Figure 1.4 A) described by Higuchi (74). TC is larger and anionic. The amino acid is cationic and since it is also smaller, it can be proposed to possess a greater charge per unit area compared to TC. In other words, not all of the positive charge becomes buried. Thus solvation may occur through interactions

between water and this relatively positive half of the ion pair. Nevertheless, these are theories which need to be investigated through ion pair characterisation studies.

2.1.4.3 Octanol-water partitioning

Octanol is widely used as a model for the membrane to determine oil-water partitioning of any given drug. A drug is more water soluble if the octanol-water partition coefficient is less than 0, whereas Log*P* greater than 0 indicates that the drug is more lipid soluble. Log*P* is a good indication for not only how freely a drug can move into a lipid membrane, but also how freely it can move out of the lipid membrane to the other side (11, 12). If Log*P* is greater than 6, the drug will readily partition into the lipid membrane, but will also find it difficult to partition out of the membrane to the other side. On the other hand if Log*P* is less than 3, its partitioning into the membrane will be very slow. Thus drugs with Log*P* values between 3 and 6 are best absorbed through the lipid membrane by passive diffusion (11, 12).

Since the solubility studies indicated L-aspartic acid to be the most appropriate counterion, partitioning of TC between the octanol and water phase was studied in L-aspartic acid solution. The results (Figure 2.30) give the Log*P* of TC as 0.0017, whereas the Log*P* of TC in L-aspartic acid solution was dependent on the concentration of the amino acid. With increasing concentration of L-aspartic acid, more TC dissolved in water and the Log*P* of TC decreased. This means that TC naturally distributes more or less equally between the aqueous and octanol phase. But in L-aspartic acid solution, TC exists in a more hydrophilic state. These results suggest and support the suggestion that TC is being ionised in L-aspartic acid solution, with the resulting polarisation increasing the drugs solubility in water, and decreasing its solubility in octanol. Further ion pair characterisation studies need to be carried out to see if any ion pair formation is occurring.

2.1.5 Conclusion

The apparent solubility of TC was found to improve with both acidic and basic amino acids. The preliminary results show that basic amino acids, L-arginine and L-lysine, are most effective in enhancing the solubility of TC. However, considering the degradation of TC which has been observed with the basic amino acids, L-aspartic acid was chosen as the optimal counterion for TC, even though the octanol-water partitioning results show that the combination of L-aspartic acid and TC results in the drug becoming more hydrophilic and therefore less able to partition into the lipid membrane.

2.2 An investigation into the synergy between tetracycline and the acidic amino acids, aspartic acid and glutamic acid, on planktonic *Staphylococcus aureus* and *Pseudomonas aeruginosa*

2.2.1 Introduction

The next phase of work was to investigate whether using amino acids as counterions leads to synergy with tetracycline on bacteria. As shown in the previous section, both basic and acidic amino acids were able to enhance the solubility of TC. Basic amino acids are greater solubility enhancers of tetracycline as compared to acidic amino acids. However, basic amino acids lead to degradation of TC over time; majority of TC degraded into toxic products within 24 hours. Considering TC is much more stable in the presence of acidic amino acids, and they act as moderate solubility enhancers of TC, these amino acids were selected whilst investigating the synergistic effect between TC and amino acids in bacteria.

For the purpose of investigating the effect of acidic amino acids on planktonic bacteria, two species, namely *S. aureus* (NCTC 8325) and *P. aeruginosa* (PA01) were chosen. The rational for this relates to the existence of intrinsic resistance in bacteria to certain antibiotics. Since resistance can be intrinsic or acquired, choosing these species allows us to investigate the effect of amino acids (AA) on the resistance to TC of intrinsically resistant *P. aeruginosa*, whilst also (see if NCTC 8325 has resistance) on a *S. aureus*, which has the ability to acquire resistance. This also allowed the investigation of AA and TC synergy in both Gram-positive (*S. aureus*) and Gram-negative (*P. aeruginosa*) bacteria.

Resistance incurred to tetracycline by bacteria can be divided into three broad categories; restriction in the access of the drug to ribosomes, binding sight alteration and TC inactivation (121, 122). Since acidic AA have been shown to increase TC solubility with the aim to enhance drug delivery, the mechanism of resistance which limits TC from accessing ribosomes captures particular interest. The access to ribosomes can be restricted by either restricting the amount of TC which permeates into the bacteria and or by utilising efflux pumps to throw back out the TC which is able to permeate (121, 122). To investigate whether AA are able to enhance drug delivery, TC accumulation was studied, which also provides insights into both drug uptake and drug efflux.

In normal circumstances the mechanism of TC uptake into the cytoplasm depends on the class to which bacteria belong; Gram-positive and Gram-negative. Since in Gram-positive

bacteria, TC only has to pass through one membrane, it can permeate via passive diffusion (123). On the other hand, in Gram-negative bacteria, TC needs to pass through two membranes, the outer and the inner to reach its target site of action. To accomplish this, TC transit occurs through two stages. The cationic stage, in chelation with magnesium, allows its passage through cation preferring porins into the periplasm. Although passive diffusion accounts for some TC being absorbed into the periplasm from the environment, the rigidity of the outer membrane restricts its extent. Once in the periplasm, the comparatively acidic state shifts equilibrium towards the neutral form of TC, allowing its diffusion into the cytoplasm through the inner membrane.

TC which does manage to reach the cytoplasm can act on ribosomes if other resistance mechanisms, mentioned above, are absent. One of these mechanism utilised by bacteria is the pumping of the drug back out and resistance is incurred when the rate of this is equal or greater than the rate of uptake (121). Tetracycline efflux pumps generally belong to the major facilitator superfamily (MFS) and span the lipid bilayer of the inner cell membrane (124). According to a 2016 review by Grossman. TH, 30 different efflux pumps specific to TC have been identified and have been split into 7 groups in accordance with their amino acid sequence and the number of transmembrane segments they possess (122). TC efflux pumps of group 1 and group 2 show the most clinical relevance. Whilst group 1 includes most common pumps found in Gram-negative bacteria such as Tet(A) and Tet(B), group 2 includes Tet(K) and Tet(L), which are the most common TC efflux pumps expressed Gram-positive bacteria (122, 124). In either case, they function as TC-H^+ antiporters to pump out TC in exchange of H^+ (122, 124).

Thus the aim of this chapter was to see if acidic amino acids act as anti-microbial agents against planktonic bacteria and whether they can be used to optimise existing antibiotics. For this we investigated the use of acidic amino acids as counterions to tetracycline, on the accumulation of the drug in planktonic *S. aureus* and *P. aeruginosa* cells. We further determined whether this translates to an effect in growth of the bacteria, whilst elucidating any other synergy between the drug and the amino acids.

Interestingly, whilst investigating the effect of amino acids on the growth of *P. aeruginosa*, pigment production was observed. Since the extent of pigment production was observed to be influenced by the concentration of amino acid used, it was decided to quantify the pigments. Pyocyanin and pyoverdine were the pigments chosen to quantify since these are the most common pigments produced by *P. aeruginosa*

2.2.2 Materials and methods

2.2.2.1 Materials

Tetracycline ≥98% (NT), L-Aspartic acid 98+% (T), L-glutamic acid 99% (N), D-(+)-glucose 99.5% GC and phosphate buffered saline tablets were from Sigma Aldrich. Ethidium bromide 10 mg/ml and tryptone soya broth was obtained from fisher scientific. KCl (sigma Aldrich), $MgCl_2$ and chloroform (fisher scientific) were gifted by technical staff. *S. aureus* strain NCTC 8325 and *P. aeruginosa* strain PAO1 was gifted by Professor Peter A. Lambert.

2.2.2.2 Determining the minimum inhibitory concentration (MIC) and minimum lethal concentration (MLC) of the amino acids and tetracycline

MIC and MLC of L-Asp, L-Glu and TC was on *S. aureus* and *P. aeruginosa* was determined. To do this, overnight cultures of *S. aureus* and *P. aeruginosa* were grown. 0.1 O.D. of each bacteria was then incubated with two-fold serial dilutions of L-Asp, L-Glu or TC. The concentrations of amino acids used ranged from 30 mM to 0.23 mM whilst the concentration of TC used ranged from 112.50 µM to 0.014 µM. TC concentration tested was capped at 112.50 µM with the solubility limitation of the antibiotic in water. Following this, the plates were incubated in a 37 °C incubator overnight. MIC was taken to be the lowest concentration with no visible growth (turbidity); generally two fold lower concentration than the MLC. To determine MLC, concentrations which showed no visible growth (turbidity) were plated on TSA agar plates and incubated at 37 °C overnight. MLC was taken to be the lowest concentration which resulted in no colony formation.

2.2.2.3 Tetracycline accumulation assay

To grow to logarithmic phase, 10 ml of overnight culture was added to 20ml of fresh TSB and incubated for one hour at 37 °C in an orbital shaking incubator. The culture was then centrifuged at 2860 g for 20 minutes and supernatant was discarded. The cell pellet was resuspended in 30 ml of 1 mM $MgCl_2$ in 0.01 M PBS. Centrifugation step was repeated following which the pellet was resuspended in 11.95 ml of same buffer. The cell suspension was split into 4 equal volumes (2.5 ml each) and to each quarter 2.5 ml of double the working concentration of the drug (made up in same buffer) along with 250µl of 1 mg/ml Ethidium Bromide (EtBr) was added. For example, if working concentration is 1mM TC, add 2.5ml of 2mM TC along with 250µl of EtBr. Aliquote 100 µl per well in 96 well plate. Observe

fluorescence every 5 minutes for 60 minutes (room temperature) at an excitation wavelength of 510 nm and an emission wavelength of 595 nm.

To check for further accumulation using amino acids, 100 µl of amino acid concentrations ranging from 30 mM to 0.23 mM made up in 1 mM $MgCl_2$, 0.01 M PBS and 100 mM glucose (to provide energy) was added to wells as required. Next 20µl of 1M KCl.was added to each well. Fluorescence was again observed as above. Controls included no drug (max AA conc), No glucose with No AA (max drug concentration used), no AA, no glucose (no drug or AA) and glucose (no drug or AA).

2.2.2.4 Growth curve susceptibility assay

Growth curves of L-Asp, L-Glu and TC were evaluated for *S. aureus* and *P. aeruginosa* in the presence of the combinations used in TC accumulation assays. To do this, overnight cultures of *S. aureus* and *P. aeruginosa* were grown. Solutions with double the working concentrations were prepared for the amino acids, TC and their combinations. 100 µL of these were then incubated with 100 µL of the culture in wells of 96 well plates. This gave working concentrations of the compounds and 0.1 O.D. of bacteria. The plates were than analysed in an incubated (37 °C) plate reader, set to read O.D. of each well every half an hour at 600 nm.

2.2.2.5 Pyocyanin Quantification

After susceptibility assay, 96 well plates were incubated in the fridge until Pyocyanin was quantified. Briefly, cell free supernatant was obtained by centrifugation at 3220 g for 10 minutes. 100 µl of chloroform was added to 150 µl of the supernatant and vigorously vortexed. The samples were then centrifuged at 2996 g for 5 minutes and the supernatant was discarded. To the remaining bottom (chloroform) layer, 60 µl of 0.2 M HCl was added, followed by vigorous vortexing. The samples were again centrifuged at 2996 g for 5 minutes and the top layer was transferred to a 96 well plate. After all the samples were processed in this manner, the 96 well plate was read for absorbance using a plate reader at 520 nm.

2.2.2.6 Pyoverdine Quantification

After susceptibility testing as described above, the 96 well plates were kept in fridge until pyoverdine was quantified. Briefly, the plates were centrifuged at 3220 g for 10 min. Cell free supernatant was transferred to Greiner black bottom plates and the concentration of

pyoverdine was quantified using a fluorescence spectrophotometer at an excitation wavelength of 395 nm and an emission wavelength of 470 nm. The results were plotted relative to control.

2.2.2.7 Statistical analysis

Statistical analysis was conducted using GraphPad Prism. Initially one way ANOVA was carried out to look for overall significance within the data. This was followed by the uncorrected Fisher's LSD test, to see where the significant difference lies. P values below 0.05 for the results were taken as statistically significant.

2.2.3 Results

2.2.3.1 MIC and MLC of *S. aureus* and *P. aeruginosa*

Concentrations of amino acids screened for MIC for each bacteria were 30, 15, 7.5, 3.75, 1.88, 0.94, 0.47, 0.23 mM whilst the concentrations of TC screened were 112.50, 56.25, 28.13, 14.06, 7.03, 3.52, 1.76, 0.88, 0.44, 0.22, 0.11, 0.055, 0.027 and 0.014 µM. Amino acid and TC concentrations were capped at 30 mM and 112.50 mM respectively, due to their solubility limitations in water. All of the amino acid concentrations that were tested for MIC and MLC were below the MIC of both *S. aureus* and *P. aeruginosa*. Working concentrations of the drug used for accumulation studies were all below the MIC determined, as presented below.

Table 2.11: TC MIC and MLC. * indicates that all concentrations tested were below MIC.

	MIC	MLC
S. aureus	7.03 µM	14.06 µM
PAO1	*	*

2.2.3.2 *S. aureus*

To assess efflux, a slightly modified accumulation assay was used which provides indirect evidence of efflux behaviour. The experiment was split into two parts, depicted on the graphs by a dashed line; first part was for 60 min and the second part was for 120 min. Whilst in the first part bacteria were loaded with EtBr by depriving them of energy needed for efflux, the second part showed whether the test substances used were able to aid in its further accumulation. Efflux of TC in *S. aureus* was investigated at the TC concentrations of 3.52, 1.76, 0.88 and 0.44 µM. To determine efflux behaviour of TC in synergism with amino acids, both L-Asp and L-Glu were used and each TC concentration was studied with amino acid concentrations ranging from 30 mM to 0.23 mM. Various controls were used to help better understand the observed patterns of efflux. The ‘no drug’ control which contained 30 mM of the respective amino acid, was used to evaluate the effect of amino acid on EtBr efflux in the absence of any competition from the drug for the efflux pump. The ‘0 mM’ AA was used to help gain insight into the effect of TC (at the concentrations used) on the efflux of EtBr in the absence of an AA, whilst ‘No Glucose and no AA’ (maximum concentration of drug only) showed this in the absence of energy. To see how efflux of EtBr is affected without any drug or AA in energised and energy deprived cells, ‘no glu’ and ‘glu’ controls were used.

2.2.3.2.1 Efflux

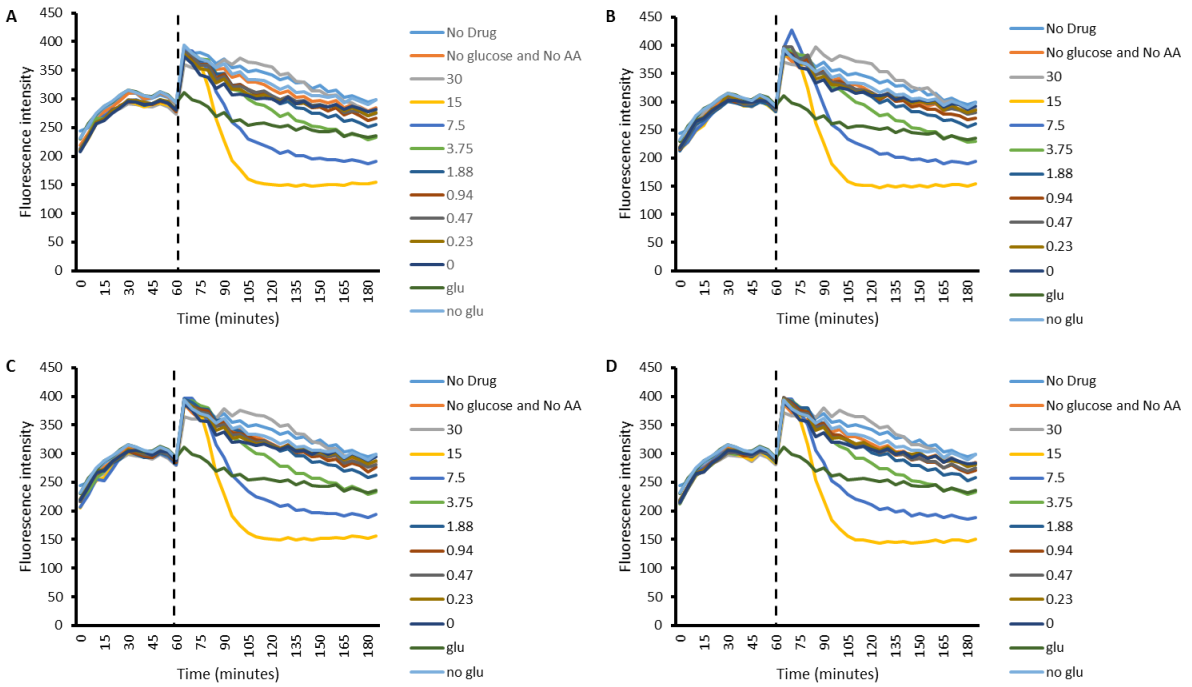

Figure 2.40: Efflux of TC in *S. aureus* using different concentrations of L-Asp (30 mM to 0.23 mM). a) 3.52 µM TC b) 1.76 µM TC c) 0.88 µM TC d) 0.44 µM TC. In the legend, numbers 0 to 30 represent amino acid concentrations in combination with respective TC concentration; n=4.

Figure 2.40 presents the efflux of TC with different concentrations of L-Asp in *S. aureus*. The pattern of efflux observed is similar (Figure 2.40a-d) irrespective of the concentration of the drug. Generally, in the second phase of the assessment, starting from the dashed line, there is a rise in intercellular EtBr, indicated by a rise in fluorescence intensity. This rise is similar to the rise in EtBr with 'no glu' used. Presence of 'glu' is the only variable which differs from this pattern; there is no substantial rise in the fluorescence intensity with 'glu' as the variable which lacks in both L-Asp and TC. The rise in fluorescence intensity is followed by a fall which varies in intensity. 15 mM L-Asp show the steepest reduction in intercellular EtBr followed by 7.5 mM L-Asp. Continuation of this pattern is observed where generally as the concentration of L-Asp is lowered, the rate of efflux of EtBr also decreases. 30 mM L-Asp is the only concentration which does not follow this pattern and has the slowest rate of reduction in fluorescence intensity. Interestingly, 'no drug' and '30 mM' amino acid follow a similar pattern. 15 mM and 7.5 mM L-Asp, once combined with TC, are the only treatments for which the fluorescence intensity decreases below the fluorescence intensity of 'glu'.

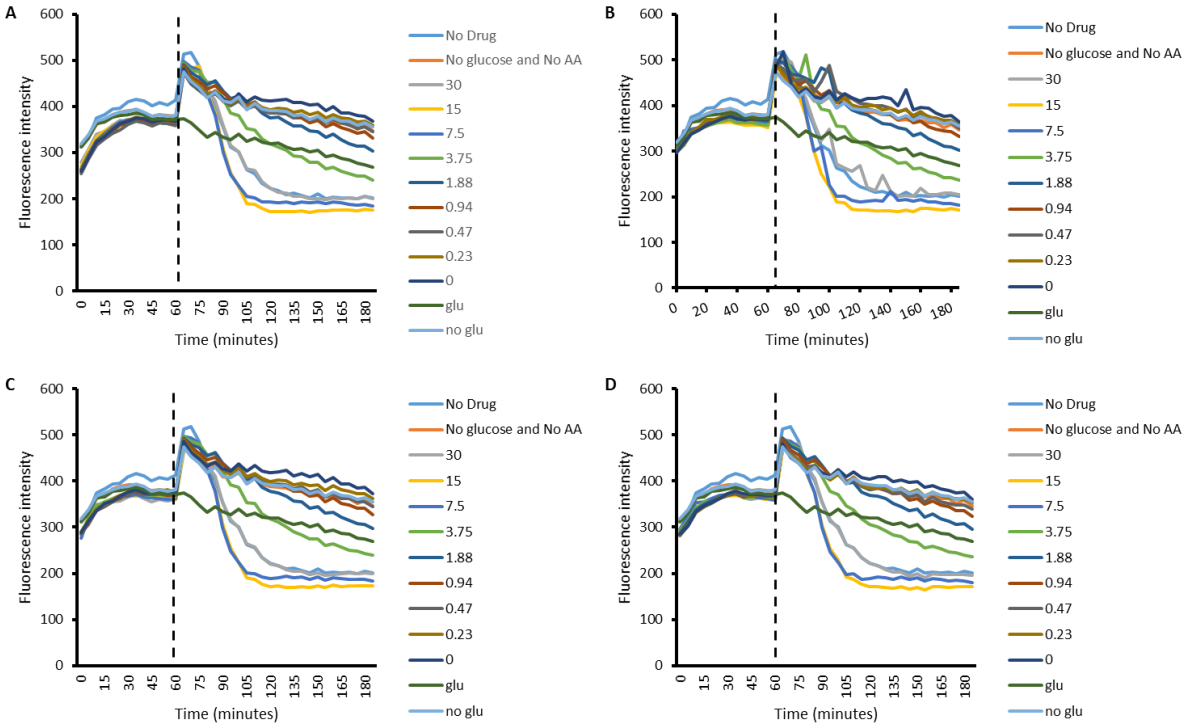

Figure 2.41: Efflux of TC in *S. aureus* using different concentrations of L-Glu (30 mM to 0.23 mM). a) 3.52 µM TC b) 1.76 µM TC c) 0.88 µM TC d) 0.44 µM TC. In the legend, numbers 0 to 30 represent amino acid concentrations in combination with respective TC concentration; n=4.

Efflux of TC by *S. aureus* in the presence of different concentrations of L-Glu is presented in Figure 2.41. The concentration of drug used (Figure 2.41a-d) does not affect the pattern of efflux observed. Like L-Asp, L-Glu causes a rise in intercellular EtBr levels with most treatments which is similar to the pattern obtained by 'no glu'; the only exception being the control 'glu' which lacks both the amino acid and the drug. A concentration dependent fall in fluorescence intensity is observed after the initial rise in the second phase of the experiment. 15 mM and 7.5 mM L-Glu show the steepest reduction in intercellular EtBr. This is followed by a pattern where generally as the concentration of L-Glu is lowered, the rate of efflux of EtBr also decreases. 0 mM L-Glu, which contains TC, shows the slowest rate of decrease in intercellular EtBr. 30 mM L-Glu is the only concentration which does not followed this patter and falls between 7.5 mM and 3.75 mM L-Glu. Interestingly, 'no drug', which contains 30 mM L-Glu and '30 mM' L-Glu follow a similar pattern. It can also be observed that the fluorescence intensity for 30 mM, 15 mM, 7.5 mM and 3.75 L-Glu and 'no drug' decreases below the fluorescence intensity of 'glu'. Also of note is that the patter observed with L-Glu is similar to the patter observed with L-Asp, except the pattern followed by 'No Drug' and '30 mM' amino acids.

2.2.3.2.2 Growth curves

To investigate how combining amino acid and TC translates to phenotypic change in *S. aureus*, growth curves were done to look for synergy between the amino acid and the drug.

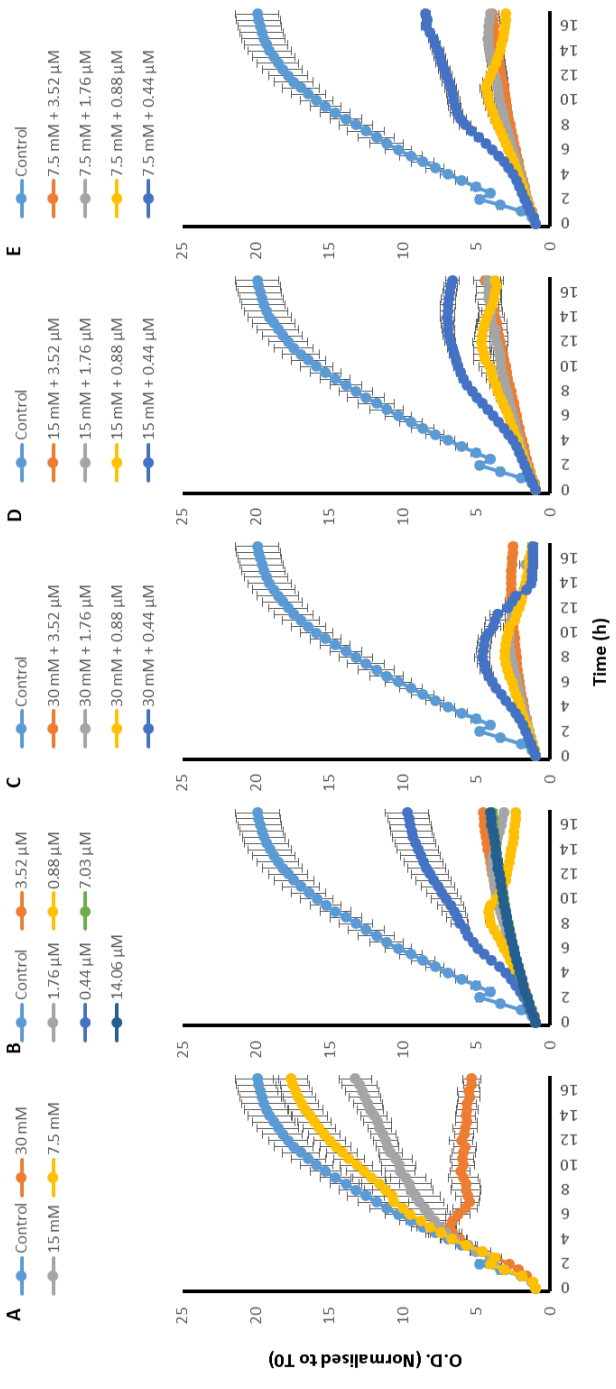

Figure 2.42: *S. aureus* growth curves with a) 30, 15 and 7.5 mM L-Asp amino acid on its own, b) with 14.06, 7.03, 3.52, 1.76, 0.88 and 0.44 µM TC on its own, c) 30 mM L-Asp combined with 3.52, 1.76, 0.88 and 0.44 µM TC, d) 15 mM L-Asp combined with 3.52, 1.76, 0.88 and 0.44 µM TC and e) 7.5 mM L-Asp combined with 3.52, 1.76, 0.88 and 0.44 µM TC; n=3.

Figure 2.42 presents the growth curves of *S. aureus* and includes curves for L-Asp on its own (Figure 2.42a), TC on its own (Figure 2.42b) and different concentrations of L-Asp combined with TC (Figure 2.42c-e) concentrations investigated in efflux experiments. L-Asp on its own (Figure 2.42a) was able to effect the growth of *S. aureus* in a concentration dependent manner where 30 mM L-Asp has the greatest effect and 7.5 mM has the lowest. TC on its own (Figure 2.42b) was also able to effect the growth of *S. aureus*. To see whether there is a synergistic effect between the amino acid and the drug, growth curves obtained by exposure to combinations (Figure 2.42c-e) were compared with growth curves obtained by amino acid (Figure 2.42a) and drug (Figure 2.42b) in isolation. Where combination showed greater reduction in growth of the bacteria compared to both the drug and the amino acid in isolation, synergy was concluded. Greatest synergy between TC and L-Asp was observed with 30 mM of the amino acid. Whilst there was a noticeable effect on the growth of *S. aureus* with 0.44 µM TC when combined with 15 mM or 7.5 mM L-Asp, a substantial effect was observed in combination with 30 mM L-Asp. With this combination (30 mM L-Asp and 0.44 µM TC), where the synergy is most prominent, the slower growth of *S. aureus*, represented by a shallower exponential phase, is followed by an early onset death phase. Combining 30 mM L-Asp with other TC concentrations also resulted in a noticeable synergistic effect.

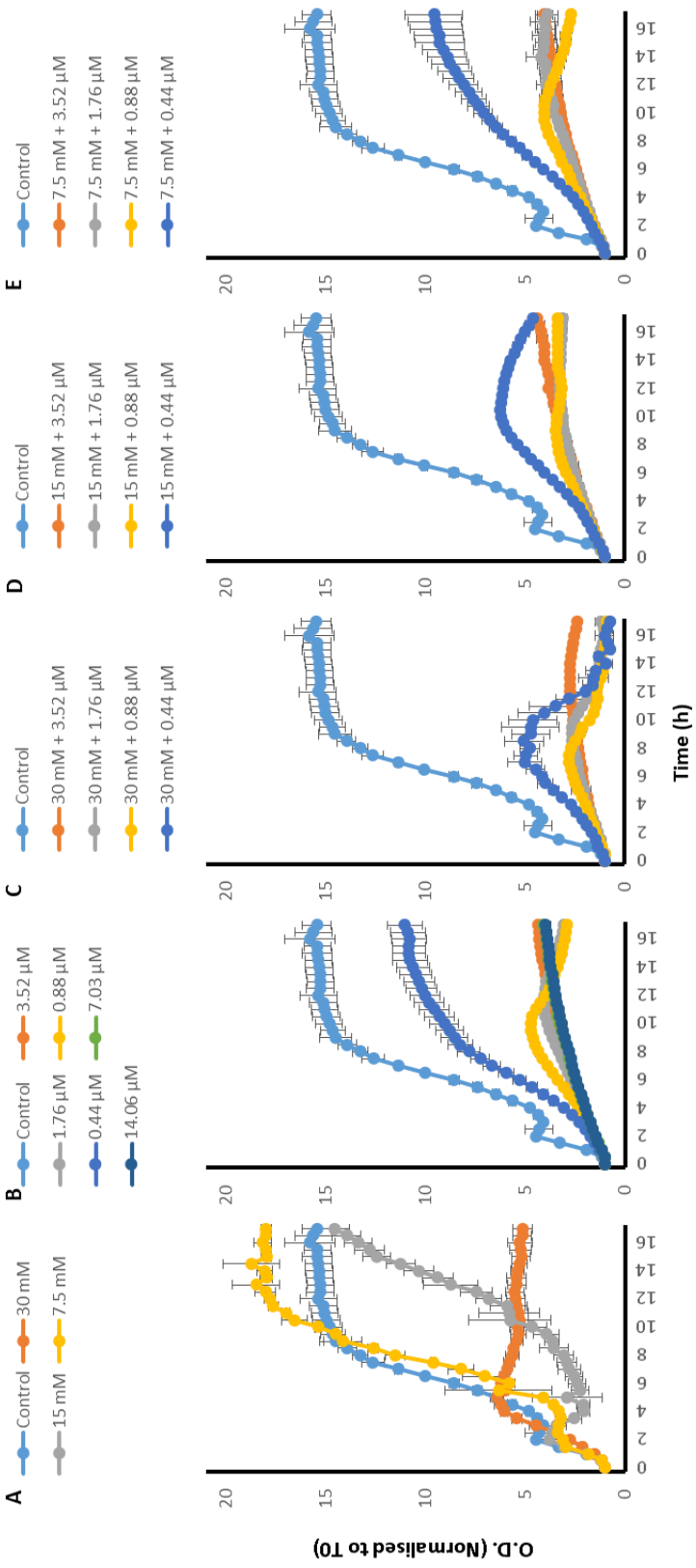

Figure 2.43: *S. aureus* growth curves with a) 30, 15 and 7.5 mM L-Glu amino acid on its own, b) with 14.06, 7.03, 3.52, 1.76, 0.88 and 0.44 µM TC on its own, c) 30 mM L-Glu combined with 3.52, 1.76, 0.88 and 0.44 µM TC, d) 15 mM L-Glu combined with 3.52, 1.76, 0.88 and 0.44 µM TC and e) 7.5 mM L-Glu combined with 3.52, 1.76, 0.88 and 0.44 µM TC; n=3.

Figure 2.43 presents the growth curves of *S. aureus* when exposed to L-Glu, (Figure 2.43a), TC (Figure 2.43b), and L-Glu and TC combinations (Figure 2.43c-e). Like L-Asp, L-Glu is also able to effect the growth of *S. aureus* in a concentration dependent manner. TC on its own (Figure 2.43b) is also able to effect the growth of *S. aureus*. Synergy was determined as before. Greatest synergy between TC and L-Glu is observed with 30 mM of the amino acid. Whilst there is noticeable effect on the growth of *S. aureus* with 0.44 µM TC when it is combined with 15 mM L-Glu, a greater effect is observed in combination with 30 mM L-Glu. With this combination (30 mM L-Asp and 0.44 µM TC), where the synergy is most striking, the slower growth of *S. aureus*, represented by a shallower exponential phase is followed by an early onset death phase. Combining 30 mM L-Glu with other 0.88, 1.75 and 3.52 µM TC also results in a substantial effect in the growth pattern of *S. aureus*.

2.2.3.3 *Pseudomonas aeruginosa*

For *P. aeruginosa* the concentrations of TC used were 112.50, 56.25, 28.13 and 14.06 µM.

2.2.3.3.1 Efflux

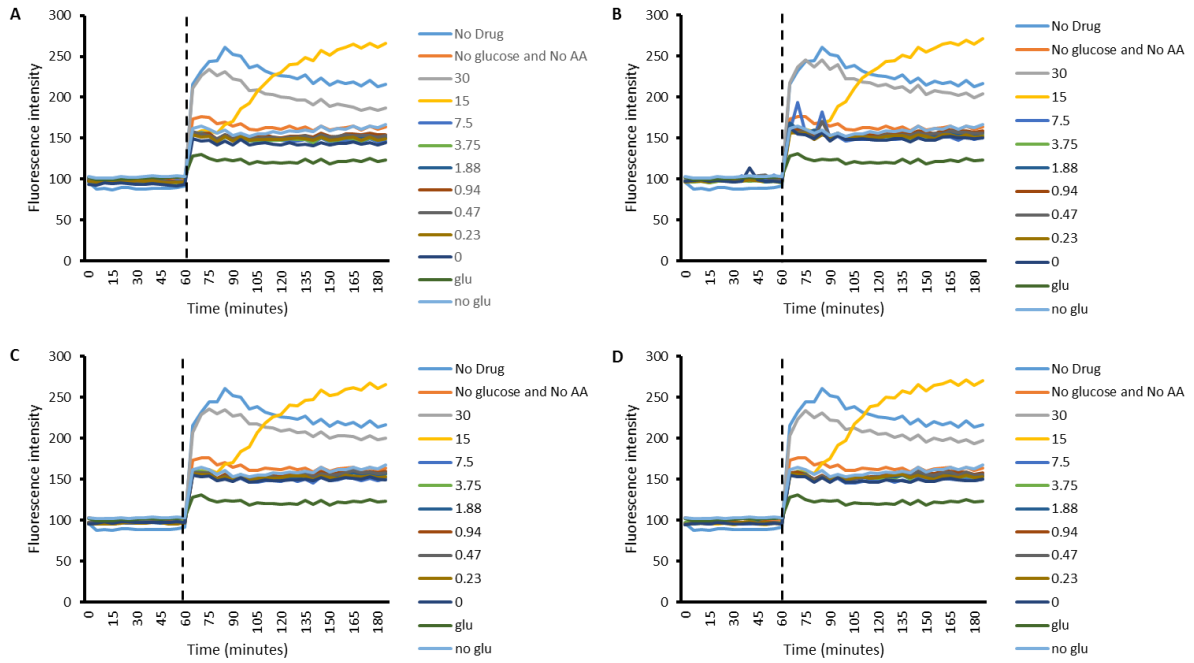

Figure 2.44: Efflux of TC in *P. aeruginosa* using different concentrations of L-Asp (30 mM to 0.23 mM). a) 112.50 µM TC b) 56.25 µM TC c) 28.13 µM TC d) 14.06 µM TC. In the legend, numbers 0 to 30 represent amino acid concentrations in combination with respective TC concentration; n=4.

Figure 2.44 presents the efflux of TC with different concentrations of L-Asp in *P. aeruginosa*. The pattern of efflux observed is similar (Figure 2.44a-d) irrespective of what concentration of drug was used, with no striking difference between TC concentrations used. Generally, in the second phase of the assessment, there is a rise in intercellular EtBr, indicated by a rise in fluorescence intensity. The steepest rise is observed for 30 mM L- Asp, which is combined with TC and 'No Drug', which contains 30 mM L-Asp on its own. Interestingly, although not substantially different, 'No Drug' reached and maintained higher fluorescence intensity compared to 30 mM L-Asp. This is followed by 15 mM L-Asp, whose fluorescence intensity continued to rise until the end of the experiment. The rise in fluorescence intensity is greatest in these three variables and is significantly greater than the rise observed with other variables, including all other L-Asp concentrations, and 'no glu' (no L-Asp and no TC). The lowest rise in fluorescence intensity was observed with the presence of 'glu' (no L-Asp and no TC) which sustained a fluorescence intensity significantly lower than all other variables.

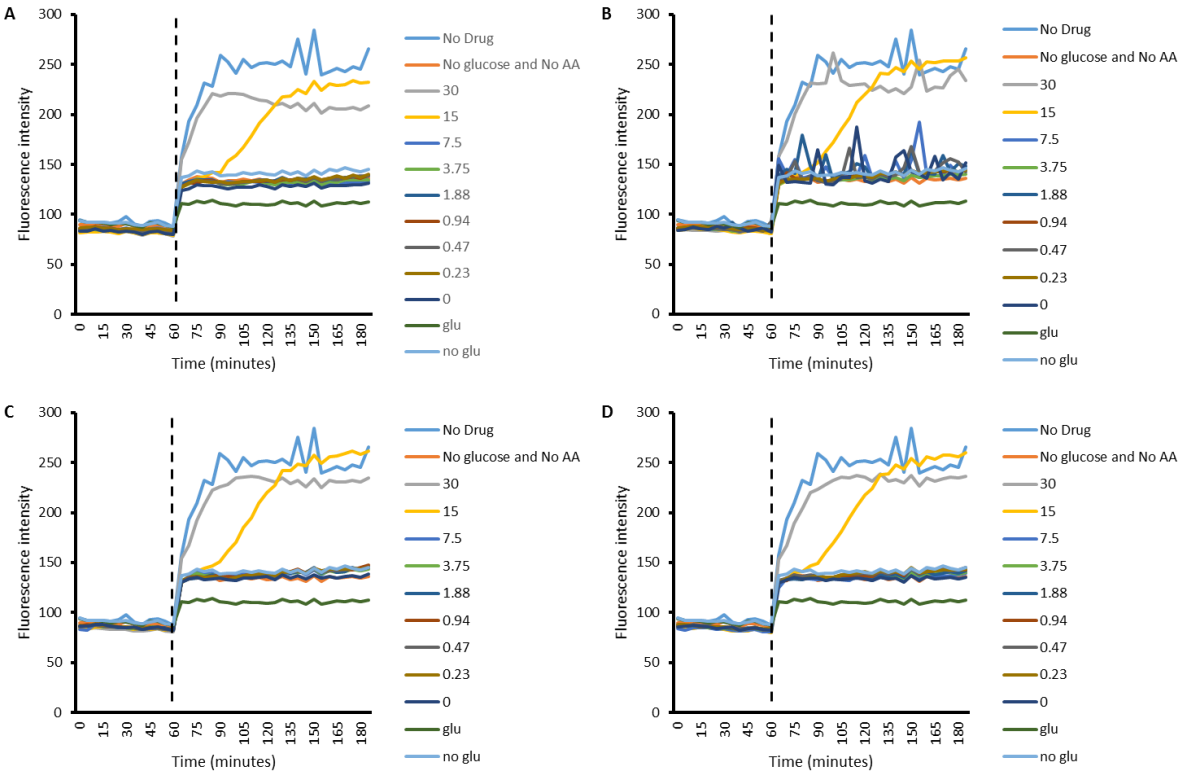

Figure 2.45: Efflux of TC in *P. aeruginosa* using different concentrations of L-Glu (30 mM to 0.23 mM). a) 112.50 µM TC b) 56.25 µM TC c) 28.13 µM TC d) 14.06 µM TC. In the legend, numbers 0 to 30 represent amino acid concentrations in combination with respective TC concentration; n=4.

Efflux experiments of TC with *P. aeruginosa* were also carried out in the presence of L-Glu and the results are presented in Figure 2.45. Again, the concentration of TC used did not affect the efflux patter observed (Figure 2.45a-d). Like with L-Asp, and following similar pattern, the steepest rise in fluorescence intensity is observed for 30 mM L-Glu and 'No Drug' which contains 30 mM L-Glu. This is followed by 15 mM L-Glu. The rise in fluorescence intensity is greatest in these three variables and pattern is strikingly different from that observed with other variables. As expected the lowest rise in fluorescence intensity was observed with the presence of 'glu' (no L-Glu and no TC) which sustained a fluorescence intensity significantly lower than all other variables.

2.2.3.3.2 Growth curves

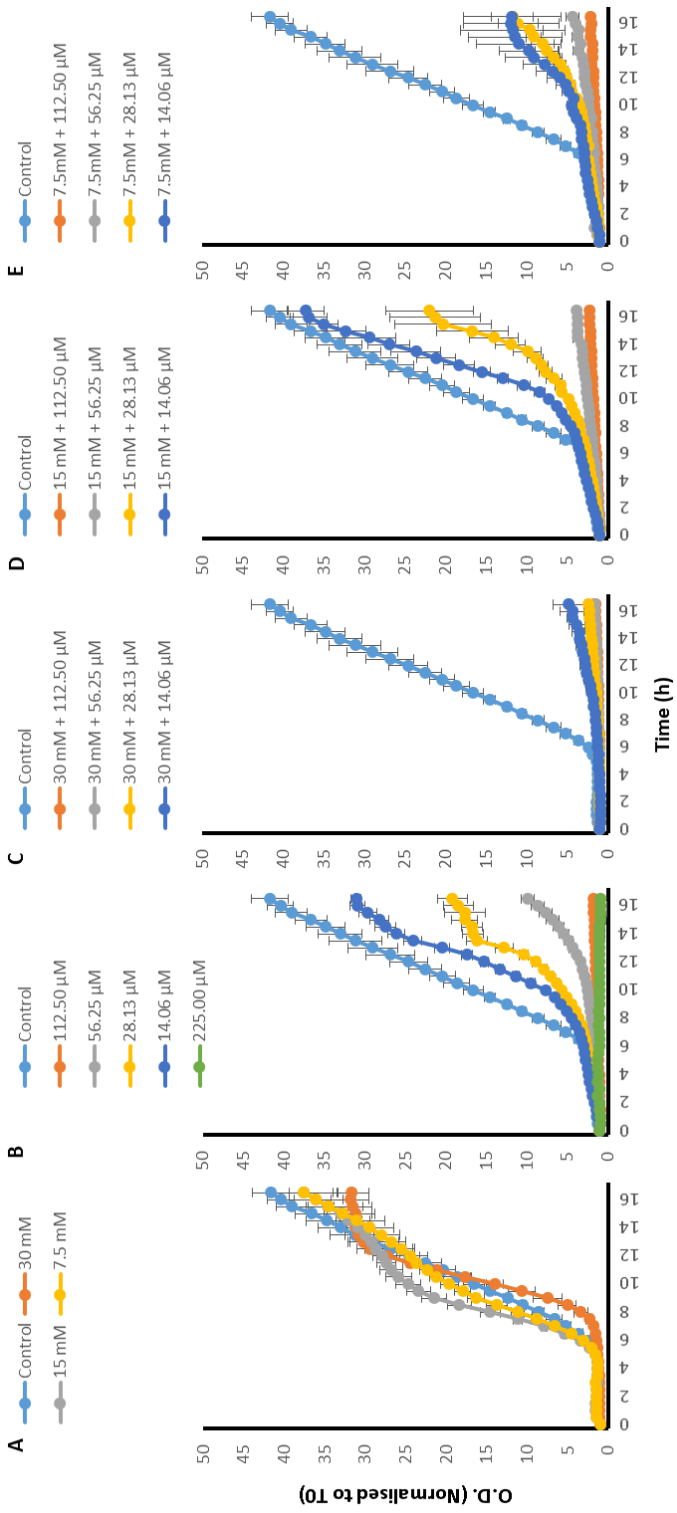

Figure 2.46: *P. aeruginosa* growth curves with a) 30, 15 and 7.5 mM L-Asp amino acid on its own, b) with 225.00, 112.50, 56.25, 28.13 and 14.06 µM TC on its own, c) 30 mM L-Asp combined with 112.50, 56.25, 28.13 and 14.06 µM TC, d) 15 mM L-Asp combined with 112.50, 56.25, 28.13 and 14.06 µM TC and e) 7.5 mM L-Asp combined with 112.50, 56.25, 28.13 and 14.06 µM TC; n=3.

Figure 2.46 presents the growth curves of *P. aeruginosa* and includes curves for L-Asp on its own (Figure 2.46a), TC on its own (Figure 2.46b) and different concentrations of L-Asp combined with TC (Figure 2.46c-e) concentrations investigated in efflux experiments. L-Asp on its own (Figure 2.46a) is unable to effect the growth of *P. aeruginosa*. On the other hand, TC on its own (Figure 2.46b) is able to effect the growth of *P. aeruginosa* in a concentration dependent manner where 112.50 µM TC has the greatest growth hindering effect and 14.06 µM has the lowest. To see whether there is a synergistic effect between the amino acid and the drug, growth curves obtained by exposure to combinations (Figure 2.46c-e) were compared with growth curves obtained by amino acid (Figure 2.46a) and drug (Figure 2.46b) in isolation. Where combination showed greater reduction in growth of the bacteria compared to both the drug and the amino acid in isolation, synergy was concluded. Greatest synergy between TC and L-Asp is observed with 30 mM of the amino acid. With 30 mM L-Asp, there was a substantial increase in the effectiveness of 56.25, 28.13 and 14.06 µM TC, represented by a concentration dependent strikingly shallower exponential phase. Other than this, a noticeable effect in growth of *P. aeruginosa* is also observed with 15 mM L-Asp combined with 56.25 µM TC and 7.5 mM L-Asp combined with 56.25, 28.13 and 14.06 µM TC.

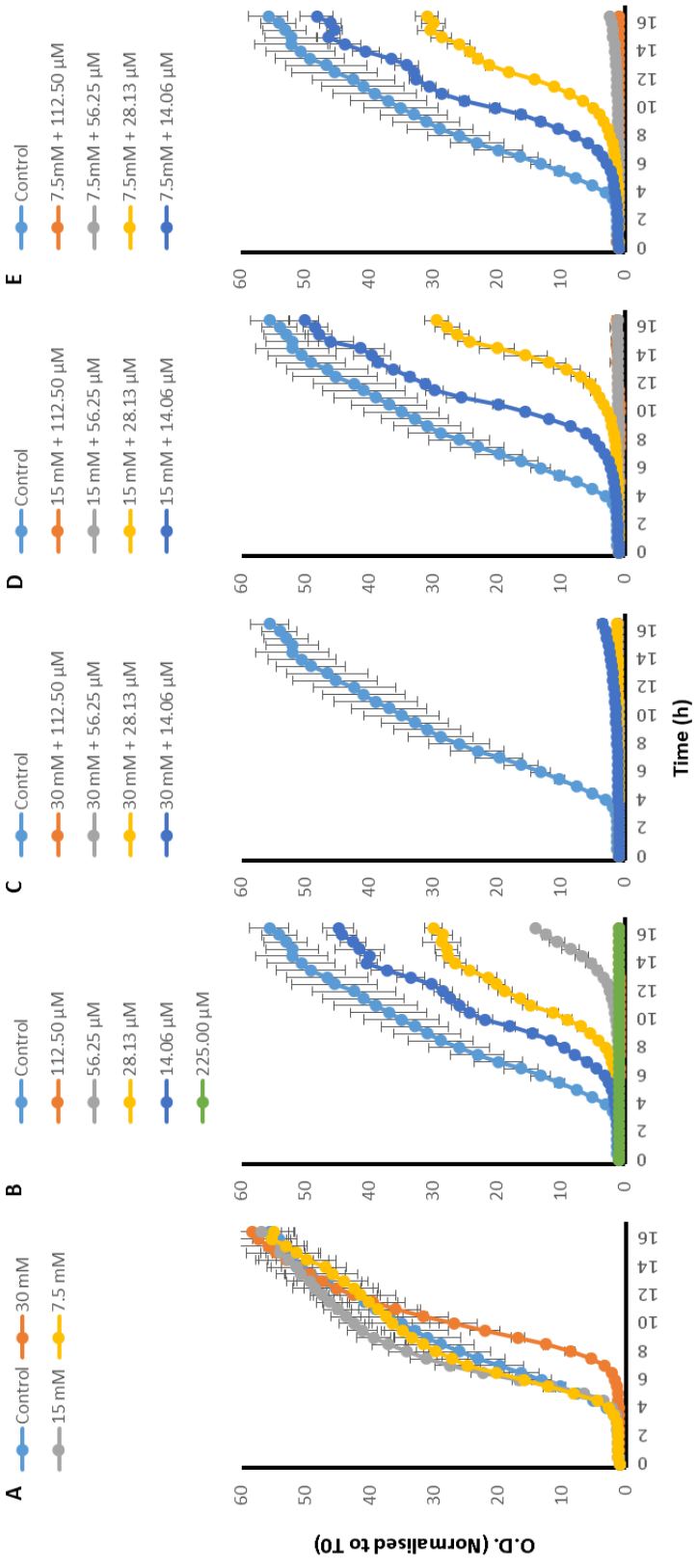

Figure 2.47: *P. aeruginosa* growth curves with a) 30, 15 and 7.5 mM L-Glu amino acid on its own, b) with 225.00, 112.50, 56.25, 28.13 and 14.06 µM TC on its own, c) 30 mM L-Glu combined with 112.50, 56.25, 28.13 and 14.06 µM TC, d) 15 mM L-Glu combined with 112.50, 56.25, 28.13 and 14.06 µM TC and e) 7.5 mM L-Glu combined with 112.50, 56.25, 28.13 and 14.06 µM TC; n=3.

Growth curves of *P. aeruginosa* are presented in Figure 2.47. The curves compare untreated growth of *P. aeruginosa* with growth in the presence of L-Glu (Figure 2.47a), TC (Figure 2.47b) and combinations of L-Glu and TC (Figure 2.47c-e). Whilst L-Glu on its own (Figure 2.47a) exhibits no effect the growth of *P. aeruginosa*, a concentration dependent inhibition is observed with TC on its own (Figure 2.47b). Synergy was again determined using the criteria described earlier. Greatest synergy between TC and L-Glu is observed with 30 mM of the amino acid. With 30 mM L-Glu, there was a significant increase in the effectiveness 56.25, 28.13 and 14.06 µM TC, represented by a substantially flatter exponential phase. There is no synergistic effect in growth of *P. aeruginosa* with 15 or 7.5 mM L-Glu.

2.2.3.3.3 Pigment production

Figure 2.48a and Figure 2.49a presents visually observed pigment production whereas Figure 2.48b and Figure 2.49b presents pyocyanin which was quantified using the chloroform and 0.2 M HCl extraction method outlined in methods section. There is a general consistency in the visually observed pigment production and the pyocyanin quantified; a more intense green colour (Figure 2.48a and Figure 2.49a) correlates with higher pyocyanin production (Figure 2.48b and Figure 2.49b). To look for statistical significance in the results, initially one way ANOVA was carried out to look for overall significance within the data. Following this uncorrected Fisher's LSD test was carried out to see where the significant difference lies. Fisher's LSD test was chosen over a test which corrects for multiple comparisons because in answering the hypothesis each comparison stood alone, such that when checking how a specific combination of amino acid and the drug compared to both its parts in isolation, its relation to other concentrations (of the amino acid, drug or any of their combinations) was not part of the hypothesis and irrelevant in answering the question posed.

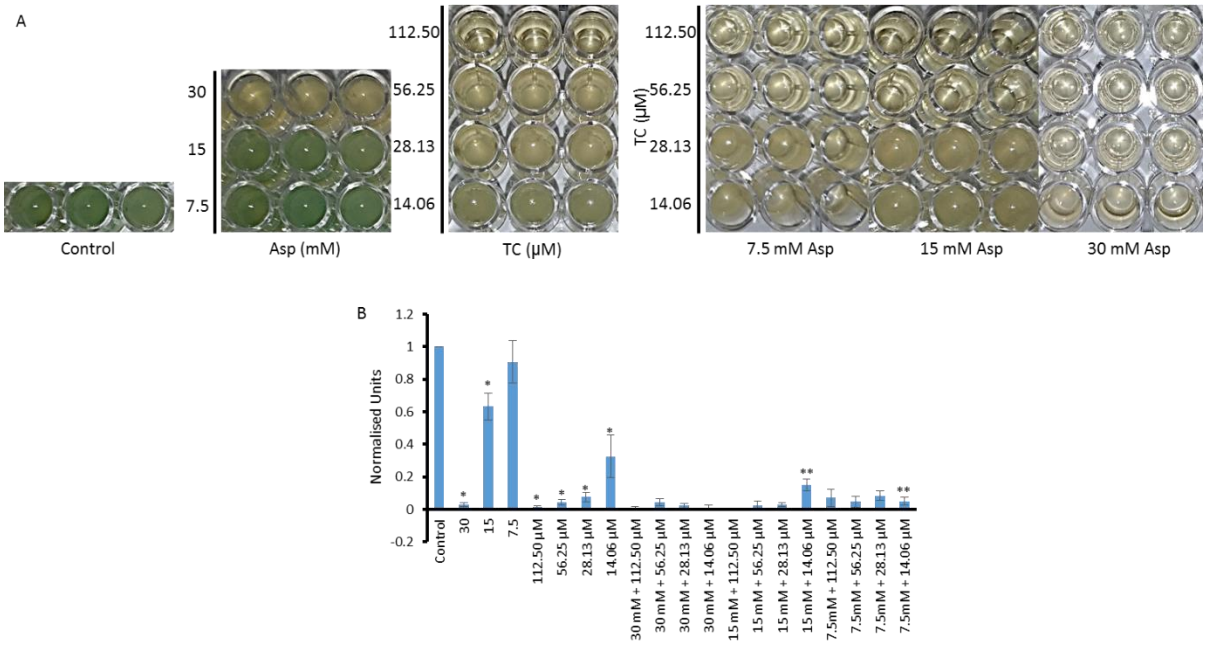

Figure 2.48: Effect of L-Asp, TC and L-Asp and TC combinations on the production of pyocyanin; n=3.

Pyocyanin production by *P. aeruginosa* in the presence of L-Asp, TC and their combinations is presented in Figure 2.48. Maximum pyocyanin production was observed with untreated *P. aeruginosa*. L-Asp and TC both used in isolation, resulted in a concentration dependent significant ($p<0.0001$) reduction in pigment production, where higher concentration of the amino acid or drug resulted in less pyocyanin production. The only concentration of L-Asp which did not show a significant reduction in pyocyanin production was 7.5 mM. To determine synergy between amino acid and drug combinations, results for L-Asp with TC were compared with the values obtained with the amino acid and the drug in isolation. Combinations which resulted in significant reduction in pigment production compared to both the amino acid on its own and the drug on its own were accepted as exhibiting positive synergy. Although synergy is observable with many L-Asp and TC combinations, statistically significant synergy was observed for 14.06 µM TC combined with 15 ($p=0.00011$) and 7.5 mM L-Asp ($p<0.0001$). Despite the combination of 15 mM and 7.5 mM L-Asp with all TC concentrations resulting in significantly lower pyocyanin production compared to the corresponding amino acid concentration in isolation, this reduction was not significant compared to the corresponding TC concentrations and hence no synergy was concluded.

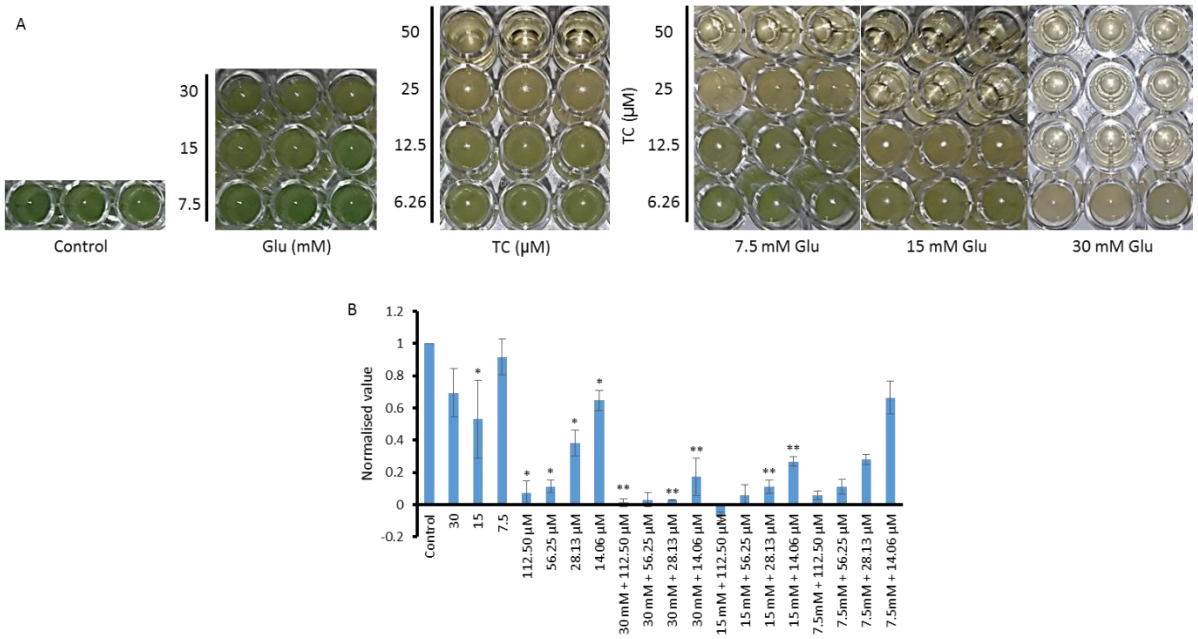

Figure 2.49: Effect of L-Glu, TC and L-Glu and TC combinations on the production of pyocyanin; n=3.

Figure 2.49 presents pyocyanin production by *P. aeruginosa* and compared the pyocyanin produced by untreated controls with that produced by L-Glu, TC and their combinations. Compared to the control, which produced most amount of pyocyanin, L-Glu on its own was able to reduce the amount of pyocyanin produced; noticeably at 30 mM and significantly at 15 mM ($p=0.034$). TC used in isolation also resulted in a significant ($p=0.000000031$, $p=0.000000047$, $p=0000015$, $p=0.00025$ for 112.50, 56.25, 28.13 and 14.06 µM TC respectively) reduction in pyocyanin production which was concentration dependent. Higher concentration of the drug resulted in less pyocyanin production. Synergy between L-Glu and TC was determined as with L-Asp. Although synergy is observable with many L-Glu and TC combinations, statistically significant synergy was observed for 30 mM and 15 mM L-Glu combined with a TC concentration of 112.50 µM ($p=0.048$ for 30 mM L-Glu only), 28.13 µM ($p=0.000011$ and $p=0.00043$ with 30 mM and 15 mM L-Glu respectively) and 14.06 µM ($p=0.000000042$ and $p=0000034$ with 30 mM and 15 mM L-Glu respectively).

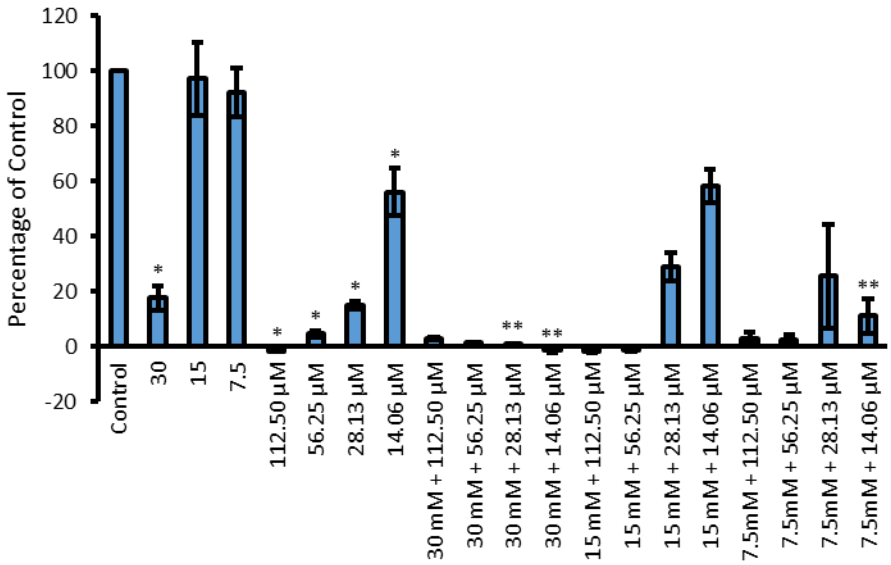

Figure 2.50: Effect of L-Asp, TC and L-Asp and TC combinations on the production of pyoverdine; n=3.

Pyoverdine production by *P. aeruginosa* in the presence of L-Asp, TC and their combinations is presented in Figure 2.50. Maximum pyoverdine production was observed with untreated *P. aeruginosa*. TC used in isolation, resulted in a concentration dependent significant ($p<0.00001$) reduction in pigment production, where higher concentration of the drug resulted in less pyoverdine production. The only concentration of L-Asp which exhibited a significant ($p=0.000012$) reduction in pyoverdine production was 30 mM. To determine synergy between amino acid and drug combinations, results for L-Asp combined with TC were compared with the values obtained with the amino acid and the drug in isolation. Combinations which resulted in significant reduction in pigment production compared to both the amino acid on its own and the drug on its own were accepted as exhibiting positive synergy. Although synergy is observable with many L-Asp and TC combinations, statistically significant synergy was observed for 14.06 µM TC combined with 30 ($p<0.00000000001$) and 7.5 mM L-Asp ($p<0.00000000001$) and 28.13 µM TC combined with 30 mM ($p=0.011$) L-Asp. Despite the combination of 15 and 7.5 mM L-Asp with all TC concentrations resulting in significantly lower pyoverdine production compared to the corresponding concentration of the amino acid on its own, the reduction was not significant compared to the corresponding TC concentrations and hence no synergy was concluded.

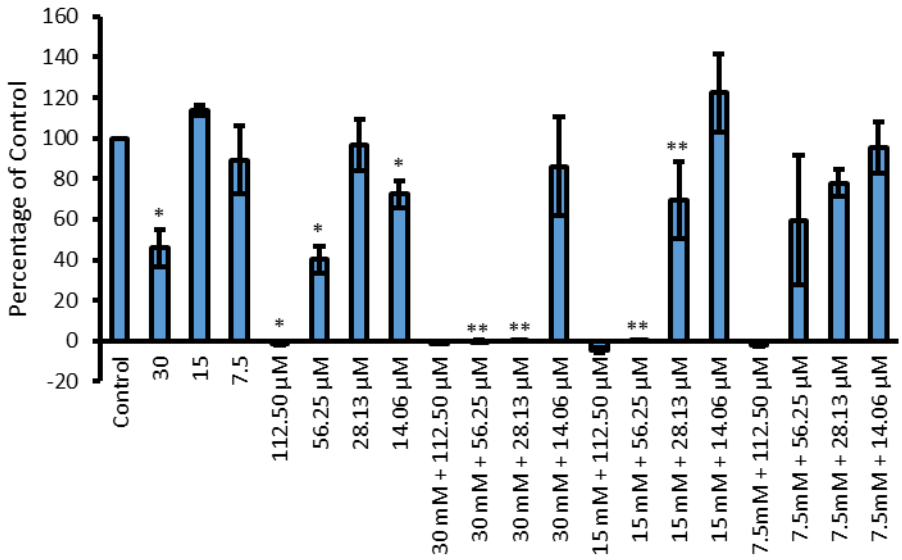

Figure 2.51: Effect of L-Glu, TC and L-Glu and TC combinations on the production of pyoverdine; n=3.

Reduced pyoverdine production was also observed with L-Glu and the results obtained with the amino acids on its own, TC on its own and their combinations is presented in Figure 2.51. Unlike the outlier 28.13 µM TC, the drug's use in isolation, generally resulted in a concentration dependent significant ($p<0.01$) reduction in pyoverdine production, where higher concentration of TC resulted in less pyoverdine production. 30 mM was the only L-Glu concentration, which when used in isolation resulted in a significant ($p=0.00070$) reduction in pyoverdine production. Synergy was determined as described above. Statistically significant synergistic reduction in pyoverdine production was seen in the middle of the four TC concentrations investigated. TC concentrations of 56.25 µM showed significant reduction in pyoverdine production in combination with 30 mM ($p=0.00035$) and 15 mM ($p=0.0004$) L-Glu when compared to the two corresponding constituents in isolation. A similar pattern was observed when 28.13 µM TC was combined with 30 mM and 15 Mm L-Glu, giving a p value of <0.00001 and 0.012 respectively.

2.2.4 Discussion

EtBr is a substrate of many efflux pumps including TC efflux pumps such as tetA (125, 126). This property allowed the indirect measurement of TC accumulation within bacteria by quantifying the amount of intracellular EtBr. Since EtBr is expected to compete with TC for being effluxed out of the cell, one can assume that higher levels of intracellular EtBr correlates with proportionally higher levels of TC within the cell.

Generally, accumulation results indicate that use of amino acids is able to raise intracellular levels of TC. This is further supported by a synergistic effect of amino acids and TC on the growth of bacteria.

Both amino acids show a similar species dependent pattern in TC accumulation hinting towards a similar underlying mechanism. The interspecies difference in the pattern observed can probably be attributed to the presence of a single membrane in *S. aureus* as compared to an outer and an inner membrane in *P. aeruginosa*. Whilst with *S. aureus* an accumulation pattern which is concentration dependent is observed, only 30 mM and 15 mM amino acids seem to effect TC accumulation in *P. aeruginosa*. This along with the fact that 30 mM amino acids enable faster accumulation of TC as compared to 15 mM, indicates that although accumulation of TC is also concentration dependent in *P. aeruginosa*, a particular amino acid threshold concentration needs to be reached.

Interestingly, with *S. aureus*, amino acid, drug or combined treatments show similar pattern to the control with no glucose, which also does not have any drug or amino acid. This shows that whatever the concentration of amino acid used, even in the presence of glucose, amino acids have a similar effect in TC accumulation as energy deplete bacteria. To add to this, increasing the concentration of amino acid seems to lead to faster efflux. Considering the bacterial growth results however, where higher amino acid concentration leads to significant reduction in bacterial growth, it is likely that this is efflux in disguise, but is in actuality cell death due to increase TC accumulation accompanied by a lowered cytoplasmic pH. Pattern observed for amino acid with *P. aeruginosa* is similar such that 0 mM to 7.5 mM show identical accumulation as the control lacking glucose. At 15 mM and 30 mM of amino acids however, EtBr accumulation is much greater. The observation that in *S. aureus* TC accumulation drops after peaking whereas in *P. aeruginosa* it does not, can be explained with the ability of Gram-negative bacteria to return cytoplasmic pH back to baseline faster than Gram-positive bacteria (127, 128). Since *P. aeruginosa* also produces detectable pigments, their production was affected synergistically with the use of amino acid and TC. The two most common pigments

of *P. aeruginosa* were quantified; pyocyanin and pyoverdine (129). The decrease in pigment production observed coincides with disruption in growth of bacteria and can be explained with fewer cells present to produce the pigments.

With 30 mM amino acid, intracellular levels of EtBr reach a higher level without the presence of TC as compared to in its presence. This is surprising since presence of TC is expected to compete with the efflux of EtBr, raising its intracellular levels. Nevertheless, this hints towards a mechanism which is efflux independent and instead involves increase rate of TC and EtBr uptake due to amino acids through mutual transporter. In such a case, presence of TC probably competes with EtBr for uptake, potentially through amino acid channels as discussed later, decreasing the amount of EtBr within the cell.

It is worth highlighting that even though the accumulation assays carried out do indicate whether amount of TC is increasing or decreasing within the cell, the assay although hints, does not conclusively distinguish between the mechanisms of this change. Elevated intracellular levels can be due both an increase in TC uptake or decrease in TC efflux. Whichever the case, raised TC levels within the cell would be detected as increased levels of intracellular EtBr. Following subsections will propose a few mechanism by which use of acidic amino acids L-Asp and L-Glu may have led to an increased uptake or a decreased efflux of TC. The likelihood that the results observed are due to a combination of both an increase in TC uptake and a decrease in its efflux cannot be ruled out.

2.2.4.1 Increase in tetracycline uptake through porins

To understand how the amino acids may be aiding in TC uptake it is important to understand the general mechanism TC uptake. *P. aeruginosa* is a Gram-negative bacteria which has two membranes; an outer membrane and an inner membrane. These membranes differ in their selectivity as barriers (130). Furthermore, the outer membrane is asymmetric, such that its inner leaflet is composed of phospholipids whereas its outer leaflet is composed of lipopolysaccharides (41). The inner membrane on the other hand is a bilayer of phospholipids. This makes the outer membrane more rigid as compared to the inner membrane and confers it comparatively more resistance to passive diffusion of hydrophobic compounds (130). This means that although an uncharged molecule may pass through the inner membrane, its ability to reach the inner membrane is somewhat hindered by the outer membrane. The outer membrane contains porins and interestingly, Mortimer and Piddock showed that porins OmpF, OmpC and PhoE are involved in the uptake of TC (130, 131). Loss of both OmpF and OmpC

reduced TC accumulation whilst in their absence, presence of PhoE enhanced TC accumulation within the cells. Interestingly, OmpF and OmpC show preference for cation uptake over anion uptake for *Escherichia coli* (*E. coli*), whilst the porin OprF of *P. aeruginosa* shows a similar preference for cations (132). Protein F plays a role in antibiotic uptake from the outer membrane and has also been suggested as a major route for the uptake of hydrophilic substances (132, 133). Furthermore, the loss of the porin OprF, also referred to in literature as protein F, has been suggested to be significant in reducing the outer membrane permeability (134). Also aiding in the influx of cationic species through the outer membrane is the presence of a high level of anions within the periplasm (135). This confers the outer membrane an interior-negative Donnan potential, which has been suggested to drive the movement of cationic species such as positively charged magnesium chelates of TC from outside of the cell into the periplasm (136, 137). It is worth noting that Mortimer and Piddock also suggest that the accumulation of a significant amounts of TC, albite a fraction of the wildtype, within cells in the absence of all major porins suggests that other mechanisms in TC uptake through the outer membrane are also involved (131). Once inside the periplasm, the drug can now work its way through the inner membrane into the cytoplasm. The concentration of the drug within the cytoplasm is in equilibrium with the periplasm (136). Whilst the mechanism of uptake through the inner membrane has been attributed to the proton motive force (PMF), this PMF seems create a pH difference which serves to keep magnesium chelated TC within the cytoplasm as opposed to aiding movement of TC through the inner membrane; lower pH in the periplasm created by the PMF shifts the equilibrium such that TC preferentially exists in the uncharged and lipophilic form which after passively diffusing through the inner membrane, forms positively charged magnesium chelates that are unable to diffuse back out (122, 137-139). In other words, it seems that PMF does not directly provide energy for the transport of TC, instead it indirectly leads to TC accumulation by preventing its diffusion back out. Argast and Beck support that the uptake of TC within bacteria is via passive diffusion which is energy independent (140). They also suggest that part of this uptake can be attributed to TC binding to phospholipids.

In view of this, a mechanism through which acidic amino acids may be enhancing TC uptake in *P. aeruginosa* is presented here. TC has three ionisable sights consisting of two acidic groups (pKa 3.3 and 7.7) and one basic (pKa 9.7). In the concentrations where substantial increase in accumulation (Figure 2.44 and Figure 2.45) was witnessed, the pH of the external solution was around 3. At this pH in accordance to the Henderson Hasselbalch equation, one acidic group (pKa 3.3) would be 33.39% ionised whilst the other (pKa 7.7) would be 0.002% ionised. The basic group on the other hand would be 100% protonated, resulting in an overall 66.61% of TC to be present in the cationic form. This cationic TC moves through porins such

as OprF through the outer membrane of *P. aeruginosa* aided by the Donnan potential attracting positively charged species into the periplasm. Once in the periplasm, the comparatively higher pH shifts the equilibrium of TC towards the unionised form which is able to passively diffuse through the phospholipid bilayer of the inner membrane.

However, Wilks and Slonczewski have shown that in *E. Coli* the pH of the cytoplasm and periplasm drops to a similar pH of the environment it is exposed to (128). Although the pH of cytoplasm shoots back to near baseline under a minute, followed by a more gradual reversion of the pH towards the baseline, the pH of the periplasm stays low for up to 5 minutes. Thus influx of hydrogen ions in the presence of cationic amino acids may negate the Donnan potential needed for TC to penetrate into the periplasm. Nevertheless, other mechanisms of cationic transport through porins are possible. Modelling shows that cations are attracted to negative charges in the pores, suggesting that cations don't just simply diffuse (141, 142). It is likely that under normal conditions, both mechanism would be involved in the movement of TC to the periplasm. Furthermore, if the pH of the periplasm in *P. aeruginosa* also drops with exposure to the acidic amino acids, equilibrium would not be expected to shift towards the unionised form of TC. In this case the 33.39% of TC which has zero net charge would be expected to diffuse through and may be what gives rise to the TC accumulation observed (Figure 2.44 and Figure 2.45). The actual percentage of TC with zero net charge would be slightly higher than this since periplasmic pH does not actually reach as low at the environmental pH (128).

Also, acidic pH has been linked to porin closure. However many of these studies are regarding the porin OmpF (142). To add to this, no effect on OmpT at low pH values suggests that the effect of pH on the porin varies from porin to porin (143). With this in mind and the observed increase in intracellular TC accumulation with exposure to acidic amino acids, makes it likely that OprF in *P. aeruginosa* may not close in response to lowered pH. Interestingly, porins like OmpF and OmpC can also close in response to voltage, whereas OprF has been shown to not be voltage gated (132, 142).

2.2.4.2 Amino acid and tetracycline ion pairing

Another mechanism leading to elevated intracellular TC levels may be uptake via amino acid channels. Uptake of prodrugs through amino acids channels such as ATB(0,+) has been reviewed in depth by Ganapathy et al. ATB(0,+) are amino acid channels with a broad substrate specificity (denoted by B) recognising both neutral (denoted by 0) and cationic amino

acids (denoted by +). Although anionic aspartic acid and glutamic acid is unlikely to be recognised by this transporter, Hatanaka et al. have shown that once these amino acids are neutralised by esterification, they are able to interact with ATB(0,+) (144, 145). This was concluded by inhibition of the transport of another ATB(0,+) substrate, glycine, in the presence of aspartate and glutamate derivatives (144). Furthermore, bacteria have many amino acid transporters belonging to both MFS and ATP-binding cassette superfamilies which are able to transport both amino acids and their derivatives (146, 147). With this in mind, a mechanism allowing uptake of TC through amino acid transporters can be proposed. Considering that at L-Asp and L-Glu concentrations of 30 mM and 15 mM, a substantial percentage of these amino acids exist in the anionic form whilst many TC molecules exist in the cationic form, a neutral ion pair is able to form between these two oppositely charged species. It is likely that such an ion pair may be recognised by amino acid transporters and taken up resulting in the enhanced accumulation of TC observed.

Of further interest is the observation that glutamic acid and ciprofloxacin exposure are able to upregulate the expression of PEPT2 which is a peptide transporter with broad substrate specificity (145, 148). PEPT2 has been linked to the transport of valacyclovir, which is a prodrug formed by esterification of the poorly bioavailable Acyclovir with the neutral amino acid valine (145). Lack of a peptide bond in this prodrugs suggests that a peptide bond is not a prerequisite for substrate to be recognised and transported through PEPT2 (149). Valacyclovir is also recognised by ATB(0,+), indicating that drugs can be coupled with neutral amino acids as esters through esterification at the α-carboxyl group of the amino acid, allowing the uptake of resulting prodrug through amino acid channels (145). If neutral amino acids are also able to increase the uptake of TC in the same way as the presented acidic amino acids, such a finding would be highly significant. Not only would this overcome the problem with antimicrobial resistance, it will also negate the pH related toxicity, which otherwise would make application of acidic amino acids at such concentrations impossible within the body.

2.2.4.3 Prevention of efflux by acidic amino acids

Earlier it was discussed that TC efflux pumps generally belong to the MFS of efflux pumps (122). Bazzone et al. showed that sugar/H^+ symporters, specifically those belonging to MFS, are inactivated by both alkaline and acidic pH (150). They suggested that whilst in a basic pH, the inactivation may be due to the lack of protons, an acidic environment would prevent deprotonation and inhibit further H^+ binding to the pump. They also highlighted that protonation or deprotonation is only affected by the pH of the compartment in which it is happening. For

example, if proton release is in the cytoplasm, acidic pH of the cytoplasm would restrict deprotonation whereas the external pH would have no effect (150). Keeping this in mind, it is likely that the use of acidic amino acids inhibits TC efflux pumps by creating a comparatively acidic environment which in turn prevents deprotonation both inside and outside the cell. Although, pH homeostasis keeps cytoplasmic pH of bacteria as close to neutral as possible once exposed to acidic environments, truly physiological pH is not reached for some time in both Gram-negative and Gram-positive bacteria (128, 151, 152). Reaching the original pH may even require the environment pH to be neutralised (152). This along with the finding by Bazzone et al that even slight decrease in pH decreases pump functionality supports the above hypothesis (150).

Another possible mechanism of anti-efflux activity of acidic amino acids may relate to the anionic form of the amino acid forming ion pairs with the metal Mg^{2+}. The TC efflux pump TetA is expressed by both *S. aureus* and *P. aeruginosa* (153, 154). Yamaguchi et al found that in inverted membrane vesicles bearing TetA, no uptake of $60Co^{2+}$ occurred in the absence of TC, concluding that the uptake of $60Co^{2+}$ required tetracycline efflux pumps (123, 155). If this means that TC requires chelation with metal cations for it to be effluxed, lack of Mg2+ as a result of scooping up by L-Asp^- and L-Glu^- may be hindering TC efflux and resulting in the elevated intracellular TC levels observed in the efflux experiments as well as the corresponding reduction in cell growth and pigment production.

2.2.5 Conclusion

Whilst amino acids are able to enhance the solubility of TC, in this subchapter the results present that they also act synergistically with TC to enhance its effectiveness against *S. aureus* and *P. aeruginosa*. It seems that the inhibition of growth of both bacteria and the reduction in pigment production by *P. aeruginosa* may be as a result of enhanced TC accumulation caused by L-Asp and L-Glu. It seems the underlying mechanism differs between Gram-positive and Gram-negative bacteria, and may include increased uptake of TC through outer membrane porins, increased uptake of TC as amino acid ion-pairs through amino acid transporters and inhibition of TC efflux through efflux transporters. However, what still remains to be seen is whether the synergy observed with amino acids is limited to TC or whether it is transferrable to other class of antibiotics too.

Chapter 3: Effect of acidic amino acids as counterions on the accumulation and efflux of ciprofloxacin in *Staphylococcus aureus* and *Pseudomonas aeruginosa*

3.1 Introduction

In the previous chapter, it was demonstrated that amino acids are able to increase intracellular accumulation of TC. Along with this an increase in the antimicrobial effectiveness of TC, as evident through a decrease in growth of both *S. aureus* and *P. aeruginosa* when combinations of amino acids and TC were used as compared to TC or amino acids on their own, was observed. Was the synergistic effect of amino acids limited to TC? Or can the synergy be used with other antimicrobial agents, potentially opening doors to broader applications. To investigate this, Ciprofloxacin (Cip) was chosen as it has been demonstrated in the past that its solubility and permeability can be enhanced using various amino acids (156).

Being active against both gram-negative and gram-positive bacteria, Cip (Figure 3.1) is often a widely used antibiotic for post-procedural prophylaxis (157, 158). It is also often a choice for many infections ranging from eye and ear infections to respiratory tract and urinary tract infections, as indicated by the British National Formulary (158, 159). Cip is one of the antibiotics of the fluoroquinolone class of antibiotics and is a bactericidal in effect. Its mechanism of action acts to stop DNA replication by inhibiting DNA-gyrase and DNA topoisomerase activity (160).

Figure 3.1: Chemical structure of Cip. Image taken from British Pharmacopeia (102).

However, like many other antibiotics, its future use is under threat. Resistance to Cip is on an ever increasing global rise (161, 162). Three main routes of resistance to Cip are discussed in literature. Firstly, mutations in the enzymes, DNA-gyrase and DNA topoisomerase renders the drug unable to act on these targets, allowing DNA replication to function normally (163, 164). The second mechanism involves restriction of Cip accumulation within the bacterial. This is either through restricting the amount of Cip that can penetrate into the bacteria and/or pumping back out the Cip which manages to get in (163, 164). Finally, bacteria can acquire resistance to Cip through plasmid-located genes (163, 164). Considering the role of amino acids in enhancing permeability of various drugs in caco-2 monolayers as well as buccal cell layers, the second mechanism is of most interest here (156, 165).

The route of uptake of Cip is certainly different between gram-positive and gram-negative bacteria, and can be attributed to the presence of an outer membrane in gram-negative bacteria. Whilst Cip most probably penetrates the membrane of gram-positive bacteria through passive diffusion, the mechanism needed for penetration into gram-negative is a little more complicated and has been discussed in detail in the previous chapter. Briefly, the asymmetric nature of the outer membrane in gram-negative bacteria makes it rigid and thus more resistant to passive diffusion of hydrophobic compounds (130). Due to this, drugs like Cip pass through the outer membrane using porins(164). Thus gram-negative bacteria can confer resistance by altering expression of these membrane proteins, limiting uptake of the drug (163).

Various efflux pumps have been identified to extrude fluoroquinolones in a number of bacteria. In *P. aeruginosa*, majority belong to the RND superfamily and include MexAB-OprM, MexCD-OprJ, MexEF-OprN and MexXY (163). Whereas, the MFS superfamily makes up most of the efflux identified currently in *S. aureus* and includes NorA, NorB, NorC and SdrM (163).

Thus, this highlights a mechanism which can be used to combat AMR, i.e. enhancing drug accumulation by increasing penetration of the drug through the membrane/s and/or hindering the efflux of the drug. These mechanisms are of particular interest here because as mentioned earlier, amino acids have been shown to enhance drug permeation into cells. This chapter thus studies whether amino acids can combat AMR through an accumulation enhancing mechanism and proposes the potential ways this could be occurring.

To investigate this, the effect of acidic amino acids on the efflux of Cip on planktonic bacteria was conducted. It was decided to use the same bacteria as were used for efflux experiments with tetracycline (TC); *S. aureus* (NCTC 8325) and *P. aeruginosa* (PA01). This holds the benefit that these pathogens are among the priority pathogens which the WHO listed in a bid to help focus research and development (47). To add to this, using these bacteria also allowed the investigation of L-Asp and L-Glu synergy with Cip in both gram-positive (*S. aureus*) and gram-negative (*P. aeruginosa*) bacteria. Furthermore it provides evidence as to whether mechanisms of TC and potentially Cip permeability enhancement are similar or different.

The aim of the study presented in this chapter was to evaluate whether the accumulation enhancing effect of the amino acids, as witnessed with tetracycline, was achievable with other antibiotics or whether the synergy was limited to optimising tetracycline only. For this we investigated the use of acidic amino acids as counterions to Cip and determined its effect on

the accumulation of the drug in planktonic *S. aureus* and *P. aeruginosa* cells. Along with the effect on efflux, we further evaluated any other synergistic effect, including the effect on bacterial growth, with the use of these counterions.

3.2 Materials and methods

3.2.1 Materials

Ciprofloxacin 98%, ethidium bromide 10 mg/ml and tryptone soya broth was obtained from fisher scientific. L-Aspartic acid 98+% (T), L-glutamic acid 99% (N), D-(+)-glucose 99.5% GC and phosphate buffered saline tablets were from Sigma Aldrich. KCl (sigma Aldrich), $MgCl^2$ and chloroform (fisher scientific) were gifted by technical staff. *S. aureus* strain NCTC 8325 and *P. aeruginosa* strain PAO1 was gifted by Professor Peter A. Lambert.

3.2.2 Determining the minimum inhibitory concentration and minimum lethal concentration of amino acids and ciprofloxacin

Minimum inhibitory concentration (MIC) and minimum lethal concentration (MLC) of L-Asp, L-Glu and Cip on *S. aureus* and *P. aeruginosa* was determined. To do this, overnight cultures of *S. aureus* and *P. aeruginosa* were grown. 0.1 O.D. of each bacteria was then incubated with two-fold serial dilutions of L-Asp, L-Glu or Cip. The concentrations of amino acids used ranged from 30 mM to 0.23 mM whilst the concentration of Cip used ranged from 135.81 µM to 2.12 µM. Following this, the plates were incubated in a 37 °C incubator overnight. MIC was taken to be the lowest concentration with no visible growth (turbidity); generally one two-fold dilution below MLC. To determine MLC, concentrations which showed no visible growth (turbidity) were plated on TSA agar plates and incubated at 37 °C overnight. MLC was taken to be the lowest concentration which resulted in no colony formation.

3.2.3 Ciprofloxacin accumulation assay

To bring to logarithmic phase, 10 ml of overnight culture was added to 20ml of fresh TSB and incubated for one hour at 37 °C in an orbital shaking incubator. The culture was then centrifuged at 2860 g for 20 minutes and supernatant was discarded. The cell pellet was resuspended in 30 ml 1 mM MgCl2 in 0.01 M PBS. Centrifugation step was repeated following which the pellet was resuspended in 11.95 ml of same buffer. The cell suspension was split into 4 equal volumes (2.5 ml each) and to each quarter 2.5 ml of double the working concentration of the drug (made up in same buffer) along with 250 µl of 1 mg/ml Ethidium Bromide (EtBr). For example if working concentration is 1 mM Cip, add 2.5 ml of 2 mM Cip along with 250 µl of EtBr. Aliquot 100 µl per well in 96 well plate. Observe fluorescence every

5 minutes for 60 minutes (room temperature) at an excitation wavelength of 510 nm and an emission wavelength of 595 nm.

To check for further accumulation using amino acids, 100 µl of amino acid concentrations ranging from 30 mM to 0.23 mM made up in 1 mM $MgCl_2$, 0.01 M PBS and 100 mM glucose (to provide energy) was added to wells as required. Next 20 µl of 1M KCl was added to each well. Controls included no drug (max AA conc), No glucose with No AA (max drug concentration used), no AA, no glucose (with no drug or AA) and glucose (with no drug or AA).

3.2.4 Growth curve susceptibility assay

Growth curves of L-Asp, L-Glu and Cip were evaluated for *S. aureus* and *P. aeruginosa* in the presence of the combinations used in Cip accumulation assays. To do this, overnight cultures of *S. aureus* and *P. aeruginosa* were grown. Solutions with double the working concentrations were prepared for the amino acids, Cip and their combinations. 100 µL of these were then incubated with 100 µL of the culture in wells of 96 well plates, in such a way that the resulting cell suspension consisted of the desired working concentrations of the test substances along with 0.1 O.D. of bacteria. The plates were than analysed in an incubated (37 °C) plate reader set to read O.D. of each well every half an hour at 600 nM.

3.2.5 Pyocyanin quantification

After susceptibility assay, 96 well plates were incubated in the fridge until Pyocyanin was quantified. Briefly, cell free supernatant was obtained by centrifugation at 3220 g for 10 minutes. 100 µl of chloroform was added to 150 µl of the supernatant and vigorously vortexed. The samples were then centrifuged at 2996 g for 5 minutes and the supernatant was discarded. To the remaining bottom (chloroform) layer, 60 µl of 0.2 M HCl was added, followed by vigorous vortexing. The samples were again centrifuged at 2996 g for 5 minutes and the top layer was transferred to a 96 well plate. After all the samples were processed in this manner, the 96 well plate was read using a plate reader at 520 nm.

3.2.6 Pyoverdin quantification

After susceptibility testing as described above, the 96 well plates were kept in fridge until pyoverdin was quantified. Briefly, the plates were centrifuged at 3220 g for 10 min. Cell free supernatant was transferred to Greiner black bottom plates and the concentration of pyoverdin

was quantified using a fluorescence spectrophotometer at an excitation wavelength of 395 nm and an emission wavelength of 470 nm. The results were plotted relative to control.

3.2.7 Statistical analysis

Statistical analysis was conducted using GraphPad Prism. Initially one way ANOVA was carried out to look for overall significance within the data. This was followed by the uncorrected Fisher's LSD test, to see where the significant difference lies. P values below 0.05 for the results were taken as statistically significant.

3.3 Results

3.3.1 MIC and MLC

Before conducting accumulation experiments, MIC and MLC of the amino acids and Cip was conducted on the *S. aureus strain* NCTC 8325 and *P. aeruginosa* strain PAO1. Concentrations of amino acids screened for MIC for each bacteria were 30, 15, 7.5, 3.75, 1.88, 0.94, 0.47, 0.23 mM whilst the concentrations of Cip screened were 0.14, 0.068, 0.034, 0.017, 0.0085, 0.0042 and 0.0021 mM. All amino acid concentrations tested were below MIC.

Table 3.1: Cip MIC and MLC.

	MIC	**MLC**
S. aureus	16.98µM	33.95 µM
PAO1	2.12µM	4.24 µM

3.3.2 *S. aureus*

Like in the TC chapter, a slightly modified accumulation assay was used for efflux assessment of Cip which allows indirect assessment of the efflux behaviour of the drug. Again the experiment was conducted in two parts. The first part was for 60 min for which bacteria were loaded with maximum EtBr by depriving them from the energy needed for efflux. The second part of the experiment was conducted for 120 min and was the main part used to assess whether the test substances used were able to effect accumulation of EtBr. The concentrations of Cip used in the assessment of efflux of Cip in *S. aureus* were 8.49 µM, 4.24 µM, 2.12 µM and 1.06 µM. The amino acids investigated for potential modulation of Cip efflux were L-Asp and L-Glu. To do this, each of the above mentioned Cip concentration were studied individually with L-Asp and L-Glu concentrations of 30 Mm,15 mM, 7.5 mM, 3.75 mM, 1.88 mM, 0.94 mM, 0.47 mM and 0.23 mM.

Along with the test compounds above, various controls were also used in a bid to better understand the observed patterns of efflux. The ‘No Drug’ control consisted of 30 mM L-Asp or L-Glu on its own and was used to gain insight into the effect of the amino acid on efflux EtBr whilst EtBr had no competition for the efflux pump in the form of Cip. On the other hand, the control ‘0 mM L-Asp or 0 mM L-Glu’ which contained Cip on its own was essential in determining whether amino acids modulated Cip efflux or not compared to Cip on its own. It

was also felt necessary to assess the efflux of EtBr in the presence (glu) and absence (no glu) of the energy source (glucose).

3.3.2.1 Efflux

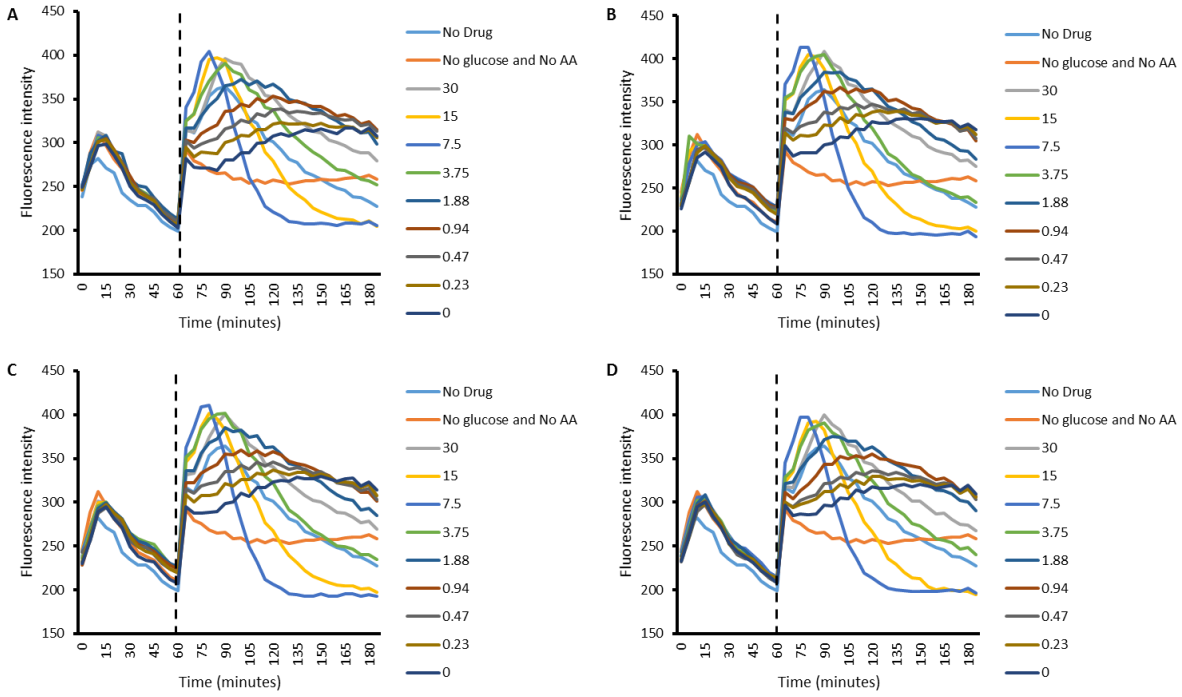

Figure 3.2: Efflux of Cip in *S. aureus* using different concentrations of L-Asp (30 mM to 0.23 mM). a) 8.49 µM TC b) 4.24 µM TC c) 2.12 µM TC d) 1.06 µM Cip. In the legend, numbers 0 to 30 represent amino acid concentrations in combination with respective Cip concentration; n=4.

Figure 3.2 presents the accumulation of Cip on its own along with its combinations with different concentrations of L-Asp in *S. aureus*. A striking observation is that the pattern of accumulation for each concentration of Cip used is similar. In other words no difference in the pattern of accumulation was observed between Cip concentration of 8.49 µM, 4.24 µM, 2.12 µM and 1.06 µM. After 60 minutes, which represents the second phase of accumulation assessment in the accumulation experiment, a general rise fluorescence intensity is observed. This indicates a rise in intracellular EtBr. After this rise, a fall in fluorescence intensity is observed, potentially indicating EtBr efflux. A concentration dependent pattern in the rise and fall of fluorescence intensity is observed between 7.5 mM L-Asp and 0 mM L-Asp; as the concentration increases the rise as well as the fall in fluorescence intensity is steeper, or it can be said that the rate of influx and efflux of EtBr decreases with a decrease in concentration of L-Asp. For some reason L-Asp concentrations of 15 mM and more so 30 mM do not follow

this pattern. It is worth noting that 0 mM L-Asp, which is basically Cip on its own shows the slowest increase and decrease in fluorescence intensity.

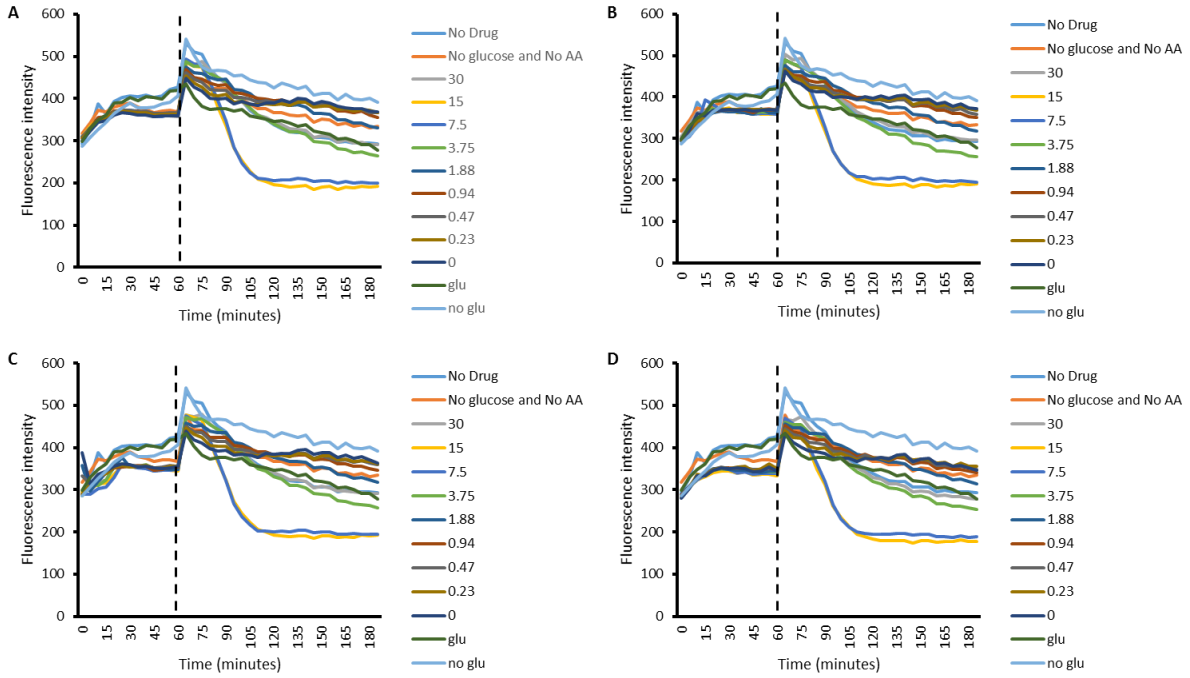

Figure 3.3: Efflux of Cip in *S. aureus* using different concentrations of L-Glu (30 mM to 0.23 mM). a) 8.49 µM TC b) 4.24 µM TC c) 2.12 µM TC d) 1.06 µM TC. In the legend, numbers 0 to 30 represent amino acid concentrations in combination with respective Cip concentration; n=4.

Efflux of Cip in *S. aureus* was also investigated in combination with different concentrations of L-Glu and is presented in Figure 3.3. Like with L-Asp, the concentration of Cip does not effect the pattern of efflux observed, only the concentration of L-Glu seems to modulate this pattern. As mentioned earlier, the second phase of the assessment (after 60 min) represents the pattern of efflux in the presence of the drug and the amino acid. In this phase, a general rise in fluorescence intensity is observed, possibly suggesting a rise in intracellular EtBr levels. Whilst lack of glucose (no glu) follows a similar pattern, least increase in fluorescence intensity is observed with the presence of glucose (glu); both of these controls lack both Cip and L-Glu, the only difference being the absence or presence of glucose, respectively. Ultimately, the rise in fluorescence intensity is followed by a gradual fall. Interestingly, 15 mM and 7.5 mM do not follow the pattern of slow reduction in fluorescence intensity and instead both show a steep reduction in fluorescence intensity which plateaus to a lower level then ever observed in part one or two of the experiment. It is also noted that 30 mM L-Glu follows a somewhat similar pattern to the no drug control. A general pattern observable in the results is that the rate of reduction in fluorescence intensity lowers with a decrease in L-Glu concentration. The main outlier in this regard is Cip in combination with 30 mM L-Glu. In other words whilst the L-Glu

concentration of 15 mM and 7.5 Mm result in fastest efflux of EtBr from within the cells, the concentrations of 0 mM, 0.23 mM and 0.47 mM show slowest efflux, only surpassed by the control (No glu) lacking energy required for efflux. The pattern of efflux observed for 15 mM and 7.5 mM L-Glu is similar to the pattern observed with L-Asp of the same concentrations, in the sense that these concentrations lead to the greatest rate of reduction in fluoresce intensity after the initial rise.

3.3.2.2 Growth curves

Although a synergy in efflux of Cip is observed between both L-Asp and L-Glu when they are combined with the drug, it raised questions with regards to whether or not this synergy translates into synergy in the effectiveness of Cip against *S. aureus*. To study this, growth curves were done to look at the effect of combining L-Asp or L-glu with the drug on the growth of *S. aureus* over a period of 16 hours.

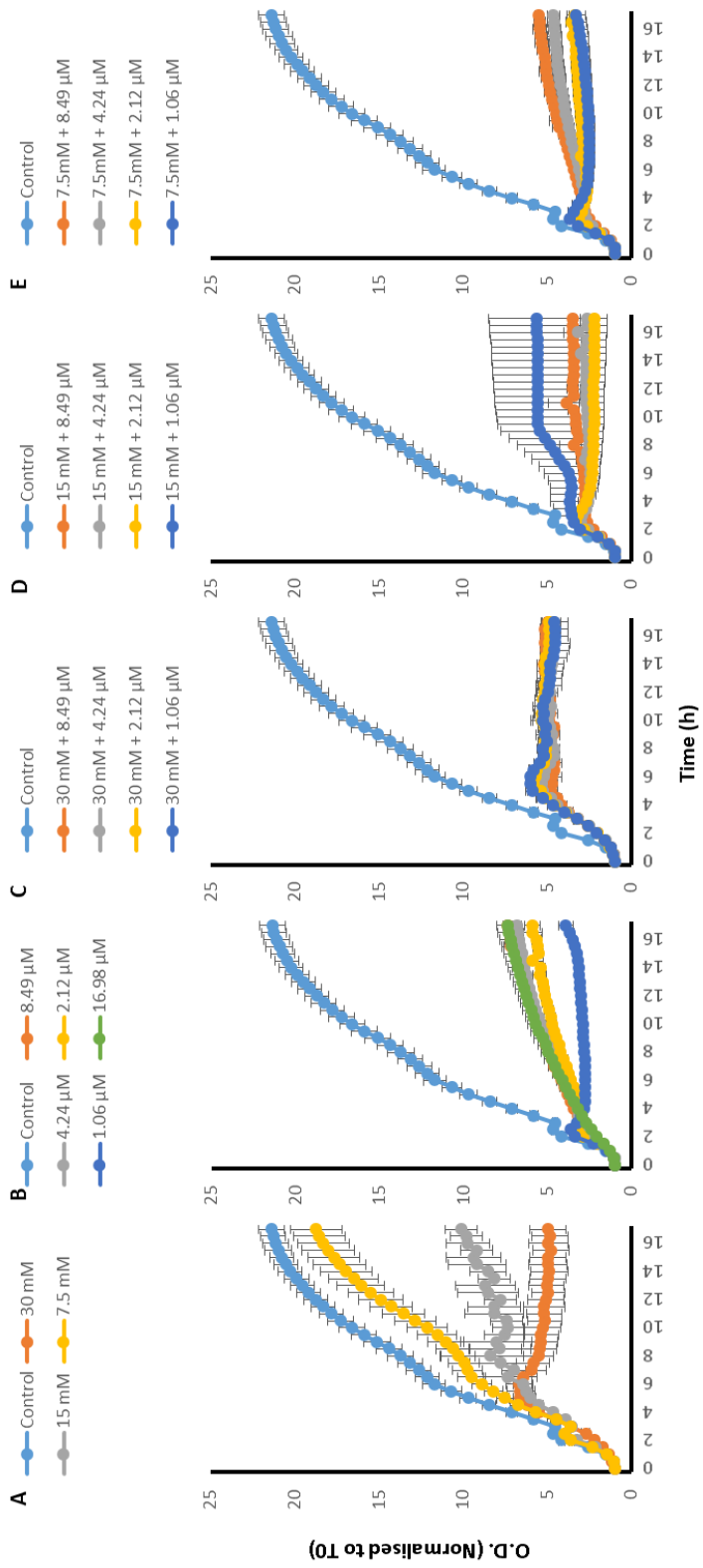

Figure 3.4: *S. aureus* growth curves with a) 30, 15 and 7.5 mM L-Asp amino acid on its own, b) with 16.98 8.49, 4.24, 2.12 and 1.06 µM Cip on its own, c) 30 mM L-Asp combined with 8.49, 4.24, 2.12 and 1.06 µM Cip, d) 15 mM L-Asp combined with 8.49, 4.24, 2.12 and 1.06 µM Cip and e) 7.5 mM L-Asp combined with 8.49, 4.24, 2.12 and 1.06 µM Cip; n=3.

Growth curves of *S. aureus* in the study with L-Asp are presented in Figure 3.4. The curves include those of L-Asp (Figure 3.4a) and Cip (Figure 3.4b) both on their own and Cip concentrations of 8.49 µM, 4.24 µM, 2.12 µM and 1.06 µM in combination with L-Asp concentrations of 30 mM (Figure 3.4c), 15 mM (Figure 3.4d) and 7.5 mM (Figure 3.4e). The curves are presented alongside each other with the same axis, enabling easy comparison between curves. A concentration dependent effect of L-Asp was observed on the growth of *S. aureus*; as the concentration of L-Asp is increased from 30 mM to 7.5 mM, a higher inhibitory effect on *S. aureus* growth is observed. On the other hand, although a concentration dependent effect is also observed with Cip alone, surprisingly, a lower concentration of Cip presents greater hindrance in the growth of *S. aureus*. Nevertheless, this shows that Cip on its own also effects the growth of *S. aureus*. Having these controls, the effect of L-Asp on its own and Cip on its own allows the comparison to their combinations when evaluating for synergistic effect. To see whether there is a synergistic effect in *S. aureus* growth when combining L-Asp and Cip, growth curves obtained by exposure to combinations (Figure 3.4c-e) were compared with growth curves obtained by the amino acid (Figure 3.4a) and the drug (Figure 3.4b) in isolation. In cases where combination showed greater reduction in growth of the bacteria compared to both the drug and the amino acid in isolation, synergy was concluded. With this rule in mind, the concentration of L-Asp which seems to present the best synergy with Cip is 15 mM, since apart from its combination with 1.06 µM Cip, the combinations noticeably hinder the growth of *S. aureus* in comparison to the corresponding Cip concentrations on their own as well as 15 mM L-Asp on its own. Combinations between 7.5 mM L-Asp and Cip, again excluding 1.06 µM Cip, also show some synergy. No synergy was observed when Cip was combined with 30 mM L-Asp.

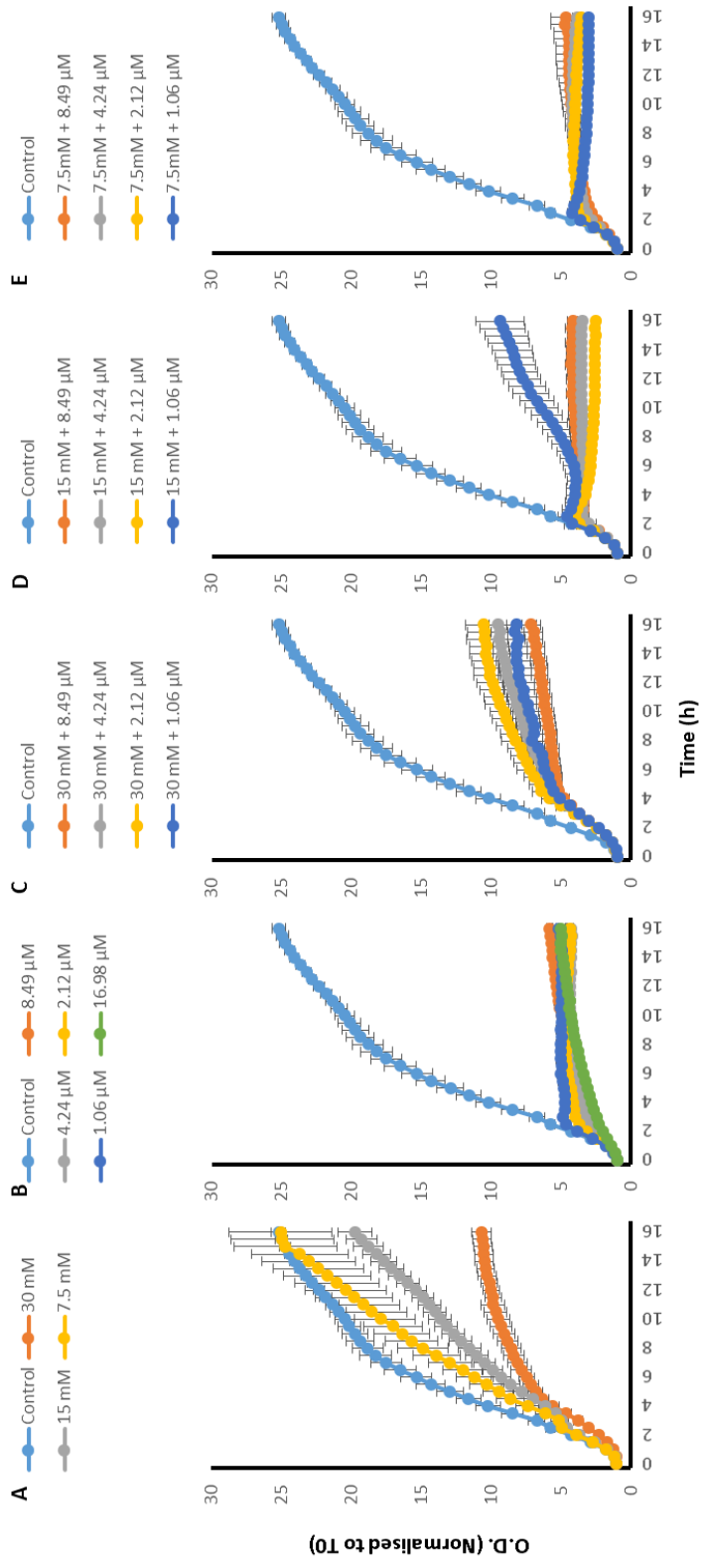

Figure 3.5: *S. aureus* growth curves with a) 30, 15 and 7.5 mM L-Glu amino acid on its own, b) with 16.98 8.49, 4.24, 2.12 and 1.06 µM Cip on its own, c) 30 mM L-Glu combined with 8.49, 4.24, 2.12 and 1.06 µM Cip, d) 15 mM L-Glu combined with 8.49, 4.24, 2.12 and 1.06 µM Cip and e) 7.5 mM L-Glu combined with 8.49, 4.24, 2.12 and 1.06 µM Cip; n=3.

When investigating the growth of *S. aureus* in the presence of L-Glu, Cip, and L-Glu and Cip combinations, similar results to those obtained with L-Asp were obtained. Figure 3.5 above presents the growth curves obtained and include those for L-Glu (Figure 3.5a) and Cip (Figure 3.5b) both on their own. To evaluate synergy, Cip concentrations of 8.49 µM, 4.24 µM, 2.12 µM and 1.06 µM in combination with L-Glu concentrations of 30 mM (Figure 3.5c), 15 mM (Figure 3.5d) and 7.5 mM (Figure 3.5e) are also presented here. Again to ease comparison between the curves, they are presented alongside each other with the same axis. Both L-Glu and Cip on its own effected the growth of *S. aureus*. However no difference was observed in the extent of growth inhibition between the different concentrations of Cip used. On the other hand, a concentration dependent inhibition in *S. aureus* growth was observed with L-Glu where apart from 7.5 mM, substantial inhibition was observed and increasing the concentration of the amino acid resulted in greater modulation of *S. aureus* growth. These curves (Figure 3.5a,b) were compared to curves obtained by combining Cip with L-Glu (Figure 3.5c-e) to look for synergy. Like before, to synergy growth curves obtained by exposure to combinations (Figure 3.5c-e) were compared with growth curves obtained by the amino acid (Figure 3.5a) and the drug (Figure 3.5b) in isolation. Combinations which showed greater reduction in growth of the *S. aureus* in comparison to both Cip and L-Glu in isolation, were concluded to exhibit positive synergy. Considering this, like with L-Asp, combining Cip with15 mM and 7.5 mM L-Glu showed best synergy where apart from combining with 1.06 µM L-Glu, all other combinations reduced *S. aureus* growth greater than their corresponding Cip and L-Glu concentrations. Cip combination with 7.5 mM L-Glu specially stands out because not only it modulates *S. aureus* growth to a similar level as 15 mM combinations does, the reduction is much greater for 7.5 mM combination than for 15 mM combination when compared to their corresponding amino acid concentration on its own; 7.5 mM L-Glu did not affect *S. aureus* much on its own. Again no synergy was observed when Cip was combined with 30 mM L-Glu.

3.3.3 *Pseudomonas aeruginosa*

Like with *S. aureus*, the possibility of synergy between the amino acids and Cip was also investigated for *P. aeruginosa*. The concentrations of Cip used were 1.06 µM, 0.53 µM, 0.27 µM and 0.13 µM. The amino acids used for to investigate this synergy were again L-Asp and L-Glu. Each Cip concentration mentioned above was studied individually as well as in combination with L-Asp and L-Glu concentrations of 30 Mm,15 mM, 7.5 mM, 3.75 mM, 1.88 mM, 0.94 mM, 0.47 mM and 0.23 mM.

3.3.3.1 Efflux

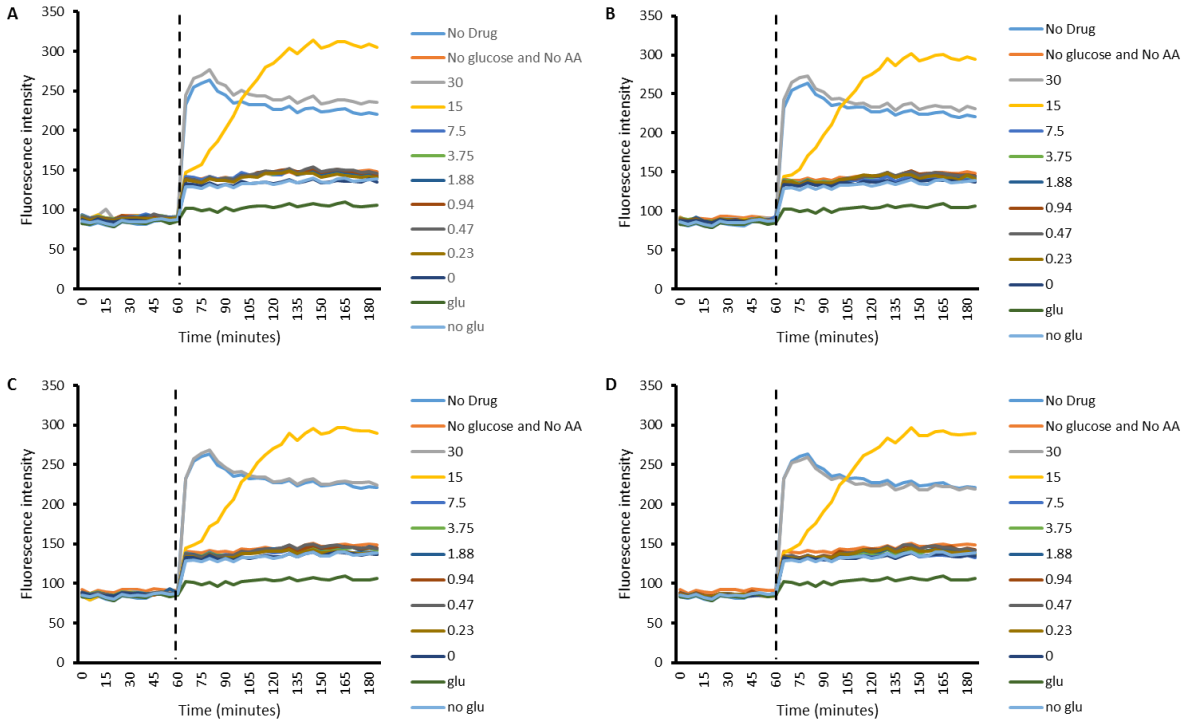

Figure 3.6: Efflux of Cip in *P. aeruginosa* using different concentrations of L-Asp (30 mM to 0.23 mM). a) 1.06 µM Cip b) 0.53 µM Cip c) 0.27 µM Cip d) 0.13 µM Cip. In the legend, numbers 0 to 30 represent amino acid concentrations in combination with respective Cip concentration; n=4.

Figure 3.6 presents the accumulation of Cip and L-Asp in *P. aeruginosa*. Results for the drug and the amino acid accumulation separately and in combinations are presented here. Figure 3.6a, Figure 3.6b, Figure 3.6c, and Figure 3.6d present Cip concentrations of 1.06, 0.53, 0.27 and 0.13 µM respectively. As with *S. aureus*, the pattern of efflux obtained from all of the Cip concentrations used is similar with no observable difference. In the second part of the accumulation experiment, a general rise in fluorescence intensity is observed, indicating a rise in intracellular accumulation of EtBr. A very distinct pattern of efflux is observed with *P.*

aeruginosa, where ‘glu’ causes a minimal rise and Cip combination with 30 mM and 15 mM L-Asp as well as ‘no drug’ which also contains 30 mM L-Asp, causes biggest increase in fluorescence intensity. The rest of the combinations, along with the energy deprived ‘no glu’ control present a moderate rise in fluorescence above ‘glu’. It is also worth noting that whilst the accumulation curve for Cip combinations with 15 mM L-Asp ends with a plateau by the end of the experiment, the curve for 30 mM L-Asp whether with Cip or without (no drug) shows a decelerating decrease in fluorescence intensity following the initial rise.

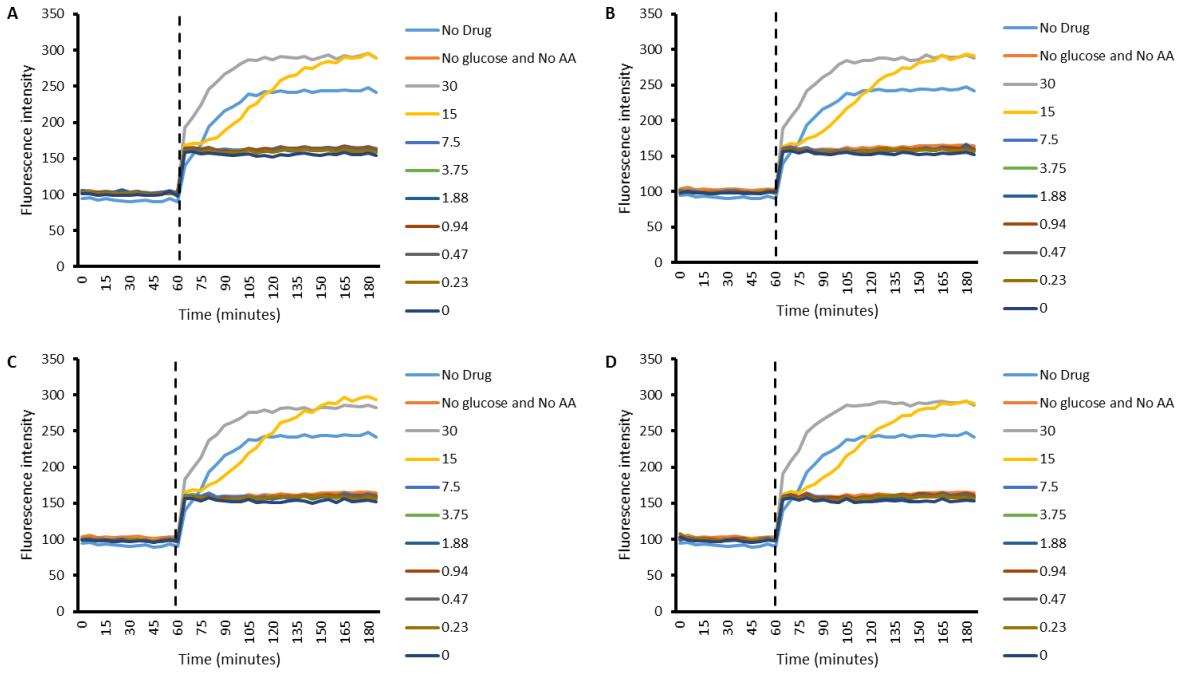

Figure 3.7: Efflux of Cip in *P. aeruginosa* using different concentrations of L-Glu (30 mM to 0.23 mM). a) 1.06 µM Cip b) 0.53 µM Cip c) 0.27 µM Cip d) 0.13 µM Cip. In the legend, numbers 0 to 30 represent amino acid concentrations in combination with respective Cip concentration; n=4.

Efflux of Cip in *P. aeruginosa* was also investigated in combination with different concentrations of L-Glu and is presented in Figure 3.7. Along with this efflux experiments were also conducted for Cip and 30 mM L-Glu on their own and these serve as controls. The concentrations of Cip used are 1.06 (Figure 3.7a), 0.53 (Figure 3.7b), 0.27 (Figure 3.7c) and 0.13 µM (Figure 3.7d). A very consistent pattern is again evident, i.e. the concentration of Cip does not affect the pattern of efflux observed, only the concentration of L-Glu seems to modulate this pattern. The second phase of the assessment (after 60 min) represents the pattern of accumulation of EtBr in the presence of the drug and the amino acid. In this a general rise in intracellular EtBr is hinted by a rise in fluorescence intensity. A very clean pattern of accumulation is observed again, like with L-Asp, where all L-Glu and Cip combinations follow the same pattern as that of Cip on its own (0 mM L-Glu). The only

deviation observed from this pattern are clearly substantial and are with Cip combinations with 30 mM and 15 mM L-Glu and 30 mM L-Glu on its own (no drug). The 30 mM combination presents with fastest rate of EtBr uptake followed by 30 mM on its own. Even though with the 15 mM combination, EtBr seems to accumulate within cells slower than with the 30 mM combination, the fluorescence intensity is equal for both by the end of the experiment, indicating that combinations allow accumulation of same amount of EtBr within the cells. Although the energised and the energy deprived controls 'glu' and 'no glu' were not included in the experiment with the amino acid L-Glu, it would be fair to assume that they follow a similar pattern as when efflux experiments on *P. aeruginosa* with L-Asp were conducted.

3.3.3.2 Growth curves

To investigate how the synergy between Cip and the amino acids observed with efflux experiments translates into the efficacy of Cip on the bacteria, growth curves were conducted for *P. aeruginosa* that was no treated and that which was treated with Cip, amino acids and Cip and amino acid combinations.

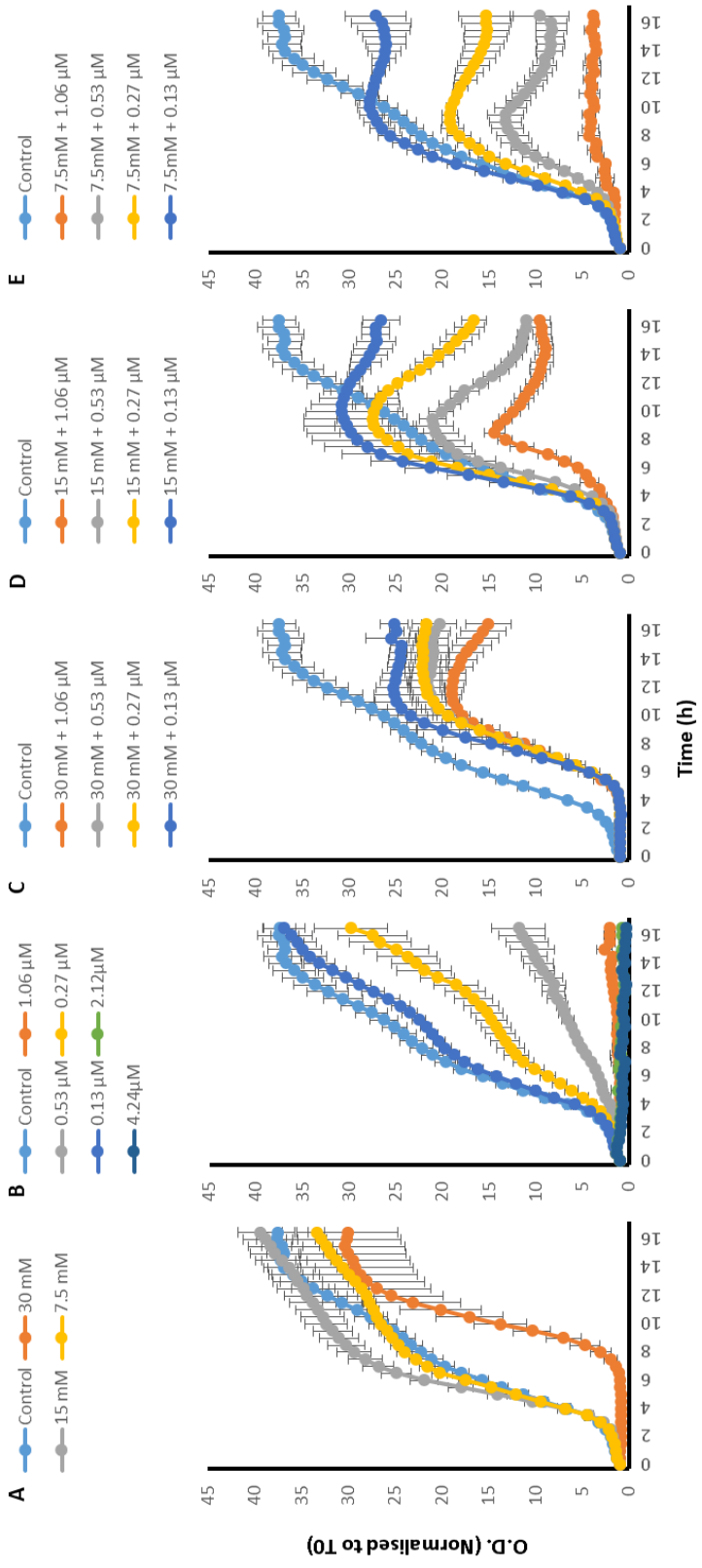

Figure 3.8: *P. aeruginosa* growth curves with a) 30, 15 and 7.5 mM L-Asp amino acid on its own, b) with 4.24, 2.12, 1.06, 0.53, 0.27 and 0.13 µM Cip on its own, c) 30 mM L-Asp combined with 1.06, 0.53, 0.27 and 0.13 µM Cip, d) 15 mM L-Asp combined with 1.06, 0.53, 0.27 and 0.13 µM Cip and e) 7.5 mM L-Asp combined with 1.06, 0.53, 0.27 and 0.13 µM Cip; n=3.

To make comparison between growth curves of L-Asp (Figure 3.8a), Cip (Figure 3.8b) and their combinations (Figure 3.8c-e) easier, the growth curves are presented alongside each other in Figure 3.8. Whilst Cip has a concentration dependent effect on the growth of *P. aeruginosa*, where a higher concentration hinders more greatly the growth of the bacteria, L-Asp on its own was generally unable to effect the growth of *P. aeruginosa*; only a delay in the onset of the exponential phase was observed with 30 mM L-Asp. In the process of evaluating the presence of synergy between L-Asp and Cip, the growth curves obtained by exposure to combinations (Figure 3.8c-e) were compared with growth curves obtained by individual parts (Figure 3.8a,b). Although, combining Cip with L-Asp leads to an early onset death phase, a very interesting pattern is observed. It seems that when L-Asp is combined with higher concentration of Cip, it reduces the effectiveness of Cip and enhances *P. aeruginosa* growth, whereas if L-Asp is combined with lower concentrations of Cip, it results in a synergistic inhibition of the growth of *P. aeruginosa*. More specifically, combining 30, 15 or 7.5 mM of L-Asp with Cip concentrations 1.06 and 0.53 µM seems to aid the growth of *P. aeruginosa*, whilst combining with 0.27 and 0.13 µM does seem to present some positive synergy resulting in the early onset of death phase mentioned earlier. Also combining the amino acids with 0.27 and 0.13 µM Cip leads to less overall *P. aeruginosa* growth, hinted lower normalised O.D. at the peaks.

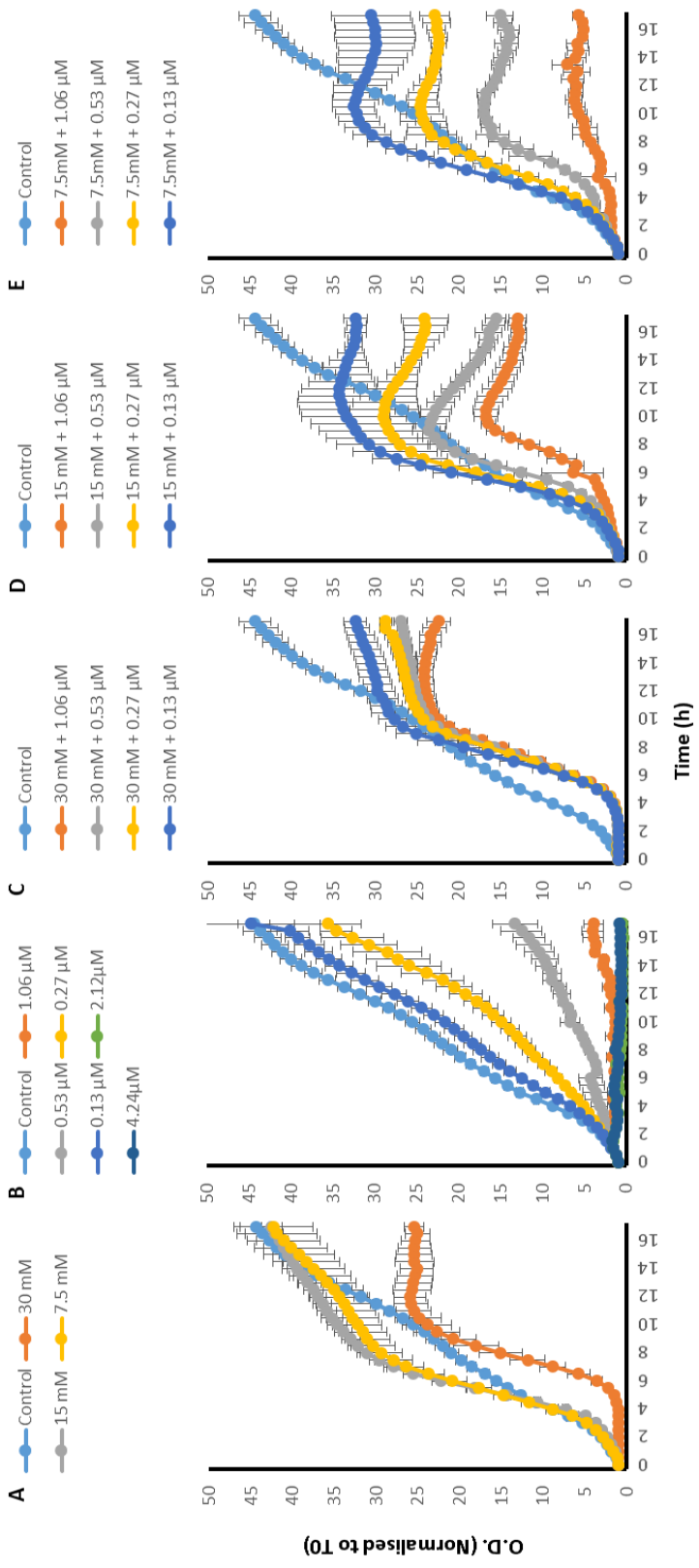

Figure 3.9: *P. aeruginosa* growth curves with a) 30, 15 and 7.5 mM L-Glu amino acid on its own, b) with 4.24, 2.12, 1.06, 0.53, 0.27 and 0.13 µM Cip on its own, c) 30 mM L-Glu combined with 1.06, 0.53, 0.27 and 0.13 µM Cip, d) 15 mM L-Glu combined with 1.06, 0.53, 0.27 and 0.13 µM Cip and e) 7.5 mM L-Glu combined with 1.06, 0.53, 0.27 and 0.13 µM Cip; n=3.

Growth curves of *P. aeruginosa* with L-Glu and L-Glu combinations with Cip (Figure 3.9) showed very similar results as to those obtained with L-Asp. Figure 3.9a presents the growth curves of *P. aeruginosa* when exposed to L-Glu concentrations of 30, 15 and 7.5 mM, whilst Figure 3.9b presents the growth curves obtained for different Cip concentrations. Alongside these are presented growth curves for Cip and L-Glu combinations (Figure 3.9c-e). Again, Cip effects the growth of *P. aeruginosa*, in a concentration dependent manner, where a higher concentration hinders more greatly the growth of the bacteria whilst a lower concentration of Cip has less of an affect. The only concentration of L-Glu which somewhat inhibits *P. aeruginosa* growth is 30 mM L-Glu. When comparing growth curves obtained with combinations with the growth curves obtained by Cip and L-Glu individually, the combinations which modulated the growth of *P. aeruginosa* more than both of the individual parts were taken to exhibit synergy. Like when using L-Asp, it seems that when L-Glu is combined with higher concentration of Cip (1.06 and 0.53 µM), it reduces the effectiveness of Cip and enhances *P. aeruginosa* growth, whereas if L-Asp is combined with lower concentrations of Cip (0.27 and 0.13 µM), it results in a synergistic inhibition of the growth of *P. aeruginosa*. Only with combinations using 30 mM L-Glu was there no synergy observed, since 30 mM L-Glu on its own inhibited *P. aeruginosa* growth to a similar level. Two main effects of synergy are observed. Firstly combining the drug with L-Glu results in an earlier onset of the death phase. And secondly, combining 15 and 7.5 mM L-Glu with 0.27 and 0.13 µM Cip leads to less overall *P. aeruginosa* growth.

3.3.3.3 Pigment production

Like with TC, pigment production during the growth curve experiments varied depending on the combinations of Cip and amino acids *P. aeruginosa* was exposed to. Due to this, it was appropriate to quantify the pigments produced. Visual production of the pigments can be seen in Figure 3.10a and Figure 3.11a. Figure 3.10b and Figure 3.11b on the other hand present pyocyanin production and was quantified using the chloroform/HCl extraction method. A relation between the pigment intensity is observed where a more intense green pigmentation (Figure 3.10a and Figure 3.11a) corresponds to higher amounts of pyocyanin (Figure 3.10b and Figure 3.11b) present. For statistical analysis, initially one way ANOVA was conducted to whether there was significant difference within the data or not. This was followed by the uncorrected Fisher's LSD test to see where this significant difference lies. Fisher's LSD test was chosen over tests which correct for multiple comparisons because in answering the hypothesis each comparison stood alone, such that when checking how a specific combination of amino acid and the drug compared to both its parts in isolation, its relation to

other concentrations (of the amino acid, drug or any of their combinations) was not part of the hypothesis and irrelevant in answering the question posed.

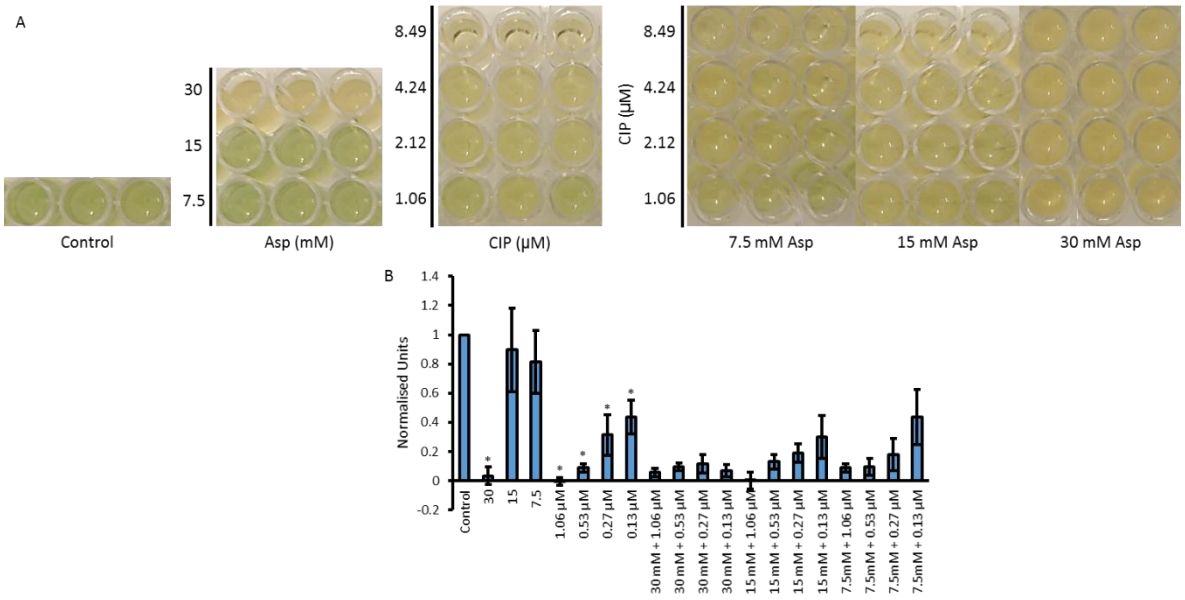

Figure 3.10: Effect of L-Asp, Cip and L-Asp with Cip combinations on the production of pyocyanin by *P. aeruginosa*; n=3.

Figure 3.10b presents pyocyanin production by *P. aeruginosa* when incubated with L-Asp, Cip and various L-Asp and Cip combinations. Cip showed a statistically significant ($p<0.0001$) concentration dependent reduction in pyocyanin production where a higher concentration of the drug led to less pigment production. The only L-Asp concentration which resulted in significant pigment reduction was 30 mM ($p<0.0001$). Synergy between Cip and L-Asp was confirmed if a particular combination resulted in less pigment production compared to both of its corresponding parts. If combination only resulted in less pigment production compared to one of the corresponding part, no synergistic effect was confirmed. Although all combinations significantly ($p<0.0001$) reduced the amount of pyocyanin produced by *P. aeruginosa*, none seem to show statistically significant synergy. Granting 0.27 and 0.13 µM Cip combined with 30 mM L-Asp did show significant reduction compared to the corresponding Cip concentrations, this was not significantly lower than 30 mM L-Asp on its own. It may be worth pointing out that although not statistically significant combinations, some synergy is witnessed with the combinations 15 mM + 0.27 µM, 15 Mm + 0.13 µM and 7.5 Mm + 0.27 µM.

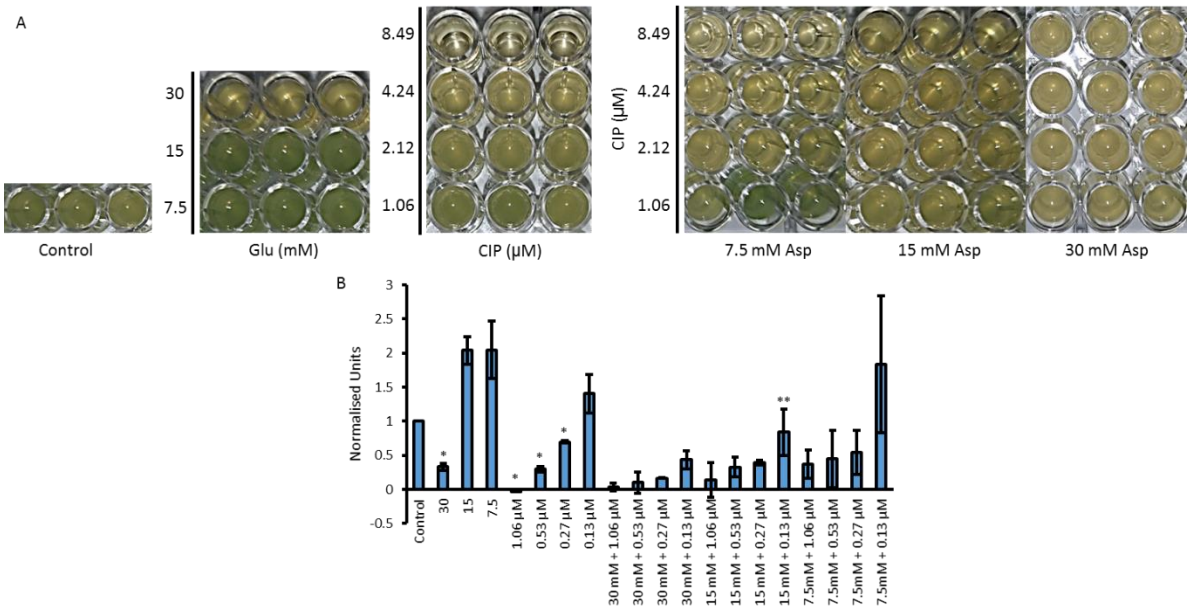

Figure 3.11: Effect of L-Glu, Cip and L-Glu with Cip combinations on the production of pyocyanin by *P. aeruginosa*; n=3.

Pyocyanin production by *P. aeruginosa* once treated with Cip, L-Glu and their combinations at various concentrations is presented in Figure 3.11. Interestingly, 15 and 7.5 mM L-Glu led to increased pyocyanin production whilst 30 mM significantly ($p=0.011$) reduced its production. Cip concentrations of 1.06 ($p<0.001$), 0.53 ($p=0.0078$) and 0.27 µM reduced pyocyanin production in a concentration dependent manner, with 1.06 µM reducing the most and 0.27 µM reducing the least. 0.13 µM Cip had no significant change on pyocyanin production. As before, synergy was established if combinations led to greater reduction in pyocyanin production compared to both Cip and L-Glu of the same concentration as that used in the combination. With this rule in mind, the only combination which showed substantial synergy ($p=0.031$) was 0.13 µM Cip combined with 15 mM L-Glu. Though Cip concentrations of 0.27 and 0.13 µM led to reduced pyocyanin production compared to the corresponding Cip concentrations, the amount of pyocyanin was not less than that produced by 30 mM L-Glu on its own. Hence these combinations did not show any synergistic effect in pyocyanin production.

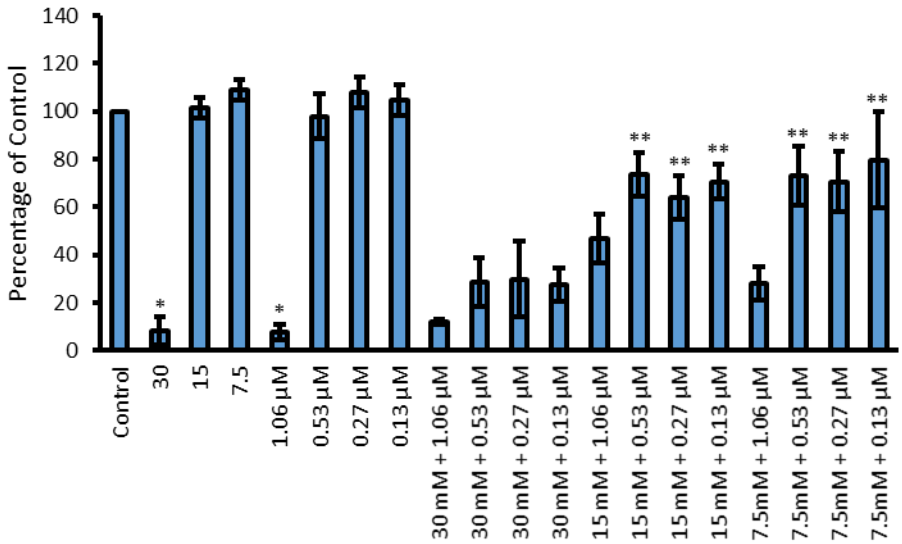

Figure 3.12: Effect of L-Asp, Cip and L-Asp and Cip combinations on the production of pyoverdine by *P. aeruginosa*; AA (mM), Cip (µM); n=3.

Pyoverdine production by *P. aeruginosa* was also quantified. Its production when exposed to Cip, L-Asp and their combinations is presented in Figure 3.12. When used in isolation only 30 mM L-Asp ($p<0.0001$) and 1.06 µM Cip ($p<0.0001$) resulted in a significant reduction in pyoverdine production. Once Cip and L-Asp were combined, synergistic decrease in pyoverdine production was observed using 15 mM ($p<0.01$) and 7.5 mM L-Asp ($p<0.01$) in combination with 0.53, 0.27 and 0.13 µM Cip. Although combining these Cip concentrations with 30 mM L-Asp hindered pigment production compared to the corresponding Cip concentrations, the amount produced was not lower than that produced with exposure to the amino acid on its own. Likewise, even though combining 1.06 µM Cip with 15 and 7.5 mM L-Asp resulted in lower pyoverdine compared to when these amino acid concentrations were used in isolation, the values obtained were not lower than that those obtained with 1.06 µM Cip. Hence no synergy is attributed to any combinations with 30 mM L-Asp or 1.06 µM Cip.

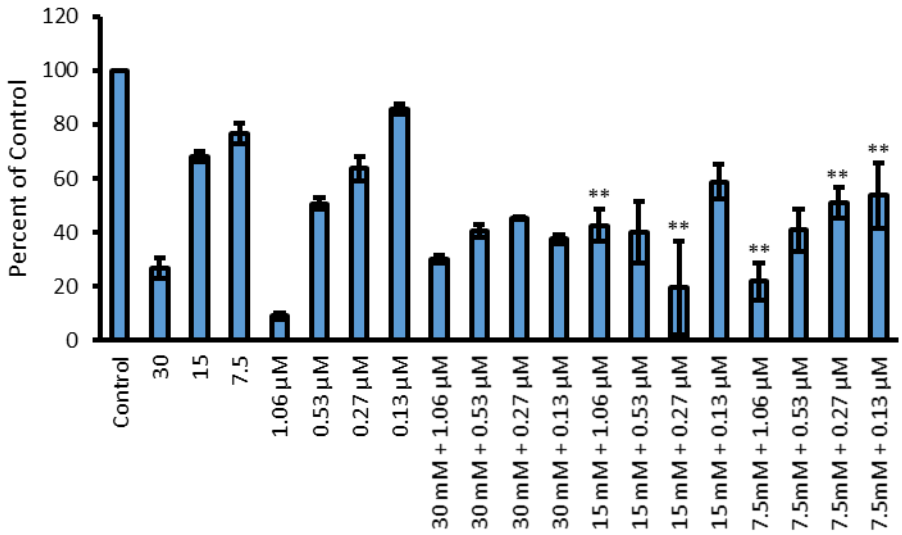

Figure 3.13: Effect of L-Glu, Cip and L-Glu and Cip combinations on the production of pyoverdine by *P. aeruginosa*; n=3.

Results for pyoverdine production when L-Glu was used as an accumulation enhancer for Cip are presented in Figure 3.13. Both L-Glu ($p<0.001$) and Cip ($p<0.05$) showed a concentration dependent reduction in pyoverdine production where a higher concentration of the amino acid and the drug resulted in less production of the pigment. Like with L-Asp, Cip combinations with 30 mM L-Glu did not result in any positive synergy, since the combinations did not decrease pyoverdine production lower than the amount produced by 30 mM L-Glu on its own. The combinations which showed significant synergy, due to being more inhibitive in pigment production than both of the corresponding parts, were 15 mM L-Glu combined with 1.06 ($p<0.0001$) and 0.27 µM ($p<0.0001$) Cip and 7.5 mM L-Glu combined with 1.06 ($p=0.022$), 0.27 ($p=0.022$) and 0.13 µM ($p<0.0001$) Cip.

3.4 Discussion

In a bid to overcome the ever growing resistance to the antibiotics in clinical use, adjuvants are in use and also form part of a research area in the field of AMR. Generally, adjuvants aim to inhibit the resistance mechanism to particular drugs. For example, if an enzyme inactivates a drug, the adjuvant would act to increase the activity of the drug by inhibiting the enzyme. Likewise, if a drug is extruded out of efflux pumps, the adjuvant would act to inhibit this efflux (67, 69, 70, 166, 167).

Unfortunately, being classified as an adjuvant, whether it has intrinsic antibiotic activity or not, does not make a substance immune from bacteria acquiring resistance against it. A good example for this is the β-lactamase inhibitor sulbactam which functions by inhibiting the β-lactamase enzyme that would otherwise inhibit the β-lactam class of antibiotics such as ampicillin (168). Although sulbactam was approved for clinical use in 1986, persistence despite sulbactam-penicillin co-administration was reported as early as 1988 (169, 170). In united states, rate of resistance to sulbactam-ampicillin was reported to be 35.2% in the period of 2003 to 2005 and rose to 44.9% and 41.2% by the period of 2006 to 2008 and the period of 2009 to 2012 respectively (168, 171). Although substances which are able to restore sulbactam activity have been identified, this approach does not seem ideal; inhibiting the resistance to adjuvants which are meant to be inhibiting the resistance to antibiotics seems inefficient (71). Furthermore, this many only be a temporary solution and resistance to such mechanisms will probably immerge.

Although sulbactam can confer intrinsic antibiotic activity, resistance is also likely to arise against adjuvants which do not (169). This is because even with the lack of intrinsic activity, the indirect antibacterial activity exhibited by combinations of the adjuvants with an antibiotic, is likely to select for phenotypes resistant to the adjuvant.

Other forms of adjuvants are those which act by the inhibition of efflux pumps and modulation of membrane permeability. To enhance the accumulation of drugs in resistant bacteria, these are the two main strategies employed (166). To the author's knowledge, naturally occurring acidic amino acids L-Asp and L-Glu have not been studied for their potential role as adjuvants to increase intracellular accumulation of drugs. Thus in this study, the amino acids which have already been proven to enhance the permeability of Cip as well as other drugs in caco-2 mono layers, were investigated as potential adjuvants to Cip in enhancing the drugs permeability in bacteria (40, 156).

The results in this chapter present that the accumulation of Cip can be enhanced within bacteria with the use of acidic amino acids as counterions. With *S. aureus* the effect is amino acid concentration dependent. On the other hand, though with *P. aeruginosa*, enhancement in accumulation only occurs with the two highest amino acid concentrations used, the efflux pattern when 15 and 30 mM L-Asp or L-Glu is used, stands out. This in turn presents as synergistic reduction in *S. aureus* and *P. aeruginosa* growth as well as reduced toxic pigment production in the latter.

The findings in this chapter are similar to those in the previous chapter which shows that L-Asp and L-Glu are able to enhance TC accumulation within both *S. aureus* and *P. aeruginosa*. Again, this was accompanied with a synergistic inhibition on the growth of both bacteria as well as reduced pigment production by *P. aeruginosa*. This shows that L-Asp and L-Glu enhance drug permeation in a manner which is independent to the drug used and thus can potentially be used to enhance accumulation of many antibiotics within a broad range of bacteria.

In this regards, it is useful to consider here that TC acts on the 30S ribosomal subunit to inhibit protein synthesis whilst Cip has its inhibitory affect by acting on DNA-gyrase and DNA topoisomerase IV, inhibiting cell replication. Meaning, the two mechanisms of action are completely different and not related. Due to this it is likely that the amino acids work in a manner which is independent to interfering with these mechanisms. Substantiating the possibility that amino acids act by a mechanism which interferes with a mutually shared process subjected to both antibiotics. Some of these mechanisms are discussed in detail in the previous chapter and will be briefly outlined later on along with another possible mechanism which will be explored in this chapter.

Interestingly, the growth curves for *S. aureus* give an indication as to why 30 mM L-Asp or L-L-Glu combined with Cip did not follow the concentration dependent efflux pattern observed with other amino acid concentrations whilst also giving insight into the steep reduction in fluorescence intensity observed with 15 mM and 7.5 mM these amino acids during efflux experiments. Growth curve data clearly shows that when 15 mM and 7.5 mM L-Asp or L-Glu are combined with Cip, *S. aureus*, growth is hindered synergistically. Keeping in mind that these combinations also cause an initial surge of EtBr and therefore Cip within the bacteria, it is possible that bactericidal activity of the increased Cip within the cells causes cell death (172). The resulting cell death would subsequently enable EtBr to leak out of cells, and since EtBr has differential intracellular and extracellular fluorescence, a great reduction in

fluorescence intensity is observed (126). This is also likely to be the reason for the efflux pattern obtained when 15 mM and 7.5 mM of the amino acids were combined with TC. In other words, the reduction in fluorescence intensity observed with Cip or TC combined with 15 mM or 7.5 mM of either amino acid is unlikely due to EtBr efflux, but rather through reduction in intracellular EtBr secondary to cell death. Since when Cip is combined with 30 mM L-Asp or L-Glu, there is no reduction in *S. aureus* growth, EtBr does not leak out and hence no drastic reduction in fluorescence is observed, explaining why the efflux pattern observed with these combinations (Cip with 30 mM L-Asp or L-Glu) present as outlier to the concentration dependent pattern observed with other concentrations.

Another interesting observation was that the pattern of efflux, though different in the two bacteria used, was similar irrespective of what concentration of Cip was used. This was the case with different Cip concentrations studied in both *S. aureus* and *P. aeruginosa*. The observation indicates that the concentration of Cip used did not affect the efflux of EtBr. Yet it is also clear that the presence of Cip does indeed effect the efflux of EtBr, as evident from the clear difference in efflux pattern between 0 mM of any amino acid used as compared to the 'glu' control; only difference between the two being the presence or absence of Cip, respectively. A potential explanation for this apparent discrepancy may be that the concentration of EtBr (~114 µM) is far greater than the concentrations of Cip used, potentially rendering negligible the difference between the Cip concentrations used. All this also holds true for TC, again reiterating that amino acids potentially use a drug independent mechanism of enhancing accumulation.

It is possible that the differences in the efflux patterns observed with *S. aureus* and *P. aeruginosa* are due to the differences in their membranes. Being gram-positive *S. aureus* has only one membrane whilst the gram-negative *P. aeruginosa* has an outer and inner membrane. As mentioned earlier the outer membrane of gram-negative bacteria confers substantial resistance to the uptake of antibiotics. Thus, 30 mM and 15 mM L-Asp and L-Glu, probably act to enhance Cip uptake by modulating the outer membranes permeability, whilst 15 mM and 7.5 mM are more effective in modulating the membrane permeability of gram-positive bacteria.

A striking observation is that despite amino acids substantially effecting the growth of *S. aureus* in a concentration dependent manner, they seem to exert no or minimal effect on the growth of *P. aeruginosa* on their own. What makes this even more interesting is that despite their lack of inhibitory effect on the growth pattern of *P. aeruginosa*, when they are combined with the drug, a substantial synergistic effect is observed. This is observed with both TC and

Cip but is more apparent with TC. Either way, this makes it more likely that the role played by amino acids in this synergism is to increase the effect of the drug, rather than exhibit intrinsic antibiotic activity, most likely through a mechanism resulting in its increased uptake or reduced efflux. However, the presence of synergy on the growth of *P. aeruginosa* between the drugs and 7.5 mM of either L-Asp or L-Glu, hints towards other mechanisms of enhancing drug effectiveness, independent of those effecting intracellular drug concentrations, to be also involved. This is because despite the synergy, Cip or TC combined with 7.5 mM of the amino acids did not show any evidence of enhanced drug uptake or a decrease in drug efflux. Nevertheless, due to the reasons discussed above, an accumulative effect of antimicrobial activity of the amino acids and Cip or TC on their own is highly unlikely to be the cause of the synergistic effect observed on *P. aeruginosa* growth.

As mentioned earlier, some of the adjuvants used and even those under research are probably liable to resistance. It seems the potential mechanisms leading to enhanced drug accumulation by the acidic amino acids used here are very non-specific. These mechanisms were discussed in detail in the earlier chapter with reference to TC and include increase in TC uptake, amino acid and TC ion pairing and prevention of efflux by acidic amino acids. It is likely that similar mechanisms also lead to enhancement of Cip accumulation and are briefly discussed later in context of Cip. Nevertheless, it is hoped that the non-specificity of the mechanisms would make it highly unlikely for resistance mechanisms to evolve against these amino acids. Utilisation of such non-specific mechanisms however will need exploration and appropriate development and control in order to avoid potential toxicity issues.

3.4.1 Enhanced ciprofloxacin accumulation through increased uptake, ion-pairing with acidic amino acids and efflux prevention

Mechanisms which may be resulting in the enhanced Cip accumulation within *S. aureus* and *P. aeruginosa* may involve increase uptake, ion-pairing between Cip and the amino acids or inhibition of efflux by the amino acids. These were discussed in the chapter presenting efflux of tetracycline and the reader is referred to it for an in-depth exploration of these mechanisms. As will be briefly discussed here the same mechanisms can leading to enhanced Cip uptake.

3.4.1.1 Increased uptake through porins

Due to the highly selective nature of the outer membrane of gram-negative bacteria, antibiotics usually utilise porins found in this membrane to penetrate within the cell (130). OprF is a major

outer membrane protein of *P. aeruginosa* (173). It has been suggested to allow antibiotic penetration, whilst showing preference to cations (132, 133, 174). Along with this, Cip is known to utilise porins too (175). Since in the presence of acidic/anionic amino acids, like TC a major proportion of Cip is likely to have been present in the cationic form, thus it may be that this charge eases the passage of Cip through porins like OprF, penetrating through the selective outer membrane and reaching the periplasm. Here the comparatively higher pH shifts the equilibrium towards more neutral molecules of Cip which are than able to passively diffuse through the inner membrane and reach the cytoplasm to carry out their function. Along with this ion-pairing between acidic amino acids and Cip may be resulting in Cip uptake too.

3.4.1.2 Ion-pairing between acidic amino acid and ciprofloxacin

As discussed in the previous chapter, amino acid channels such as ATB(0,+) which are able to transport not only amino acids, but also prodrugs formed by reactions such as esterification of a drug with the amino acids (144, 145). Interestingly bacteria also express transporters that are able to carry out a similar function. Transporters belonging to the MFS and ABC-binding cassette superfamilies have been suggested to transport amino acids and their derivatives (146, 147). Thus, since in the given Cip and amino acid concentrations, both exist not only as neutral species but also as oppositely charged species, ion-pairs are likely to form between the cationic Cip and the anionic acidic amino acids, conferring the newly formed species the ability to be recognised and taken up through these amino acid channels.

3.4.1.3 Amino acids inhibit ciprofloxacin efflux in *S. aureus*

Majority of the efflux pumps present in *S. aureus* belong to the MFS superfamily (163). Interestingly, it has been shown that transporters such as those which belong to the MFS superfamily, which function by substance/H^+ symport, can be inhibited by acidic pH (150). This is because the acidic pH probably prevents deprotonation of the symporter thus preventing any further transport (150). This gives reason as to why the pattern of TC and Cip accumulation caused by amino acids is similar, and highlights again that mechanisms not specific to drugs are probably at play. It may be that the acidic pH of the surrounding environment caused by the L-Asp and L-Glu prevents deprotonation of the symporter, rendering it inhibited.

3.4.2 Amino acids based Mg^{2+} and Ca^{2+} chelation

Another possible mechanism, not explored earlier, relates to the ability of amino acids to act as chelating agents. Ethylenediaminetetraacetic acid (EDTA), an anionic substance has been well studied for its ability to chelate cations like Ca^{2+} and Mg^{2+}, leading to outer membrane disorganisation, consequently resulting in enhanced permeability of otherwise hard to permeate drugs. These cations play a crucial role in outer membrane integrity by binding to adjacent lipopolysaccharide molecules. Without this, the negative charges present on lipopolysaccharide molecules found on the outer leaflet would cause repulsion between them, resulting in loss of integrity for the outer membrane (176). Thus Ca^{2+} and Mg^{2+} act by neutralising the negatively charged lipopolysaccharides, maintaining outer leaflet and thus outer membrane stability (176). Hence like EDTA, here it is proposed that acidic amino acids, a substantial proportion of which would be present as anions, act as Ca^{2+} and Mg^{2+} chelators. This exposes the negative charges present on the lipopolysaccharide molecules, causing repulsion between them. With repulsion between its constituents, the outer membrane loses stability and becomes permeable to Cip and TC, presenting as the enhanced accumulation of these drugs observed in *P. aeruginosa*. Supporting this hypothesis is that amino acids, aspartic acid and glutamic acid, are known to act as chelators of metals including Ca^{2+} and Mg^{2+} (177). The above proposed mechanisms are depicted in Figure 3.14.

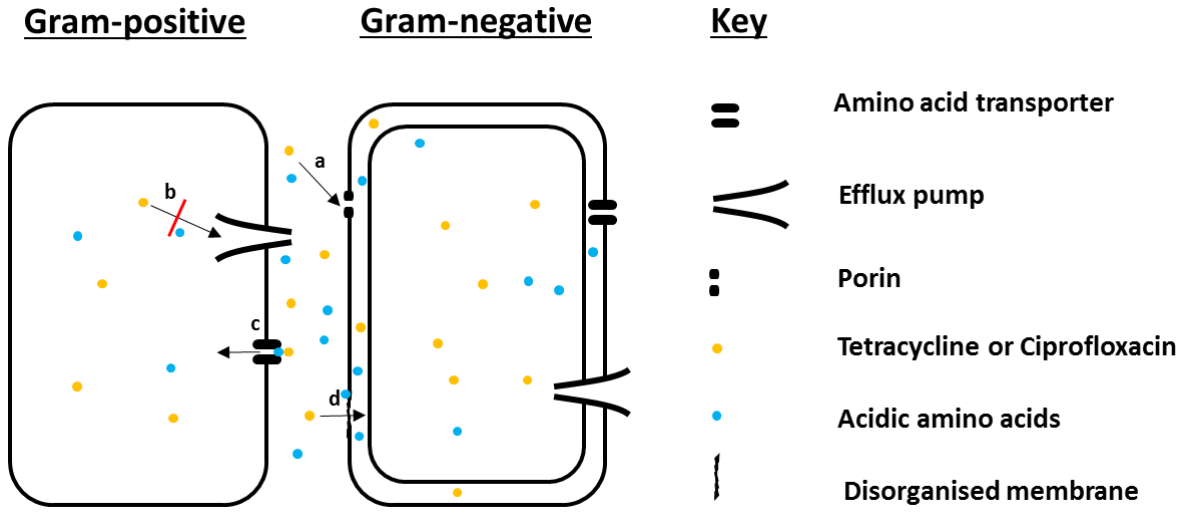

Figure 3.14: Diagram depicting possible mechanisms utilised by acidic amino acids in enhancing TC and Cip accumulation within both Gram-positive *S. aureus* (single membrane) and Gram-negative *P. aeruginosa* (two membranes). These mechanisms include a) charge triggered permeation through porins, b) efflux pump inhibition, c) permeation as ion-pairs through amino acid transporters and d) disorganisation of the outer membrane via chelation of otherwise stabilising cations such as Mg^{2+} and Ca^{2+} by acidic amino acids.

3.5 Conclusion

In conclusion, acidic amino acids have been shown in this chapter to act as adjuvants able to overcome resistance to Cip in both *S. aureus* and *P. aeruginosa*, synergistically inhibiting the growth of bacteria. Likewise synergistic reduction in pigment production by *P. aeruginosa* was also observed by combining the amino acids with the drug. This appears to result from the ability of L-Asp and L-Glu to enhance the accumulation of Cip within these bacteria. These findings may hold a key to strategies for overcoming the ever increasing AMR and it is hoped that the potential underlying mechanisms will make it substantially rarer for resistance to emerge.

It seems that amino acids probably function through multiple mechanisms, allowing the uptake of antibiotics belonging to different classes. Whilst the results suggest that the mechanism utilised are not drug-dependent, they probably depend on whether the bacteria in question is gram-negative or gram-positive, requiring traversing through two or one membrane respectively. Thus the uptake of both TC and Cip in *P. aeruginosa* is probably due to one or a combination of factors such as the effect of L-Asp and L-Glu on porin permeability, permeation as ion-pairs through amino acid transporters, efflux pump inhibition and disorganisation of the outer membrane via chelation of otherwise stabilising cations by amino acids, catering for permeation through both membranes. On the other had permeation into *S. aureus* only requires crossing through one membrane and is probably due to permeation through amino acid transporters after ion-pair formation and/or pH dependent inhibition of the efflux pumps.

Chapter 4: Anti-eDNA: insights into a new mechanism of *Staphylococcus aureus* biofilm inhibition and dispersal using acidic amino acids

4.1 Introduction

Biofilms are communities of sessile microorganisms (bacteria or fungi) living in a self-produced matrix (matrix of extracellular polymeric substances) which aids the survival of these microorganisms (58). The formation of biofilm can be divided into stages. Firstly planktonic bacteria attach to a surface reversibly (58). At this stage the bacteria are still susceptible to antibiotics. Hence prophylaxis in alloplastic surgery proves very useful as at this stage since the antibiotics are able to act on the planktonic forms which become reversibly attached (57). In the absence of a challenge during the next stage, the bacteria become irreversibly attached through self-adhesion structures such as pili, multiply and form colonies. Furthermore, extracellular polymeric substances, which form the matrix are secreted and deposited around the colonies (57). The matrix is a key structural component of the biofilm community and consists of water, polysaccharides, proteins, lipids and DNA (57). Hydrogen bonding between water molecules and hydrophilic polysaccharides holds water within the biofilms whilst polymers such as glycopeptides, lipids and lipopolysaccharides aid in scaffolding and holding the biofilm together (57). As the biofilm grows thicker, it becomes mature; a process which is coordinated through quorum sensing and other signalling pathways (57). Finally, the sessile bacteria in the biofilm are able to become free and spread to other surfaces to form new biofilms (57, 58).

Biofilm forming bacteria are commonly associated with chronic infections, which are infections that persist despite antibiotic therapy and the body's immune response (57). This is because the therapy and immune response are able to overcome planktonic bacteria, but are unable to penetrate the biofilm defences. After a while, when the individual seems to be cured, the sessile communities in biofilms give rise to planktonic forms, which in turn leads to a relapse of the disease state (58). Since the bacteria in biofilms have evolved complex survival strategies, biofilms act as a persistent base which poses constant pathogenicity to the body through continuous release of virulence factors and planktonic forms (57). Hence a chronic state of infection is maintained due to the inability of the immune system or drugs to eradicate the biofilm.

Biofilm formation on abiotic surfaces can result in complications with implants as well as catheters. A good example which highlights the danger associated with biofilms is a biliary stent in which the growth of *Escherichia coli* (*E.coli*) biofilm lead to repeated incidents of sepsis(57). In this case, antibiotic therapy was of no avail and the second episode of sepsis proved fatal. DNA typing revealed that the same *E.coli* clonal type was present in the biofilm

as the one responsible for sepsis (57). On the other hand, biofilms are also implicated on biotic surfaces such as acute and chronic wounds. In such cases, along with the disease state of infection, biofilms also hinder wound healing (178).

The problem is exacerbated by the fact that resistance to antibiotics can be up to 1000 times higher for bacteria in biofilms and the underlying mechanisms of resistance are likely to be a combination of conventional resistance mechanisms found in planktonic phenotypes as well as those specific to biofilm phenotypes (58). Such specific mechanisms include retardation of antibiotic diffusion by the biofilm matrix as well as slowed growth of bacteria due to decreased metabolic rate in biofilms (57). The latter leads to resistance because most antibiotics have their effect on rapidly dividing cells (58).

There is an urgent need therefore for strategies which can successfully and safely prevent as well as those which can treat infections where biofilms are implicated. The strategies studied can be divided into four major categories; prevention of biofilm formation, weakening of the biofilm, disruption or dispersal of the biofilm and killing of bacteria particularly the subpopulation which persists (58).

One strategy utilises D-amino acids to inhibit and disperse biofilms. Their role was seen after D-leucine, D-methionine, D-tryptophan and D-tyrosine, isolated prior to disassembly of *Bacillus subtilis* biofilms, were found to prevent new biofilm formation as well as cause its dispersal. It was found that D-amino acids caused cells in the biofilm to release amyloid fibres which are involved in linking cells in the biofilm together. YqxM is a protein required in the formation and anchoring of the Tas A amyloid fibres (amyloid fibres which in their composition contain Tas A protein) to the cell wall (64). These amyloid fibres give structural integrity to the biofilm. Strains with mutations in this protein were able to form biofilms in the presence of D-amino acids, indicating that the anti-biofilm activity of these amino acids was dependent on the strain with the wild type YqxM protein (65).

Since this finding, D-amino acids have also proved to be effective as strategies for the prevention and dispersal of *Staphylococcus epidermidis, Staphylococcus aureus* (*S. aureus*) *and Pseudomonas aeruginosa* (*P. aeruginosa* biofilms) (66, 179). Studies have demonstrated their effectiveness in combination with antimicrobials in a bid to overcome the antimicrobial resistance of biofilms (66). It is generally claimed that L-amino acids have no effect and literature attributing anti-biofilm activity to these isomers is limited (65, 180, 181).

S. aureus was used in this study as it is one of the most clinically prominent bacteria and is frequently the causative agent in both acute and chronic infections. Its infections can range from relatively mild skin infections to life-threatening infections such as endocarditis and pneumonia (182). Furthermore, other D-amino acids have been shown to prevent its biofilm formation as well as cause its dispersal. *S. aureus* NCTC 8325, a strain with a well-defined genotype, was used for this investigation.

Amino acids are able to increase the solubility of Ciprofloxacin (Cip) (156). It was hypothesised that this solubility enhancing property of various amino acids, along with their potential anti-biofilm activity, can be utilised as a dual approach to decrease antimicrobial resistance within bacterial biofilms, through amino acid-drug synergy.

Thus the primary aim of the study presented in this chapter was to determine whether the amino acids exhibit anti-biofilm activity and whether this can be used with Cip to synergistically enhance the antibiotics activity on biofilms. To achieve this we investigated the effect of using D-isomers of acidic amino acids on *S. aureus* biofilm inhibition and dispersal, specifically on their effect on biofilm density, colony forming unites (CFU) and biofilm architecture. The presence of synergy when combining amino acids and Cip was investigated by determining biofilm density and CFU.

4.2 Materials and methods

4.2.1 Materials

S. aureus strain NCTC 8325 was gifted by Professor Peter A. Lambert. Tryptone soya broth (TSB), tryptone soya agar (TSA), Ciprofloxacin 98%, D(-)-aspartic acid 99+%, D(-)-glutamic acid 99+% were all obtained from Fisher Scientific whereas L-aspartic acid 98+% and L-glutamic acid 99% were obtained from Sigma Aldrich. Crystal violet (CV) was obtained from Sigma Aldrich. Phosphate buffered saline (PBS) tablets and LIVE/DEAD™ BacLight™ Bacterial Viability Kit were obtained from Thermofisher Scientific.

4.2.2 General methods

The biofilm formation, quantification and dispersal assays were adapted from published protocols (66, 183, 184). For inoculum preparation, 10 ml TSB was inoculated with a colony of *S. aureus* and incubated overnight at 37°C in an aerobic orbital shaker at ~50 cycles/min. The optical density (OD) was measured using a spectrophotometer at a wavelength of 600 nm, and the culture was diluted with TSB to adjust the O.D. to 0.1. Minimum lethal concentration (MLC) of Cip against planktonic forms of *S. aureus* was previously determined and found to be 3.75×10^{-6} g/ml.

4.2.3 Biofilm dispersal assay

The biofilms were grown for appropriate number of hours (6, 12, 24, 48 and 72 h) before addition of the amino acids. To do this, 500 µl of the diluted culture was added to each well of the 24 well plate. The plates were then incubated in a static incubator for 37 °C.

To examine the dispersal effects of amino acids, 40 mM solutions of aspartic acid (Asp), glutamic acid (Glu) and aspartic acid combined with glutamic acid (AA) were prepared in the broth followed by filter sterilisation using 0.22 µm syringe filters. Broth was used for serial dilution to attain working concentrations of 40, 20, 10, 5, 2.5 mM for the amino acids from the stock solution. After 72 h of incubation, the wells were washed once with PBS. 500 µl of media with various concentrations of amino acids were added to the wells. Negative control was TSB without any amino acids. The plates were then incubate overnight at 37 °C, washed and quantified by crystal violet staining. Cip and Cip in combination with amino acids was assessed in a similar way.

4.2.4 Biofilm Inhibition assay

To determine the inhibitory effects of amino acids, Cip and Cip combined with AA, the biofilms were allowed to grow whilst being exposed to these test substances from the start of the experiment. For this the culture was mixed with the D-amino acids before it was incubated for 6, 12, 24, 48 and 72 h. Briefly, after achieving appropriate culture (0.1 OD) and test substance concentration within each well, the plates were left in a 37 °C incubator for the desired time before the biofilm density was quantified. Again for negative control biofilms, TSB lacking any test substance was used.

4.2.5 Crystal violet staining

The media was removed from the plates through gentle shaking into a beaker and followed by gentle dabbing of the plates on a bed of paper towels to remove excess media. Each well was then washed once with 500 µl PBS followed by staining with 500 µl of 0.1% CV (w/v) for 30 min. The wells were then washed three times by submerging the plates in a tub of distilled water and by gently dabbing in a bed of paper towels to remove any excess stain. The plates were then left overnight or for a few hours (until dry) before proceeding.

Once dry 625 µl of 30% (v/v) acetic acid was added to each well to dissolve the CV. Plates were left to incubate for 15 min after which the solubilised crystal violet was transferred into a new plate and the biofilm was quantified by determining the O.D. using a plate reader at the wavelength of 570 nm.

4.2.6 Colony forming units

To determine the colony forming units, excess media was removed from the wells and the wells were washed with PBS once as described earlier. Next 500µl of TSB was added to each well and the biofilm was resuspended in the media by scraping and re-pipetting. This detached the biofilm from the well surface whilst also breaking up any free floating aggregates of the biofilm in the media. After vortexing the suspension, the Miles and Misra method was used to determine the CFU/ml (185).

4.2.7 Rate of cell attachment

Rate of cell attachment to a glass surface was determined through live imaging obtained using ZEISS Celldiscoverer 7. Images were obtained every 5 min over 2.5 h. Since the focus of lens was set at the surface of the glass, the clearly visible cells were taken to be those which had attached to the surface. ZEISS Celldiscoverer 7 software was used to quantify the number of cells which had attached.

4.2.8 Fluorescence and Confocal Imaging of Biofilms

Glass coverslips were sterilised with 70% (v/v) ethanol and placed in wells of 6 well plates. Biofilms were grown on coverslips as detailed under biofilm inhibition assay and washed with 0.85% (v/v) sodium chloride whilst dabbing on a bed of paper towel to maximise drainage. Dyes SYTO 9 and propidium iodide (PI) from the LIVE/DEAD BacLight Bacterial Viability Kit were used to stain the cells. Staining solution was made in deionised water at a concentration of 3 µl/ml of each dye from a stock of 3.34 mM SYTO9 and 20 mM PI. The plates were then incubated for 90 min at 37 °C with 500 µl of the staining solution in each well. The wells were then rinsed with RNA free water, and the plates left upside down to drain for 10-15 min. The coverslip were then mounted onto slides using BacLight mounting oil. The biofilm samples were then analysed using confocal microscopy using CLSM TCS SP5 II system (Leica Microsystems GmbH, UK) using a x63 and a x100 oil immersion lens. An argon laser was used to excite SYTO 9 fluorophores and a helium-neon laser was used to excite PI fluorophores at a wavelength of 488 nm and 543 nm respectively. The emission analyser filters were set between the range of 493 nm to 530 nm for SYTO 9 and 625 nm to 676 nm for PI. For fluorescence imaging, biofilms were stained in a similar way within the wells of a 24 well plate and analysed on the same day using Leica Widefield Fluorescence Microscope (Leica Microsystems GmbH, UK).

4.2.9 Statistical analysis

One-way ANOVA was followed by a post-hoc t-test Bonferroni correction to determine where the significant difference lay within the data set. P value <0.05 was taken to be significant.

4.3 Results

4.3.1 Biofilm inhibition and dispersal using D-Asp and D-Glu

The concentration of amino acids used were 2.5 mM, 5 mM, 10 mM, 20 mM and 40 mM. Upper limit was capped at 40 mM considering the solubility limitations of these amino acids in water. Figure 4.1a and Figure 4.1b show the effect on biofilm density of D-Asp and D-Glu whilst they were used separately as inhibiting and dispersing agents. Concentration dependent anti-biofilm activity (Figure 4.1a-d) was observed with each time point (Figure 4.1c,d) whether amino acids were used in isolation or in combination. However, greater anti-biofilm activity (Figure 4.1c,d) was observed by combining D-Asp and D-Glu (D-AA). Figure 4.1a-d also show that D-AA were effective in both preventing (inhibition) the formation of new biofilms, as well as the breakdown (dispersal) of already formed biofilms. Significant inhibition was achieved with the lowest concentration (2.5 mM) of D-AA used whereas minimum of 5 mM D-AA concentration was required to obtain statistically significant dispersal. The maximum inhibition and dispersal effect was obtained with the higher concentrations of D-AAs used i.e. 20 mM and 40 mM. The D-AA were better at inhibition than dispersal. Anti-biofilm activity was investigated on biofilms grown for 6, 12, 24, 48 and 72 h. The amino acids were similar in effectiveness at all the time points. Therefore, considering that bacteria are most resistant once the biofilm has matured, the 72 h time point was considered appropriate for conducting further work (186). For biofilms grown for 72 h, at 40 mM 37.55% of biofilm was dispersed whereas 96.89% was inhibited from forming (Figure 4.1c,d).

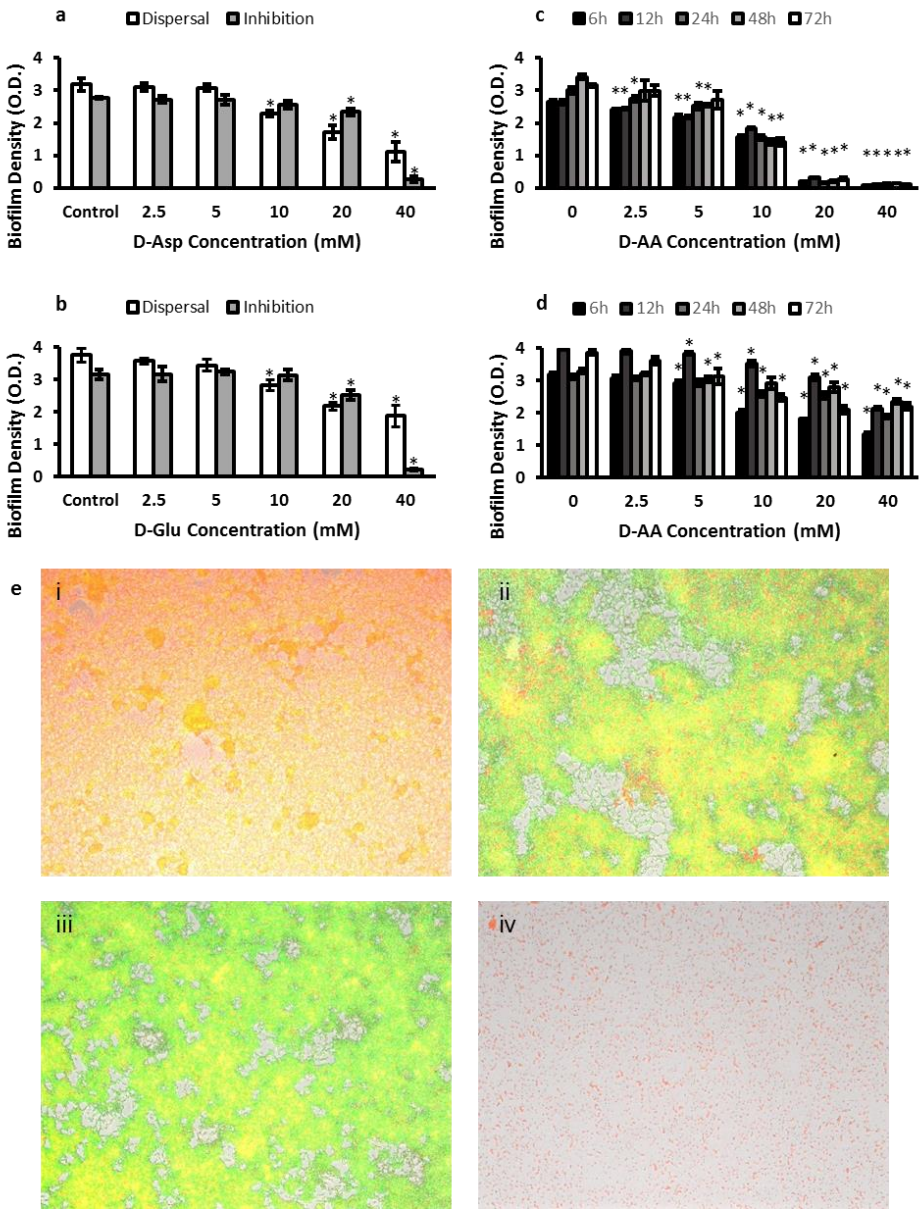

Figure 4.1: a) Inhibition and dispersal of *S. aureus* biofilm using 2.5, 5, 10, 20 and 40 mM D-Asp. b) Inhibition and dispersal of *S. aureus* biofilm using 2.5, 5, 10, 20 and 40 mM D-Glu. c) Inhibition of *S. aureus* biofilm using equimolar concentrations of D-AA. d) Dispersal of *S. aureus* biofilm using equimolar concentrations of D-AA. a-d) One-way ANOVA showed an overall significant difference within the data and was followed by a post-hoc t-test with Bonferroni correction to see which concentration significantly ($p<0.0083$ was taken as significant; indicated by *) significantly inhibited or dispersed biofilms; n=3, ±S.D. e) Fluoresence imaging showing 72 h biofilm formation. i) Control ii) inhibited with 40 mM D-Asp iii) inhibited with 40 mM D-Glu iv) inhibited with equimolar concentrations of D-Asp and D-Glu (40 mM of each); D-Asp = D-Aspartic acid; D-Glu = D-Glutamic acid; D-AA = D-Asp and D-Glu.

Fluorescence images in Figure 4.1e confirm that both D-Aspartic acid and D-Glutamic acid have anti-biofilm activities and that combining both amino acids is more efficacious. High levels of extracellular DNA (eDNA) was evident in the untreated biofilm (Figure 4.1e i) compared to those treated (Figure 4.1e ii,iii,iv). Use of amino acids leads to patchy (Figure 4.1e ii,iii) and incomplete (Figure 4.1e iv) biofilm formation. Equimolar combination of both

amino acids was therefore chosen for further investigations. The work presented here was obtained using combination of both aspartic acid and glutamic acid such that if 40mM D-AA is stated, it means that 40mM of D-Asp and 40mM of D-Glu was used together.

4.3.2 L-AA also inhibit and disperse biofilms

It was important to investigate whether the anti-biofilm activity of D-AA is restricted to the isomeric form. For this, combination of L-Asp and L-Glu (L-AA) were investigated for their anti-biofilm properties, whilst using the same concentrations as D-AA. L-AA showed a similar, concentration dependent dispersal and inhibition profile (Figure 4.2) to D-isomers whilst inhibiting and dispersing biofilms.

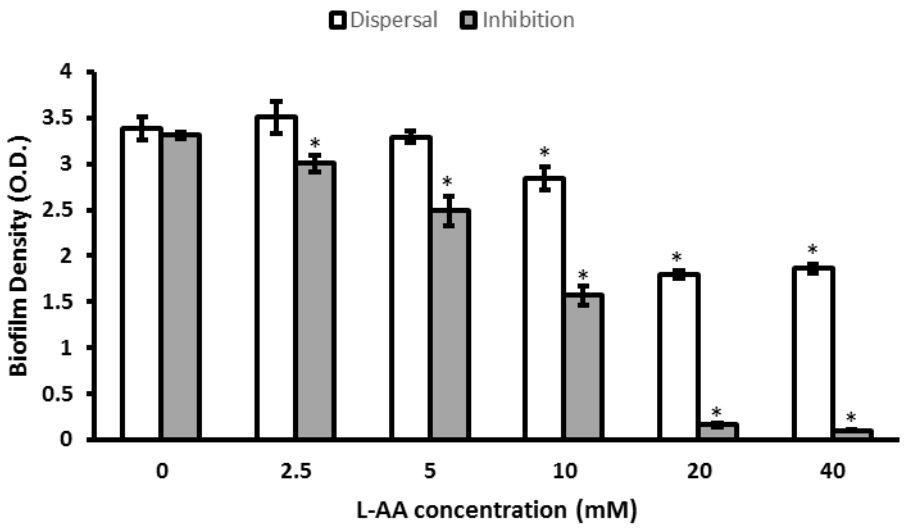

Figure 4.2: Dispersal and Inhibition of *S. aureus* biofilm using L-AA (equimolar combination of L-Asp and L-Glu) was dependent on the concentration of amino acids used. One-way ANOVA showed an overall significant difference within the data and was followed by a post-hoc t-test with Bonferroni correction to see which concentration significantly ($p<0.0083$ was taken as significant; indicated by *) significantly inhibited and dispersed biofilms; n=3, ±S.D; L-Asp = L-Aspartic acid; L-Glu = L-Glutamic acid; L-AA = L-Asp and L-Glu.

4.3.3 Synergistic effect of D-AA and Cip on biofilm inhibition and dispersal

Although, Cip on its own also has anti-biofilm activity, potential synergistic effect of using Cip with amino acids was investigated. Anti-biofilm activity of Cip and D-AA alone was compared to combined D-AA (2.5 – 40 mM) + Cip (1 MLC, 4 MLC and 8 MLC; number represents x times MLC) at various concentration combinations (Figure 4.3a-e). 40 mM D-AA showed significantly greater biofilm inhibiting ($p<0.001$) and dispersing ($p<0.0001$) activity as compared to 8 MLC Cip. Whilst 40 mM D-AA + Cip (8 MLC, 4 MLC or 1 MLC) maintained the anti-biofilm activity of the amino acid, there was no synergistic effect observed of these combinations on biofilm density (Figure 4.3a). However, at specific combinations with lower concentrations of D-AA, significant synergistic effect was observed (Figure 4.3b-e); 10 mM D-AA + 1 MLC Cip and 20 mM D-AA + 4 MLC Cip showed significant synergy in biofilm inhibition whilst 5 mM D-AA + 4 MLC Cip showed significant synergy in biofilm dispersal.

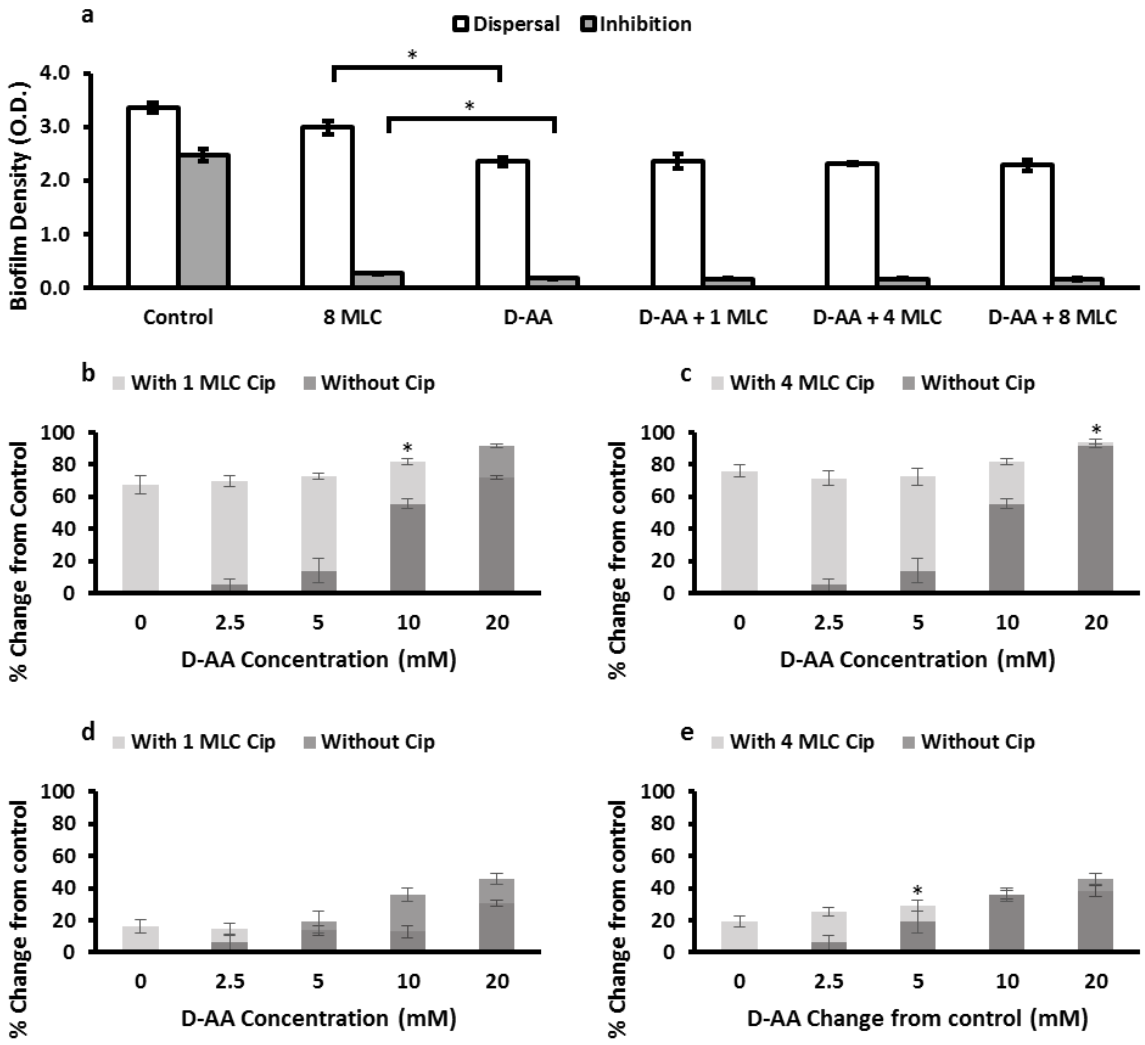

Figure 4.3: a) Efficacy of 8 MLC Cip, 40mM D-AA and 40mM D-AA combined with 1 MLC, 4 MLC and 8 MLC Cip on biofilm density whilst inhibiting and dispersing *S. aureus* biofilms. Two tailed T-test revealed that D-AA have a significantly (indicated by *) greater anti-biofilm activity (inhibition p<0.001, dispersal p<0.0001) as compared to 8x MLC of Cip. One-way ANOVA showed no significant synergistic effect (p>0.05) on biofilm density between D-AA and when D-AA and Cip are used in combination. a-e) Synergistic effect of using combination of 1 MLC (b, d) or 4 MLC (c, e) Cip with 2.5, 5, 10 and 20mM D-AA on biofilm inhibition (b, c) and dispersal (d, e). One-way ANOVA showed an overall significant difference for amino D-AA + Cip data (b-e). This was followed by a post-hoc t-test with Bonferroni correction to see which concentration of D-AA + Cip had significantly higher (p<0.01) anti-biofilm activity as compared Cip on its own. Next one-tail t test was done to see whether this combination of D-AA + Cip had significantly (p<0.05) improved anti-biofilm activity as compared to the corresponding D-AA on its own. b) 10 mM D-AA + 1 MLC Cip was significantly (*) able to inhibit greater biofilm formation compared to both Cip and D-AA on their own (p<0.001 and p<0.00001 respectively). c) 20 mM D-AA + 4 MLC Cip was significantly (*) able to inhibit greater biofilm formation compared to both Cip and D-AA on their own (p=0.00014 and p=0.014 respectively). d) No combination was significantly able to disperse greater biofilm compared to both Cip and D-AA on their own e) 5 mM D-AA + 4 MLC Cip gave significant (*) rise in biofilm dispersal activity compared to both Cip and D-AA on their own (p=0.0045 and p=0.018 respectively). a-e) D-AA = 40 mM D-Aspartic acid and 40 mM D-Glutamic acid; x MLC = x times minimum lethal concentration; Cip = ciprofloxacin; n=3, ±S.D.

4.3.4 Effect on colony forming units

Since biofilms are composed of bacterial cells and extracellular matrix, it was necessary to distinguish how the anti-biofilm activity of amino acids was distributed between these two components. Measuring biofilm density is a quantitative method that does not distinguish between matrix and cells. To determine the effect of amino acids and Cip on the viability of cells residing in *S. aureus* biofilms, viability assays were carried out by estimating the CFU/mL. Figure 4.4 compares the $\log_{10}$ CFU/ml of untreated biofilms with biofilms treated with 40mM D-AA, 40mM L-AA, and 40mM D-AA + 8 MLC Cip. Experiments for dispersal showed greater than 1 log reduction (≥91.89%) decrease in $\log_{10}$ CFU/ml for biofilms dispersed with 40mM D-AA and 40mM L-AA, as compared to untreated biofilms. Whereas for inhibition using the same treatments, there was greater than 2 log reduction (≥99.85%) in the number of viable bacterial cells attached to the surface.

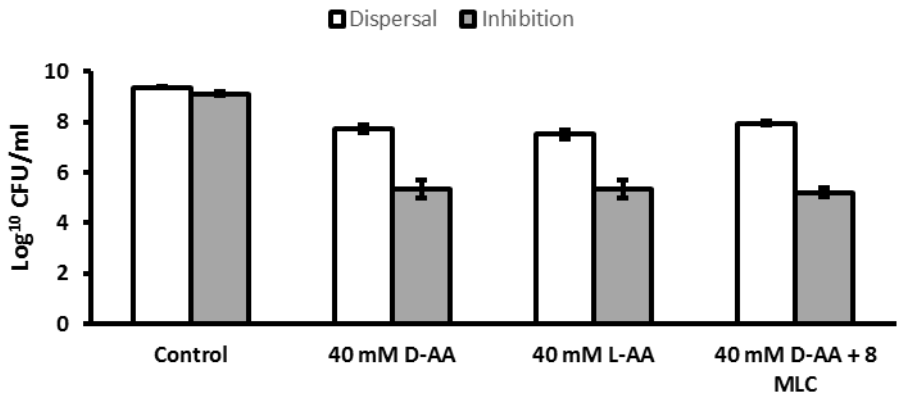

Figure 4.4: Effect of 40 mM D-AA, 40 mM L-AA and 40 mM D-AA + 8 MLC on CFU after biofilm inhibition and dispersal. ≥99.85% (inhibition) and ≥91.89% (dispersal) reduction in CFU from control was observed for D-AA, L-AA and D-AA + 8 MLC; D-AA = 40 mM D-Aspartic acid and 40 mM D-Glutamic acid; x MLC = x times minimum lethal concentration of ciprofloxacin; n=3, ±S.D.

4.3.5 D-AA treatment prevents eDNA meshwork formation

For confocal imaging, biofilms were grown on glass coverslips. After the treatment experiments, biofilms were stained with the dyes SYTO 9 and PI which stain nucleic acids in live and dead cells respectively. When both dyes are used in conjunction, the SYTO 9 channel generally represents the nucleic acid which is present within intact membranes and the PI channel enables the visualisation of nucleic acids outside cells (eDNA) or cells with a compromised cell membrane. The images taken through confocal microscopy are presented in Figure 4.5, Figure 4.6 and appendix Figure 1. Images of inhibited (Figure 4.5) and dispersed (Figure 4.6) biofilms from both, the SYTO 9 channel and the PI channel along with their overlay are presented. In this way the structure of eDNA can be more easily visualised whilst also being able to see how it spatially relates to both live and dead cells.

Untreated *S. aureus* biofilm covers the whole field of view and it has the highest cell density. In comparison, cells within all inhibited and dispersed biofilms have a patchy or clustered distribution. *S. aureus* cells in the control biofilms are interconnected and held in position by an organised distribution of eDNA throughout (Figure 4.5.1 and Figure 4.6.1). This meshwork of eDNA is filamentous in nature and almost seems to represent a honeycomb like structure. Furthermore, there is a uniformity in the thickness of eDNA between cells within the biofilms, raising the question as to whether the intercellular distance within the biofilm is precisely controlled and not without purpose.

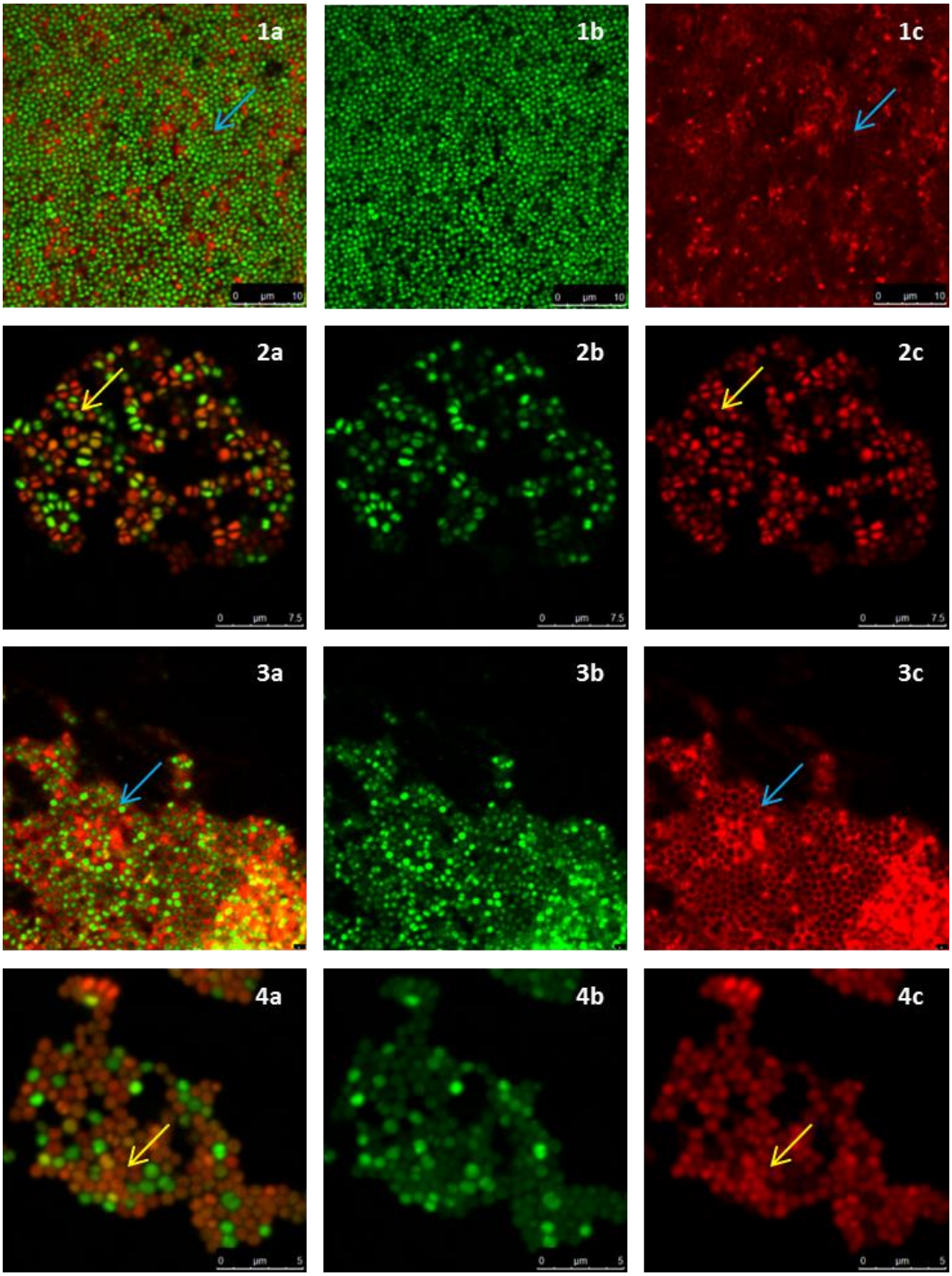

Figure 4.5: Confocal images of inhibited *S. aureus* biofilms. a) combined channel; b) SYTO 9 channel; c) Promidium Iodide channel; 1) control biofilm; 2) inhibited with 40mM D-AA (40mM D-Asp and 40mM D-Glu); 3) treated with Cip; 4) treated with 40mM D-AA and 8 MLC Cip; blue arrow) presence of intercellular eDNA; yellow arrow) lack of intercellular eDNA; green arrow) eDNA presence is inconclusive. 1) Untreated *S. aureus* biofilms are reinforced by an organised honeycomb like meshwork made of interconnected intercellular eDNA. eDNA forms a filamentous mesh like structure within the biofilm and surrounds all cells. 2) Biofilms inhibited with D-AA show a complete lack of eDNA. 3) Biofilms inhibited by Cip express a lower population of *S. aureus* cells. A dense eDNA meshwork provides structure to these persisting cells. 4) Biofilm treated with a combination of D-AA and 8 MLC Cip lack in eDNA meshwork structure; D-AA = 40 mM D-Aspartic acid and 40 mM D-Glutamic acid; x MLC = x times minimum lethal concentration; Cip = ciprofloxacin.

From visual analysis of the confocal images it is clear that both inhibited and dispersed biofilms exposed to D-AA, whether in isolation (Figure 4.5.2 and Figure 4.6.2) or in combination with Cip (Figure 4.5.4 and Figure 4.6.4), not only lack this organised structure of eDNA, but lack eDNA altogether. Considering the clear lack of eDNA within inhibited biofilms, any eDNA present within biofilms dispersed by these agents is most probably a result of being entrapped within the complex matrix. Like cells within biofilms treated with D-AA and D-AA + Cip, *S. aureus* cells within biofilms treated with Cip on its own are also distributed in clusters. However, Cip-only treated biofilms do not lack eDNA (Figure 4.5.3 and Figure 4.6.3). Moreover, the eDNA which is present in these biofilms seems to be more densely structured as compared to that of untreated biofilms. Dispersing with Cip-only also reveals an interesting feature; the eDNA seems to be present as patches or in boundaries, with number of viable cells decreasing as we move away from these boundaries (Figure 4.6.3 and appendix Figure 1).

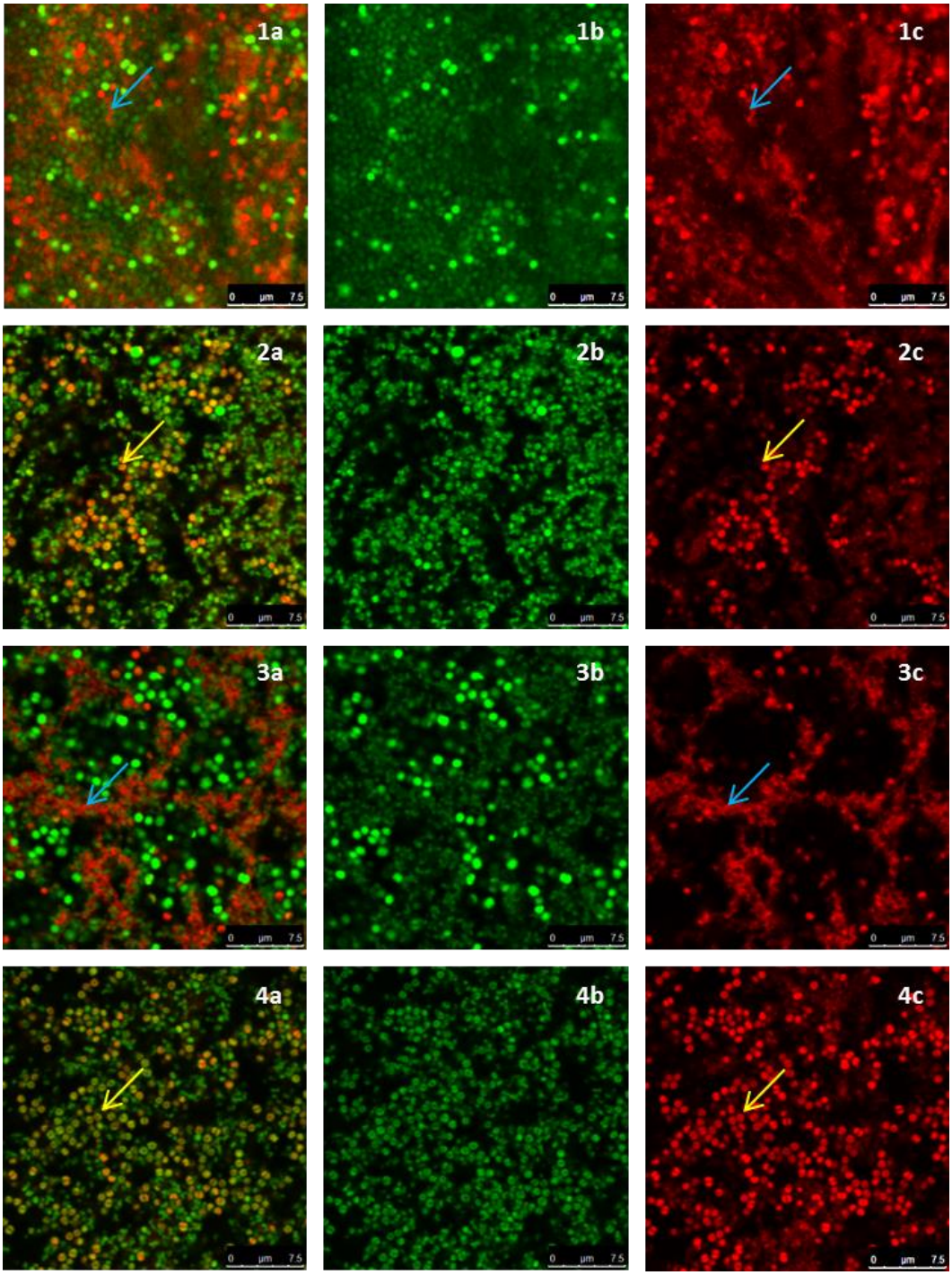

Figure 4.6: Confocal images of dispersed *S. aureus* biofilms. a) combined channel; b) SYTO 9 channel; c) Promidium Iodide channel; 1) control biofilm; 2) dispersed with 40mM D-AA (40mM D-Asp and 40mM D-Glu); 3) dispersed with Cip; 4) dispersed with 40mM D-AA and 8 MLC Cip; blue arrow) presence of intercellular eDNA; yellow arrow) lack of intercellular eDNA. 1) Untreated *S. aureus* biofilms are reinforced by an organised honeycomb like meshwork made of interconnected intercellular eDNA. eDNA forms a filamentous mesh like structure within the biofilm and surrounds all cells. 2) Biofilms dispersed with D-AA lack majority of the eDNA. The pan-biofilm eDNA network is lost, any remaining eDNA is likely to be that entrapped between other matrix substances. 3) Presence of eDNA networks provides structure to persisting cells in biofilms treated with Cip on its own. 4) Biofilm treated with a combination of D-AA and 8 MLC Cip lack in eDNA meshwork structure and have minimal eDNA; eDNA = extracellular DNA; eDNA = extracellular DNA; D-AA = 40 mM D-Aspartic acid and 40 mM D-Glutamic acid; x MLC = x times minimum lethal concentration; Cip = ciprofloxacin.

4.3.6 D-AA reduce the rate of cell attachment

Since attachment of cells to a surface is the key initial stage of biofilm formation, it was appropriate to investigate the effect of D-AA on cell attachment. Figure 4.7 shows that exposing *S. aureus* cells to 40 mM D-AA reduces the rate of cell attachment compared to untreated cells. Throughout the attachment assay, a gradual increase in the percentage reduction in cell attachment was observed, starting from 43.45% at 5 min to 69.50% at 150 min.

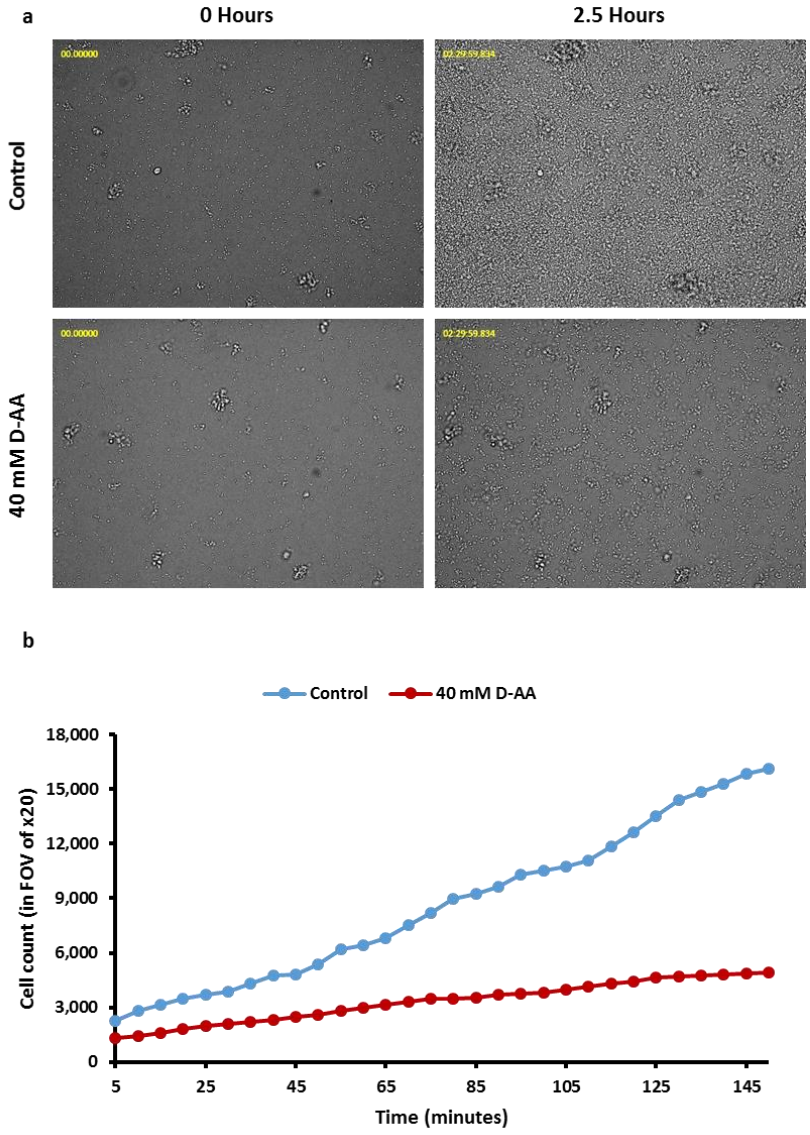

Figure 4.7: 40 mM D-AA considerably reduce the number of cells attached to the plate surface over 2.5 hours of incubation. b) The rate of *S. aureus* attachment is also slower in cells treated with 40mM D-AA as compared to control; D-AA = 40 Mm D-Aspartic acid and D-Glutamic acid. FOV = field of view; n=2.

4.4 Discussion

Aspartic acid and glutamic acid are known to enhance the solubility of Cip (156). Considering that one of the mechanisms of antimicrobial resistance in biofilms is the hindrance of drug diffusion through their matrix, it was decided to utilise these solubility enhancers of Cip in order to overcome this mechanism of antimicrobial resistance in *S. aureus* biofilms. Along with this, since amino acids themselves are known to possess anti-biofilm activity, whether D-Asp and D-Glu confer anti-biofilm activity was also investigated, whilst also studying the nature of this activity.

Although the effectiveness of D-isomers of amino acids as anti-biofilm agents is somewhat under debate (65, 180, 181), much attention has been given to them over the past decade and their role in inhibiting and dispersing biofilms. On the other hand, most publications agree on a lack of anti-biofilm activity of L-amino acids, and some even attribute pro-biofilm activity to them (187-189). Literature claiming that L-amino acids have anti-biofilm activity is rare (180, 181). It was therefore appropriate to choose D-isomers as solubility enhancers for Cip. A hypothesis was drawn that any potential anti-biofilm activity specific to D-isomers would supplement the above proposed biofilm perfusion enhancing mechanism and may further enhance the efficacy of Cip.

Due to age dependent variation in cells and matrix of a biofilm, Vidakovic *et al.* (2018), hypothesized that susceptibility to the antimicrobial agent (phage) may vary depending on age of the biofilm. They found that younger biofilms (<48 h) were more susceptible to phage activity than older (>60 h) ones (190). Similarly, Yang *et al.* (2015) found that younger biofilms (24 h) were more susceptible to inhibition by D-Asp than biofilms grown for 48 h and 72 h (181). Data presented here shows that whilst inhibiting, generally the anti-biofilm activity of D-AAs is independent of age, since in most concentrations, the percentage reduction in biofilm formation is similar regardless of how long the biofilm was incubated for (appendix Figure 2). On the other hand, dispersing already formed biofilm becomes less effective as the biofilm ages from 6h to 48h. At 72h, however the efficacy of amino acids again rises (appendix Figure 3), probably due to endogenous dispersal mechanisms also being involved at this point.

It seems Tong *et al.* (2014) were the first to attribute anti-biofilm activity to L-amino acids, shortly followed by Yang *et al.* (2015) (181). Whilst Yang *et al.* (2015) found that D and L-Asp were able to inhibit and disperse *S. aureus* biofilms, Tong *et al.* (2014) only reported inhibition of *Streptococcus mutants* biofilms (180, 181). However, the latter found inhibition with both D

and L-isomers of both of the acidic amino acids. In this chapter we show that either isomer of both Asp and Glu are able to inhibit and disperse *S. aureus* NCTC 8325 biofilms (Figure 4.1-Figure 4.6). To our knowledge, this is a previously unreported biofilm forming strain to be tested with these amino acids.

Contrary to our findings with *S. aureus*, L-Glu has been reported to enhance biofilm formation of *Azotobacter chroococcum (A. chroococcum)*. The concentration (40mM) we present to be most potent in anti-biofilm activity, Velmourougane *et al.* (2017) show, possess the highest pro biofilm activity (189). However their results in another paper seem to suggest that eDNA may be low if at all present in *A. chroococcum* biofilms (191). Furthermore, it seems that the importance of eDNA in forming biofilms and their role in stability after biofilm formation varies from species to species (192). Absence of eDNA is probably unlikely, as even without any specific DNA releasing mechanisms, eDNA is a natural product of dead cells. It is more likely therefore, that eDNA does not play a pivotal role in the formation of *A. chroococcum* biofilms, rendering the anti-eDNA mechanism of L-Glu presented later on in this chapter unchallenged. Hence, with no disruption to biofilm structure, the pro-biofilm effects L-Glu, as observed by Velmourougane *et al.* become more pronounced.

The ability of the dyes SYTO 9 and PI to distinguish between live and dead cells can be attributed firstly, to the inability of PI to enter live cells possessing intact membranes (except in exceptional cases), whereas SYTO 9 is able to enter both live and dead cells (193, 194). Secondly, PI has higher affinity for, and is able to, displace SYTO 9 from nucleic acids (194); despite the presence of SYTO 9 within dead cells or within extracellular matrix, SYTO 9 is unable to compete against PI for nucleic acids. Hence, DNA within both dead cells and the extracellular matrix (eDNA) is detected through the fluorescence of PI bounded to it. This is made feasible by the fact that the fluorescence of both dyes is substantially lower when unbound; fluorescence of both dyes is enhanced greatly when the dyes are attached to nucleic acids. As a result, despite the presence of SYTO 9, it is not detected in the presence of PI. This allowed confident localisation of eDNA through confocal imaging (Figure 4.5 and Figure 4.6). It seems that under specific conditions PI may also enter live cells. Kirchhoff *et al.* (2017) showed that PI can enter live cells if there are changes to membrane potential, resulting in yellow/orange cells as opposed to the expected green or red (193). It is likely that the orange cells seen in Figure 4.5.2 and Figure 4.6.2 are due to some uptake of PI which binds to DNA within the cells (193). Since the rest of the DNA within the cells has SYTO 9 bounded to it, fluorescence of both red and green makes cells appear orange in the overlay. This uptake of PI through intact membranes may be due to a change of membrane potential or an increase in the permeability of PI through other mechanism caused by amino acids (40, 193).

With amino acid exposure, one cause for the reduction in biofilm CFU/ml and in the rate of cell attachment (Figure 4.4 and Figure 4.7) is likely due to reduction in planktonic cell viability (appendix Figure 4). However another important cause suggested by confocal findings is lack of eDNA (Figure 4.5 and Figure 4.6). Recently, Sugimoto *et al.* (2018) showed that eDNA is the most common component of *S. aureus* biofilms suggesting it to be a prime target for anti-biofilm therapeutics (195). This chapter proposes that a way to target this vital structural matrix component is acidic amino acids; the biofilms inhibited and dispersed with D-AA at 40mM concentration were unable to form (Figure 4.5.2) or lost (Figure 4.6.2) their eDNA honeycomb meshwork, respectively. Since eDNA is important in initial bacterial attachment to a surface and also for further biofilm growth, including cell aggregation, the lack of eDNA or its inability to form a structural framework means that the biofilm is neither able to build a strong foundation nor is able to mature, ultimately stunting its growth (196, 197). Furthermore, with the continuous role of aggregating cells and providing stability to the already formed biofilms, lack of eDNA leads to the breakdown of already formed biofilms, at least partially. Thus the low number of viable cells in inhibited biofilms can be attributed to the inability of the cells to attach and aggregate. Whereas in dispersed biofilms, this would be due to destabilisation of the eDNA mediated intercellular bonding mechanism; the cells are released from the biofilm due to the lack of eDNA which would otherwise hold them together.

Whilst the cells within a *S. aureus* biofilm are interconnected through cell wall structures, matrix components also play a major role in the stabilisation of the biofilm (198). The major components of the extracellular matrix in *S. aureus* biofilms are the polysaccharide intercellular adhesin (PIA) and as aforementioned, extracellular DNA (eDNA). The mechanisms involved in the release of eDNA from *S. aureus* cells is not yet clear. However it seems to be highly dependent on autolysis which has been attributed to many systems including those leading to a reduction in cell wall integrity (199, 200). As discussed later, findings reported in this chapter highlight that eDNA release may also be derived by externally influenced lysis. Nevertheless, this eDNA has been described as an electrostatic net that anchors cells together (197). However, for eDNA to serve its purpose in the matrix, *S. aureus* seems to employ certain moonlighting proteins i.e. enolase and GAPDH (glyceraldehyde-3-phosphate dehydrogenase) which are attached to the cell surface (201). Although these proteins are cytoplasmic in origin, they serve a second function in the matrix acting as a bridge between the cells and the eDNA. The removal of these proteins by increasing the pH causes the release of eDNA from the *S. aureus* biofilms; showing that the role of eDNA in the structural stability of the biofilm is dependent on these cell surface proteins (197). These proteins are proposed as an ideal bridge because they are thought to be positively charged, and hence

are able to interact with and connect the negatively charged cells on one side with the negatively charged eDNA on the other (197).

It seems that eDNA in a healthy biofilm surrounds all cells individually (Figure 4.5.1 and Figure 4.6.1), helping them aggregate and provides structural stability and integrity to the biofilm. Das *et al.* (2011) suggest that bacterial aggregation mediated by eDNA is due to acid-base interactions (202). We propose that acidic amino acids prevent the formation of eDNA meshwork, and if already present, break it down by interfering with these acid-base interactions. The mechanism that may be employed by acidic amino acids is depicted in Figure 4.8. Negatively charged eDNA helps aggregate cells by interacting with positively charged *S. aureus* surface proteins (enolase and GAPDH) on multiple cells; thus acting as an intercellular electrostatic bridge (Figure 4.8a). The importance of these proteins in intercellular bridging is highlighted by their presence, at varying concentrations, along the entire surface of bacteria (203-209). Since at the pH value of 4.01, the ionised acidic amino acids are negatively charged, they are able to interact with these positively charged proteins. Resulting ion-pair formation, neutralises the positive charge on enolase and GAPDH, rendering eDNA unable to interact with these proteins. Therefore, during inhibition intercellular bridges do not form, neither are cells able to aggregate (Figure 4.8c). Dispersal with amino acids utilises a similar mechanism. Anionic amino acids displace enolase and GAPDH associated eDNA. Release of eDNA causes a release of cells from the biofilm since they are now unable to aggregate with each other (Figure 4.8b). Greater effectiveness of D-AA in combination as compared to their use individually can be explained through the presence of a greater number of anions in combination. More anions present greater obstruction for eDNA-protein interaction, resulting in combined D-AA exhibiting greater anti-eDNA activity. Support for the role of charge in the underlying mechanism is provided by the observation that neutralising the acidic amino acids using NaOH halts anti-biofilm activity (appendix Figure 5) of the amino acids.

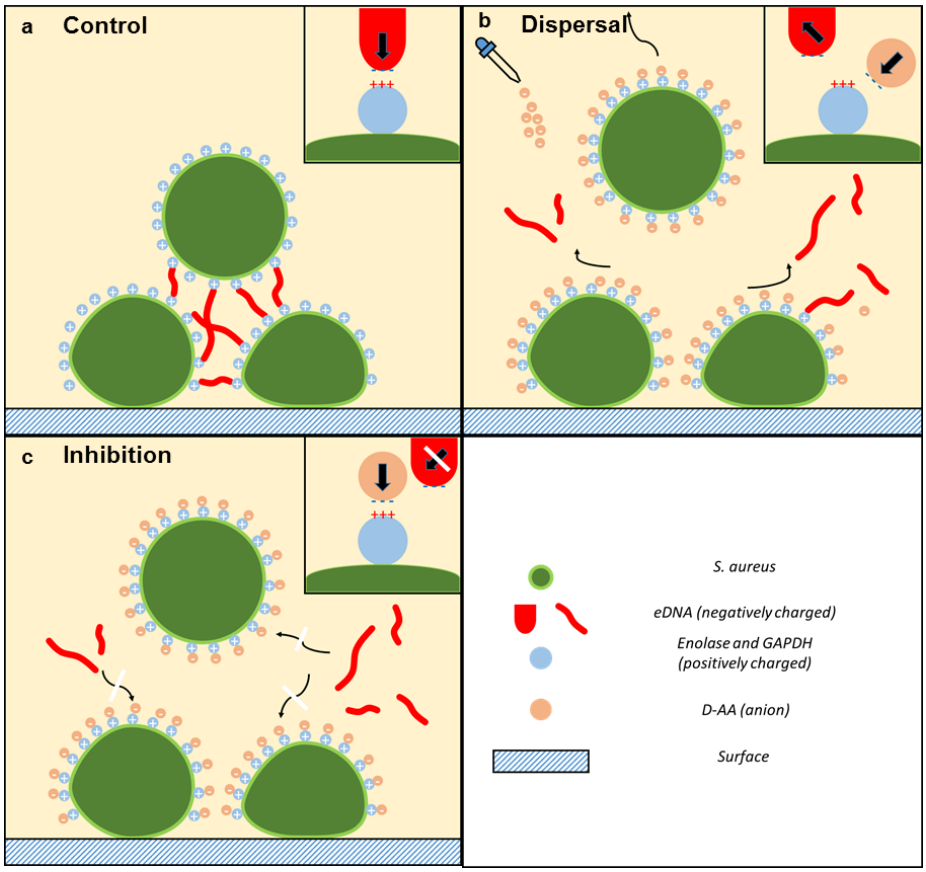

Figure 4.8: Mechanism of biofilm inhibition and dispersal using D-AA. D-AA exhibit anti-eDNA activity. a) Normal conditions: eDNA forms intercellular bridges by interacting with surface bound positively charged proteins (enolase and GAPDH) via acid-base interactions. b) Dispersal: addition of anionic D-AA displaces eDNA from the surface bound positively charged proteins. eDNA is released and the intercellular bridges are broken. c) Inhibition: the present D-AA interact with surface bound positively charged proteins preventing eDNA from associating with these proteins; intercellular bridges are unable to form; eDNA = extracellular DNA; D-AA = D-Aspartic acid and D-Glutamic acid; GAPDH = glyceraldehyde-3-phosphate dehydrogenase.

In dispersed biofilms, it is likely that other matrix components are still present which would explain why there is a greater percentage reduction in viable cell number (Figure 4.4 and appendix Table 1) as compared to total biofilm density (Figure 4.1 and appendix Table 1). This is because with the release of eDNA, the cells are unable to stay aggregated and are released from the biofilm. However, other matrix components remain unaffected and constitute to the remaining biofilm density (Figure 4.1a,b,d,e and appendix Figure 3) observed after dispersal experiments. This also gives reason as to why D-AA seem to appear more efficacious at reducing biofilm density whilst inhibiting than whilst dispersing. Conversely, cell number and eDNA are not the only effected components in inhibited biofilms. Clearly, other matrix components are also unable to become established and form a consequential part of the percentage reduction observed in biofilm density (appendix Table 2). This further highlights the role of eDNA in not only the aggregation of cells but also the establishment of other matrix components.

Confocal images show that use of treatment with Cip on its own leads to biofilms with seemingly denser eDNA structures (Figure 4.5.3 and Figure 4.6.3). This is a visual reminder as to why biofilms are a major cause of chronic infections. Whilst an antibiotic may get rid of majority of the bacterial load from the body, persister cells remain unharmed within biofilms. Biofilms are then able to re-establish once treatment is stopped and ultimately, the infection recurs. Interestingly, treating already formed biofilms with Cip alone reveals eDNA localised in a seemingly well-fortified boundaries (Figure 4.6.3 and appendix Figure 1). Here we hypothesis two potential implications of these findings. Firstly, these boundaries suggest that within a biofilm eDNA structures have weak and strong points. Cells away from these boundaries are released upon treatment giving rise to voids within treated biofilms. Since these boundaries seem circular in morphology, they may be boundaries to microcolonies within the biofilm. Previous studies have shown eDNA to be highly concentrated around *P. aeruginosa* microcolonies (210, 211). A second possibility is that upon threat, cells which are to persist within the biofilm are able to further fortify and make dense the eDNA structures surrounding them. This is made feasible due to the excess of eDNA present as a result of antibiotic triggered cell death. In either case, it is appropriate to speculate that these strong points within eDNA meshwork are likely responsible for cell persistence and antimicrobial resistance.

Despite the ability of acidic amino acids to enhance the solubility of Cip (156), no synergistic effect of combining 40Mm D-AA and Cip was found in biofilm density or on cell viability. The reasons may be different for inhibition and dispersal. When inhibiting biofilms, 40Mm amino acids are alone able to inhibit 96.89% of the biofilm from forming. This leaves minimal room for improvement for any amounts of Cip which may be added in biofilms in combinations with the amino acids. Similarly, with a reduction of 97.60% CFU in biofilms dispersed with D-AAs, there are not many viable cells within the biofilm left for Cip to act on. In either case, any effect of Cip has probably gone unnoticed. Therefore it seemed likely that a synergistic effect may be more pronounced at lower concentrations of D-AAs. Further experiments were carried out which confirmed that at lower but specific concentrations, a synergistic effect on biofilm density is achievable by combining Cip with D-AA (Figure 4.3b,c,e).

4.5 Conclusion

Acidic amino acids are able to disperse already formed biofilms and inhibit new *S. aureus* biofilm formation. This coincides with a lack of eDNA present in treated biofilms, suggesting that eDNA is a target for the observed D-AA anti-biofilm activity. Hence, an anti-eDNA mechanism is proposed; D-AA modulate the acid-base interactions which are essential for anchoring eDNA to cells. The findings further confirm that eDNA is critical to *S. aureus* biofilms, both in formation stages as well as once established. Targeting matrix components not only helps fight biofilms on its own, but may also be used to increase the efficacy of other antimicrobial agents. Furthermore, the role of antibiotics in increasing antimicrobial resistance is reiterated, whilst suggesting that the mechanisms of acquiring antimicrobial resistance is not limited to cells but may extend to the matrix. Therefore, to fight antimicrobial resistance drugs that target cells alone should be used in conjunction with ways to disrupt the matrix or inhibit its formation. The findings from this work can lead to applications where amino acids act as anti-biofilm agents to coat catheters, implants and in wound dressings.

Chapter 5: Investigating the effect of acidic and basic amino acids on the solubility, caco-2 monolayer permeability and efflux ratio of digoxin

5.1 Introduction

Being one of the oldest drugs used for cardiovascular care, digoxin (Figure 5.1) is frequently used to treat atrial fibrillation and for patients suffering with heart failure (212). Its mechanism of action relates to inhibition of sodium-potassium adenosine triphosphatase (ATPase) which ultimately results in lower heart rates and increased myocardial contractility due to lengthening of the cardiac action potential (212).

Figure 5.1: Chemical structure of digoxin. Image taken from British Pharmacopeia (102).

BCS classification is a system which puts drugs into four groups depending on their solubility and permeability profiles. Surprisingly, in literature, digoxin has been grouped into classes I, II, and IV (213-215). However according to Caldeira TG et al, digoxin was grouped into classes I and II only provisionally without taking into consideration the effect on permeability of efflux transporters(213). Valizadeh et al, through conducting permeability experiments on rat jejunum suggested that digoxin belongs to BCS class IV (216). In summary, digoxin is both poorly soluble and has poor permeability.

Finding ways to overcome solubility and permeability limitations for digoxin can reduce toxicity to patients as well as costs for the pharmaceutical companies. Our group has previously shown that amino acids possess the ability to enhance drug permeation through both caco-2 monolayers as well as buccal cell layers (165). Therefore in this study, we aim to investigate

the effect of acidic and or basic amino acids on the solubility profile of digoxin as well as their effect on the permeability of the drug through caco-2 monolayers.

Digoxin is taken up into cells via passive diffusion but its uptake into the body is limited by efflux. It is a well-known substrate for P-glycoprotein (P-gp), so much so that it is also sometimes used to validate the integrity caco-2 monolayers (217, 218). Caco-2 cells serve as a well-established in vitro model of the enterocytes. Once cultured on permeable cell inserts (transwells), under appropriate conditions they form monolayers which are well differentiated. These differentiated cells are highly polarised, possess microvilli, exhibit tight junctions and express similar transporters to those present in intestinal epithelium, resulting in an appropriate selective barrier for the study of both passive and active drug transport. Like enterocytes they possess distinct apical and basolateral features allowing for the investigation of drug absorption and secretion through apical to basolateral and basolateral to apical studies respectively.

The primary aim of the study in this chapter was to evaluate the role of charged amino acids on solubility and the in vitro permeability of digoxin. This was done by first setting up a HPLC method and determining the saturated solubility of digoxin in different concentrations of amino acids in aqueous medium. Finally permeability experiments using caco-2 monolayers were conducted to determine the permeability enhancing ability of the solubility optimised amino acids.

5.2 Materials and methods

5.2.1 Materials

Digoxin was purchased from Acros Organics whereas L-Aspartic acid (Asp), L-Glutamic acid (Glu), L-Arginine (Arg), L-Histidine (His), L-Lysine (Lys) were purchased from Sigma Aldrich. HPLC grade Acetonitrile was purchased from Fisher Scientific UK. Caco-2 cells were purchased from Public Health England (PHE). Minimum essential medium eagle (EMEM), Dimethyl sulfoxide (DMSO), Thiazoyl Blue Tetrazolium Bromide (MTT) and Corning® Transwell® polycarbonate membrane cell culture inserts were obtained from Sigma Aldrich. Gibco™ Fetal bovine serum and Gibco™ Hank's balanced salt solution (HBSS; no calcium, no magnesium and no phenol red) and digoxin (95%; ACROS Organics™) was obtained from Fisher Scientific. Eagle's minimum essential medium (MEM) Non-essential amino acids solution (without L-glutamine), penicillin-streptomycin (pen-strep) and L-glutamine solution (200 mM) was obtained from as well as Sigma Aldrich. Trypsin used was 0.25% trypsin, 2.21 mM EDTA in HBSS w/o calcium, magnesium and sodium bicarbonate (Corning™). 0.4% Trypan Blue solution was purchased from Sigma Aldrich.

5.2.2 HPLC analysis

HPLC was used for obtaining a calibration curve and further sample quantification using the Agilent Technologies 1260 infinity. Eclipse Plus C18 3.5µm 150 x 4.6 mm column was used. The method was adapted from British Pharmacopoeia. Mobile phase consisted of Water and Acetonitrile (70:30 v/v). Analysis was carried out at ambient temperature with the flow rate of 1 ml/min and an injection volume of 40 µL. λmax for digoxin was determined using Genesys 10s UV-Vis Spectrophotometer to be 220 nm and hence the UV detector for HPLC analysis was set at 220 nm.

To obtain the calibration curve, stock solution was prepared by dissolving digoxin in DMSO at a concentration of 20mM. This stock solution was used to make chromatographic standard solutions by diluting with appropriate volume of water.

5.2.3 Digoxin solubility study

Saturated solubility of digoxin in different concentrations of amino acids were determined. Stock solution of amino acids (arginine, lysine, histidine, glutamic acid and aspartic acid) with

a concentration of 4500 µg/ml was prepared. Dilutions were prepared from this stock solution ranging from 4500 µg/ml down to 62.5 µg/ml. Excess amounts of digoxin was added to each dilution of each amino acid solution. The mixture was stirred at ambient temperature for up to 24 hours until excess drug had deposited. The pH of the solution was obtained (Xisherbrand Hydrus 500 pH meter) after which the supernatant was filtered through 0.45 µm syringe filter. The concentration of the filtrate was determined through HPLC using the method detailed above.

5.2.4 Cell revival

Caco-2 cells were obtained from Public Health England. The frozen vial was wrapped with tissue soaked in 70% ethanol which was followed by loosening of the lid to release excess liquid nitrogen. The lid was retightened and the frozen vial was thawed in a 37 °C water bath. The vial was again wiped with 70% ethanol soaked tissue before opening in a sterile biological safety cabinet/ tissue culture hood. The contents of the vial was then added to T25 flask containing 6ml of media. The media used for culturing caco-2 cells was EMEM supplemented with 10% FBS, 1% non-essential amino acids, 1% 200 mM L-glutamine and 0.5% pen-strep. After 24 hour incubation in 37 °C incubator with 5% CO_2, the media was changed to remove unattached cells.

5.2.5 Caco-2 cell culture, routine maintenance and cell splitting

As above, Caco-2 cells were purchased from PHE and were received at passage 43 (P 43). The passages used throughout the study ranged from P 47 to a maximum of P 60. Cells were grown at 37 °C and 5% CO_2 in T75 flasks and the media used was EMEM supplemented with 10% FBS, 1% non-essential amino acids, 1% 200 mM L-glutamine and 0.5% pen-strep. The media was changed every 2-3 days which replenished nutrients for the cells and removed dead cells.

To maintain caco-2 cells for experiments, the cells were split at around 80% confluence. To do this cells were washed with sterile HBSS which allowed removal of serum which would otherwise deactivate the trypsin. This was followed by incubation with 3 ml trypsin and subsequent incubation at 37 °C for a couple of minutes. The flasks were gently tapped to aid detachment of cells from the solid surface. Once sufficient cells were detached, as visualised by an inverted light microscope the cell culture media was quickly added to halt trypsin activity.

The resulting cell suspension was split into 4 new flasks and incubated at 37 °C with 5% CO_2 until needed for permeability experiments or further splitting.

5.2.6 Cell counting

To count cells, a clean a grease free haemocytometer was used. A coverslip was affixed onto the haemocytometer by applying slight moisture; newton's rings observed once coverslip fixed onto haemocytometer appropriately. When ready, it was ensured that the cell suspension to be counted was thoroughly mixed. Next, a small volume of the suspension was diluted with 0.4% trypan blue. 10 µL of this diluted suspension was then pipetted at the edge of the mounted coverslip and allowed to run under. The haemocytometer was then visualised under a light microscope and live cells were counted on multiple big squares. Average of the squares was then taken and cell concentration per ml calculated using the following formula.

$$\text{Average No. of cells per square} \times \text{ dilution factor } \times 1 \times 10^4$$

5.2.7 Determining Digoxin and amino acid concentrations for permeability experiments using the MTT assay

5.2.7.1 Determining optimal concentration of Caco-2 cells for MTT assay

For MTT assay to be carried out, the optimal cell density for seeding was first determined. This was done by seeding 100 µl of caco-2 cell suspension in cell culture media with serial dilutions ranging from a concentration of 500000.00 cells/ml to 975.56 cells/ml in wells of a 96 well plate. The cells were then incubated for 24h at 37 °C with 5 % CO_2. Next day, after removal of media, 100 µl of 0.5 mg/ml of MTT was added to each well. Next the plate was again incubated under same conditions for 2-4 hours, until intracellular purple pigmentation was clearly visible through light microscopy. After this the supernatant (MTT) was removed and 100 µl of DMSO was added to each well. The plate was left shaking for 30 min at 37 °C. The optical density was then read at 570 nm and a graph was plotted. A concentration from the linear portion of the graph was chosen for conducting further MTT assays.

5.2.7.2 MTT assay

For the MTT assay, 100 µl of 250000 cells/ml cell suspension was added to each well of a 96 well plate and incubated for 24h at 37 °C with 5% CO_2. Next day the media was removed and

100 µl of test concentrations of the amino acids (30 mM to 30 pM) and digoxin (100 µM to 100 fM) was added to each well. The plates were then incubated at 37 °C with 5% CO_2 for 4 h. After 4h, supernatant was removed and 100 µl of 0.5 mg/ml (10µl of 5 mg/ml MTT stock added to 90µl HBSS) of MTT (made up in HBSS) was added to each well. The plate was then further incubated for 2h (until intercellular punctate purple precipitate is visible) under same conditions. Next the supernatant containing MTT was removed and 100 µl of DMSO was added to each well and the plate was left to shake at 37 °C for 30 min (until the cells have lysed and the purple crystals have dissolved). Finally the O.D. was determined by reading the plate using a plate reader at 570nm.

5.2.8 Measurement of TEER

Transepithelial electrical resistance (TEER) was measured with an EVOM epithelial voltohmmeter (World Precision Instruments). TEER was measured at room temperature each time. To ensure this, monolayers were left at room temperature for 15 minutes before measuring TEER. TEER was measured whilst growing caco-2 monolayers to follow monolayer development and confirm its integrity. TEER was also measured before, during and after each permeability experiment. It was ensured that the TEER probe was sterilised in 70% ethanol between reading different transwells. The pre-experimental TEER was measured with monolayers still in the media, whilst the TEER measurements during the permeability experiments were performed in HBSS. After the experiments, HBSS was replaced with media in each compartment before taking the TEER measurements. Only those monolayers with a TEER of above 250 Ωcm^2, after correction with blanks, were used for the permeability experiments. To calculate TEER net resistance (which is resistance of the blank subtracted from the resistance of the monolayer) was multiplied by the cell growth area (4.67 cm^2).

5.2.9 Caco-2 permeability assay

After reviving cells, passaging was carried out at least twice before seeding caco-2 cells on transwells for permeability experiments. Cells were seeded at a density of 1.3 x 10^5 cells/cm_2 on polycarbonate-coated transwell membranes. This translates to 1.5 ml of cell suspension of a concentration of 4 x 10^5 cells/ml added to each 6 well transwell. The cells were allowed to grow to form a monolayer for ~21 days. Media was changed every 2-3 days to allow healthy development of the monolayer.

Culture media was changed a day before the transport experiments were to be carried out. This prevented the cells from changing to a starved phenotype (18). On the day of the experiment, all solutions were pre-warmed. Donor solutions were prepared with appropriate concentration of digoxin and amino acid.

The membranes and monolayers were washed with HBSS by transferring the transwells into new wells containing HBSS and replacing apical media with HBSS. Following the wash, the transwells were incubated with HBSS for 15 minutes before starting the transport experiments. Transport experiments were performed in the apical to basolateral (A-B) or B-A direction by pipetting the donor solution in the apical or basolateral side respectively. Either way, final volume for apical side was kept at 1.5ml and 2.5ml at basolateral side. Donor solutions were either digoxin on its own or digoxin with various molar ratios (1:5, 1:10, 1:30, 1:100, 1:300 and 1:600) of L-arg, L-lys and L-his made up in HBSS. For determining the concentration of the receiver compartment, 500 µl samples were withdrawn at each time-point, making sure to replace the volume with HBSS. The time-points used is this study were 0, 15, 30, 45, 60, 120 and 180 min. The transwells were incubated at 37°C with 5% CO_2 between each time point to allow permeation at a physiological temperature. A final sample was taken from the donor compartment to calculate mass balance.

5.2.10 Data analysis

5.2.10.1 Papp

After permeability experiments in A-B and B-A direction, the apparent permeability coefficient (Papp) was calculated using the equation:

$$Papp = (\frac{dQ}{dt})/(C_0 A)$$

In this equation, dQ/dt is the rate of permeation of the drug (digoxin) into the receiver compartment, whilst A is the surface are of transwell or Caco-2 monolayer and C_0 is the initial donor compartment concentration. In this case, we took the slope of the linear portion of the plot of the concentration in the receiver compartment by time to be dQ/dt. Surface area of the transwell was 4.67 cm^2, whilst C_0 was measured by taking a sample and determining the concentration by HPLC.

5.2.10.2 Efflux ratio

After determining Papp in both directions, A-B and B-A, it was possible to determine the efflux ratio (ER) using the following equation:

$$ER = \frac{Papp\ B - A}{Papp\ A - B}$$

Here, the Papp B-A is the Papp determined as previously described for the basolateral to apical direction of permeability experiments whilst Papp A-B is for the apical to basolateral direction.

5.2.11 Statistics

One way ANOVA (multiple comparison) was used to look for overall statistical significance within the data and was followed by Tukey's multiple comparisons test to see exactly where the significant difference was. GrapPad Prism was used for statistical analysis and adjusted P values below 0.05 were taken as statistically significant.

5.3 Results

5.3.1 Digoxin solubility in the presence of amino acid

Solubility of digoxin was investigated in aqueous solutions of both acidic (L-aspartic acid and L-glutamic acid) and basic (L-arginine, L-lysine and L-histidine) amino acids. The concentration range of the amino acids used was from 62.5 µg/ml to 4500 µg/ml.

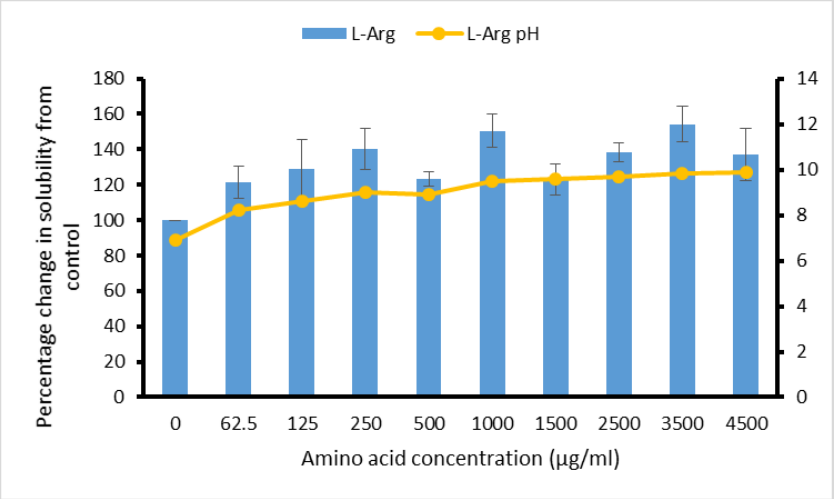

Figure 5.2: Apparent solubility of digoxin in the presence of L-Arg. Generally the solubility of digoxin increased in the presence of L-Arg. Significant rise in digoxin solubility was observed with 125 (p=0.017), 250 (p=0.00078), 1000 (p<0.0001), 2500 (p=0.0013), 3500 (p<0.0001) and 4500 µg/ml (p=0.0018) of L-Arg; n=3.

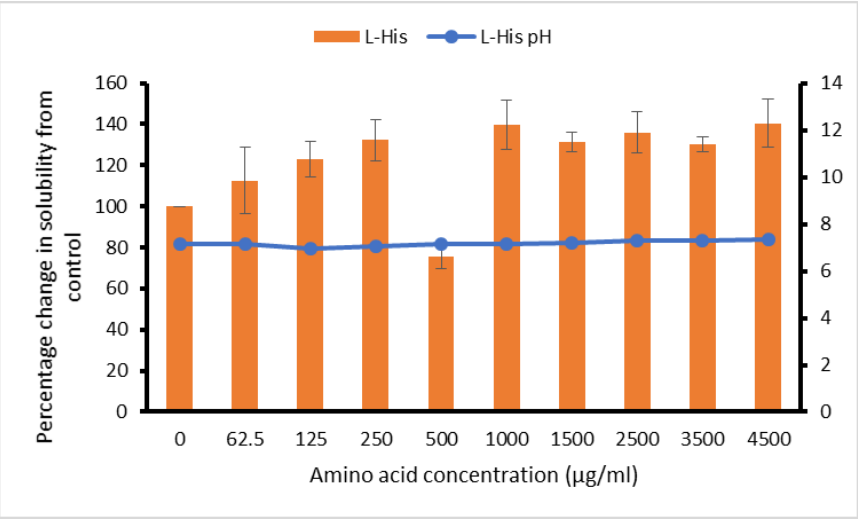

Figure 5.3: Apparent solubility of digoxin in the presence of L-His. Generally the solubility of digoxin increased in the presence of L-His. Significant rise in digoxin solubility was observed with 125 (p=0.048), 250 (p=0.0033), 500 (p=0.031), 1000 (p=0.00039), 1500 (P=0.0041), 2500 (p=0.0011), 3500 (p=0.0062) and 4500 µg/ml (p=0.00032) of L-His; n=3.

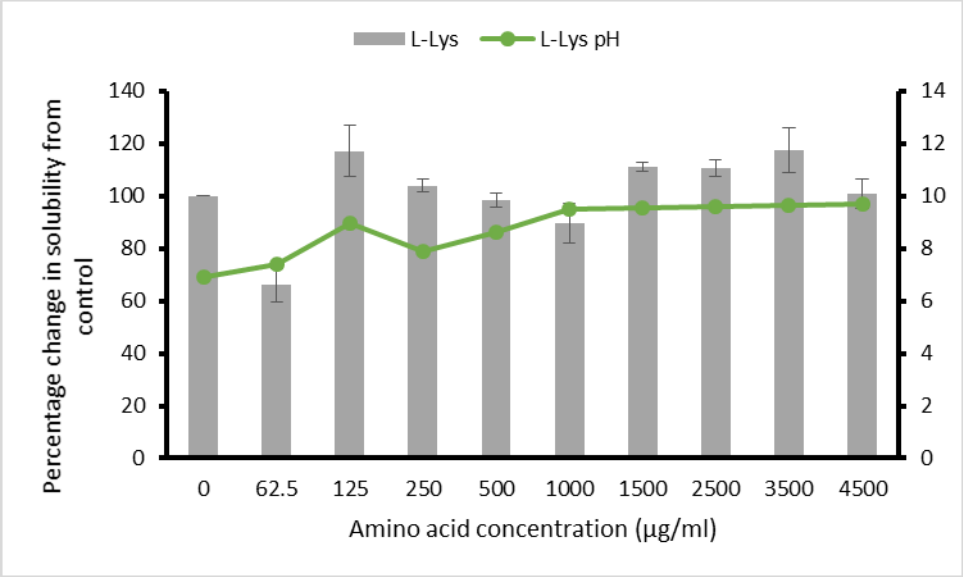

Figure 5.4: Apparent solubility of digoxin in the presence of L-Lys. Significant rise in digoxin solubility was observed with 125 (p=0.011), and 3500 µg/ml (p=0.0089) of L-Lys; n=3.

Overall, with the exception of a few outliers, the solubility of digoxin increased with increasing concentration of the basic amino acids, especially L-Arg and L-His (Figure 5.2 to Figure 5.4). In L-Arg solution of 3500 µg/ml, there was a 1.54 fold increase (Figure 5.2) in digoxin solubility compared to control, representing the highest amount of digoxin dissolved with this amino acid. Same concentration of L-Lys lead to a 1.17 fold increase (Figure 5.4) in digoxin solubility compared to control, representing the highest enhancement in digoxin solubility with the amino acid. A 1.40 fold increase (Figure 5.3) in solubility was observed with L-His concentration of 4500 µg/ml representing the highest amount of drug able to dissolve in the concentration range of this amino acid.

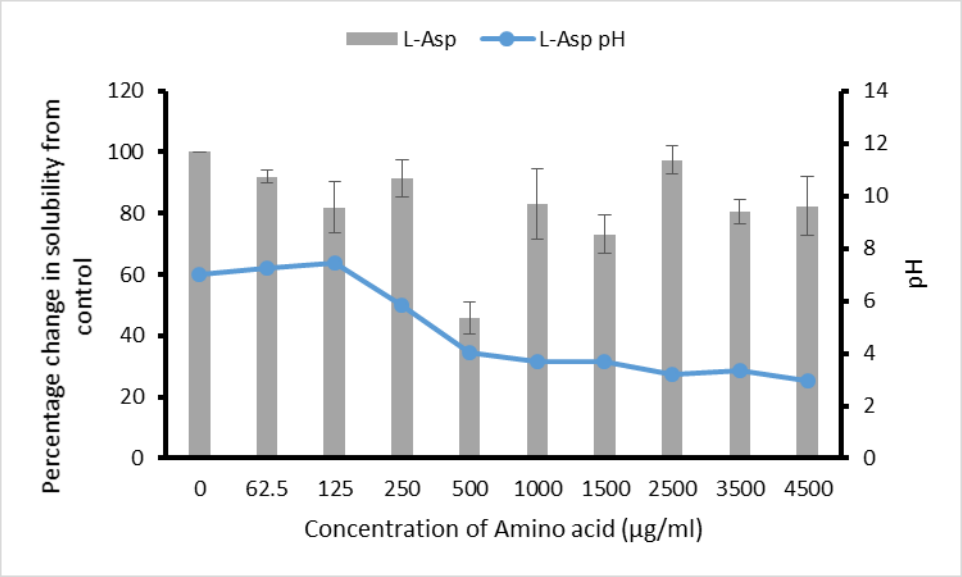

Figure 5.5: Apparent solubility of digoxin in the presence of L-Asp. No significant rise in digoxin solubility was observed with L-Asp; n=3.

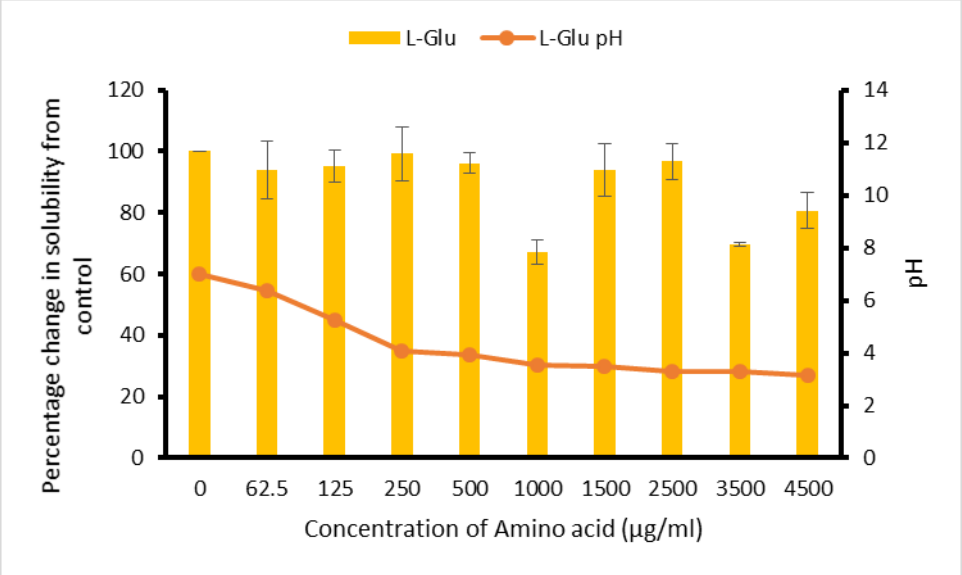

Figure 5.6: Apparent solubility of digoxin in the presence of L-Glu. No significant rise in digoxin solubility was observed with L-Glu; n=3.

Unlike basic amino acids, no significant increase in digoxin solubility was observed with the acidic amino acids, L-Asp and L-Glu (Figure 5.5 and Figure 5.6). It is also worth noting that the chromatogram for digoxin exposed to the acidic amino acids showed two peaks instead of the one peak observed whilst obtaining the calibration curve and whilst experimentation with basic amino acids.

5.3.2 Digoxin permeability through caco-2 monolayer in the presence of basic amino acids

5.3.2.1 MTT assay

To investigate whether amino acid are able to increase digoxin permeability, it was essential that concentrations that are not cytotoxic to the caco-2 cells were used. To determine the optimal concentration of cells needed for carrying out the MTT assay, different concentrations of cells were investigated (Figure 5.7). Optical density (O.D.) increased with increasing concentrations of cells. From the straight portion of the graph, 250000 cells/ml was chosen to proceed with for MTT assays as it gave decent confluence (Figure 5.8) within 24 hours and reduced the chance of requiring more cells than could be harvested if 500000 cells/ml was chosen.

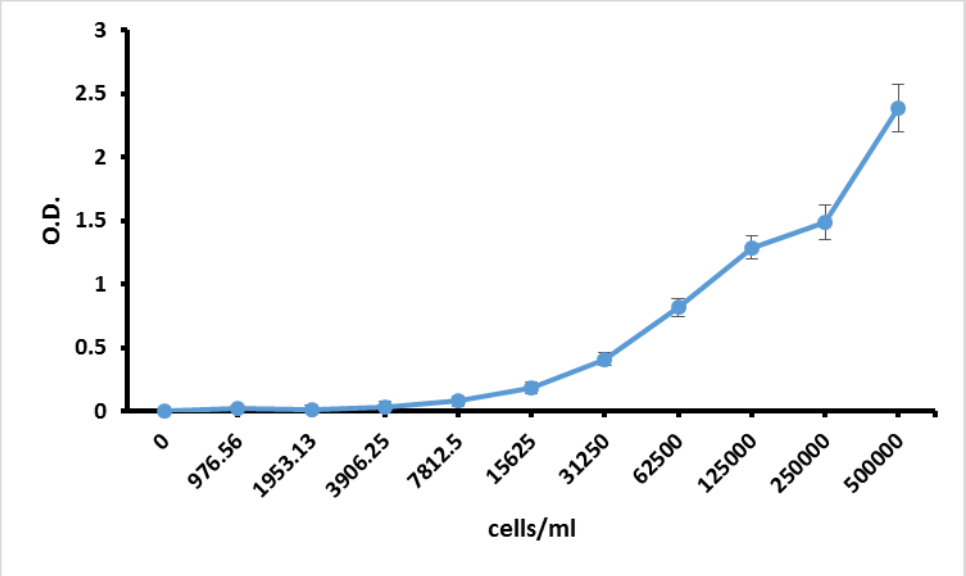

Figure 5.7: Caco-2 cell concentration plotted against O.D. measured at 570 nm to determine the optimal concentration of cells for MTT assay; n=16.

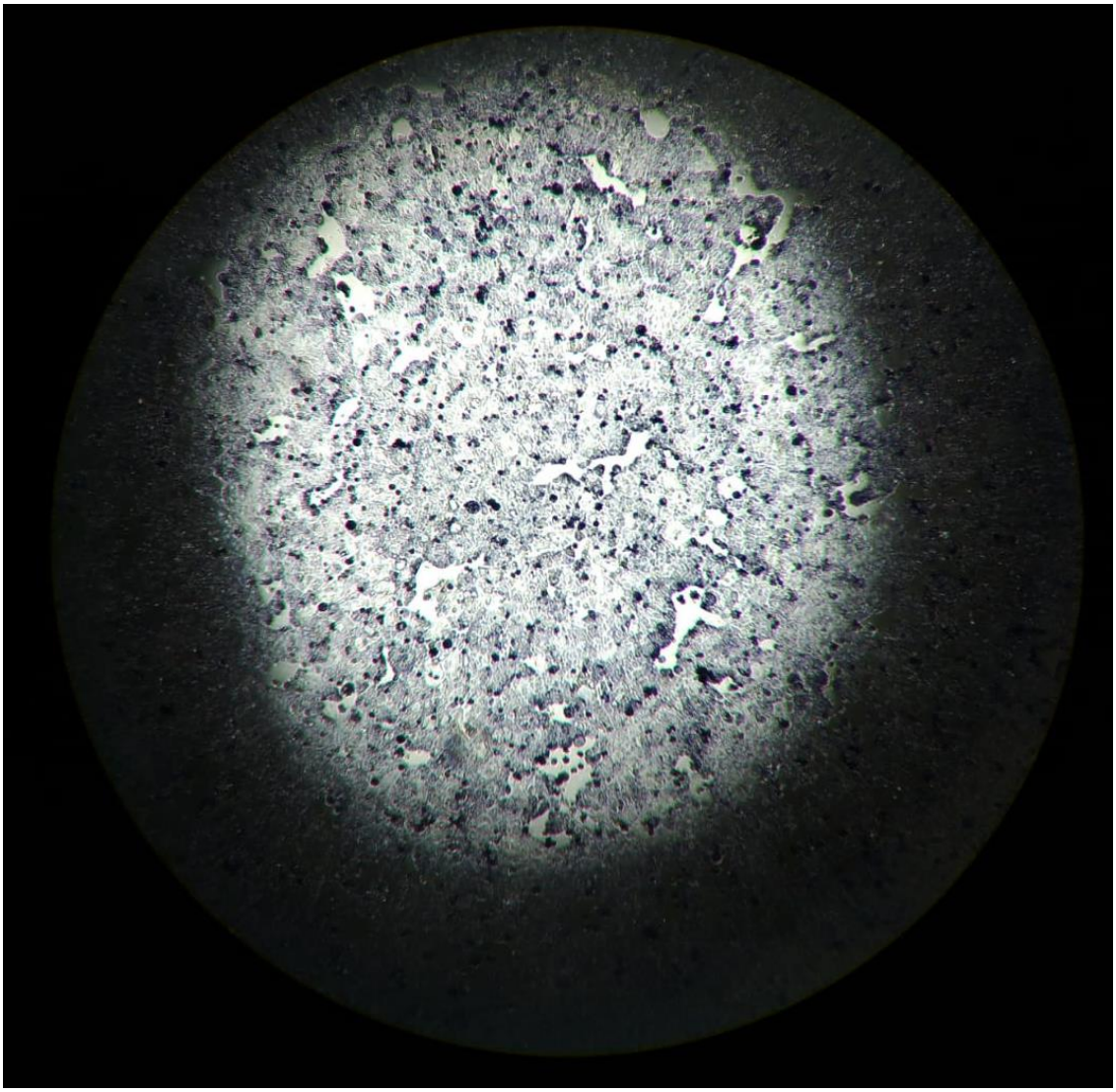

Figure 5.8: Acceptable (>80%) cell confluence achieved within 24h with 250000 cells/ml for MTT assay.

MTT assays were then conducted for the three basic amino acids, L-arg, L-lys and L-his (Figure 5.9) as well as digoxin (Figure 5.10) and percentage cell viability plotted. With all amino acids there was an initial decrease in caco-2 cell viability with increasing concentration of the amino acid. Further increase had the opposite effect and the cell viability reverted back to normal. With L-arg, reduction in cell viability was observed at 3 nM to 300 µM of the amino acid ($p<0.01$). With L-lys however, significant reduction was only seen at a concentration of 3 nM ($p<0.05$). Significant reduction with L-histidine was observed between the concentration range of 3 nM to 30 µM ($p<0.05$). Digoxin exhibited a concentration dependent cytotoxicity on caco-2 cells where an increase in concentration led to a reduction in cell viability. Significant reduction in cell viability with digoxin was observed above 100 nM of digoxin, where the p value for 100 nM was <0.05 and for 1, 10 and 100 µM was <0.0001.

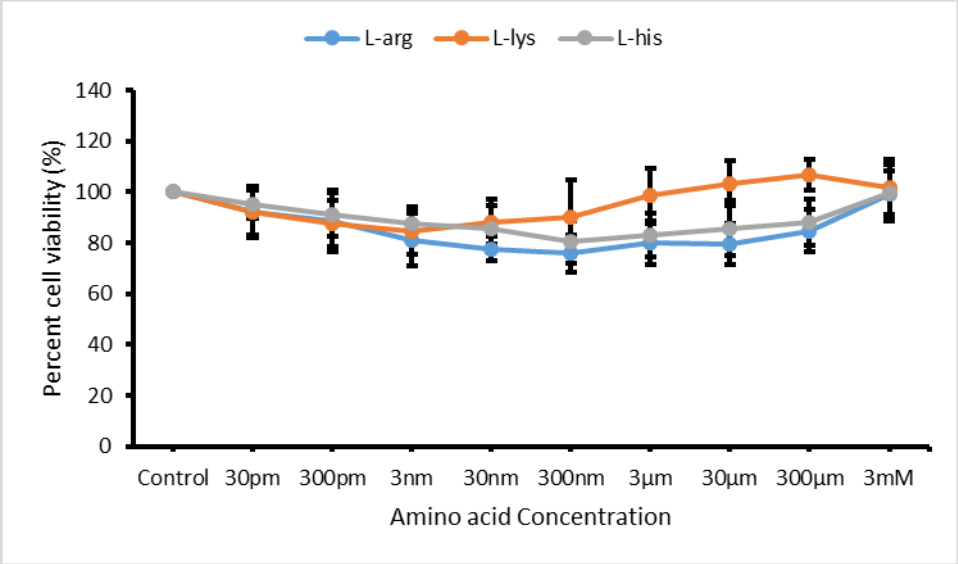

Figure 5.9: MTT assay was conducted to check for amino acid cytotoxicity. Percentage caco-2 cell viability at different concentrations of L-arg, L-lys and L-his; n=8.

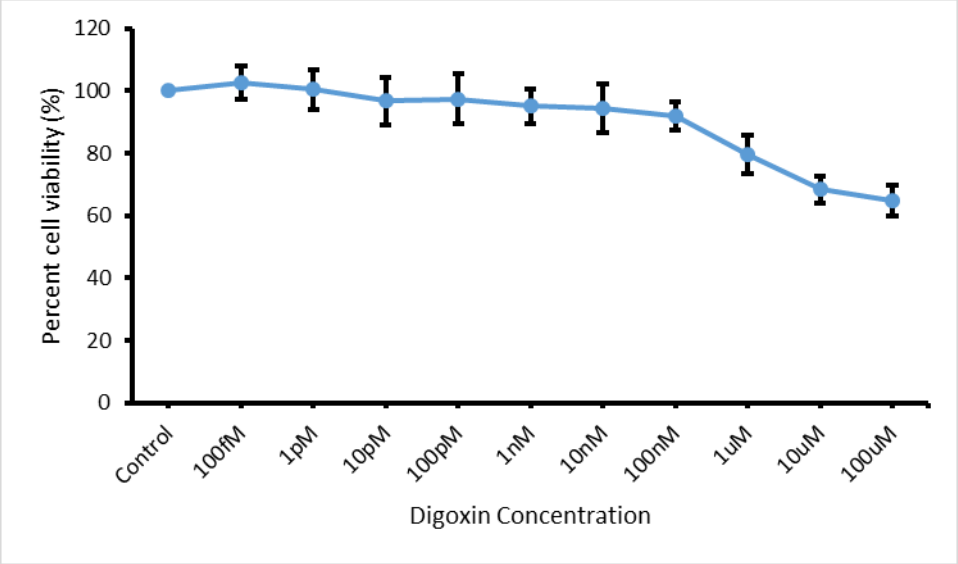

Figure 5.10: MTT assay was conducted to check for digoxin cytotoxicity. Percentage caco-2 cell viability at different concentrations of digoxin; n=8.

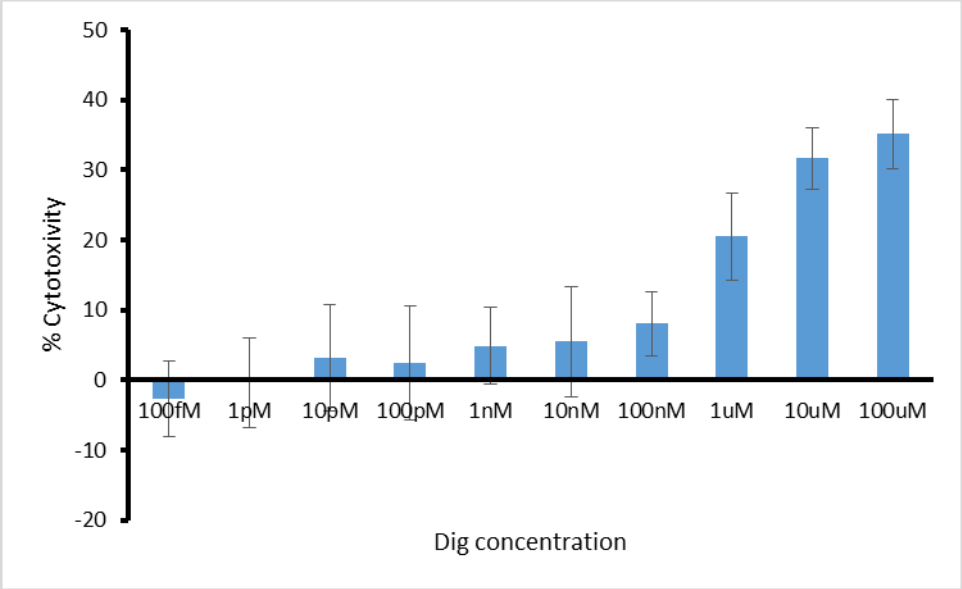

Figure 5.11: Percentage cytotoxicity of digoxin (Dig) on caco-2 cells. Cytotoxicity increased with increasing concentration of digoxin; n=8.

The percentage cytotoxicity of the drug was calculated using the equation below.

$$\%\ cytotoxicity = 100 - \%\ cell\ viability$$

5.3.2.2 Permeation enhancement of Digoxin with basic amino acids

Before starting the permeability experiments, it was crucial to ensure that the caco-2 monolayers grown were of good integrity. To check for this, TEER measurements were carried out over a 24 day period (Figure 5.12). This also allowed determination of the optimal number of days to carry out the permeability experiments post seeding. There was a shallow rise in TEER value up to day 13 followed by a steep rise until day 19. The peak TEER was measured on day 19 after which TEER value again started falling. Hence optimal days to carry out permeability experiments were determined to be around day the days 19-21.

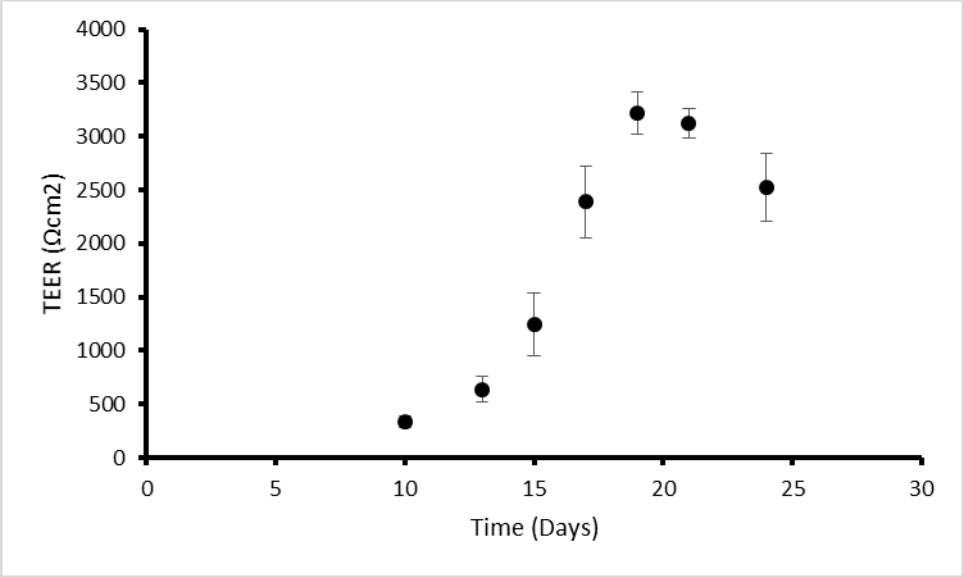

Figure 5.12: Transepithelial electrical resistance of caco-2 monolayer grown for 24 days on transwells with surface area of 4.67 cm^2; n=12.

Due to digoxin solubility enhancement by only the basic amino acids and the presence of an additional peak in the chromatogram of digoxin during solubility experiments with acidic amino acids, it was decided to proceed with permeability studies using only the basic amino acids. Permeability of digoxin on its own (control) and in the presence of digoxin to amino acid molar ratios of 1:5, 1:10, 1:30, 1:100, 1:300 and 1:600 were conducted in the apical to basolateral (A-B) direction. Significant permeation enhancement, was observed with L-Arg and L-Lys and not with L-His. Due to this, permeability experiments in the basolateral to apical (B-A) direction were only conducted for digoxin in the presence of L-Arg and L-Lys, specifically at the concentrations that gave statistically significant enhancement in digoxin permeability.

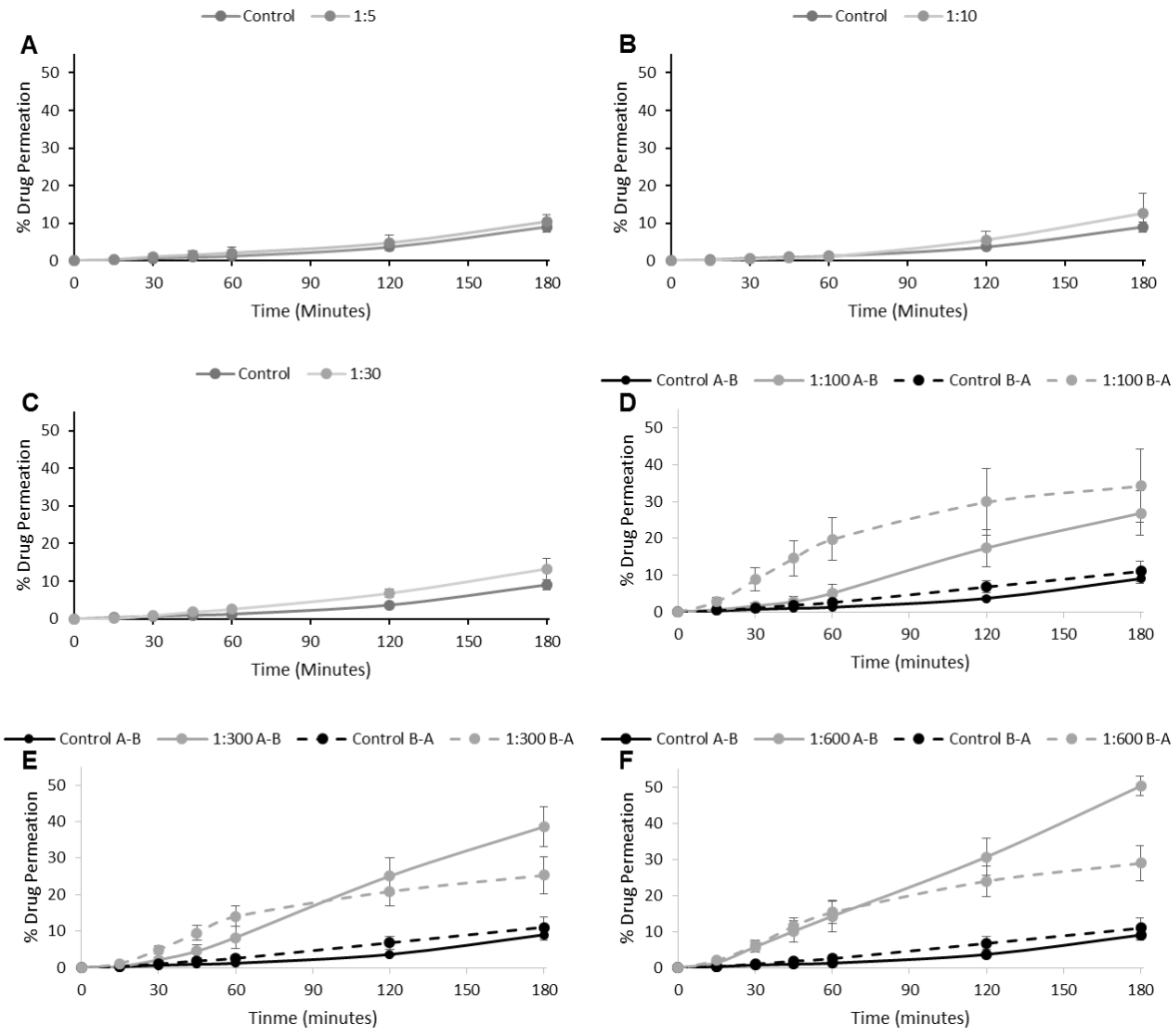

Figure 5.13: digoxin permeability through caco-2 monolayers on its own and in the presence of L-Arg at digoxin to amino acid molar ratios of A) 1:5, B) 1:10, C) 1:30, D) 1:100, E) 1:300 and F) 1:600. Percentage dug permeation from apical to basolateral direction (A-B) are presented for all molar ratios whereas for basolateral to apical (B-A) direction, only 1:100, 1:300 and 1:600 molar ratios were studied. A-B represented by solid line whereas B-A is represented by dashed line; n=3.

In the apical to basolateral (A-B) direction, a time dependent permeation of digoxin through Caco-2 monolayers, both in the presence and absence of L-Arg was observed. Also generally, the percentage of drug permeating through the caco-2 monolayers increased with increasing concentration of L-Arg at each time-point. The maximum digoxin permeation of 50.31% and was achieved with a digoxin to L-Arg molar ratio of 1:600 at 180 min. Statistically significant enhancement in digoxin permeation was observed with the digoxin to L-Arg molar ratios of 1:100, 1:300 and 1:600, though only at time points of 120 min and 180 min. For these molar ratios, along with the control, permeability experiments in the basolateral to apical (B-A) direction were also conducted. Digoxin permeation in the B-A direction also increased with time. This allowed the determination of efflux rate in the presence and absence L-Arg.

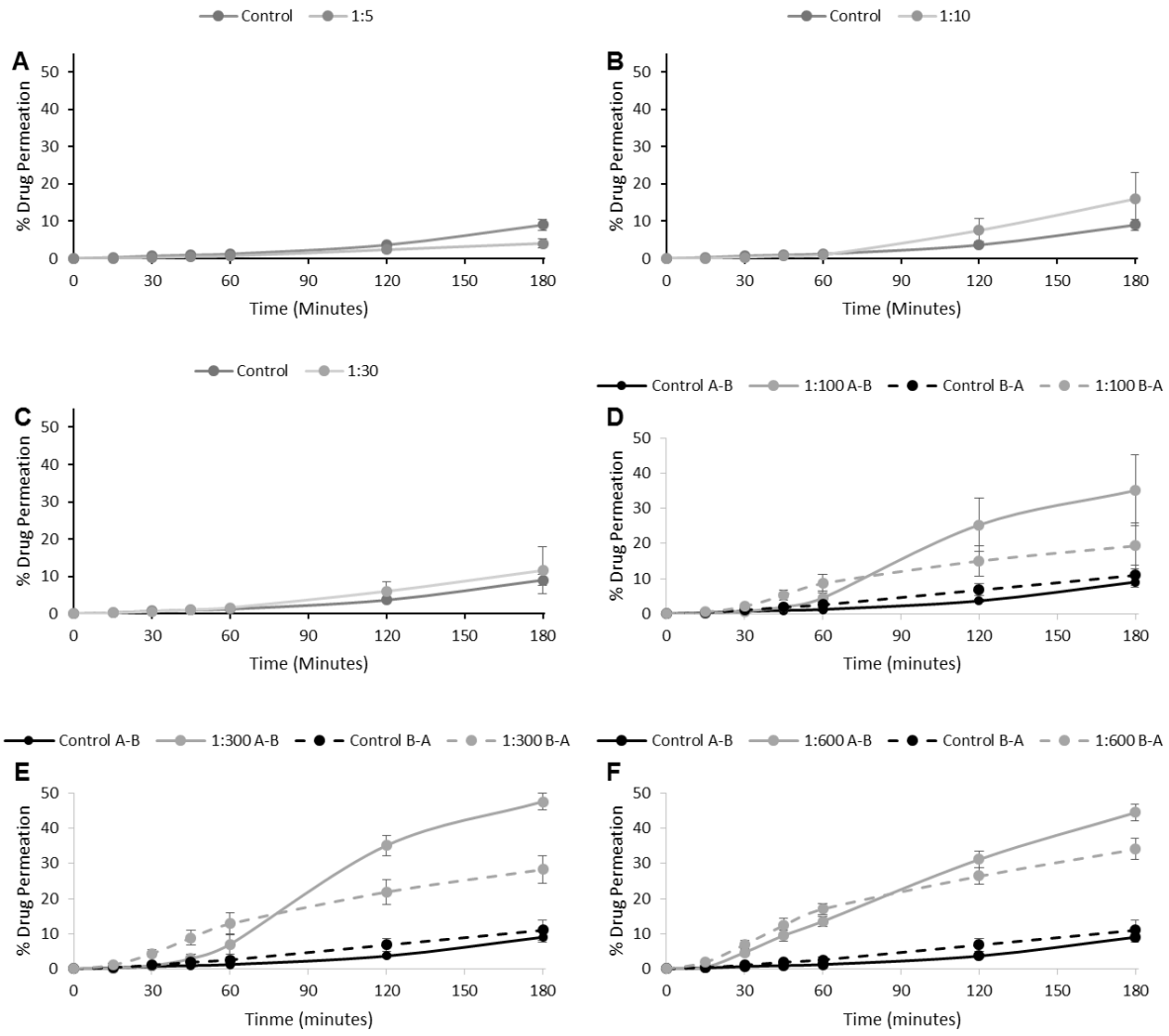

Figure 5.14: Digoxin permeability through caco-2 monolayers on its own and in the presence of L-Lys at digoxin to amino acid molar ratios of A) 1:5, B) 1:10, C) 1:30, D) 1:100, E) 1:300 and F) 1:600. Percentage dug permeation from apical to basolateral direction (A-B) are presented for all molar ratios whereas for basolateral to apical (B-A) direction, only 1:100, 1:300 and 1:600 molar ratios were studied. A-B represented by solid line whereas B-A is represented by dashed line; n=3.

Overall with L-Lys a similar pattern to L-Arg was observed in the permeation behaviour of digoxin. Like with L-Arg, a time dependent permeation of digoxin through Caco-2 monolayers, both in the presence and absence of L-Lys was observed in the A-B direction. However, the maximum digoxin permeation of 47.61 % and was achieved with a digoxin to L-Lys molar ratio of 1:300, unlike the 1:600 observed with L-Arg, again at 180 min. Again, significant enhancement in digoxin permeation was observed with the digoxin to L-Lys molar ratios of 1:100, 1:300 and 1:600 at time points of 120 min and 180 min. Permeability experiments in the B-A direction were conducted for these molar ratios as well as the control, allowing calculation of the efflux rate of digoxin in the presence of L-Lys. Digoxin permeation in the B-A direction also increased with time.

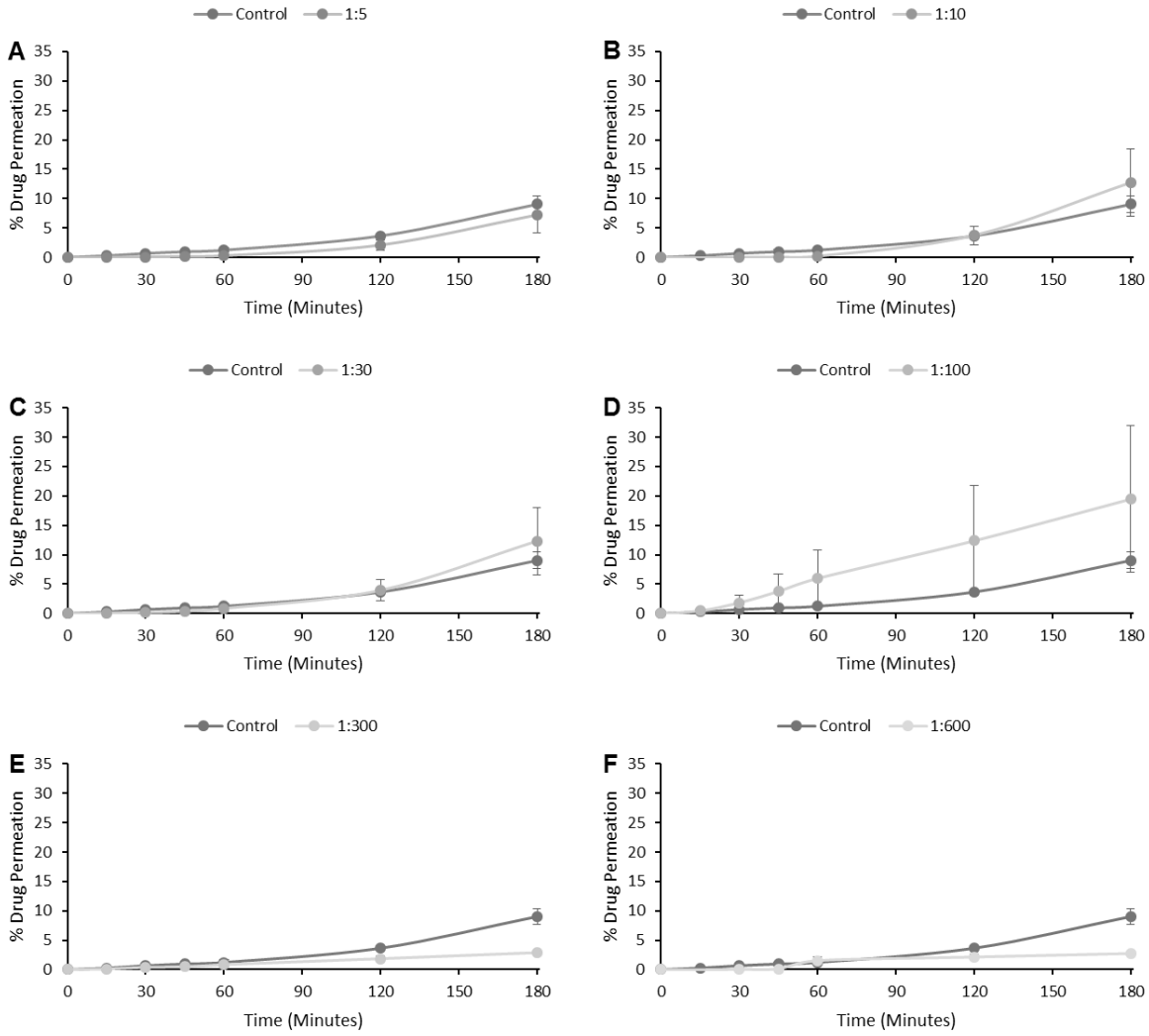

Figure 5.15: Digoxin permeability through caco-2 monolayers on its own and in the presence of L-His at digoxin to amino acid molar ratios of A) 1:5, B) 1:10, C) 1:30, D) 1:100, E) 1:300 and F) 1:600. Percentage dug permeation from apical to basolateral direction (A-B) are presented for all molar ratios; n=3.

Permeability experiments in the A-B direction were also done with L-His as a potential permeability enhancer. However, unlike L-Arg and L-Lys, L-His showed no statistically significant enhancement in digoxin permeability as compared to digoxin on its own. Due to this, no permeability experiments in the B-A direction were conducted with L-His.

Table 5.1: Table representing apparent permeability coefficient (Papp) and efflux ratio of digoxin (DIG) and digoxin combined with L-Arg and L-Lys at digoxin to amino acid molar ratios of 1:100, 1:300 and 1:600. Papp values for both the apical to basolateral (A-B) and basolateral to apical (B-A) direction are presented; * p<0.05, **p<0.005 and *** p<0.001; n=3.

TEST AGENT/S	PAPP A-B (10^{-6} CM/S)	PAPP B-A (10^{-6} CM/S)	EFFLUX RATIO
DIG	1.39 ± 0.47	2.49 ± 1.07	2.06
DIG:ARG 1:100	3.50 ± 1.59*	3.18 ± 1.97	1.23
DIG:ARG 1:300	4.46 ± 0.43***	4.60 ± 0.50	0.61
DIG:ARG 1:600	5.52 ± 0.30***	5.08 ± 1.90	0.63
DIG:LYS 1:100	3.88 ± 1.14	4.32 ± 2.14	0.85
DIG:LYS 1:300	5.41 ± 0.76*	3.35 ± 1.16	1.05
DIG:LYS 1:600	6.43 ± 0.55**	4.04 ± 0.32	0.93

From the permeability data obtained, the permeability coefficient (Papp) of digoxin on its own and in combination with various concentrations of L-Arg and L-Lys was calculated in the A-B and B-A direction. Digoxin which was combined with L-Arg or L-Lys gave higher Papp values. Furthermore, increasing the concentration of the amino acid led to higher Papp, especially for the A-B direction. Significant change in Papp was achieved with 1:100, 1:300 and 1:600 molar ratios of digoxin to L-Arg. Whereas, whilst combining with L-Lys, digoxin to L-Lys molar ratios of 1:300 and 1:600 were significantly different from control.

From the Papp values, the efflux ratio was calculated, which allowed the assessment of the efflux behaviour of digoxin on its own in comparison to its efflux behaviour in the presence of basic amino acids L-Arg and L-Lys. Combining digoxin with either L-Arg or L-Lys decreased the efflux ratio of digoxin.

Table 5.2: Transepithelial electrical resistance across caco-2 monolayers measured before, during (after each time point; 0 min, 15 min, 30 min, 45 min, 60 min, 120 min and 180 min) and after (24 h and 96 h) the permeability experiment. * Only some of the caco-2 monolayers exposed to 1:600 concentration of amino acid recovered to a TEER value above 200 Ωcm^2; n=3.

	Time point	*TEER (Ωcm^2)*	*S.D.*
Digoxin	Before experiment	2009.66	35.05
	0 min	1782.38	52.07
	15 min	1151.93	37.75
	30 min	1066.32	70.26
	45 min	1130.14	37.07
	60 min	965.13	17.68
	120 min	443.65	49.42
	180 min	189.91	31.09
	24h	1997.20	5.39
	96h	1346.52	5.39
1:10	Before experiment	1438.36	69.11
	0 min	1131.70	26.96
	15 min	544.83	11.75
	30 min	249.07	215.70
	45 min	375.16	17.68
	60 min	345.58	60.71
	120 min	259.96	14.27
	180 min	175.90	5.39
	24h	2154.43	123.06
	96h	1008.72	93.75
1:30	Before experiment	2758.41	21.06
	0 min	2154.43	17.68
	15 min	529.27	53.92
	30 min	337.80	25.72
	45 min	412.52	31.09
	60 min	389.17	60.23
	120 min	364.26	4.67
	180 min	244.40	63.58
	24h	3240.98	8.09
	96h	801.68	222.03
1:600	Before experiment	1712.33	23.96
	0 min	1179.95	15.01

15 min	259.96	7.13
30 min	110.52	16.40
45 min	99.63	25.72
60 min	85.62	5.39
120 min	118.31	11.75
180 min	12.45	7.13
24h	59.15	18.87
96h	372.04*	158.53

In a bid to check the effect of different digoxin and L-Arg/Lys concentrations on monolayer integrity during permeability experiments, TEER measurements were carried out for selected combinations across the range of concentrations used. The test agents selected for this include digoxin on its own as well as digoxin in combination with L-Arg/Lys at digoxin to L-Arg/Lys molar ratios of 1:10, 1:30 and 1:600. It was found that the TEER values dropped over time during the permeability experiments with values being lowest at 180 min. Although higher amino acid concentrations led to more abrupt drops in TEER value, digoxin on its own also led to substantial drops. Nevertheless, to check whether the monolayer integrity is recoverable or not, the monolayers were again incubated with cell culture medium under the general conditions detailed under methods. Monolayers exposed to digoxin, 1:10 and 1:30 recovered to TEER values of 2000 Ωcm^2 or above within 24 hours. However at 96 hours after the experiment, only some of the monolayers exposed to 1:600 recovered to a TEER value of 372.04 Ωcm^2. Nevertheless, it was observed that all monolayers exposed to 1:600 recovered to an acceptable TEER above 250 Ωcm^2 if left long enough.

5.4 Discussion

5.4.1 Digoxin solubility in acidic and basic amino acids

Solubility studies of digoxin in amino acids show that basic amino acids serve as its suitable counterions. We were unable to find experimental pKa values for digoxin, however pKa values have been predicted to be 7.15 and -3 for its strongest acidic and strongest basic ionisable site respectively. If these estimates are correct, in the basic pH of the solutions achieved by

all three amino acids, the strongest acidic ionisable site of digoxin is likely to be ionised more so than digoxin on its own in water. The percentage ionisation of this site would be in an equilibrium dependent on the particular pH of the solution, and is likely to increase with an increase in the concentration of the amino acid due to the accompanying increase in pH. Although it is possible to calculate the percentage ionisation of the sites, it was not done so due to the unavailability of experimental pKa. Nevertheless, in basic amino acid solutions, the proportion of anionic digoxin is likely to have increased. This results in the increased digoxin solubility observed, since the resulting increase in the proportion of polar drug molecules are able to interact with polar water molecules, or in other words become solubilised; polar molecules have higher hydrophilicity.

Unlike with basic amino acids, acid amino acids did not enhance digoxin solubility. However this can be explained by the degradation of digoxin in the presence of acidic amino acids. According to literature, an acidic environment causes hydrolysis of digoxin resulting in its degradation (219). Digoxigenin, digoxigenin bisdigitoxoside and digoxigenin monodigitoxoside have been identified as degradation products (219, 220). Multiple degradation products formed by the hydrolysis of digoxin also explains why an extra peak was seen upon HPLC analysis of digoxin in acidic amino acids solutions.

5.4.2 Digoxin permeability

5.4.2.1 Efflux of digoxin and the effect of L-Arg and L-Lys on P-gp

For digoxin on its own, Papp in the B-A direction was around 2 fold greater than the Papp in the A-B direction giving an efflux ratio of 2.06. Since digoxin is a substrate of P-gp, making it highly prone to efflux through caco-2 cells, an efflux rate greater than two is expected since it is suggested that an efflux ratio greater than two indicates the presence of efflux mechanism (221). The efflux ratio is in line with literature, since a broad range of digoxin efflux ratios in caco-2 cells ranging from 2.57 to 28 have been reported (222-224). Hence, the results presented above suggest digoxin used on its own is effluxed out of the cells. Interestingly permeability studies of digoxin in the presence of L-Arg and L-Lys in digoxin to amino acid molar ratios of 1:100, 1:300 and 1:600 all showed a decrease in efflux ratio due to Papp in B-A direction being either closer to or less than the Papp values obtained for A-B direction. This means that in the presence of these basic amino acids, there is a decrease in efflux of digoxin. Since digoxin is a substrate of P-gp, it is likely that amino acid interfere with efflux of digoxin through P-gp.

Interestingly, majority of P-gp substrates are hydrophobic indicating, its preference for pumping out hydrophobic compounds (225, 226). With this in mind, the decrease in efflux of digoxin in the presence of basic amino acids might be due to more digoxin being present in the hydrophilic form and losing its ability to be recognised as a substrate by P-gp. Although many drugs with positive charges are also recognised by P-gp, digoxin is not likely to be present in the cationic form in the presence of basic amino acids (226).

Al-Ali AA et al observed an increase in digoxin permeation in the A-B direction using permeation enhancers (223). However, considering that the permeation enhancers did not decrease permeation in the B-A direction, they suggested that the underlying mechanism is unrelated to P-gp inhibition. Since in the results presented here (Figure 5.13, Figure 5.14 and Table 5.1) both L-Arg and L-Lys increased the permeation of digoxin in not only the A-B direction but also the B-A direction, this is a stronger indication that the underlying mechanism does not involve inhibition of P-gp. This is because if P-gp was inhibited by the amino acids, a decrease in permeation of digoxin in the B-A direction compared to control would be expected. Although this seems like an appropriate interpretation, at this stage P-gp inhibition cannot be ruled out. The reason is that if the increase in permeation enhancing mechanism (like one proposed next) is significantly greater than the inhibition of P-gp, the latter may go unnoticed; a decrease in digoxin efflux may be concealed by significantly greater permeation from the B-A direction.

5.4.2.2 Ion-pair hypothesis

Reduction in ionisation is one of the mechanisms which can be employed to enhance drug permeability (227). Along with a decrease in efflux, an increase in digoxin uptake can also present as a reduced efflux ratio observed in the presence of L-Arg and L-Lys. This leads to the hypothesis of another mechanism which may possibly explain the increase in digoxin permeability; ion pair formation between anionic digoxin and cationic L-Arg and L-Lys. Although digoxin present in the unionised form can freely diffuse through the caco-2 monolayer, ionised digoxin wold require other mechanisms (228, 229). This leads to the ion-pair theory where ion-pair formation occurs between the anionic digoxin molecules and cationic amino acid molecules. The resulting digoxin -Arg or digoxin -Lys ion pairs would have zero net charge allowing the newly formed lipophilic complexes to passively diffuse through the cell membrane (230, 231). This is aided by the fact that in our experiments, there were sufficiently excess moles of amino acid present to form ion pairs, allowing any amount of

anionic digoxin to have a cationic pair. Once the pair is absorbed and enters the blood circulation, it would become diluted. It is suggested that at this point ion-pair would dissociated allowing digoxin to carry out its required function (230).

5.4.2.3 Recovery of caco-2 monolayer TEER value indicates paracellular route of permeation

Since there was a decrease in TEER value with each experiment whether in the presence of amino acids or in its absence, it warranted an investigation to see if this TEER value was recoverable. As presented earlier, the TEER does recover, although more slowly for digoxin to amino acid molar ratio of 1:600, past an acceptable level of 250 Ωcm^2 (224, 232). Nevertheless, this suggests that L-Arg and L-Lys led permeation enhancement may be due to a reversible tight junction modulation rather than damage to the cells which is not reversible (223, 233). TEER values for the caco-2 cell monolayers are known to decrease with the opening of tight junctions (233). Interestingly during MTT assay, it was noticed that the intracellular distance increased (Figure 5.16) whether exposed to amino acids or not, again hinting towards tight junction modulation. Despite the increase in distance between adjacent caco-2 cells, metabolic activity was evident by the presence of purple precipitate within the cells.

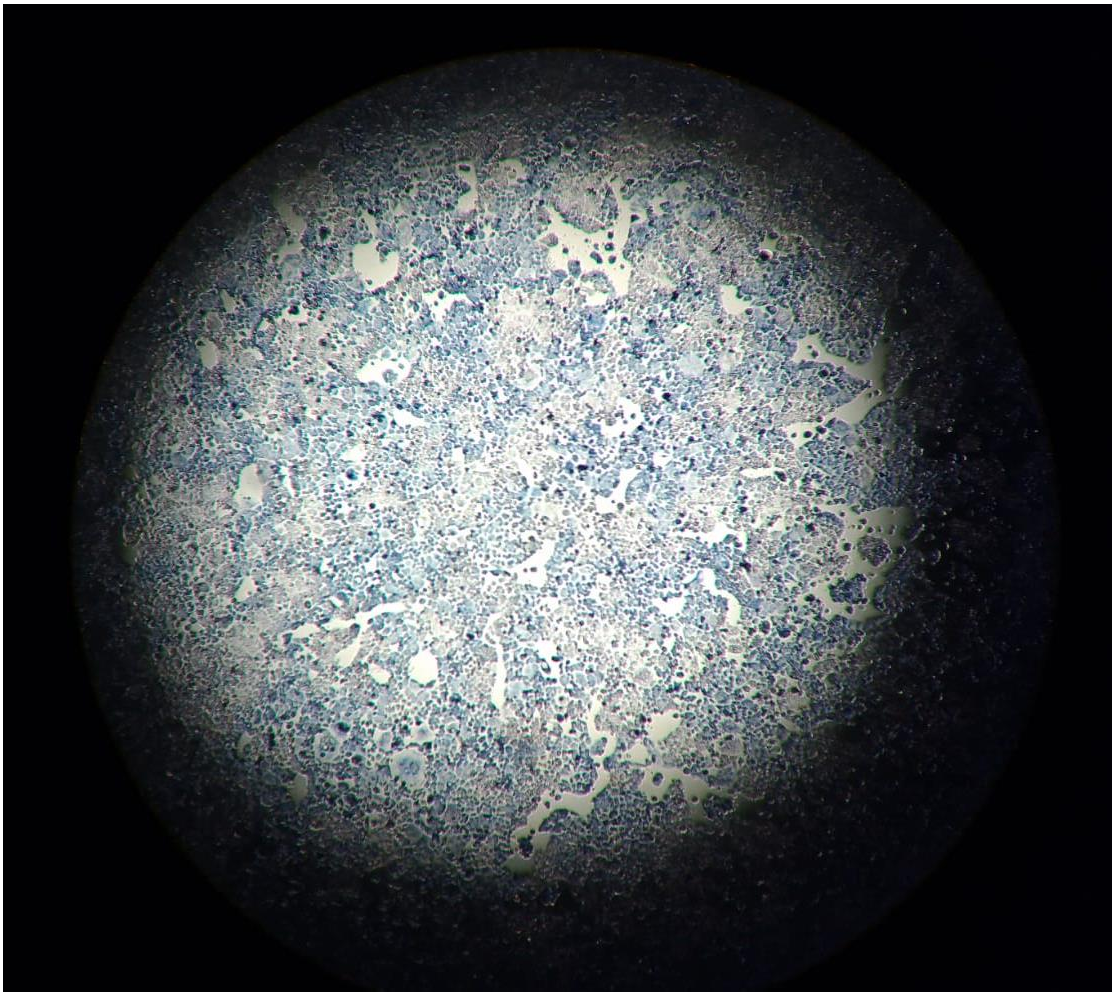

Figure 5.16: Increase in distance between viable caco-2 cells observed during MTT assay in the presence and absence of amino acids.

Contrary to the findings presented here, Iyire A et al who also studied basic amino acids as permeation enhancers insulin, found that TEER values after the experiments were maintained with L-Arg (165). However this can easily be explained by considering that the concentrations of the amino acid used by them were greatly lower than those which gave significant enhancement in digoxin permeation in this study. Also Iyire A et al used a different cell line which may respond differently to amino acids. Nevertheless, Iyire A does report a reduction in TEER value for some concentrations of L-Lys used in permeability assays (165). Elshaer A et al on the other hand did use the caco-2 cell line and also used amino acids as permeation enhancers but for the insoluble drug indomethacin (40). Although they maintained TEER values above 300 Ωcm^2 throughout the experiments, there was a slight drop in TEER value. Furthermore, their transport experiments were only for 90 minutes and they also used considerably lower amino acid concentrations. Nonetheless, this highlights that although amino acids do serve as permeability enhancers for a broad array of drugs, their concentration required for significant permeation enhancement is dependent on the drug being used.

5.5 Conclusion

In conclusion, basic amino acids serve as suitable counterions enabling a concentration dependent enhancement of digoxin solubility. Furthermore, high concentrations of basic amino acid L-Arg and L-Lys also serve a second function, increasing the permeation of digoxin through caco-2 monolayers through mechanisms which may involve increase paracellular transport, transcellular transport or inhibition of digoxin efflux by P-gp. Although the integrity of caco-2 monolayers was put to question, the recovery of TEER values confirmed non-toxic mechanism of permeability enhancement. These amino acids may also hold the potential in the delivery of other poorly soluble and permeable drugs; concentration of amino acids required will probably depend on the drug candidate.

Chapter 6: General discussion and future work

6.1 General discussion

Antimicrobial resistance (AMR) is on a rise, whilst majority of the newly discovered drugs are unable to reach systemic circulation through oral routes, hindered by their solubility and permeability. In a bid to unite researchers and help focus in most crucial aspects of AMR, the world health organisation (WHO) set out 5 main objectives in their global action plan. Whilst these objectives highlight the need of new antimicrobial agents, they also remind researchers to find new ways of overcoming AMR of existing antibiotics. On the other hand tools like the biopharmaceutical classification system can be used by formulation scientists, allowing it to be used as a criteria where one can modulate the physiochemical properties of a drug with the aim for their model drug to move up this solubility and permeability dependent class ladder.

One of the ways to enhance the activity of antibiotics for which bacteria have developed resistance is the use of adjuvants (67). Antibiotic adjuvants aim to overcome antibiotics resistance by interfering with the resistance mechanisms. Although adjuvants such as β-lactamase inhibitors are in use and in clinical development, researches are cautious of bacteria becoming resistant to these as well, ultimately giving rise to the undesired extensive drug resistance (70). Additionally, the use of a second compound along with the antibiotic introduces increased risk of potential side effects (167). Likewise, although many techniques into solubility and permeability enhancement have been researched into, these often involve complex processes and usually enhance one or the other.

Amino acids have been shown by ElShaer A et al, to not only enhance the solubility but also the caco-2 monolayer permeability of indomethacin through ion pair formation. They also showed that the solubility and permeability of Cip can also be enhanced using these amino acids. Whilst enhancing the solubility of insulin, Iyire A et al, showed amino acids to improve the permeability of Insulin through buccal cell layers. This prompted exploration of the ion-pair concept in tackling AMR in planktonic cells as well as biofilms. Additionally, solubility and permeability of two other drugs, TC and digoxin was also investigated.

Solubility of TC and digoxin was explored in the presence of all naturally occurring acidic and basic amino acids. Acidic amino acids included aspartic acid and glutamic acid, whilst the basic amino acids were arginine, lysine and histidine. A concentration dependent enhancement in TC solubility was observed with both acidic and basic amino acids. The maximum increase was seen with 4500 µg/ml L-arginine and L-lysine representing a 16.30 and 25.70 fold increase from control, respectively. Despite this, due to degradation of TC

which was likely mediated by oxidation and resulted in colour change from yellow to brown, acidic amino acids, which were less effective solubility enhancers were decided to be suitable counterions for TC. Nevertheless a substantial, 3.94 and 2.21 fold enhancement in TC solubility was observed with 4500 µg/ml L-aspartic acid and glutamic acid respectively. Along with this octanol/water partitioning showed that an increase in L-aspartic acid concentration resulted in TC becoming more hydrophilic, represented by a decrease in Log*P*. Acidic amino acids on the other hand led to degradation of digoxin. Digoxin solubility enhancement with basic amino acids though statistically significant, was substantially less than that seen for TC. Solubility of digoxin increased to a maximum of 1.54, 1.40 and 1.17 fold higher than control in the presence of 3500 µg/ml L-Arg, 4500 µg/ml L-His and 3500 µg/ml L-Lys respectively. In the case of both TC and digoxin, the increase in solubility has been attributed to an increase in the presence of their ionised form. The ionised form is in an equilibrium with the unionised form with the proportion of both dependent on the pH of the solution. Thus generally, as the concentration of the amino acid changes, so does the pH of the solution and hence the proportion of the drug in ionised form. Ultimately the ionised forms of the drugs are more easily able to interact with the polar water molecules and become solubilised, resulting in the increase in TC and digoxin solubility observed.

Permeability studies of digoxin in caco-2 cells were carried out in the A-B direction. For this purpose, only basic amino acids were used as potential permeability enhancers due to the instability of digoxin in acidic solutions. Substantial increase in digoxin permeability was observed with L-Arg and L-Lys, but only at higher digoxin to amino acid ratios (1:100, 1:300 and 1:600). Thus permeability studies in the B-A directions were only obtained for these combinations and Papp for both directions were calculated. It was found that addition of amino acids decreases the Papp B-A/Papp A-B ratio. This ratio is known as the efflux ratio and the observed pattern is likely due to either an increase in digoxin permeation which is hinted by increase in Papp in the A-B direction, a decrease in efflux of digoxin hinted by Papp in the B-A direction being closer to the values obtained for Papp in the A-B direction, or a combination of increase in permeation and a decrease in efflux.

Being the suitable counterions for TC, acidic amino acids were used to study their effect in the permeability of TC. For this purpose, accumulation with experiments were conducted which give indirect evidence of efflux. These studies were carried out on *S. aureus* and *P. aeruginosa*. Both pathogens exert high clinical implications and are listed as priority pathogens by the WHO (47). To study efflux, intracellular accumulation of ethidium bromide (EtBr) was measured which is expected to compete with TC for the efflux pump. Thus, an increase is EtBr accumulation represents an increase in accumulation of the drug. Although both L-Asp

and L-Glu are able to increase TC accumulation in both bacteria, a species dependent pattern in TC accumulation was observed, hinting that the mechanism may be different between species. Whilst with *S. aureus* the increase in TC accumulation was concentration dependent, only 30 and 15 mM of the amino acids led to an increase in TC accumulation within *P. aeruginosa*. To see the effect of enhanced drug accumulation on bacteria, growth curves were done. Both amino acids on their own adversely affected the growth of *S. aureus* in a concentration dependent manner, whilst their combination with TC resulted in synergy which was greatest when 30 mM of the amino acids were used. Whilst L-Asp or L-Glu did not affect the growth of *P. aeruginosa* on their own, their combination with TC showed remarkable synergy, especially when TC was combined with 30 mM of the amino acids. The synergy was so great that despite 30 mM of the acidic amino acids exerting little to no effect on *P. aeruginosa* growth, their combination with 14.06 µM TC hindered the growth of the bacteria to similar levels as 112.50 µM TC on its ow. In other words, only 12.50 % of TC was needed when used in conjunction with L-Asp or L-Glu to get similar inhibitory effects as the maximum concentration of TC used on its own. Along with the effect on growth, TC and acidic amino acid combinations also resulted in synergistic reduction in the production of the toxic pigments, pyocyanin and pyoverdine (234, 235).

The effects of acidic amino acids on planktonic bacteria were not restricted to TC but were found to enhance Cip accumulation and activity too. Due to the similar patterns of accumulation obtained, it can be assumed that the mechanism of enhancing drug accumulation by the amino acids is similar irrespective of what drug is used. However, the mechanism seems to be dependent on the species of bacteria used, since accumulation patterns differ between the two species used. Again when Cip is combined with different concentrations of L-Asp or L-Glu, an amino acid concentration dependent accumulation pattern is observed in *S. aureus*, whilst in *P. aeruginosa* only 30 and 15 mM of the amino acids lead to enhanced accumulation of the drug. L-Asp concentration of 15 mM and L-Glu concentrations of 15 and 7.5 mM showed noticeable synergy in *S. aureus* growth when combined with 8.49, 4.24 and 2.12 µM Cip. Synergy between the amino acids and Cip on the growth of *P. aeruginosa* was a bit more complicated, where the effectiveness of higher drug concentrations was decreased whilst that of lower concentrations was increased. Nevertheless, decreasing the dose of drug required is always welcome due to lower risk of side effects as well lower costs. Furthermore, as when combined with TC, combining with Cip also resulted in synergistic reduction in pigment production by *P. aeruginosa*.

Biofilm are communities of bacteria which attach themselves to biotic or abiotic surfaces, secreting substances which form a matrix surrounding the community and conferring its

inhabitants enhanced AMR. One of the ways biofilms confer resistance is by retarding diffusion of antibiotics through the matrix. This gave hope to acidic amino acids, known solubility enhancers of Cip, in potentially overcoming AMR associated with biofilms and confirmed the need to investigate further. Along with this, D-isomers of various amino acids are known to possess intrinsic anti-biofilm activity (187). Hence, the anti-biofilm activity of D-Asp and D-Glu was studied on *S. aureus* biofilms. Synergistic effect of combining D-amino acids with Cip was also investigated as a potential means to overcome antimicrobial resistance in these biofilms. For this purpose biofilm were grown in 24 well plates and their density quantified using the crystal violet staining method. Interestingly at equimolar combinations, D-Asp and D-Glu were able to significantly disperse (at 20 mM and 40 mM) established biofilms and inhibit (at 10 mM, 20 mM and 40 mM) new biofilm formation in the absence of an antibiotic. This confirmed that acidic amino acids also exhibit intrinsic anti-biofilm activity. Moreover, our study successfully confirmed L-amino acids also exhibit anti-biofilm activity; a finding contrary to the popular view found in published literature (65, 180, 181). The synergistic effect of acidic amino acids with Cip was observed at lower concentration ranges (<40 mM and <90.54 µM, respectively).

Confocal imaging revealed *S. aureus* to possess an interesting structure of the extracellular DNA (eDNA) which confers the biofilm structural stability whilst keeping the individual cells aggregated through acid-base interactions (202). Furthermore, the amino acids used were found to disrupt the honeycomb-like extracellular DNA (eDNA) meshwork whilst also preventing its formation. Thus it seems that D-Asp and D-Glu exert their inhibitory and dispersal effects through an anti-eDNA mechanism, potentially interfering with the acid-base interactions which binds the eDNA with the cells. Ultimately this results in eDNA unable to bind to (during inhibition) or eDNA release from (during dispersal) *S. aureus* cell surface, preventing biofilm growth or causing biofilm breakdown respectively. These findings highlight that targeting matrix components such as eDNA not only helps fight biofilms on its own, but may also be used to potentially enhance the effectiveness of antibiotics which the bacteria is potentially resistant to, thus acting as adjuvants. Furthermore, the role of antibiotics in increasing antimicrobial resistance is reiterated by the presence of seemingly denser eDNA structures when Cip is used on its own compared to control biofilms. This also confirms that the mechanisms of acquiring antimicrobial resistance is not limited to cells but also extends to the matrix. Thus emphasising the need to use antibiotics in conjunction with ways to disrupt the matrix or inhibit its formation.

Many of the adjuvants in use and under research and development, such as β-lactamase inhibitors, work in a way where mutation in bacteria can lead to them becoming resistant to

the same adjuvant which is meant to exhibit anti-resistance activity. One such example is the β-lactamase inhibitor sulbactam (168). Thus though these adjuvants do help overcome resistance to antibiotics, the effect seems only temporary, ultimately leading to the need of developing drugs which inhibit resistance to the adjuvants, which once were inhibiting resistance to an antibiotic (71). This identifies a major gap in research in the field of AMR, for ways of overcoming AMR which themselves are not susceptible to resistance. Since the amino acids used in the research presented here seem to generally work in a non-specific manner, using mechanisms such as modulation of acid-base interactions and ionic interactions such as ion-pair formation, it may be that acquiring resistance to such mechanisms may be difficult if not impossible for bacteria.

To the authors knowledge, natural acidic amino acids have been shown for the first time to act as adjuvants increasing the effectiveness of antibiotics, in both planktonic cells as well as biofilms. This introduces a multi-mechanistic approach to overcoming AMR using the said substances. Providing useful insights into potential mechanisms employed by amino acids in their diverse functionality including those leading to solubility enhancement, permeability enhancements in caco-2 cells and bacteria as well as mechanisms employed in anti-biofilm activity, this thesis sets the groundwork for exploring individually and in detail the mechanisms.

The thesis highlights that amino acids may be used as potential adjuvants with the role of enhancing solubility and permeability of otherwise less soluble and permeable drugs to be taken orally. Apart from this, it brings to light the potential application of amino acids as substances to overcome AMR. They can be used in diverse applications including wound care, medical devices as well as disinfectants. Whilst in disinfectants they may aid in decreasing the required concentration of the active ingredients, medical devises can be adopted with slow release of amino acids or those coated with amino acids based hydrogels, preventing bacterial attachment and biofilm formation on their surfaces. Use of amino acids in wound care may prove especially useful since in chronic wounds biofilm formation is a major issue. To start off, their application in wound healing, can be investigated in simple scratch test based wound models using fibroblasts (236, 237). It is hoped that whilst the anti-biofilm activity is likely to prevent infection of the wound model, the acidic pH of the amino acids may aid wound healing through increasing fibroblast activity (238). In vivo however, the acidic pH is like to have many other benefits including alterations in protease activity, increase in macrophage activity as well as angiogenesis (238).

6.2 Future work

- Investigating into the mechanisms through which amino acids are able to enhance accumulation of drugs within bacteria. This can involve the use of transporter specific blockers to elucidate the underlying mechanisms.
- Investigating anti-biofilm properties of basic amino acids and determining whether these have anti-eDNA properties too.
- Quantifying the amount of e-DNA in the supernatant of treated and untreated biofilms and characterising the differences between the two.
- Determining the underlying mechanism of the anti-eDNA properties of acidic amino acids, including investigations into the in vitro interactions between the amino acids, e-DNA and the proteins, enolase and GAPDH.
- Exploring the wound healing properties of amino acids using monoculture, co-culture or three dimensional cell culture wound healing models. The effect of biofilms (as a model for biofilm infected wounds) on wound healing can be explored along with the effect of amino acids as potential anti-biofilm wound healing agents.
- Investigating the gene and protein expression of both planktonic and biofilm bacteria as well as caco-2 cells upon exposure to acidic amino acids and combinations with respective drugs.

References

1. Pereira DA, Williams JA. Origin and evolution of high throughput screening. British journal of pharmacology. 2007;152(1):53-61.
2. Housman G, Byler S, Heerboth S, Lapinska K, Longacre M, Snyder N, et al. Drug resistance in cancer: an overview. Cancers (Basel). 2014;6(3):1769-92.
3. Zaman SB, Hussain MA, Nye R, Mehta V, Mamun KT, Hossain N. A Review on Antibiotic Resistance: Alarm Bells are Ringing. Cureus. 2017;9(6):e1403-e.
4. Cowen LE, Sanglard D, Howard SJ, Rogers PD, Perlin DS. Mechanisms of Antifungal Drug Resistance. Cold Spring Harb Perspect Med. 2014;5(7):a019752-a.
5. Strasfeld L, Chou S. Antiviral drug resistance: mechanisms and clinical implications. Infect Dis Clin North Am. 2010;24(2):413-37.
6. Ma JKH, Hadzija B. Basic Physical Pharmacy: Jones & Bartlett Learning; 2012.
7. Pandit NK. Introduction to the Pharmaceutical Sciences: Lippincott Williams & Wilkins; 2007.
8. Savjani KT, Gajjar AK, Savjani JK. Drug solubility: importance and enhancement techniques. ISRN Pharm. 2012;2012:195727.
9. Gupta S, Kesarla R, Omri A. Formulation strategies to improve the bioavailability of poorly absorbed drugs with special emphasis on self-emulsifying systems. ISRN Pharm. 2013;2013:848043.
10. Aulton ME, Taylor K. Aulton's Pharmaceutics: The Design and Manufacture of Medicines: Churchill Livingstone/Elsevier; 2013.
11. Hillery AM, Lloyd AW, Swarbrick J. Drug Delivery and Targeting: For Pharmacists and Pharmaceutical Scientists: Taylor & Francis; 2003.
12. Palmer M, Chan A, Dieckmann T, Honek J. Notes to Biochemical Pharmacology: Wiley; 2013.
13. Savjani KT, Gajjar AK, Savjani JK. Drug solubility: importance and enhancement techniques. ISRN pharmaceutics. 2012;2012:195727-.
14. Aungst BJ. Novel formulation strategies for improving oral bioavailability of drugs with poor membrane permeation or presystemic metabolism. J Pharm Sci. 1993;82(10):979-87.
15. Smith BT. Remington Education: Physical Pharmacy: Pharmaceutical Press; 2015.
16. Solubility of organic compounds: University of Calgary; [Available from: http://www.chem.ucalgary.ca/courses/351/laboratory/351expt_01_solubility.pdf.
17. Finkel R, Clark MA, Cubeddu LX. Pharmacology: Lippincott Williams & Wilkins; 2009.
18. Hubatsch I, Ragnarsson EGE, Artursson P. Determination of drug permeability and prediction of drug absorption in Caco-2 monolayers. Nat Protoc. 2007;2(9):2111-9.
19. Clinical Pharmacology Baghdad, Republic of Iraq: Baghdad University; [Available from: http://www.codental.uobaghdad.edu.iq/uploads/lectures/Pharma%20lectures/2%20Pharmacokinetics%20finishing%20with%20bioavailibility.pdf.
20. Waiver of In Vivo Bioavailability and Bioequivalence Studies for Immediate-Release Solid Oral Dosage Forms Based on a Biopharmaceutics Classification System - Guidance for Industry FDA; 2017 [Available from: https://www.fda.gov/about-fda/center-drug-evaluation-and-research/biopharmaceutics-classification-system-bcs-guidance.
21. Benet LZ. The role of BCS (biopharmaceutics classification system) and BDDCS (biopharmaceutics drug disposition classification system) in drug development. J Pharm Sci-Us. 2013;102(1):34-42.
22. Lipinski CA, Lombardo F, Dominy BW, Feeney PJ. Experimental and computational approaches to estimate solubility and permeability in drug discovery and development settings. Advanced Drug Delivery Reviews. 1997;23(1):3-25.
23. Armstrong JD, Hubbard RE, Chemistry RSo, Farrell T, Maiguashca B. Structure-based Drug Discovery: An Overview: Royal Society of Chemistry; 2006.
24. Mohsin K, Alamri R, Ahmad A, Raish M, Alanazi FK, Hussain MD. Development of self-nanoemulsifying drug delivery systems for the enhancement of solubility and oral bioavailability of fenofibrate, a poorly water-soluble drug. Int J Nanomedicine. 2016;11:2829-38.

25. Balata GF, Essa EA, Shamardl HA, Zaidan SH, Abourehab MA. Self-emulsifying drug delivery systems as a tool to improve solubility and bioavailability of resveratrol. Drug design, development and therapy. 2016;10:117-28.
26. Alqahtani S, Alayoubi A, Nazzal S, Sylvester PW, Kaddoumi A. Enhanced Solubility and Oral Bioavailability of gamma-Tocotrienol Using a Self-Emulsifying Drug Delivery System (SEDDS). Lipids. 2014;49(8):819-29.
27. Wang Y, Wang S, Firempong CK, Zhang H, Wang M, Zhang Y, et al. Enhanced Solubility and Bioavailability of Naringenin via Liposomal Nanoformulation: Preparation and In Vitro and In Vivo Evaluations. AAPS PharmSciTech. 2016.
28. Fong SY, Martins SM, Brandl M, Bauer-Brandl A. Solid Phospholipid Dispersions for Oral Delivery of Poorly Soluble Drugs: Investigation Into Celecoxib Incorporation and Solubility-In Vitro Permeability Enhancement. J Pharm Sci. 2016;105(3):1113-23.
29. Choonara BF, Choonara YE, Kumar P, du Toit LC, Tomar LK, Tyagi C, et al. A Menthol-Based Solid Dispersion Technique for Enhanced Solubility and Dissolution of Sulfamethoxazole from an Oral Tablet Matrix. Aaps Pharmscitech. 2015;16(4):771-86.
30. Sanka K, Munjulury VS, Mohd AB, Diwan PV. Enhancement of solubility, dissolution release profile and reduction in ulcerogenicity of piroxicam by inclusion complex with skimmed milk. Drug Deliv. 2014;21(7):560-70.
31. Ganesh M, Jeon UJ, Ubaidulla U, Hemalatha P, Saravanakumar A, Peng MM, et al. Chitosan cocrystals embedded alginate beads for enhancing the solubility and bioavailability of aceclofenac. Int J Biol Macromol. 2015;74:310-7.
32. Rashid R, Kim DW, Yousaf AM, Mustapha O, Fakhar Ud D, Park JH, et al. Comparative study on solid self-nanoemulsifying drug delivery and solid dispersion system for enhanced solubility and bioavailability of ezetimibe. Int J Nanomedicine. 2015;10:6147-59.
33. Yousaf AM, Mustapha O, Kim DW, Kim DS, Kim KS, Jin SG, et al. Novel electrosprayed nanospherules for enhanced aqueous solubility and oral bioavailability of poorly water-soluble fenofibrate. Int J Nanomedicine. 2016;11:213-21.
34. Ashour EA, Majumdar S, Alsheteli A, Alshehri S, Alsulays B, Feng X, et al. Hot melt extrusion as an approach to improve solubility, permeability and oral absorption of a psychoactive natural product, piperine. J Pharm Pharmacol. 2016;68(8):989-98.
35. Sadeghi F, Ashofteh M, Homayouni A, Abbaspour M, Nokhodchi A, Garekani HA. Antisolvent precipitation technique: A very promising approach to crystallize curcumin in presence of polyvinyl pyrrolidon for solubility and dissolution enhancement. Colloid Surface B. 2016;147:258-64.
36. Simon S, Schubert R. Inhibitory effect of phospholipids on P-glycoprotein: Cellular studies in Caco-2, MDCKII mdr1 and MDCKII wildtype cells and P-gp ATPase activity measurements. Bba-Mol Cell Biol L. 2012;1821(9):1211-23.
37. Weinheimer M, Fricker G, Burhenne J, Mylius P, Schubert R. The application of P-gp inhibiting phospholipids as novel oral bioavailability enhancers - An in vitro and in vivo comparison. Eur J Pharm Sci. 2016.
38. Whitehead K, Karr N, Mitragotri S. Safe and Effective Permeation Enhancers for Oral Drug Delivery. Pharmaceutical Research. 2008;25(8):1782-8.
39. Lozoya-Agullo I, Gonzalez-Alvarez I, Gonzalez-Alvarez M, Merino-Sanjuan M, Bermejo M. Development of an ion-pair to improve the colon permeability of a low permeability drug: Atenolol. Eur J Pharm Sci. 2016;93:334-40.
40. ElShaer A, Hanson P, Mohammed AR. A novel concentration dependent amino acid ion pair strategy to mediate drug permeation using indomethacin as a model insoluble drug. Eur J Pharm Sci. 2014;62:124-31.
41. Silhavy TJ, Kahne D, Walker S. The bacterial cell envelope. Cold Spring Harbor perspectives in biology. 2010;2(5):a000414-a.
42. Nikaido H. Prevention of drug access to bacterial targets: permeability barriers and active efflux. Science. 1994;264(5157):382-8.

43. Delcour AH. Outer membrane permeability and antibiotic resistance. Biochimica et Biophysica Acta (BBA) - Proteins and Proteomics. 2009;1794(5):808-16.
44. Hill WG, Rivers RL, Zeidel ML. Role of leaflet asymmetry in the permeability of model biological membranes to protons, solutes, and gases. J Gen Physiol. 1999;114(3):405-14.
45. Lande MB, Donovan JM, Zeidel ML. The relationship between membrane fluidity and permeabilities to water, solutes, ammonia, and protons. J Gen Physiol. 1995;106(1):67-84.
46. WHO. Global action plan on antimicrobial resistance: World Health Organisation; 2015 [Available from: https://apps.who.int/iris/bitstream/handle/10665/193736/9789241509763_eng.pdf?sequence=1.
47. WHO. Prioritization of pathogens to guide discovery, research and development of new antibiotics for drug-resistant bacterial infections, including tuberculosis: World Health Organization; 2017 [Available from: https://www.who.int/medicines/areas/rational_use/PPLreport_2017_09_19.pdf?ua=1.
48. Bhullar K, Waglechner N, Pawlowski A, Koteva K, Banks ED, Johnston MD, et al. Antibiotic resistance is prevalent in an isolated cave microbiome. PloS one. 2012;7(4):e34953-e.
49. Sandner-Miranda L, Vinuesa P, Cravioto A, Morales-Espinosa R. The Genomic Basis of Intrinsic and Acquired Antibiotic Resistance in the Genus Serratia. Front Microbiol. 2018;9:828.
50. Munita JM, Arias CA. Mechanisms of Antibiotic Resistance. Microbiology spectrum. 2016;4(2):10.1128/microbiolspec.VMBF-0016-2015.
51. WHO. Global Antimicrobial Resistance Surveillance System (GLASS). 2015.
52. Hall CW, Mah T-F. Molecular mechanisms of biofilm-based antibiotic resistance and tolerance in pathogenic bacteria. FEMS Microbiology Reviews. 2017;41(3):276-301.
53. Wishart DS, Knox C, Guo AC, Shrivastava S, Hassanali M, Stothard P, et al. DrugBank: a comprehensive resource for in silico drug discovery and exploration. Nucleic acids research. 2006;34(Database issue):D668-72.
54. Kapoor G, Saigal S, Elongavan A. Action and resistance mechanisms of antibiotics: A guide for clinicians. J Anaesthesiol Clin Pharmacol. 2017;33(3):300-5.
55. Kon K, Rai M. Antibiotic Resistance: Mechanisms and New Antimicrobial Approaches: Elsevier Science; 2016.
56. Tenson T, Lovmar M, Ehrenberg M. The Mechanism of Action of Macrolides, Lincosamides and Streptogramin B Reveals the Nascent Peptide Exit Path in the Ribosome. Journal of molecular biology. 2003;330(5):1005-14.
57. Hoiby N, Ciofu O, Johansen HK, Song ZJ, Moser C, Jensen PO, et al. The clinical impact of bacterial biofilms. Int J Oral Sci. 2011;3(2):55-65.
58. Gupta P, Sarkar S, Das B, Bhattacharjee S, Tribedi P. Biofilm, pathogenesis and prevention--a journey to break the wall: a review. Arch Microbiol. 2016;198(1):1-15.
59. Stoodley P, Sauer K, Davies DG, Costerton JW. Biofilms as complex differentiated communities. Annu Rev Microbiol. 2002;56:187-209.
60. Lawrence JR, Korber DR, Hoyle BD, Costerton JW, Caldwell DE. Optical sectioning of microbial biofilms. J Bacteriol. 1991;173(20):6558-67.
61. Lewis K. Persister cells and the riddle of biofilm survival. Biochemistry (Mosc). 2005;70(2):267-74.
62. Brooun A, Liu S, Lewis K. A dose-response study of antibiotic resistance in Pseudomonas aeruginosa biofilms. Antimicrob Agents Chemother. 2000;44(3):640-6.
63. Mah TF, O'Toole GA. Mechanisms of biofilm resistance to antimicrobial agents. Trends Microbiol. 2001;9(1):34-9.
64. Romero D, Vlamakis H, Losick R, Kolter R. An accessory protein required for anchoring and assembly of amyloid fibres in B. subtilis biofilms. Mol Microbiol. 2011;80(5):1155-68.
65. Kolodkin-Gal I, Romero D, Cao S, Clardy J, Kolter R, Losick R. D-amino acids trigger biofilm disassembly. Science. 2010;328(5978):627-9.

66. Sanchez CJ, Jr., Akers KS, Romano DR, Woodbury RL, Hardy SK, Murray CK, et al. D-amino acids enhance the activity of antimicrobials against biofilms of clinical wound isolates of Staphylococcus aureus and Pseudomonas aeruginosa. Antimicrob Agents Chemother. 2014;58(8):4353-61.
67. Wright GD. Antibiotic Adjuvants: Rescuing Antibiotics from Resistance. Trends in Microbiology. 2016;24(11):862-71.
68. Basak S, Singh P, Rajurkar M. Multidrug Resistant and Extensively Drug Resistant Bacteria: A Study. J Pathog. 2016;2016:4065603.
69. González-Bello C. Antibiotic adjuvants – A strategy to unlock bacterial resistance to antibiotics. Bioorganic & Medicinal Chemistry Letters. 2017;27(18):4221-8.
70. Douafer H, Andrieu V, Phanstiel O, Brunel JM. Antibiotic Adjuvants: Make Antibiotics Great Again! J Med Chem. 2019.
71. McLeod SM, Shapiro AB, Moussa SH, Johnstone M, McLaughlin RE, de Jonge BLM, et al. Frequency and Mechanism of Spontaneous Resistance to Sulbactam Combined with the Novel beta-Lactamase Inhibitor ETX2514 in Clinical Isolates of Acinetobacter baumannii. Antimicrob Agents Chemother. 2018;62(2).
72. Marcus Y, Hefter G. Ion pairing. Chemical reviews. 2006;106(11):4585-621.
73. Quintanar-Guerrero D, Allémann E, Fessi H, Doelker E. Applications of the ion-pair concept to hydrophilic substances with special emphasis on peptides. Pharmaceutical research. 1997;14(2):119-27.
74. Higuchi T, Michaelis A, Tan T, Hurwitz A. Ion pair extraction of pharmaceutical amines. Role of dipolar solvating agents in extraction of dextromethorphan. Anal Chem. 1967;39(8):974-9.
75. Diamond RM. THE AQUEOUS SOLUTION BEHAVIOR OF LARGE UNIVALENT IONS. A NEW TYPE OF ION-PAIRING1a. The Journal of Physical Chemistry. 1963;67(12):2513-7.
76. Esch TEH, Smid J. Studies of Contact and Solvent-Separated Ion Pairs of Carbanions. I. Effect of Temperature, Counterion, and Solvent. Journal of the American Chemical Society. 1966;88(2):307-18.
77. Reichardt C, Welton T. Solvents and Solvent Effects in Organic Chemistry: Wiley; 2011.
78. Burger K. Solvation, Ionic and Complex Formation Reactions in Non-Aqeuous Solvents: Elsevier Science; 2012.
79. ElShaer A, Khan S, Perumal D, Hanson P, Mohammed AR. Use of amino acids as counterions improves the solubility of the BCS II model drug, indomethacin. Curr Drug Deliv. 2011;8(4):363-72.
80. Izutsu K. Electrochemistry in Nonaqueous Solutions: Wiley; 2009.
81. Coury L. Conductance Measurements Part 1: Theory. Current Separations. 1999;18(3):92.
82. Irwin GM, Kostenbauder HB, Dittert LW, Staples R, Misher A, Swintosky JV. Enhancement of gastrointestinal absorption of a quaternary ammonium compound by trichloroacetate. J Pharm Sci. 1969;58(3):313-5.
83. Lage H. ABC-transporters: implications on drug resistance from microorganisms to human cancers. Int J Antimicrob Agents. 2003;22(3):188-99.
84. Van Bambeke F, Balzi E, Tulkens PM. Antibiotic efflux pumps - Commentary. Biochem Pharmacol. 2000;60(4):457-70.
85. Li X-Z, Nikaido H. Efflux-Mediated Drug Resistance in Bacteria: an Update. Drugs. 2009;69(12):1555-623.
86. Blair JMA, Piddock LJV. Structure, function and inhibition of RND efflux pumps in Gram-negative bacteria: an update. Current Opinion in Microbiology. 2009;12(5):512-9.
87. Venter H, Mowla R, Ohene-Agyei T, Ma S. RND-type Drug Efflux Pumps from Gram-negative bacteria: Molecular Mechanism and Inhibition. Frontiers in Microbiology. 2015;6.
88. Hunter J, Hirst BH. Influence of Secretory Systems on Drug Delivery/TargetingIntestinal secretion of drugs. The role of P-glycoprotein and related drug efflux systems in limiting oral drug absorption. Advanced Drug Delivery Reviews. 1997;25(2):129-57.
89. Zdanowicz MM, Pharmacists ASoH-S. Concepts in Pharmacogenomics: American Society of Health-System Pharmacists; 2010.

90. Wilson K, Walker J. Principles and Techniques of Biochemistry and Molecular Biology. 7th ed: Cambridge University Press; 2010.
91. Wu G. Amino Acids: Biochemistry and Nutrition: Taylor & Francis; 2013.
92. Petsko GA, Ringe GAPD, Ringe D. Protein Structure and Function: New Science Press; 2004.
93. Bettelheim FA, Brown WH, Campbell MK, Farrell SO, Torres O. Introduction to Organic and Biochemistry: Cengage Learning; 2012.
94. Chopra I, Roberts M. Tetracycline Antibiotics: Mode of Action, Applications, Molecular Biology, and Epidemiology of Bacterial Resistance. Microbiology and Molecular Biology Reviews. 2001;65(2):232-60.
95. Agwuh KN, MacGowan A. Pharmacokinetics and pharmacodynamics of the tetracyclines including glycylcyclines. J Antimicrob Chemoth. 2006;58(2):256-65.
96. Clive DLJ. Chemistry of tetracyclines. Quarterly Reviews, Chemical Society. 1968;22(4):435-56.
97. Lemke TL, Williams DA. Foye's Principles of Medicinal Chemistry: Wolters Kluwer Health; 2012.
98. Jiao SJ, Zheng SR, Yin DQ, Wang LH, Chen LY. Aqueous photolysis of tetracycline and toxicity of photolytic products to luminescent bacteria. Chemosphere. 2008;73(3):377-82.
99. Sigma-Aldrich. Tetracycline - Product Information Saint Louis, Missouri, USA2003 [
100. Karcher SJ. Molecular Biology: A Project Approach: Elsevier Science; 1995.
101. Sigma-Aldrich. Tetracycline Hydrochloride - Product Information Saint Louis, Missouri, USA2003 [
102. Commission BP. The British Pharmacopoeia 2016: London: TSO; 2016.
103. Liang YL, Denton MB, Bates RB. Stability studies of tetracycline in methanol solution. J Chromatogr A. 1998;827(1):45-55.
104. Grobbenverpoorten A, Dihuidi K, Roets E, Hoogmartens J, Vanderhaeghe H. Determination of the Stability of Tetracycline Suspensions by High-Performance Liquid-Chromatography. Pharm Weekblad. 1985;7(3):104-8.
105. Pena A, Carmona A, Barbosa A, Lino C, Silveira I, Castillo B. Determination of tetracycline and its major degradation products by liquid chromatography with fluorescence detection. J Pharm Biomed Anal. 1998;18(4-5):839-45.
106. Allen LV. Remington: An Introduction to Pharmacy: Pharmaceutical Press; 2013.
107. Nelson M, Hillen W, Greenwald RA. Tetracyclines in Biology, Chemistry and Medicine: Birkhäuser Basel; 2012.
108. United States Pharmacopeia - National Formulary. USP 39-NF 34 ed: The United States Pharmacopeial Convention; 2016.
109. Nasipuri D. Stereochemistry of Organic Compounds: Principles and Applications: Wiley Eastern Limited; 1994.
110. Walton VC, Howlett MR, Selzer GB. Anhydrotetracycline and 4-epianhydrotetracycline in market tetracyclines and aged tetracycline products. J Pharm Sci. 1970;59(8):1160-4.
111. Castellari M, García-Regueiro JA. HPLC Determination of Tetracyclines in Lamb Muscle Using an RP-C18 Monolithic Type Column. Chromatographia. 2003;58(11-12):789-92.
112. OECD. Test No. 107: Partition Coefficient (n-octanol/water): Shake Flask Method: OECD Publishing.
113. Sangster J. Octanol-Water Partition Coefficients: Fundamentals and Physical Chemistry: Wiley; 1997.
114. Manuelsweb. Determine drug absorption by pKa [Available from: https://www.manuelsweb.com/pka.htm.
115. Reviewer Guidance: Validation of Chromatographic Methods: Center for Drug Evaluation and Research, Washington; 1994 [Available from: http://www.fda.gov/downloads/Drugs/.../Guidances/UCM134409.pdf.
116. Bressolle F, BrometPetit M, Audran M. Validation of liquid chromatographic and gas chromatographic methods - Applications to pharmacokinetics. J Chromatogr B. 1996;686(1):3-10.

117. Tongaree S, Goldberg AM, Flanagan DR, Poust RI. The effects of pH and PEG 400-water cosolvents on oxytetracycline-magnesium complex formation and stability. Pharm Dev Technol. 2000;5(2):189-99.
118. Hasan T, Allen M, Cooperman BS. Anhydrotetracycline Is a Major Product of Tetracycline Photolysis. J Org Chem. 1985;50(10):1755-7.
119. Sah H. Degradation patterns of tetracycline antibiotics in reverse micelles and water. Biomed Chromatogr. 2006;20(11):1142-9.
120. Narukawa M, Matsumi Y, Matsumoto J, Takahashi K, Yabushita A, Sato K, et al. Real-time analysis of secondary organic aerosol particles formed from cyclohexene ozonolysis using a laser-ionization single-particle aerosol mass spectrometer. Anal Sci. 2007;23(5):507-12.
121. Speer BS, Shoemaker NB, Salyers AA. Bacterial-Resistance to Tetracycline - Mechanisms, Transfer, and Clinical-Significance. Clinical Microbiology Reviews. 1992;5(4):387-99.
122. Grossman TH. Tetracycline Antibiotics and Resistance. Cold Spring Harb Perspect Med. 2016;6(4):a025387-a.
123. Tamura N, Konishi S, Yamaguchi A. Mechanisms of drug/H+ antiport: complete cysteine-scanning mutagenesis and the protein engineering approach. Current Opinion in Chemical Biology. 2003;7(5):570-9.
124. Thaker M, Spanogiannopoulos P, Wright GD. The tetracycline resistome. Cellular and Molecular Life Sciences. 2010;67(3):419-31.
125. Arioli S, Guglielmetti S, Amalfitano S, Viti C, Marchi E, Decorosi F, et al. Characterization of tetA-like gene encoding for a major facilitator superfamily efflux pump in Streptococcus thermophilus. Fems Microbiol Lett. 2014;355(1):61-70.
126. Blair JMA, Piddock LJV. How to Measure Export via Bacterial Multidrug Resistance Efflux Pumps. Mbio. 2016;7(4).
127. Kitko RD, Cleeton RL, Armentrout EI, Lee GE, Noguchi K, Berkmen MB, et al. Cytoplasmic Acidification and the Benzoate Transcriptome in Bacillus subtilis. Plos One. 2009;4(12).
128. Wilks JC, Slonczewski JL. pH of the cytoplasm and periplasm of Escherichia coli: Rapid measurement by green fluorescent protein fluorimetry. Journal of Bacteriology. 2007;189(15):5601-7.
129. BH I. Medical Microbiology. 4th edition ed. University of Texas Medical Branch at Galveston: Galveston (TX); 1996.
130. Zgurskaya HI, Löpez CA, Gnanakaran S. Permeability Barrier of Gram-Negative Cell Envelopes and Approaches To Bypass It. ACS Infect Dis. 2015;1(11):512-22.
131. Mortimer PG, Piddock LJ. The accumulation of five antibacterial agents in porin-deficient mutants of Escherichia coli. The Journal of antimicrobial chemotherapy. 1993;32(2):195-213.
132. Benz R, Hancock RE. Properties of the large ion-permeable pores formed from protein F of Pseudomonas aeruginosa in lipid bilayer membranes. Biochimica et biophysica acta. 1981;646(2):298-308.
133. Woodruff WA, Hancock REW. Pseudomonas-Aeruginosa Outer-Membrane Protein-F - Structural Role and Relationship to the Escherichia-Coli Ompa Protein. Journal of Bacteriology. 1989;171(6):3304-9.
134. Nicas TI, Hancock RE. Pseudomonas aeruginosa outer membrane permeability: isolation of a porin protein F-deficient mutant. Journal of Bacteriology. 1983;153(1):281-5.
135. Stock JB, Rauch B, Roseman S. Periplasmic Space in Salmonella-Typhimurium and Escherichia-Coli. J Biol Chem. 1977;252(21):7850-61.
136. Nikaido H, Thanassi DG. Penetration of lipophilic agents with multiple protonation sites into bacterial cells: tetracyclines and fluoroquinolones as examples. Antimicrob Agents Chemother. 1993;37(7):1393-9.
137. Schnappinger D, Hillen W. Tetracyclines: antibiotic action, uptake, and resistance mechanisms. Arch Microbiol. 1996;165(6):359-69.

138. Yamaguchi A, Ohmori H, Kaneko-Ohdera M, Nomura T, Sawai T. Delta pH-dependent accumulation of tetracycline in Escherichia coli. Antimicrob Agents Chemother. 1991;35(1):53-6.
139. McMurry LM, Cullinane JC, Petrucci RE, Levy SB. Active uptake of tetracycline by membrane vesicles from susceptible Escherichia coli. Antimicrobial Agents and Chemotherapy. 1981;20(3):307-13.
140. Argast M, Beck CF. Tetracycline diffusion through phospholipid bilayers and binding to phospholipids. Antimicrobial agents and chemotherapy. 1984;26(2):263-5.
141. Im W, Roux B. Ions and counterions in a biological channel: a molecular dynamics simulation of OmpF porin from Escherichia coli in an explicit membrane with 1 M KCl aqueous salt solution. Journal of molecular biology. 2002;319(5):1177-97.
142. Delcour AH. Outer membrane permeability and antibiotic resistance. Biochimica et biophysica acta. 2009;1794(5):808-16.
143. Duret G, Simonet V, Delcour AH. Modulation of Vibrio cholerae porin function by acidic pH. Channels. 2007;1(2):70-9.
144. Hatanaka T, Haramura M, Fei YJ, Miyauchi S, Bridges CC, Ganapathy PS, et al. Transport of amino acid-based prodrugs by the Na+- and Cl- -coupled amino acid transporter ATB(0,+) and expression of the transporter in tissues amenable for drug delivery. J Pharmacol Exp Ther. 2004;308(3):1138-47.
145. Ganapathy ME, Ganapathy V. Amino Acid Transporter ATB0,+ as a delivery system for drugs and prodrugs. Current drug targets Immune, endocrine and metabolic disorders. 2005;5(4):357-64.
146. Saier MH. Families of transmembrane transporters selective for amino acids and their derivatives. Microbiol-Sgm. 2000;146:1775-95.
147. Hosie AH, Poole PS. Bacterial ABC transporters of amino acids. Res Microbiol. 2001;152(3-4):259-70.
148. A E. Amino acids in oral drug delivery: salts, ion-pairs and transcriptomics 2013.
149. Ganapathy ME, Huang W, Wang H, Ganapathy V, Leibach FH. Valacycloviv: A substrate for the intestinal and renal peptide transporters PEPT1 and PEPT2. Biochem Bioph Res Co. 1998;246(2):470-5.
150. Bazzone A, Madej MG, Kaback HR, Fendler K. pH Regulation of Electrogenic Sugar/H+ Symport in MFS Sugar Permeases. PloS one. 2016;11(5):e0156392-e.
151. Cotter PD, Hill C. Surviving the acid test: responses of gram-positive bacteria to low pH. Microbiology and molecular biology reviews : MMBR. 2003;67(3):429-53.
152. O'Driscoll B, Gahan C, Hill C. Two-Dimensional Polyacrylamide Gel Electrophoresis Analysis of the Acid Tolerance Response in Listeria monocytogenes LO28. Appl Environ Microb. 1997;63(7):2679-85.
153. Ginn SL, Brown MH, Skurray RA. The TetA(K) Tetracycline/H⁺ Antiporter from Staphylococcus aureus: Mutagenesis and Functional Analysis of Motif C. Journal of Bacteriology. 2000;182(6):1492-8.
154. Leesukon P, Wirathorn W, Chuchue T, Charoenlap N, Mongkolsuk S. The selectable antibiotic marker, tetA(C), increases Pseudomonas aeruginosa susceptibility to the herbicide/superoxide generator, paraquat. Arch Microbiol. 2013;195(9):671-4.
155. Yamaguchi A, Udagawa T, Sawai T. Transport of Divalent-Cations with Tetracycline as Mediated by the Transposon Tn10-Encoded Tetracycline Resistance Protein. J Biol Chem. 1990;265(9):4809-13.
156. ElShaer A OD, Hanson P, Mohammed AR. Preparation and Evaluation of Amino Acid Based Salt Forms of Model Zwitterionic Drug Ciprofloxacin. Journal of Pharmaceutics and Drug Delivery Research. 2013.
157. Turner B, Pati J, Nargund V, Claxton A, Longstaff V, Sarkar S, et al. Ciprofloxacin Resistance: A Review of Patients in East London Undergoing Prostate Biopsy. Urologic nursing. 2016;36(4):173-82.
158. Committee JF. British National Formulary (online): London: BMJ Group and Pharmaceutical Press; [Available from: http://www.medicinescomplete.com.

159. Sharma D, Patel RP, Zaidi STR, Sarker MMR, Lean QY, Ming LC. Interplay of the Quality of Ciprofloxacin and Antibiotic Resistance in Developing Countries. Frontiers in Pharmacology. 2017;8(546).
160. Campoli-Richards DM, Monk JP, Price A, Benfield P, Todd PA, Ward A. Ciprofloxacin. A review of its antibacterial activity, pharmacokinetic properties and therapeutic use. Drugs. 1988;35(4):373-447.
161. Reis ACC, Santos SRdS, Souza SCd, Saldanha MG, Pitanga TN, Oliveira RR. CIPROFLOXACIN RESISTANCE PATTERN AMONG BACTERIA ISOLATED FROM PATIENTS WITH COMMUNITY-ACQUIRED URINARY TRACT INFECTION. Rev Inst Med Trop Sao Paulo. 2016;58:53-.
162. Mulder M, Kiefte-de Jong JC, Goessens WHF, de Visser H, Hofman A, Stricker BH, et al. Risk factors for resistance to ciprofloxacin in community-acquired urinary tract infections due to Escherichia coli in an elderly population. J Antimicrob Chemoth. 2016;72(1):281-9.
163. Fàbrega A, Madurga S, Giralt E, Vila J. Mechanism of action of and resistance to quinolones. Microb Biotechnol. 2009;2(1):40-61.
164. Jacoby GA. Mechanisms of Resistance to Quinolones. Clinical Infectious Diseases. 2005;41(Supplement_2):S120-S6.
165. Iyire A, Alaayedi M, Mohammed AR. Pre-formulation and systematic evaluation of amino acid assisted permeability of insulin across in vitro buccal cell layers. Scientific reports. 2016;6:32498-.
166. Liu Y, Li R, Xiao X, Wang Z. Antibiotic adjuvants: an alternative approach to overcome multi-drug resistant Gram-negative bacteria. Critical Reviews in Microbiology. 2019;45(3):301-14.
167. Melander RJ, Melander C. The Challenge of Overcoming Antibiotic Resistance: An Adjuvant Approach? ACS Infect Dis. 2017;3(8):559-63.
168. Yang Y, Fu Y, Lan P, Xu Q, Jiang Y, Chen Y, et al. Molecular Epidemiology and Mechanism of Sulbactam Resistance in Acinetobacter baumannii Isolates with Diverse Genetic Backgrounds in China. Antimicrobial Agents and Chemotherapy. 2018;62(3):e01947-17.
169. Noguchi JK, Gill MA. Sulbactam: a beta-lactamase inhibitor. Clinical pharmacy. 1988;7(1):37-51.
170. Fischer J, Ganellin CR. Analogue-based Drug Discovery: Wiley; 2006.
171. Zilberberg MD, Kollef MH, Shorr AF. Secular trends in Acinetobacter baumannii resistance in respiratory and blood stream specimens in the United States, 2003 to 2012: A survey study. J Hosp Med. 2016;11(1):21-6.
172. Silva F, Lourenço O, Queiroz JA, Domingues FC. Bacteriostatic versus bactericidal activity of ciprofloxacin in Escherichia coli assessed by flow cytometry using a novel far-red dye. The Journal Of Antibiotics. 2011;64:321.
173. Hancock REW, Brinkman FSL. Function of Pseudomonas Porins in Uptake and Efflux. Annu Rev Microbiol. 2002;56(1):17-38.
174. Hancock RE, Siehnel R, Martin N. Outer membrane proteins of Pseudomonas. Mol Microbiol. 1990;4(7):1069-75.
175. Fernandes F, Neves P, Gameiro P, Loura LM, Prieto M. Ciprofloxacin interactions with bacterial protein OmpF: modelling of FRET from a multi-tryptophan protein trimer. Biochimica et biophysica acta. 2007;1768(11):2822-30.
176. Sahalan AZ, Abd Aziz AH, Lian HH, Abd Ghani MK. Divalent Cations (Mg2+, Ca2+) Protect Bacterial Outer Membrane Damage by Polymyxin B. Sains Malays. 2013;42(3):301-6.
177. Park M-G, Choi MH. Method for preparation of amino acid chelate. Google Patents; 2008.
178. Percival SL, Hill KE, Williams DW, Hooper SJ, Thomas DW, Costerton JW. A review of the scientific evidence for biofilms in wounds. Wound Repair and Regeneration. 2012;20(5):647-57.
179. Ramon-Perez ML, Diaz-Cedillo F, Ibarra JA, Torales-Cardena A, Rodriguez-Martinez S, Jan-Roblero J, et al. D-Amino acids inhibit biofilm formation in Staphylococcus epidermidis strains from ocular infections. J Med Microbiol. 2014;63:1369-76.

180. Tong Z, Zhang L, Ling J, Jian Y, Huang L, Deng D. An in vitro study on the effect of free amino acids alone or in combination with nisin on biofilms as well as on planktonic bacteria of Streptococcus mutans. PloS one. 2014;9(6):e99513-e.
181. Yang H, Wang MY, Yu JP, Wei HP. Aspartate inhibits Staphylococcus aureus biofilm formation. Fems Microbiol Lett. 2015;362(7).
182. Cassat JE, Lee CY, Smeltzer MS. Investigation of biofilm formation in clinical isolates of Staphylococcus aureus. Methods Mol Biol. 2007;391:127-44.
183. O'Toole GA. Microtiter Dish Biofilm Formation Assay. Journal of Visualized Experiments : JoVE. 2011(47):2437.
184. Sanchez CJ, Mende K, Beckius ML, Akers KS, Romano DR, Wenke JC, et al. Biofilm formation by clinical isolates and the implications in chronic infections. BMC Infectious Diseases. 2013;13:47-.
185. Harrigan WF, McCance ME. Laboratory Methods in Microbiology: Elsevier Science; 2014.
186. Ito A, Taniuchi A, May T, Kawata K, Okabe S. Increased antibiotic resistance of Escherichia coli in mature biofilms. Appl Environ Microbiol. 2009;75(12):4093-100.
187. Hochbaum AI, Kolodkin-Gal I, Foulston L, Kolter R, Aizenberg J, Losick R. Inhibitory Effects of d-Amino Acids on Staphylococcus aureus Biofilm Development. Journal of Bacteriology. 2011;193(20):5616-22.
188. Leiman SA, May JM, Lebar MD, Kahne D, Kolter R, Losick R. d-Amino Acids Indirectly Inhibit Biofilm Formation in Bacillus subtilis by Interfering with Protein Synthesis. Journal of Bacteriology. 2013;195(23):5391-5.
189. Velmourougane K, Prasanna R. Influence of l-amino acids on aggregation and biofilm formation in Azotobacter chroococcum and Trichoderma viride. J Appl Microbiol. 2017;123(4):977-91.
190. Vidakovic L, Singh PK, Hartmann R, Nadell CD, Drescher K. Dynamic biofilm architecture confers individual and collective mechanisms of viral protection. Nat Microbiol. 2018;3(1):26-31.
191. Velmourougane K, Prasanna R, Singh SB, Kumar R, Saha S. Sequence of inoculation influences the nature of extracellular polymeric substances and biofilm formation in Azotobacter chroococcum and Trichoderma viride. FEMS Microbiol Ecol. 2017;93(7).
192. Tang L, Schramm A, Neu TR, Revsbech NP, Meyer RL. Extracellular DNA in adhesion and biofilm formation of four environmental isolates: a quantitative study. FEMS Microbiol Ecol. 2013;86(3):394-403.
193. Kirchhoff C, Cypionka H. Propidium ion enters viable cells with high membrane potential during live-dead staining. Journal of Microbiological Methods. 2017;142:79-82.
194. Stiefel P, Schmidt-Emrich S, Maniura-Weber K, Ren Q. Critical aspects of using bacterial cell viability assays with the fluorophores SYTO9 and propidium iodide. BMC microbiology. 2015;15:36-.
195. Sugimoto S, Sato F, Miyakawa R, Chiba A, Onodera S, Hori S, et al. Broad impact of extracellular DNA on biofilm formation by clinically isolated Methicillin-resistant and -sensitive strains of Staphylococcus aureus. Scientific reports. 2018;8(1):2254-.
196. Das T, Sharma PK, Busscher HJ, van der Mei HC, Krom BP. Role of extracellular DNA in initial bacterial adhesion and surface aggregation. Appl Environ Microbiol. 2010;76(10):3405-8.
197. Dengler V, Foulston L, DeFrancesco AS, Losick R. An Electrostatic Net Model for the Role of Extracellular DNA in Biofilm Formation by Staphylococcus aureus. Journal of Bacteriology. 2015;197(24):3779-87.
198. Moormeier DE, Bayles KW. Staphylococcus aureus biofilm: a complex developmental organism. Mol Microbiol. 2017;104(3):365-76.
199. DeFrancesco AS, Masloboeva N, Syed AK, DeLoughery A, Bradshaw N, Li GW, et al. Genome-wide screen for genes involved in eDNA release during biofilm formation by Staphylococcus aureus. Proceedings of the National Academy of Sciences of the United States of America. 2017;114(29):E5969-E78.
200. Mann EE, Rice KC, Boles BR, Endres JL, Ranjit D, Chandramohan L, et al. Modulation of eDNA Release and Degradation Affects Staphylococcus aureus Biofilm Maturation. PLOS ONE. 2009;4(6):e5822.

201. Foulston L, Elsholz AKW, DeFrancesco AS, Losick R. The Extracellular Matrix of Staphylococcus aureus Biofilms Comprises Cytoplasmic Proteins That Associate with the Cell Surface in Response to Decreasing pH. Mbio. 2014;5(5):e01667-14.
202. Das T, Krom BP, van der Mei HC, Busscher HJ, Sharma PK. DNA-mediated bacterial aggregation is dictated by acid–base interactions. Soft Matter. 2011;7(6):2927-35.
203. Alvarez RA, Blaylock MW, Baseman JB. Surface localized glyceraldehyde-3-phosphate dehydrogenase of Mycoplasma genitalium binds mucin. Molecular Microbiology. 2003;48(5):1417-25.
204. GilNavarro I, Gil ML, Casanova M, OConnor JE, Martinez JP, Gozalbo D. The glycolytic enzyme glyceraldehyde-3-phosphate dehydrogenase of Candida albicans is a surface antigen. Journal of Bacteriology. 1997;179(16):4992-9.
205. Bergmann S, Rohde M, Hammerschmidt S. Glyceraldehyde-3-phosphate dehydrogenase of Streptococcus pneumoniae is a surface-displayed plasminogen-binding protein. Infection and immunity. 2004;72(4):2416-9.
206. Bergmann S, Rohde M, Chhatwal GS, Hammerschmidt S. α-Enolase of Streptococcus pneumoniae is a plasmin(ogen)-binding protein displayed on the bacterial cell surface. Molecular Microbiology. 2001;40(6):1273-87.
207. Pancholi V, Fischetti VA. alpha-enolase, a novel strong plasmin(ogen) binding protein on the surface of pathogenic streptococci. J Biol Chem. 1998;273(23):14503-15.
208. Terao Y, Yamaguchi M, Hamada S, Kawabata S. Multifunctional glyceraldehyde-3-phosphate dehydrogenase of Streptococcus pyogenes is essential for evasion from neutrophils. J Biol Chem. 2006;281(20):14215-23.
209. Antikainen J, Kuparinen V, Lähteenmäki K, Korhonen TK. pH-dependent association of enolase and glyceraldehyde-3-phosphate dehydrogenase of Lactobacillus crispatus with the cell wall and lipoteichoic acids. Journal of bacteriology. 2007;189(12):4539-43.
210. Chiang W-C, Nilsson M, Jensen PØ, Høiby N, Nielsen TE, Givskov M, et al. Extracellular DNA shields against aminoglycosides in Pseudomonas aeruginosa biofilms. Antimicrobial agents and chemotherapy. 2013;57(5):2352-61.
211. Allesen-Holm M, Barken KB, Yang L, Klausen M, Webb JS, Kjelleberg S, et al. A characterization of DNA release in Pseudomonas aeruginosa cultures and biofilms. Molecular Microbiology. 2006;59(4):1114-28.
212. Virgadamo S, Charnigo R, Darrat Y, Morales G, Elayi CS. Digoxin: A systematic review in atrial fibrillation, congestive heart failure and post myocardial infarction. World J Cardiol. 2015;7(11):808-16.
213. Caldeira TG, Ruiz-Picazo A, Lozoya-Agullo I, Saúde-Guimarães DA, González-Álvarez M, de Souza J, et al. Determination of intestinal permeability using in situ perfusion model in rats: Challenges and advantages to BCS classification applied to digoxin. International Journal of Pharmaceutics. 2018;551(1):148-57.
214. Malm-Erjefalt M, Ekblom M, Vouis J, Zdravkovic M, Lennernas H. Effect on the Gastrointestinal Absorption of Drugs from Different Classes in the Biopharmaceutics Classification System, When Treating with Liraglutide. Molecular pharmaceutics. 2015;12(11):4166-73.
215. Papich MG, Martinez MN. Applying Biopharmaceutical Classification System (BCS) Criteria to Predict Oral Absorption of Drugs in Dogs: Challenges and Pitfalls. AAPS J. 2015;17(4):948-64.
216. Valizadeh H, Mehtari M, Zakeri-Milani P. Evidence for Enhanced Intestinal Absorption of Digoxin by P-Glycoprotein Inhibitors. Tropical Journal of Pharmaceutical Research. 2012;11:939-45.
217. Aungst BJ. Intestinal permeation enhancers. J Pharm Sci. 2000;89(4):429-42.
218. Parr A, Hidalgo IJ, Bode C, Brown W, Yazdanian M, Gonzalez MA, et al. The Effect of Excipients on the Permeability of BCS Class III Compounds and Implications for Biowaivers. Pharmaceutical research. 2016;33(1):167-76.
219. Gault MH, Charles JD, Sugden DL, Kepkay DC. Hydrolysis of digoxin by acid. J Pharm Pharmacol. 1977;29(1):27-32.

220. Sonobe T, Hasumi S, Yoshino T, Kobayashi Y, Kawata H, Nagai T. Digoxin degradation in acidic dissolution medium. J Pharm Sci. 1980;69(4):410-3.
221. Fang Y, Cao W, Xia M, Pan S, Xu X. Study of Structure and Permeability Relationship of Flavonoids in Caco-2 Cells. Nutrients. 2017;9(12):1301.
222. Zheng Y, Benet LZ, Okochi H, Chen X. pH Dependent but not P-gp Dependent Bidirectional Transport Study of S-propranolol: The Importance of Passive Diffusion. Pharmaceutical research. 2015;32(8):2516-26.
223. Al-Ali AAA, Steffansen B, Holm R, Nielsen CU. Nonionic surfactants increase digoxin absorption in Caco-2 and MDCKII MDR1 cells: Impact on P-glycoprotein inhibition, barrier function, and repeated cellular exposure. International Journal of Pharmaceutics. 2018;551(1):270-80.
224. Oga EF, Sekine S, Shitara Y, Horie T. P-glycoprotein mediated efflux in Caco-2 cell monolayers: the influence of herbals on digoxin transport. J Ethnopharmacol. 2012;144(3):612-7.
225. Loo TW, Clarke DM. Recent progress in understanding the mechanism of P-glycoprotein-mediated drug efflux. J Membr Biol. 2005;206(3):173-85.
226. Al-Shawi MK, Omote H. The remarkable transport mechanism of P-glycoprotein: a multidrug transporter. J Bioenerg Biomembr. 2005;37(6):489-96.
227. Gross G. Chapter 27 - Strategies for Enhancing Oral Bioavailability and Brain Penetration. In: Wermuth CG, Aldous D, Raboisson P, Rognan D, editors. The Practice of Medicinal Chemistry (Fourth Edition). San Diego: Academic Press; 2015. p. 631-55.
228. Mooradian AD. Digitalis. An update of clinical pharmacokinetics, therapeutic monitoring techniques and treatment recommendations. Clinical pharmacokinetics. 1988;15(3):165-79.
229. Cavet ME, West M, Simmons NL. Transport and epithelial secretion of the cardiac glycoside, digoxin, by human intestinal epithelial (Caco-2) cells. Br J Pharmacol. 1996;118(6):1389-96.
230. Samiei N, Mangas-Sanjuan V, González-Álvarez I, Foroutan M, Shafaati A, Zarghi A, et al. Ion-pair strategy for enabling amifostine oral absorption: Rat in situ and in vivo experiments. European Journal of Pharmaceutical Sciences. 2013;49(4):499-504.
231. Miller JM, Dahan A, Gupta D, Varghese S, Amidon GL. Enabling the Intestinal Absorption of Highly Polar Antiviral Agents: Ion-Pair Facilitated Membrane Permeation of Zanamivir Heptyl Ester and Guanidino Oseltamivir. Molecular pharmaceutics. 2010;7(4):1223-34.
232. Djnv A, Nilsen OG. Caco-2 Cell Methodology and Inhibition of the P-glycoprotein Transport of Digoxin by Aloe vera Juice. Phytother Res. 2008;22(12):1623-8.
233. Moghimipour E, Tabassi SAS, Ramezani M, Handali S, Löbenberg R. Brush border membrane vesicle and Caco-2 cell line: Two experimental models for evaluation of absorption enhancing effects of saponins, bile salts, and some synthetic surfactants. J Adv Pharm Technol Res. 2016;7(3):75-9.
234. Kirienko DR, Kang D, Kirienko NV. Novel Pyoverdine Inhibitors Mitigate Pseudomonas aeruginosa Pathogenesis. Frontiers in microbiology. 2019;9:3317-.
235. Liu PV. Extracellular Toxins of Pseudomonas aeruginosa. The Journal of Infectious Diseases. 1974;130:S94-S9.
236. Liang C-C, Park AY, Guan J-L. In vitro scratch assay: a convenient and inexpensive method for analysis of cell migration in vitro. Nat Protoc. 2007;2:329.
237. Planz V, Wang J, Windbergs M. Establishment of a cell-based wound healing assay for bio-relevant testing of wound therapeutics. Journal of Pharmacological and Toxicological Methods. 2018;89:19-25.
238. Nagoba BS, Suryawanshi NM, Wadher B, Selkar S. Acidic Environment and Wound Healing: A Review. Wounds. 2015;27(1):5-11.

Appendices

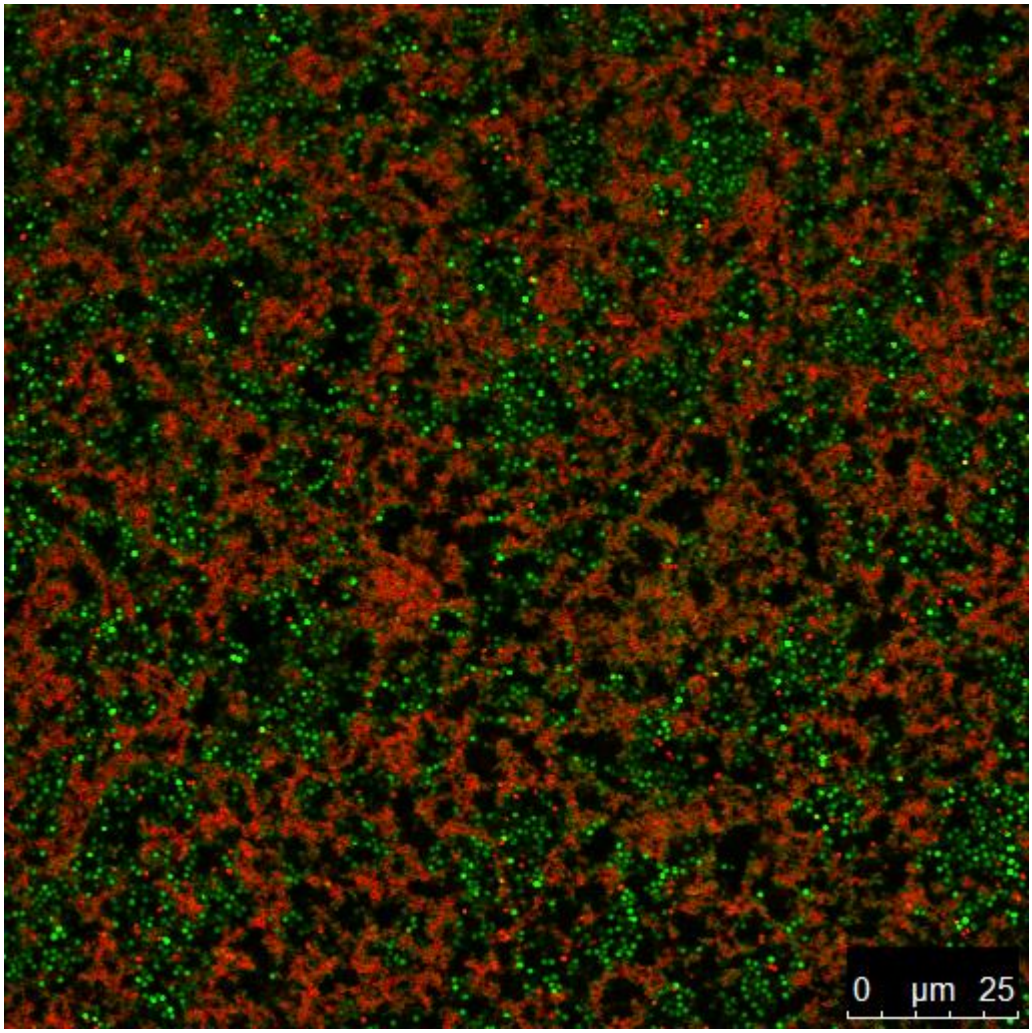

Appendix figure 1: Confocal Image of biofilm dispersed with Cip alone. eDNA is present as seemingly well-fortified boundaries, enclosing persisting *S. aureus* cells.

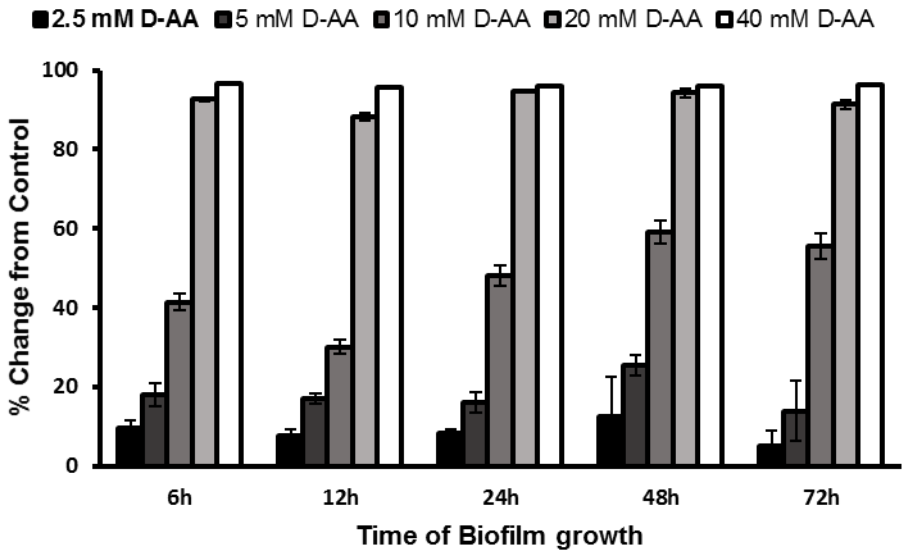

Appendix figure 2: Percentage change from control upon biofilm inhibition; n=3.

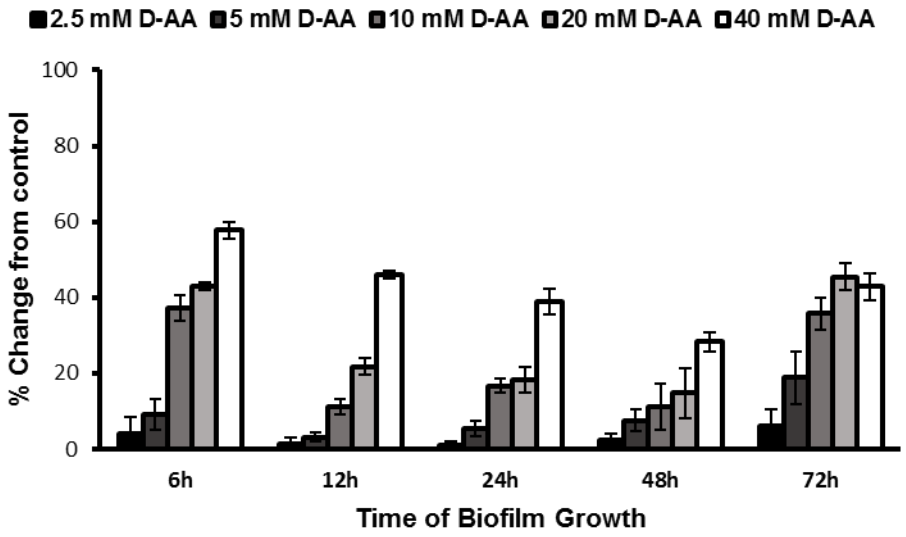

Appendix figure 3: Percentage change from control upon biofilm dispersal; n=3.

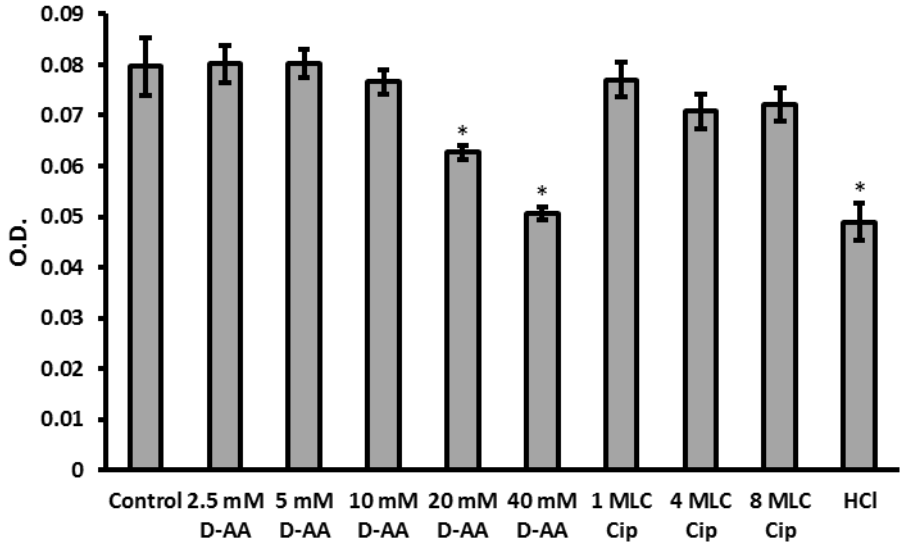

Appendix figure 4: Effect of D-AA at concentrations of 2.5, 5, 10, 20 and 40mM, and Cip at concentrations of 1 MLC, 4 MLC and 8 MLC on the Optical density of planktonic *S. aureus* growth after 30 minutes of exposure. One-way ANOVA showed an overall significant difference within the data and was followed by a post-hoc t-test with Bonferroni correction to see which concentration significantly ($p<0.005$ was taken as significant; indicated by *) killed or effected planktonic growth of *S. aureus* compared to the control. Significant effect on planktonic growth of *S. aureus* was observed with 20mM and 40mM D-AA; n=6.

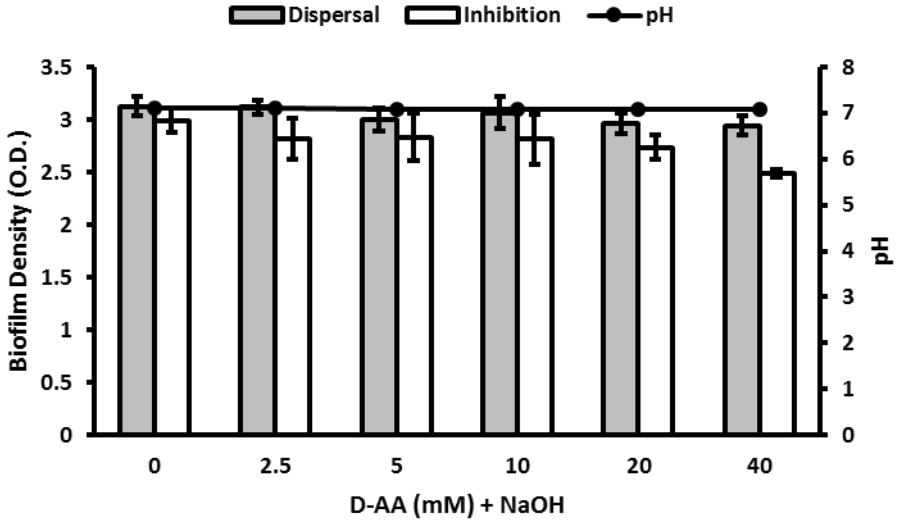

Appendix figure 5: Effect of NaOH on the anti-biofilm activity of D-AA. Neutralising acidic amino acids using NaOH resulted in the anti-biofilm activity of these agents to be halted; n=4.

Appendix table 1: Comparison of percent change in biofilm density with percent change in viable cells for dispersed biofilms. There is a greater reduction in number of viable cells as compared to the reduction in total biomass. This pattern is more prominent in dispersed biofilms than inhibited.

Dispersing agent	Percent reduction in biofilm density	Percent reduction in cell viability
40mM D-AA	30.16	97.59
40mM L-AA	44.92	98.55
40mM D-AA + 8 MLC	32.00	96.09

Appendix table 2: Comparison of percent change in biofilm density with percent change in viable cells for inhibited biofilms. There is a greater reduction in number of viable cells as compared to the reduction in total biomass. This pattern is more prominent in dispersed biofilms than inhibited.

Inhibiting agent	Percent reduction in biofilm density	Percent reduction in cell viability
40mM D-AA	92.78	99.98
40mM L-AA	97.01	99.98
40mM D-AA + 8 MLC	93.58	99.99